Finite Alphabet Blind Separation

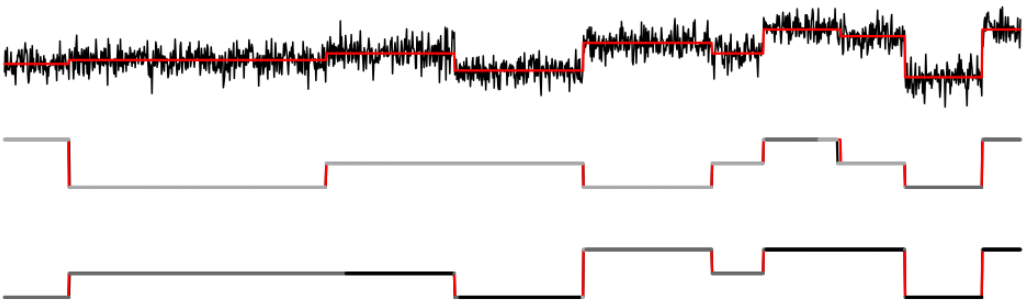

Dissertation
zur Erlangung des mathematisch-naturwissenschaftlichen Doktorgrades
“Doctor rerum naturalium”
der Georg-August-Universität zu Göttingen

im Promotionsprogramm
“PhD School of Mathematical Sciences (SMS)”
der Georg-August University School of Science (GAUSS)

vorgelegt von
Merle Behr
aus Papenburg

Göttingen, 2017

Betreuungsausschuss:

Prof. Dr. Axel Munk
Institut für Mathematische Stochastik, Universität Göttingen

Prof. Dr. Max Wardetzky
Institut für Numerische und Angewandte Mathematik, Universität Göttingen

Mitglieder der Prüfungskommission:

Referent:
Prof. Dr. Axel Munk
Institut für Mathematische Stochastik, Universität Göttingen

Korreferent:
Prof. Dr. Max Wardetzky
Institut für Numerische und Angewandte Mathematik, Universität Göttingen

Weitere Mitglieder der Prüfungskommission:

Prof. Dr. Stefan Halverscheid
Mathematisches Institut, Universität Göttingen

Prof. Dr. Dieter Hogrefe
Institut für Informatik, Universität Göttingen

Jun.-Prof. Dr. Daniel Rudolf
Institut für Mathematische Stochastik, Universität Göttingen

Prof. Dr. Dominic Schuhmacher
Institut für Mathematische Stochastik, Universität Göttingen

Tag der mündlichen Prüfung: 6.12.2017

"The best thing about being a statistician is that you get to play in everyone's backyard."

— John Tukey

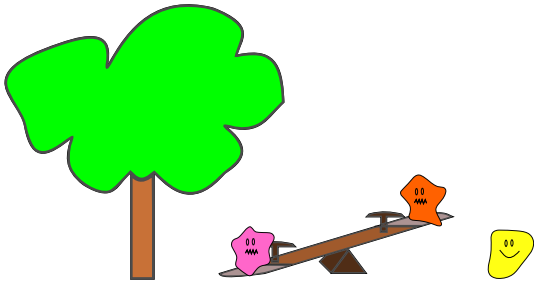

Acknowledgments

First of all, I would like to thank Prof. Axel Munk for being such a wonderful supervisor and mentor during my last four years in his research group. His incredibly broad expertise in so many fields shaped my knowledge of statistics. Without his constant support, motivating advice, and our enlightening discussions this work would have been impossible.
I would also like to thank Prof. Max Wardetzky for taking on the Korreferat.
I was very happy to work with Prof. Chris Holmes on this project, who introduced me to applications in genetics. I always had a great time in Oxford and felt very welcome at the Department of Statistics and Wellcome Trust Centre for Human Genetics. In particular, I would like to thank Prof. Christopher Yau and Prof. Jean-Baptiste Cazier for their time to explain me various aspects of copy-number variations in cancer genetics.
Further, I would like to thank Prof. Martin Wainwright, Prof. Anita Schöbel, Prof. Boaz Nadler, and Prof. Christian Clason for fruitful discussions about my work in this thesis and related projects.
Special thanks go to all members of the IMS, who provided a lovely working environment. In particular, I would like to thank Anne Hein, Carla Tameling, Claudia König, Henning Höllwarth, Dr. Katharina Proksch, Laura Fee Schneider, Manuel Diehn, Max Sommerfeld, and Miguel Del Alamo. You are not just the best colleagues one can image, you are also wonderful friends! Also, I want to thank Claudia König, Malte Behr, and Markus Schmitt for proofreading this thesis.
With the end of my PhD will soon come the end of my time in Göttingen. Burkhard Blobel, Thomas Kotzott, Luisa Huchting, and Christina Jänicke, I thank you so much for making this place my home.
Am meisten möchte ich mich aber bei meinen Eltern, Meike Hager-Behr und Martin Behr, meinem Bruder, Malte Behr, meiner Großmutter, Ingeborg Hager, und meinem Freund, Markus Schmitt, bedanken. Es ist alles unglaublich viel leichter, wenn man weiß, dass man einen solchen Rückhalt hat! Vor allem Markus hat mich wie kein anderer beim Erstellen dieser Arbeit begleitet. Wie einer der Begründer der Wahrscheinlichkeitstheorie, Blaise Pascal, schon bemerkt hat: “Ein Tropfen Liebe ist mehr als ein Ozean an Wille und Verstand”.

Preface

In blind source separation (BSS) problems one observes M mixtures of m sources and aims to recover the original sources from the available observations, where the blindness refers to the fact that neither the sources nor the mixing weights are known. BSS appears in many different applications and is a widely discussed topic in the signal processing, but also in the statistics literature. A prominent example is the separation of a mixture of audio or speech signals, which has been picked up by several microphones, simultaneously. In this case the different speech signals correspond to the sources and the recordings of the microphones to the mixture of signals with unknown mixing weights. From this mixture the individual signals have to be separated. To ensure identifiability various assumptions on the sources exist. Among the most well known are stochastic independence, as in independent component analysis (Comon, 1994), non-negativity, as in non-negative matrix factorization (Lee and Seung, 1999), and sparsity of the signals (Li et al., 2006).

Fundamental to this thesis is a different assumption which has received relatively few attention so far: It is assumed that the sources take only values in a known finite set, called the alphabet. This is denoted as *finite alphabet blind separation (FABS)*. FABS occurs in many applications, for instance in digital communications with mixtures of multilevel pulse amplitude modulated digital signals (Talwar et al., 1996; Sampath et al., 2001). The main motivation for this thesis, however, comes from cancer genetics, where one aims to infer copy number aberrations of different clones in a tumor (Liu et al., 2013).

The first part of this thesis in Chapter 2 provides identifiability conditions for FABS. In Chapter 3 FABS is considered in a statistical change-point regression setting for single mixtures ($M = 1$). Estimators for sources and mixing weights with almost optimal convergence rates and confidence statements for all quantities are derived. Moreover, a consistent model selection procedure and lower confidence bounds for the number of sources are proposed. For arbitrary number of sources M (without a change-point regression structure) FABS can be reformulated as a linear model where the design matrix is only known up to a selection matrix, a model which recently has perceived great interest (Marques et al., 2009; Unnikrishnan et al., 2015; Pananjady et al., 2016, 2017). When the number of sources m is fixed and both, number of observations and mixtures M, tend to infinity, in Chapter 4 minimax prediction and estimation rates are obtained. The theoretical results of this thesis are accompanied by algorithms in Chapter 5, a simulation study in Chapter 6, and a real data example from cancer genetics in Chapter 7. An outlook and discussion for further research is given in Chapter 8.

Previous publications Large parts of this thesis have already been published in (Behr and Munk, 2017a), (Behr et al., 2017), and (Behr and Munk, 2017b). Behr and Munk (2017a) consider the identifiability issue, Behr et al. (2017) consider FABS in a statistical change-point regression setting, and Behr and Munk (2017b) consider minimax rates for FABS with multiple mixtures. More precisely, parts of Chapter 1, Section 2.1, Section 2.3.1, and Section 2.4.1 are taken from (Behr and Munk, 2017a) with few modifications. Parts of Chapter 1, some parts of Section 2.2, Chapter 3 (apart from Section 3.6), some parts of Section 5.1, Section 6.1, and the first part of Chapter 7 are taken from (Behr et al., 2017) with few modifications. Parts of Chapter 1, some parts of Section 2.2 and 2.3, Chapter 4, Section 5.2, Section 6.3, and parts of Chapter 8 are taken from the preprint (Behr and Munk, 2017b) with few modifications.

Contents

List of Symbols **xiii**

1 Introduction **1**
- 1.1 Applications . . . 1
- 1.2 Finite alphabet blind separation . . . 5
- 1.3 Main results . . . 7
  - 1.3.1 Identifiability . . . 8
  - 1.3.2 FABS for change-point regression . . . 10
  - 1.3.3 Multivariate FABS . . . 20
- 1.4 Algorithms and implementation . . . 21
- 1.5 Literature survey: contrasted and compared . . . 22
- 1.6 Summary . . . 26

2 Identifiability and model-regularization **27**
- 2.1 Identifiability . . . 27
  - 2.1.1 Combinatorial characterisation of identifiability . . . 28
  - 2.1.2 Separability . . . 29
- 2.2 Exact and stable recovery . . . 32
- 2.3 Restrictiveness of separability . . . 34
  - 2.3.1 Separability of stochastic processes . . . 35
  - 2.3.2 Alphabet separation boundary . . . 36
  - 2.3.3 Known vs. unknown number of sources . . . 39
- 2.4 Extensions . . . 41
  - 2.4.1 Arbitrary mixing weights . . . 41
  - 2.4.2 Unknown alphabet . . . 43

3 Multiscale segmentation of single mixtures **45**
- 3.1 Confidence region for the weights . . . 45
- 3.2 Estimation of source functions . . . 48
- 3.3 Confidence bands for the source functions . . . 49
- 3.4 Consistency and rates . . . 49
- 3.5 Selection of the threshold parameter . . . 52
- 3.6 Model selection . . . 52

3.6.1 Lower confidence bounds for m . . . 54
3.6.2 Model selection consistency . . . 55
3.6.3 Inference on ω and f for unknown m . . . 56

4 Minimax rates for multiple mixtures 59
4.1 Minimax rates for prediction error . . . 60
4.2 Estimation error . . . 61

5 Implementation 63
5.1 Multiscale methods . . . 63
5.2 Clustering based algorithm . . . 65

6 Simulations 67
6.1 SLAM . . . 67
6.1.1 Number of source functions m . . . 67
6.1.2 Number of alphabet values k . . . 68
6.1.3 Confidence levels α and β . . . 70
6.1.4 Prior information on minimal scale λ . . . 72
6.1.5 Robustness of SLAM . . . 72
6.2 SLAM-selector . . . 75
6.2.1 Comparision with AIC, BIC, and LRM . . . 75
6.2.2 Lower Confidence Bounds . . . 78
6.3 LS approximation . . . 79

7 Applications in cancer genetics 85

8 Outlook and discussion 89

A Proofs 95
A.1 Proofs of Chapter 2 . . . 95
A.1.1 Proofs of Section 2.1 . . . 95
A.1.2 Proofs of Section 2.2 . . . 96
A.1.3 Proofs of Section 2.3 . . . 99
A.1.4 Proofs of Section 2.4 . . . 106
A.1.5 Additional lemmas on the ASB . . . 109
A.2 Proofs of Chapter 3 . . . 111
A.2.1 Proofs of Section 3.6 . . . 120
A.3 Proofs of Chapter 4 . . . 122
A.3.1 Additional lemmas . . . 128
A.4 Proof of Chapter 5 . . . 130
A.5 Proof of Chapter 8 . . . 131

B Additional figures from Section 6.2 133

Bibliography **137**

List of Symbols

$\mathrm{E}(X), \mathrm{Med}(X)$	expected value and median of a random variable X
$\mathcal{N}(\mu, \sigma^2)$	normal distribution with mean μ and variance σ^2
$\mathbb{N}$	set of positive integers
$\mathbb{R}$	set of real numbers
$\mathbb{R}_+$	set of non-negative real numbers
$\mathbb{1}_A$	indicator function with $\mathbb{1}_A(x) = 1$ if $x \in A$ and $\mathbb{1}_A(x) = 0$ otherwise
$\|x\|$	Frobenius norm (for matrices) and Euclidean norm (for vectors)
$\|x\|_\infty$	supremum norm
$\mathrm{imag}(g)$	the image set $\{g(x) : \ x \in [0,1)\}$ for $g : [0,1) \to \mathbb{R}$
$\mathrm{imag}(A)$	column space $\{Ax : \ x \in \mathbb{R}^n\} \subset \mathbb{R}^m$ for $A \in \mathbb{R}^{n \times m}$
$\mathrm{rank}(A)$	rank of a matrix $A \in \mathbb{R}^{n \times m}$
$\mathrm{span}(S)$	linear span of a set of vectors S
$\dim(V)$	dimension of a vector space V
$I_{m \times m}$	$m \times m$ identity matrix
e^i	i-th unit vector $(e^i)_j = \mathbb{1}_{i=j}$
$g\|_I$	restriction of function g on interval I
$\#S$	number of elements in a set S
$\lesssim, \gtrsim$	inequalities up to a universal constant
$x^\top$	transposed of a vector or matrix x
B^c	complement of an event B
$\lfloor a \rfloor$	largest integer smaller or equal to a
$a_n \in O(b_n)$	$\limsup_{n \to \infty} \lvert a_n / b_n \rvert < \infty$

CHAPTER 1

Introduction

This thesis provides statistical methodology for the Finite Alphabet Blind Separation (FABS) problem, where one aims to recover the underlying unknown mixing weights and unknown finite alphabet sources from a linear mixture. More precisely, for a given (ordered) set $\mathfrak{A} = \{a_1, \ldots, a_k\} \subset \mathbb{R}$ of distinctive values $a_1 < \ldots < a_k$, denoted as the *alphabet*, we consider the mixture structure

$$\boldsymbol{g} = \boldsymbol{f}\boldsymbol{\omega} = \sum_{i=1}^{m} \boldsymbol{f}^i \omega_i, \tag{1.1}$$

with sources $\boldsymbol{f} = (\boldsymbol{f}^1, \ldots, \boldsymbol{f}^m) \in \mathfrak{A}^{n \times m}$, which are known to take only values in the given alphabet $\mathfrak{A}$. The mixing weights $\boldsymbol{\omega} = (\omega_1, \ldots, \omega_m)^\top \in \mathbb{R}^{m \times M}$ are arbitrary numbers. Further, n is the number of samples, m is the number of sources, and M is the number of mixtures. The aim in FABS is to infer from (a possibly noisy version of) the mixture $\boldsymbol{g}$ and the alphabet $\mathfrak{A}$

1. the number of sources m,
2. the mixing weights $\boldsymbol{\omega} = (\omega_1, \ldots, \omega_m)^\top$,
3. and the sources $\boldsymbol{f} = (\boldsymbol{f}^1, \ldots, \boldsymbol{f}^m)$.

Before introducing FABS further, including details on identifiability, statistical modeling, and inference, we give some motivating examples.

1.1 Applications

FABS appears in many different areas, for instance in digital communications and multiuser detection (Proakis, 2007; Talwar et al., 1996; Verdu, 1998; Zhang and Kassam, 2001; Sampath et al., 2001). In wireless digital communication, several digital signals (e.g., binary signal with $\mathfrak{A} = \{0, 1\}$) are modulated (e.g., with pulse amplitude modulation (PAM)), transmitted through several wireless channels (each having different channel response), and received by (several) antennas. In signal processing this is known as MIMO (multiple input multiple output) and (ignoring time shifts, i.e., considering instantaneous mixtures) can be described by FABS when the channel response is unknown, see (Talwar et al., 1996; Love et al., 2008). Here, the m sources correspond to m digital signals $\boldsymbol{f}^1, \ldots, \boldsymbol{f}^m$ and the M mixing vectors $\boldsymbol{\omega}_{\cdot 1}, \ldots, \boldsymbol{\omega}_{\cdot M}$ correspond to the response of M different channels. The M mixture signals $\boldsymbol{g}_{\cdot 1}, \ldots, \boldsymbol{g}_{\cdot M}$ correspond to the received signals at M different antennas (usually corrupted by noise).

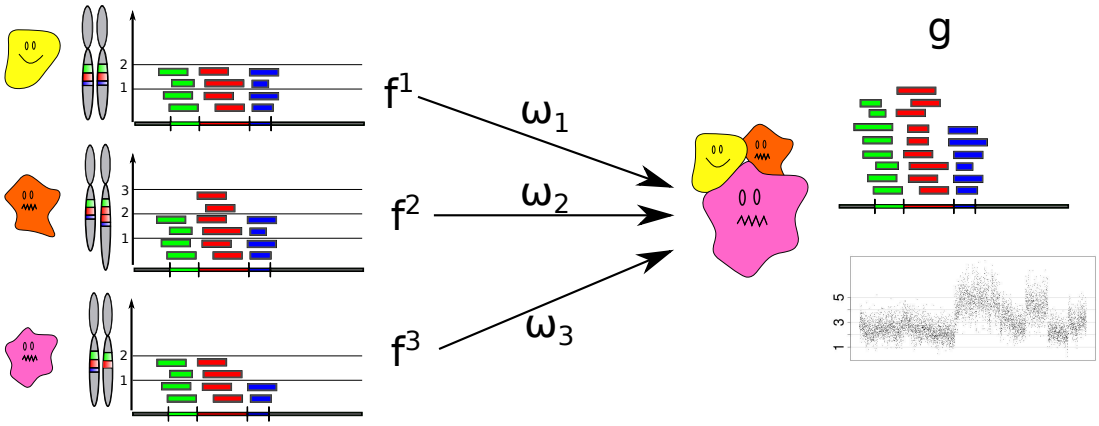

Figure 1.1: Illustration of a FABS problem in cancer genetics.

The major motivation, however, for this thesis comes from a cooperation with the Wellcome Trust Centre for Human Genetics at the University of Oxford in the field of cancer genetics, namely, from assigning copy number aberrations (CNA's) in cell samples taken from tumors to its clones (Yau et al., 2011; Carter et al., 2012; Liu et al., 2013; Ha et al., 2014). In Chapter 7, we decompose a cancer tumor into its clones with the proposed method.

CNA's refer to stretches of DNA in the genome of cancer cells which are under copy number (CN) variation, that is, some parts of the genome are either deleted or multiplied (relative to the inherited germline state present in normal tissue). This is illustrated in Figure 1.1. The yellow cartoon represents normal tissue (healthy cells). Each region of its DNA appears exactly twice, as there are two copies of each chromosome. Hence, the green, red, and blue marked regions in its DNA all have CN 2. The orange cartoon represents tumor cells with a duplication of the red region. Hence, its red region has CN 3, while the blue and the green region have (normal) CN 2. The pink cartoon represents tumor cells with a deletion of the blue region in its DNA. Hence, its blue region has CN 1, while the green and red region have CN 2. In total, the CN of a tumor (that is the number of copies of DNA stretches at a certain locus) of a single clone's genome is a step function mapping chromosomal loci to a value $i \in \{0, 1, \ldots, k\}$ corresponding to i copies of DNA at a locus, with reasonable biological knowledge of k. For instance, in the data example which will be analyzed in Chapter 7 the maximal CN is $k = 5$. CNA's are known to be key drivers of tumor progression through the deletion of "tumor suppressing" genes and the duplication of genes involved in processes such as cell signaling and division. Understanding where, when and how CNA's occur during tumorgenesis, and their consequences, is a highly active and important area of cancer research, see e.g., (Beroukhim et al., 2010).

CNA's can be measures with whole genome sequencing (WGS), where the DNA is fragmented into pieces, the single pieces are sequenced using short "reads", and the reads are aligned to a reference genome by a computer. Thus, for example, in a region with CN 1 there are (on average) only half as many reads aligned as in a region with CN 2 (see Figure 1.1 for an illustration). Modern high-throughput technologies allow for routine WGS of cancer samples and major international efforts are underway to characterize the genetic make up of all cancers,

for example The Cancer Genome Atlas, `http://cancergenome.nih.gov/`.

A key component of complexity in cancer genetics is the "clonal" structure of many tumors (heterogeneity), which relates to the fact that tumors usually contain distinct cell populations of genetic sub-types (clones) each with a distinct CNA profile, see e.g., (Greaves and Maley, 2012; Shah et al., 2012). This is illustrated in Figure 1.1, where the tumor sample originates from three different types of DNA: the normal tissue (represented by the yellow cartoon) and two different cancer clones each with different CNA's (represented by the orange and pink cartoon). High-throughput sequencing technologies act by bulk measurement of large numbers of pooled cells in a single sample, extracted by a micro-dissection biopsy (or blood sample for hematological cancers). Hence, for WGS data of a heterogeneous tumor the number of reads at a certain locus is proportional to the sum of the CN's of the single clones at that locus weighted by the relative proportion of each clone in the cell sample.

Summing up, with the notation of FABS in (1.1), in this example the number of sources $\boldsymbol{m}$ corresponds to the number of clones (plus normal tissue), the source functions $\boldsymbol{f}^i$ correspond to the CN profile of the single clones (with CN's only taking values in the finite alphabet $\{0, 1, 2, \ldots, k\}$), the mixing weights $\boldsymbol{\omega}_i$ correspond to the relative proportion of the clone in the tumor, and the mixture $\boldsymbol{g}$ corresponds to the overall CN of the tumor. If a cell sample of a tumor is taken at several locations or time points (each with a possibly different relative proportion of the single clones), this correspond to FABS with several mixtures, where M is the number of different probes.

The estimation of the mixed function $\boldsymbol{g}$, i.e., estimating the locations of varying overall CN's, has perceived considerable interest in the past, see (Olshen et al., 2004; Zhang and Siegmund, 2007; Tibshirani and Wang, 2008; Jeng et al., 2010; Chen et al., 2011; Yau et al., 2011; Niu and Zhang, 2012; Frick et al., 2014; Du et al., 2015). However, the corresponding demixing problem, that is, jointly estimating the number of clones, their proportion, and their CNAs, has been only recognized more recently as an important issue and hence received very little attention in a statistical context so far and is a major motivation for this thesis.

We illustrate the ability of the procedure which will be proposed in this thesis (called SLAM) to recover the number of clones, their relative proportion, and their CNA's by utilizing it on real genetic sequencing data (see Chapter 7). In collaboration with the University of Oxford, we analyzed a data set from a colorectal cancer, which comes from two different clones and normal tissue. The data has the special feature that sequencing data of the single clones is available, something which is not the case for patient cancer samples. Figure 1.2 shows raw data of chromosomes $4, 5, 6, 18$ and 20. The x-axis represents the position on the chromosome and the y-axis the number of reads at a certain position (recall the illustration in Figure 1.1). The top row shows data which comes from normal tissue (germline) and the subsequent rows show two different clones. As sequencing produces artifacts, we preprocess the data with a smoothing filter and binning (see Chapter 7 for details). Dividing the data by the average number of reads per CN, which is 26 for normal tissue and 14 for the clones in this example, yields baseline correction. The resulting data is displayed in Figure 1.3, where the first row shows a mixture with mixing weights $\boldsymbol{\omega}^\top = (\omega_{\text{Normal}}, \omega_{\text{Clone1}}, \omega_{\text{Clone2}}) = (0.2, 0.35, 0.45)$. Only the

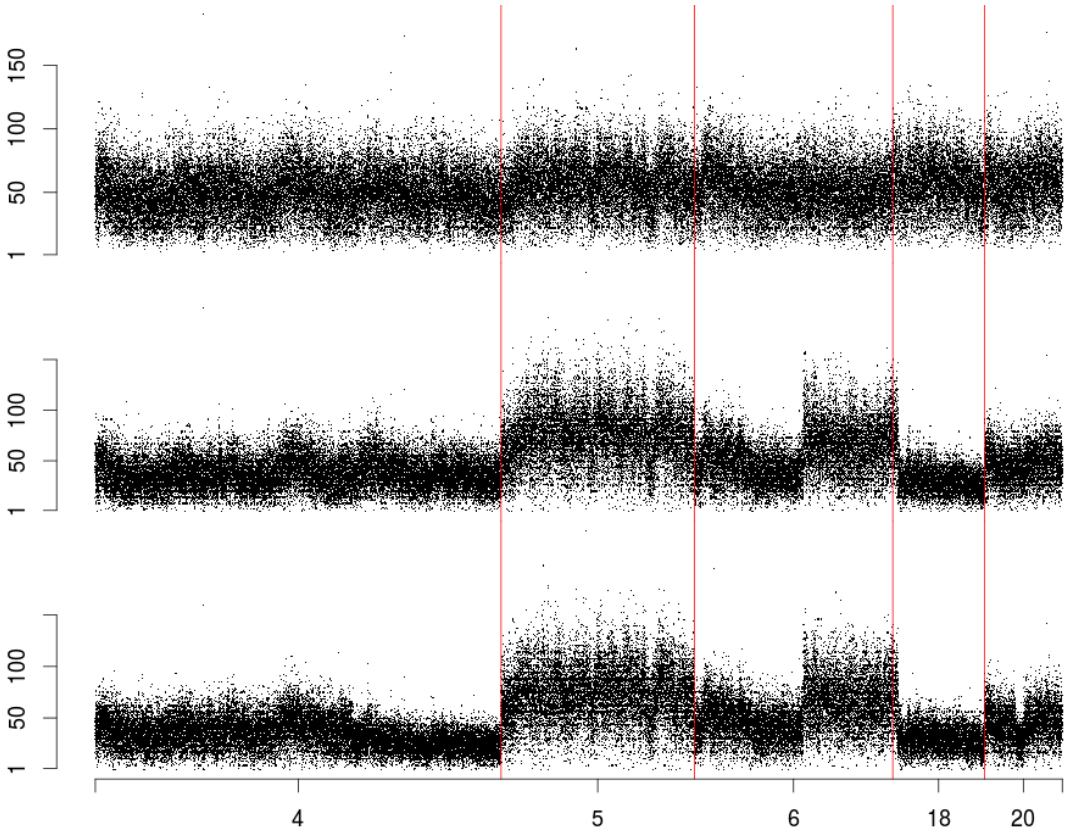

Figure 1.2: Raw WGS data from cell line LS411. Displayed are chromosomes 4,5,6,18, and 20. The x-axis represents the position on the chromosome and the y-axis the number of reads at a certain position. Top row: germline data. Row 2 and 3: two different clones.

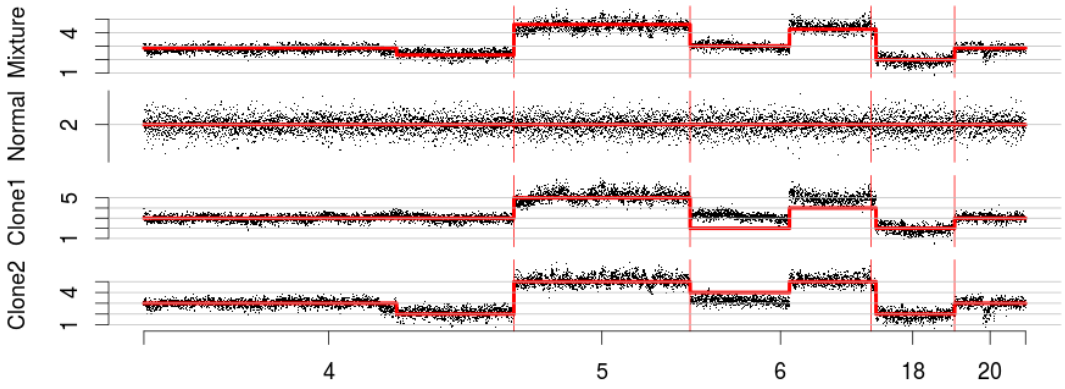

Figure 1.3: Preprocessed WGS data from Figure 1.2. Top row: total CN of the mixture with $\boldsymbol{\omega}^\top = (\omega_{\text{Normal}}, \omega_{\text{Clone1}}, \omega_{\text{Clone2}}) = (0.2, 0.35, 0.45)$. Second row: germline data. Row 3 and 4: two different clones. The red lines show SLAM's estimates. Threshold parameters, as explained in the following, were $q_n(\alpha) = -0.15$ (selected with MVT-method from Section 3.5) and $q_n(\beta) = 20$.

data in the first row of Figure 1.3 enters the estimation procedure, the data of the single clones in subsequent rows serves as ground truth and is used for validation only. SLAM estimates the

number of components $m = 3$ correctly, the mixing weights as $\hat{\omega} = (0.11, 0.36, 0.52)$, and the CNA profile as the red lines in Figure 1.3. This shows that SLAM can provides accurate estimates for the number of clonal components, their relative proportion, and their CNA profiles, something which has not been obtainable prior to now.

1.2 Finite alphabet blind separation

In the following, we introduce FABS in more detail. In FABS the unknown weights ω and unknown sources f are not identifiable from the mixture g, in general, even if the number of sources m is known. Consequently, in order to to achieve the goals 1. - 3. the first major task in FABS is to impose conditions on both, ω and f, which guarantee identifiability and stable recovery, see Section 1.3.1 and Chapter 2. Motivated from the application in cancer genetics, where ω corresponds to physical mixing proportions, we assume that the weights ω_i are positive and sum up to one. This assumption simplifies identifiability conditions to decompose ω and f uniquely. Results for arbitrary weights are given in Section 2.4.1. More precisely, for a given number of sources m and a given number of mixtures M, the set of possible mixing weights ω is defined as

$$\Omega_{m,M} := \left\{ \omega \in \mathbb{R}_+^{m \times M} : \ 0 < \|\omega_{1\cdot}\| \leq \ldots \leq \|\omega_{m\cdot}\|, \ \sum_{i=1}^{m} \omega_{ij} = 1 \ \forall j = 1, ..., M \right\}. \tag{1.2}$$

For a single mixture ($M = 1$) we define $\Omega_m := \Omega_{m,1}$. Note that a fixed ordering of the row-sums is necessary as otherwise for any permutation matrix P one finds that $g = f\omega = fPP^{-1}\omega$ with ω and $P^{-1}\omega$ both valid mixing weights. We address FABS for two statistical settings.

1. A univariate *change-point (c.p.) regression setting* with *one mixture ($M = 1$)*. That is, the weights ω_i in (1.1) are one-dimensional such that a single mixture g of the sources $f^1, \ldots, f^m$ is observed. In this setting, the sources f^i and the mixture g are assumed to be piecewise constant functions mapping from the interval $[0, 1)$ to $\mathbb{R}$. This allows to allocate local information about the unknown weights ω and sources f from the step function g. Such a setting appears, for instance, in the CNA-example explained in Section 1.1, where a piecewise constant source function f^i corresponds to the CNA profile of a clone in some tumor, from which a single ($M = 1$) probe is available.

2. *Multivariate FABS* with *several mixtures ($M \geq 1$)*. That is, the weights ω_i in (1.1) are M-dimensional such that one observes M mixtures $g_{\cdot 1}, \ldots, g_{\cdot M}$ of the sources $f^1, \ldots, f^m$. Here, f is regarded as an arbitrary matrix in $\mathfrak{A}^{n \times m}$ (without c.p. structure). Such a setting appears, for instance, in wireless digital communications (recall Section 1.1), where MIMO techniques use several antennas ($M \geq 1$) to separate digital ($\mathfrak{A} = \{0, 1\}$) signals f^i from m sources, each being an arbitrary sequence of 0's and 1's.

Change-point regression setting The *Statistical Blind Separation Regression (SBSR)* model assumes independent observations

$$Y_j = \boldsymbol{g}(x_j) + \epsilon_j, \qquad j = 1, \dots, n, \tag{1.3}$$

for fixed sampling points $x_j := (j-1)/n$ and independent, identically distributed (i.i.d.), additive Gaussian error terms $(\epsilon_1, \dots, \epsilon_n)^\top \sim \mathcal{N}(0, \sigma^2 I_{n\times n})$, with standard deviation $\sigma > 0$. The true underlying regression function $\boldsymbol{g}$ is assumed to be of FABS mixture structure as in (1.1). The $\boldsymbol{m}$ source functions $\boldsymbol{f}^i$, $i = 1, \dots, \boldsymbol{m}$, consist of arrays of constant segments, i.e., step functions with unknown jump sizes, numbers, and locations of c.p.'s. More precisely, for an alphabet $\mathfrak{A}$ each source function is in the class of step functions on $[0, 1)$

$$\mathcal{S}(\mathfrak{A}) := \left\{ \sum_{j=0}^{K} \theta_j \mathbb{1}_{[\tau_j, \tau_{j+1})} : \theta_j \in \mathfrak{A}, 0 = \tau_0 < \dots < \tau_K < \tau_{K+1} = 1, K \in \mathbb{N} \right\}. \tag{1.4}$$

Note that this implies that for each source function the number $K(\boldsymbol{f}^i)$ of c.p.'s is assumed to be finite, possibly different, and unknown. We assume $\theta_j \neq \theta_{j+1}$ for $j = 0, \dots, K$ to ensure identifiability of the c.p.'s τ_j. Moreover, define the set of all possible (linear) mixtures with $\boldsymbol{m}$ components each in $\mathcal{S}(\mathfrak{A})$ as

$$\mathcal{M}_{\boldsymbol{m}} := \mathcal{M}_{\boldsymbol{m}}(\mathfrak{A}) = \left\{ f\omega = \sum_{i=1}^{\boldsymbol{m}} \omega_i f^i : \omega \in \Omega_{\boldsymbol{m}} \text{ and } f \in \mathcal{S}(\mathfrak{A})^{\boldsymbol{m}} \right\}. \tag{1.5}$$

For a set $\tilde{\Omega} \subset \Omega_{\boldsymbol{m}}$ we define $\mathcal{M}_{\boldsymbol{m}}(\mathfrak{A}, \tilde{\Omega})$ analogously.

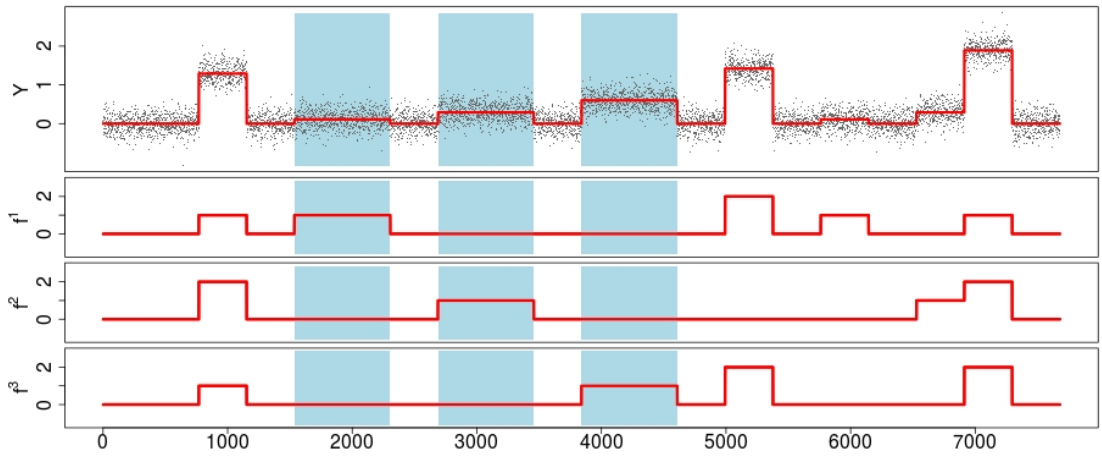

Figure 1.4: Mixture $\boldsymbol{g} = 0.11\boldsymbol{f}^1 + 0.29\boldsymbol{f}^2 + 0.6\boldsymbol{f}^3$ with observations Y (gray dots), and sources $\boldsymbol{f}^1$, $\boldsymbol{f}^2$, $\boldsymbol{f}^3$ from Example 1.2.1 (from top to bottom). A separable region is marked blue.

Example 1.2.1. In Figure 1.4 a mixture $\boldsymbol{g}$ with $\boldsymbol{\omega}^\top = (0.11, 0.29, 0.6)$ of $\boldsymbol{m} = 3$ sources $\boldsymbol{f}^1$, $\boldsymbol{f}^2$, $\boldsymbol{f}^3$, taking values in the alphabet $\mathfrak{A} = \{0, 1, 2\}$, is displayed. Normal noise with $\sigma = 0.22$ is added according to the SBSR model (1.3), $n = 7680$. The marked blue region shows a separable region, which guarantees identifiability of $\boldsymbol{\omega}$ from $\boldsymbol{g}$ (see Section 1.3.1).

In Chapter 3 for the SBSR model we will address estimation of

1. the number of source components $\boldsymbol{m}$,
2. the weights $\boldsymbol{\omega} = (\boldsymbol{\omega}_1, \ldots, \boldsymbol{\omega}_{\boldsymbol{m}})^\top$ and
3. the source functions $\boldsymbol{f}^i$, $i = 1, \ldots, \boldsymbol{m}$, i.e. their
   (a) number of c.p.'s $K(\boldsymbol{f}^i)$,
   (b) c.p. locations τ^i_j, $j = 1, \ldots, K(\boldsymbol{f}^i)$, and
   (c) function values $\boldsymbol{f}^i(x)$ ($\in \mathfrak{A}$) at locations $x \in [0, 1)$.

In addition, we will construct

4. uniform lower confidence bounds for $\boldsymbol{m}$,
5. uniform confidence regions $C_{1-\alpha}$ for the weights $\boldsymbol{\omega}$, and
6. asymptotically uniform multivariate confidence bands for the sources $\boldsymbol{f} = (\boldsymbol{f}^1, \ldots, \boldsymbol{f}^{\boldsymbol{m}})$.

Multivariate FABS FABS can be considered in a multivariate matrix factorization setting, where the sources $\boldsymbol{f}$ are associated with an unknown matrix $\boldsymbol{F} \in \mathfrak{A}^{n \times \boldsymbol{m}}$ and the mixing weights with an unknown matrix $\boldsymbol{\omega} \in \Omega_{\boldsymbol{m},M} \subset \mathbb{R}^{\boldsymbol{m} \times M}$. In *Multivariate finite Alphabet Blind Separation (MABS)* one models an observation matrix $Y \in \mathbb{R}^{n \times M}$ as

$$Y = \boldsymbol{F}\boldsymbol{\omega} + Z, \tag{1.6}$$

with unknown source matrix $\boldsymbol{F} \in \mathfrak{A}^{n \times \boldsymbol{m}}$, unknown weight matrix $\boldsymbol{\omega} \in \Omega_{\boldsymbol{m},M}$, and additive noise matrix $Z \in \mathbb{R}^{n \times M}$, which in this work is assumed to be i.i.d. Gaussian, that is $Z_{ij} \sim \mathcal{N}(0, \sigma^2)$ for $i = 1, \ldots n$, $j = 1, \ldots, M$. Note that this corresponds to a multivariate linear model with design matrix $\boldsymbol{F}$ and parameter matrix $\boldsymbol{\omega}$, with the additional difficulty that the design matrix $\boldsymbol{F}$ is not completely known. Namely, only a finite set of possible values (the alphabet) for the entries of the design matrix $\boldsymbol{F}$ is given.

1.3 Main results

This section gives an overview of the main results of this thesis. Throughout the following bold letters $\boldsymbol{m}, \boldsymbol{f}$ (or $\boldsymbol{F}$), $\boldsymbol{\omega}, \boldsymbol{g}$ denote the underlying truth of the observations Y in (1.3) and (1.6), respectively. For simplicity, we use the same notation in Chapter 2, where identifiability of FABS is analyzed (independent of a specific data model as in (1.3) and (1.6)), to distinguish between two different mixtures $(\boldsymbol{f}, \boldsymbol{\omega})$ and (f, ω). Moreover, throughout the following, we assume a fixed, given (ordered) alphabet $\mathfrak{A}$, where w.l.o.g. $a_1 = 0$ and $a_2 = 1$, that is

$$\mathfrak{A} = \{0, 1, a_3, \ldots, a_k\} \quad \text{with} \quad 1 < a_3 < \ldots < a_k. \tag{1.7}$$

Otherwise, one may instead consider the observations $(Y_j - a_1)/(a_2 - a_1)$ with alphabet $\mathfrak{A} = \{0, 1, \frac{a_3-a_1}{a_2-a_1}, \ldots, \frac{a_k-a_1}{a_2-a_1}\}$ in (1.3) and (1.6).

1.3.1 Identifiability

A minimal requirement underlying any recovery algorithm of $\boldsymbol{m}$, $\boldsymbol{f}$ and $\boldsymbol{\omega}$ from (a possibly noisy version of) $\boldsymbol{g}$ in (1.1) to be valid is identifiability, that is, a unique decomposition of the mixture $\boldsymbol{g}$ into finite alphabet sources $\boldsymbol{f}$ and weights $\boldsymbol{\omega}$. For illustration, consider a binary alphabet $\mathfrak{A} = \{0, 1\}$ with two sources $\boldsymbol{m} = 2$ and a single mixture $M = 1$. The red line in Figure 1.5 shows an example of a possible mixture $\boldsymbol{g}$. The question is as following: Is it possible to uniquely recover the underlying weights $\boldsymbol{\omega}$ and sources $\boldsymbol{f}$ from the mixture $\boldsymbol{g} = \boldsymbol{f}\boldsymbol{\omega}$? Or may there exist $(\omega, f) \neq (\boldsymbol{\omega}, \boldsymbol{f})$ such that $\boldsymbol{g} = \boldsymbol{f}\boldsymbol{\omega} = f\omega$? In this example the answer is simple: The smallest possible function value for $\boldsymbol{g}$ is 0, which corresponds to both sources taking the smallest alphabet value $\boldsymbol{f}^1 = \boldsymbol{f}^2 = 0$. Analog, when $\boldsymbol{f}^1 = 0$ and $\boldsymbol{f}^2 = 1$, $\boldsymbol{g}$ takes the second smallest possible value, namely $\boldsymbol{\omega}_1$ (recall that $0 \leq \boldsymbol{\omega}_1 \leq \boldsymbol{\omega}_2$ and $\boldsymbol{\omega}_1 + \boldsymbol{\omega}_2 = 1$). Similar, the third smallest value for $\boldsymbol{g}$ equals $\boldsymbol{\omega}_2$ with $\boldsymbol{f}^1 = 0, \boldsymbol{f}^2 = 1$ and the largest value equals 1 with $\boldsymbol{f}^1 = \boldsymbol{f}^2 = 1$. Thus, one can (almost) always uniquely identify $\boldsymbol{\omega}$ and $\boldsymbol{f}$ from $\boldsymbol{g}$. There are just two situations where this goes wrong:

1. If $\boldsymbol{\omega}_1 = \boldsymbol{\omega}_2$, one cannot distinguish from $\boldsymbol{g}$ whether $\boldsymbol{f}^1 = 0, \boldsymbol{f}^2 = 1$ or $\boldsymbol{f}^1 = 1, \boldsymbol{f}^2 = 0$.
2. If $\boldsymbol{f}^1 = \boldsymbol{f}^2$, one cannot obtain $\boldsymbol{\omega}_1, \boldsymbol{\omega}_2$.

Consequently, in order to guarantee identifiability (in this simple example), we have to assume that these two situations do not occur. That is, we need to exclude from the parameter space the single weight vector $\boldsymbol{\omega} = (0.5, 0.5)$ (the only one with $\boldsymbol{\omega}_1 = \boldsymbol{\omega}_2$) and sources $\boldsymbol{f} = (\boldsymbol{f}^1, \boldsymbol{f}^2)$ with equal components $\boldsymbol{f}^1 = \boldsymbol{f}^2$ (or equivalently $\boldsymbol{\omega}_1, \boldsymbol{\omega}_2 \notin \operatorname{imag}(\boldsymbol{g})$). Clearly, this is not very restrictive, in most situations.

Now we turn to the general case, of arbitrary $\mathfrak{A}$, $\boldsymbol{m}$, and M. It turns out that identifiability has a complete combinatorial characterization via the given alphabet, see Section 2.1.1 (Theorem 2.1.3), and that the above assumptions can be extended to a universal (for any $\mathfrak{A}, \boldsymbol{m}, M$) simple sufficient condition, called separability, which guarantees identifiability even when the number of sources $\boldsymbol{m}$ is unknown (see Section 2.1.2, Theorem 2.1.5, Theorem 2.1.9).

First, we discuss conditions on $\boldsymbol{\omega}$. For fixed $\boldsymbol{\omega}$ the mixture $\boldsymbol{g}$ can take any of at most $k^{\boldsymbol{m}}$ (recall that the alphabet $\mathfrak{A}$ has size k) values of the form $e\boldsymbol{\omega} = \sum_{i=1}^{\boldsymbol{m}} e_i\boldsymbol{\omega}_i$ with $e = (e_1, \ldots, e_m) \in \mathfrak{A}^{\boldsymbol{m}}$ (elements in $\mathfrak{A}^{\boldsymbol{m}}$ are considered as row vectors). Clearly, if for any two $e \neq e' \in \mathfrak{A}^{\boldsymbol{m}}$ it holds that $e\boldsymbol{\omega} = e'\boldsymbol{\omega}$, then $\boldsymbol{f}$ is not identifiable as it cannot be distinguished from $\boldsymbol{g}$ whether $\boldsymbol{f} = e$ or $\boldsymbol{f} = e'$. For the situation where $e\boldsymbol{\omega}$ is corrupted by noise as in the SBSR (1.3) and MABS model (1.6), it is important to understand stability when any two of these values are very close, that is, $\|e\boldsymbol{\omega} - e'\boldsymbol{\omega}\| < \delta$ for small $\delta > 0$. We denote the minimal distance between any two of these values, which depends on $\boldsymbol{\omega}$, as *alphabet separation boundary (ASB)*,

$$ASB(\boldsymbol{\omega}) = ASB(\boldsymbol{\omega}, \mathfrak{A}) := \min_{e \neq e' \in \mathfrak{A}^{\boldsymbol{m}}} \left\| e\boldsymbol{\omega} - e'\boldsymbol{\omega} \right\|. \tag{1.8}$$

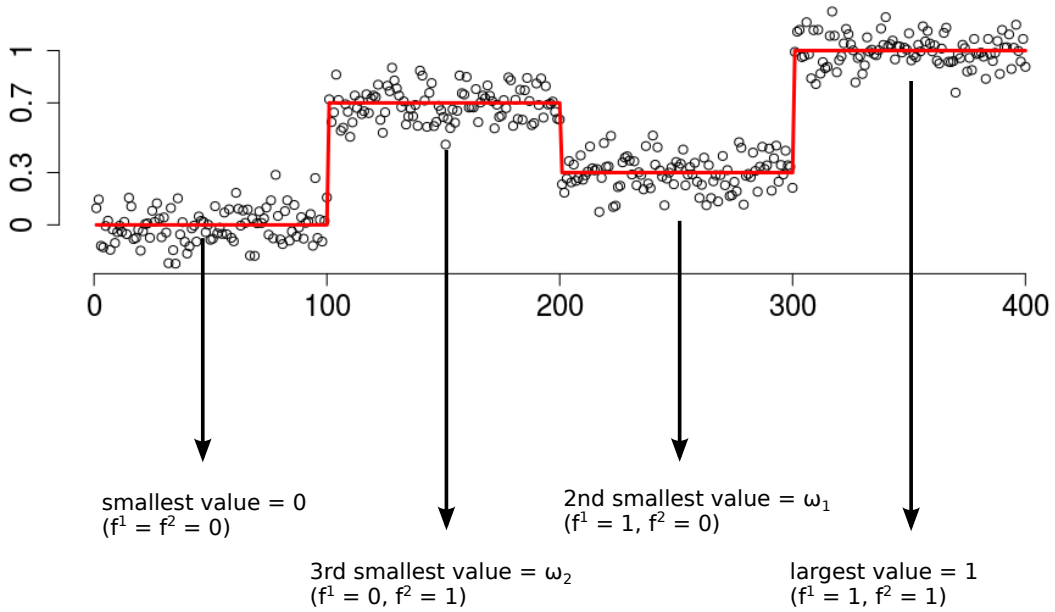

Figure 1.5: Example of a mixture $\boldsymbol{g}$ (red line) from the SBSR model (1.3) with $\mathfrak{A} = \{0, 1\}$, $\boldsymbol{m} = 2$, $M = 1$. The ordering structure of the possible different function values of $\boldsymbol{g}$ is illustrated.

Note that for $\mathfrak{A} = \{0, 1\}$, $\boldsymbol{m} = 2$, $M = 1$ as in Figure 1.5 the condition $ASB(\boldsymbol{\omega}) > 0$ is equivalent to $\boldsymbol{\omega}_1 \neq \boldsymbol{\omega}_2$. Further, note that in the c.p. setting of the SBSR model (1.3) $ASB(\boldsymbol{\omega}) > 0$ implies that any jump in the source vector $\boldsymbol{f}$ (i.e., at least one source $\boldsymbol{f}^i$ jumps) occurs as well in the mixture $\boldsymbol{g} = \boldsymbol{f}\boldsymbol{\omega}$ and that $ASB(\boldsymbol{\omega})$ coincides with the minimal possible jump height of $\boldsymbol{g}$. Clearly, as $\boldsymbol{m} \nearrow \infty$ the ASB converges to 0, as it describes the minimal distance between $k^{\boldsymbol{m}}$ values in the bounded set $[0, a_k]^M$ (see Theorem 2.3.10). For instance, in SBSR with $M = 1$ this gives $ASB(\omega) \leq a_k/(k^{\boldsymbol{m}} - 1)$, which corresponds to the minimal jump height and, hence, scales with the standard deviation σ. Thus, no method can detect $\boldsymbol{m}$ signals when $\sigma \notin O(k^{-\boldsymbol{m}})$. This shows that for practical applications of FABS the number of sources should be small (relative to the noise variance with $\boldsymbol{m} \lesssim \ln(1/\sigma)$).

Second, we discuss conditions on $\boldsymbol{f}$. In order to identify $\boldsymbol{\omega}$ from $\boldsymbol{g}$ it is necessary that the sources differ sufficiently much. For instance, if $\boldsymbol{f}^1 = \ldots = \boldsymbol{f}^{\boldsymbol{m}}$ then $\boldsymbol{g} = \boldsymbol{f}^1$ irrespective of $\boldsymbol{\omega}$. The *separability*[1] condition (see Section 2.1.2) provides a sufficient variability of $\boldsymbol{f}$ which guarantees identifiability, in particular even when the number of sources $\boldsymbol{m}$ is unknown. Separability guarantees that for each $i = 1, \ldots, \boldsymbol{m}$ there exists some $j = 1, \ldots, n$ where $\boldsymbol{f}^i$ takes the second smallest alphabet value and all other sources take the smallest alphabet value. Note that, as the alphabet is of the form (1.7), this is equivalent to

$$\boldsymbol{\omega}_1, \ldots, \boldsymbol{\omega}_{\boldsymbol{m}} \in \{\boldsymbol{g}_1, \ldots, \boldsymbol{g}_n\} \quad \Leftrightarrow \quad e^1, \ldots, e^{\boldsymbol{m}} \in \{\boldsymbol{f}_{1\cdot}, \ldots, \boldsymbol{f}_{n\cdot}\}, \tag{1.9}$$

[1]The notation *separable* is borrowed from identifiability conditions for nonnegative matrix factorization (Donoho and Stodden, 2004; Arora et al., 2012; Bittorf et al., 2012).

where e^i denotes the i-th unit vector. Note that this is analog to $\boldsymbol{f}^1 \neq \boldsymbol{f}^2$ for $\mathfrak{A} = \{0, 1\}, \boldsymbol{m} = 2, M = 1$ as in Figure 1.5. In Figure 1.4 a separable region is marked blue.

In summary, a pair $(\boldsymbol{\omega}, \boldsymbol{f})$ in FABS is denoted as *δ-separable* if $AS\,B(\boldsymbol{\omega}) \geq \delta$ and (1.9) holds for the sources $\boldsymbol{f}$. In Section 2.2 we quantify how difficult it is to recover the sources $\boldsymbol{f}$ in dependence on δ. It turns out that δ-separability regularizes FABS via the parameter δ and yields exact recovery for the sources $\boldsymbol{f}$ (as well as for the number of sources $\boldsymbol{m}$) in a neighborhood of the mixture $\boldsymbol{g}$, that is for $(\boldsymbol{\omega}, \boldsymbol{f}), (\omega, f)$ both δ-separable

$$\max_{j=1,\dots,n} \left\|(\boldsymbol{f}\boldsymbol{\omega})_{j\cdot} - (f\omega)_{j\cdot}\right\| < c(\delta) \quad \Rightarrow \quad \boldsymbol{f} = f \text{ and } \max_{i=1,\dots,\boldsymbol{m}} \|\boldsymbol{\omega}_i - \omega_i\| < c(\delta), \tag{1.10}$$

where $c(\delta) \to 0$ as $\delta \to 0$, see Theorem 2.2.3 and 2.2.5.

Imposing δ-separability in FABS naturally leads to the question how restrictive this condition is, which is the topic of Section 2.3. Clearly, this depends on the specific weights $\boldsymbol{\omega}$ and sources $\boldsymbol{f}$. It turns out that in many practical situations it is not very restrictive. For instance, when $\boldsymbol{f}$ is modeled as a Markov process, it is separable with probability converging exponentially fast to one, see Theorem 2.3.1, and when $\boldsymbol{\omega}$ is drawn uniformly, then $AS\,B(\boldsymbol{\omega}) \geq \delta$ with probability $1 - O(\delta)$, where the constant depends on the specific alphabet, see Theorem 2.3.4. Moreover, this remains true even when $\boldsymbol{m}$ is unknown, see Theorem 2.3.12.

1.3.2 FABS for change-point regression

In the following, the main results of Chapter 3 on the SBSR model (1.3) are presented. In a first step, it is assumed that the number of sources $\boldsymbol{m}$ in (1.1) is known and $\boldsymbol{\omega}$ and $\boldsymbol{f}$ are inferred conditioned on the correct model dimension $\boldsymbol{m}$. In a second step, a model selector for $\boldsymbol{m}$ is proposed (see Section 3.6). In order to guarantee identifiability, we employ δ-separability. To regularize the separability condition on $\boldsymbol{f}$ in (1.9) we further introduce a minimal scale λ (minimal interval length between successive jumps). Thus, for given $\delta, \lambda > 0$, given standard deviation σ, a given finite alphabet $\mathfrak{A}$ as in (1.7), and given number of sources $\boldsymbol{m} \in \mathbb{N}$ we consider the SBSR model (1.3) with

$$\boldsymbol{g} \in \mathcal{M}_{\boldsymbol{m}}^{\delta,\lambda} := \left\{f\omega : \ f \in \mathcal{S}(\mathfrak{A})_\lambda^{\boldsymbol{m}}, \ \omega \in \Omega_{\boldsymbol{m}} \text{ with } AS\,B(\omega) \geq \delta\right\}, \tag{1.11}$$

and

$$\begin{aligned}\mathcal{S}(\mathfrak{A})_\lambda^{\boldsymbol{m}} :=& \Bigg\{ \sum_{j=0}^{K} \theta_j \mathbb{1}_{[\tau_j,\tau_{j+1})} : \theta_j \in \mathfrak{A}^{\boldsymbol{m}}, \tau_{i+1} - \tau_i \geq \lambda, \\ & \tau_0 = 0, \tau_{K+1} = 1, e^1, \dots, e^{\boldsymbol{m}} \in \{\theta_0, \dots, \theta_K\}, K \in \mathbb{N}\Bigg\}.\end{aligned} \tag{1.12}$$

Note that the condition $e^1, \dots, e^{\boldsymbol{m}} \in \{\theta_0, \dots, \theta_K\}$ in (1.12) coincides with separability in (1.9).

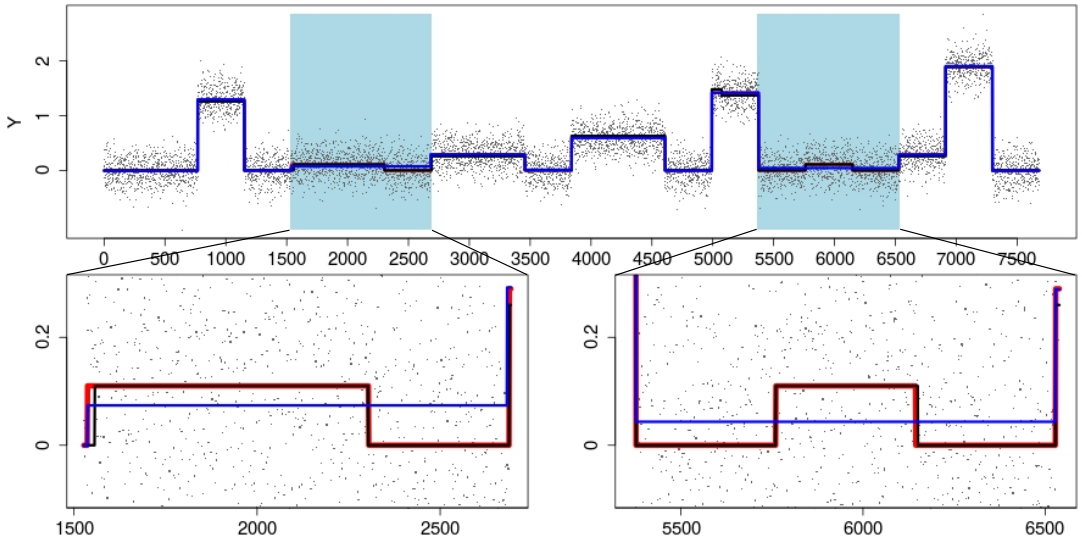

Figure 1.6: Observations Y from Example 1.2.1 (gray dots), together with true underlying mixture $\boldsymbol{g}$ (red line). The blue line shows the c.p. estimate from Frick et al. (2014), which does not incorporate the mixture structure. The red line shows the estimate with the proposed method (see Figure 1.9 for the estimate of $\boldsymbol{f}$). The blue areas display a region where $\boldsymbol{g}$ has a small jump (red line), which is not detected by the c.p. estimator (Frick et al., 2014) (blue line), but by the proposed method (black line). The bottom plots show a zoom in of the blue regions.

First attempts

In order to motivate the (quite involved) methodology to recover all quantities in (1.1) simultaneously, some attempts which may come to mind at first glance are briefly discussed. As a first approach to estimate $\boldsymbol{\omega}$ and $\boldsymbol{f}$ from the data Y in the SBSR model (1.3), one might pre-estimate the mixture $\boldsymbol{g}$ with some standard c.p. procedure, ignoring its underlying mixture structure, and then try to reconstruct $\boldsymbol{\omega}$ and $\boldsymbol{f}$ afterwards. One problem is that the resulting step function cannot be decomposed into weights $\boldsymbol{\omega} \in \Omega_m$ and sources $\boldsymbol{f} \in \mathcal{S}^m(\mathfrak{A})$, in general, as the given alphabet $\mathfrak{A}$ leads to restrictions on the function values of $\boldsymbol{g}$. But already for the initial step of reconstructing the mixture $\boldsymbol{g}$ itself, a standard c.p. estimation procedure (which ignores the mixture structure) is unfavorable as it discards important information on the possible function values of $\boldsymbol{g}$ (induced by $\mathfrak{A}$). For example, if $\boldsymbol{g}$ has a small jump in some region, this might be easily missed (see Figure 1.6 for an example). Consequently, subsequent estimation of $\boldsymbol{f}$ and $\boldsymbol{\omega}$ will fail as well. In contrast, a procedure which takes the mixture structure explicitly into account right from its beginning is expected to have better detection power for a jump. As a conclusion, considering SBSR as a standard c.p. problem discards important information and does not allow for demixing, in general.

A second approach, which comes to mind, is to first use some clustering algorithm to pre-estimate the function values of $\boldsymbol{g}$, ignoring its serial c.p. structure, and infer the mixing weights $\boldsymbol{\omega}$ from this. This pre-clustering approach has been pursued in several papers (Diamantaras, 2006; Li et al., 2003; Gu et al., 2010) for the particular case of a binary alphabet, i.e., $k = 2$. However, as the number of possible function values of $\boldsymbol{g}$ equals k^m (recall that k is the size

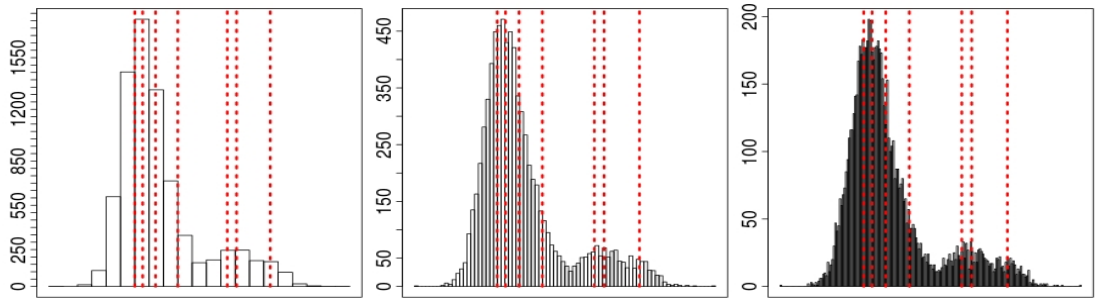

Figure 1.7: Histogram of the data from Example 1.2.1 with 20, 100, and 200 equidistant bins, respectively (from left to right). The vertical red lines indicate the true function values (modes) of $\boldsymbol{g}$ which have to be identified.

of the alphabet), recovery of these values in a statistical context by clustering is a difficult task in general, as it amounts to estimate the location of (at most) k^m modes correctly from the marginal distributions of the observations Y_j. In fact, this corresponds to mode hunting with potentially large number of modes which is known to be a hard problem, see e.g., (Cheng and Hall, 1999; Tibshirani et al., 2001; Dümbgen and Walther, 2008). We illustrate the difficulty of this in Figure 1.7 employing histograms of the Y_j's in Example 1.2.1 with different bin widths. From this, it becomes obvious that a pre-clustering approach is not feasible for the present data. Summing up, ignoring either of both, the c.p. and the finite alphabet mixture structure, in a first pre-estimation step discards important information, which is indispensable for statistically efficient recovery. It should be emphasized that we are not aware of any existing method taking both aspects into account, in contrast to the method presented in this thesis, called *SLAM (Separates Linear Alphabet Mixtures)*, which is briefly described now.

In a first step, a confidence region $C_{1-\alpha}$ and an estimator for $\boldsymbol{\omega}$ is constructed. This can be characterized by the acceptance region of a specific multiscale test with test statistic $T_n(Y, \boldsymbol{g})$, which is particularly well suited to capture both, c.p. and mixture structure, of $\boldsymbol{g}$. The confidence level is determined by a threshold $q_n(\alpha)$ such that for any $\boldsymbol{g} = \sum_{i=1}^{m} \omega_i \boldsymbol{f}^i \in \mathcal{M}_m^{\delta,\lambda}$ in (3.17)

$$\{\boldsymbol{\omega} \in C_{1-\alpha}(Y)\} \supseteq \{T_n(Y, \boldsymbol{g}) \leq q_n(\alpha)\}. \tag{1.13}$$

In a second step, we estimate $\boldsymbol{f}$ based on a multiscale constraint again. In the following this procedure is introduced in more detail. The multiscale approach underlying SLAM is crucial as jumps of $\boldsymbol{f}$ potentially can occur at any location and scale (interval length).

Multiscale statistic and confidence boxes underlying SLAM

Recall that a reasonable estimator must explore both, the c.p. and the finite alphabet structure. Roughly speaking, c.p. structure means that observations which are close to each other (on the time scale) are more likely to share the same distribution than observations which are far apart. To explore this structure, one has to allocate local information (on single intervals). As the jump locations may occur at any place, it becomes necessary to do this in a multiscale

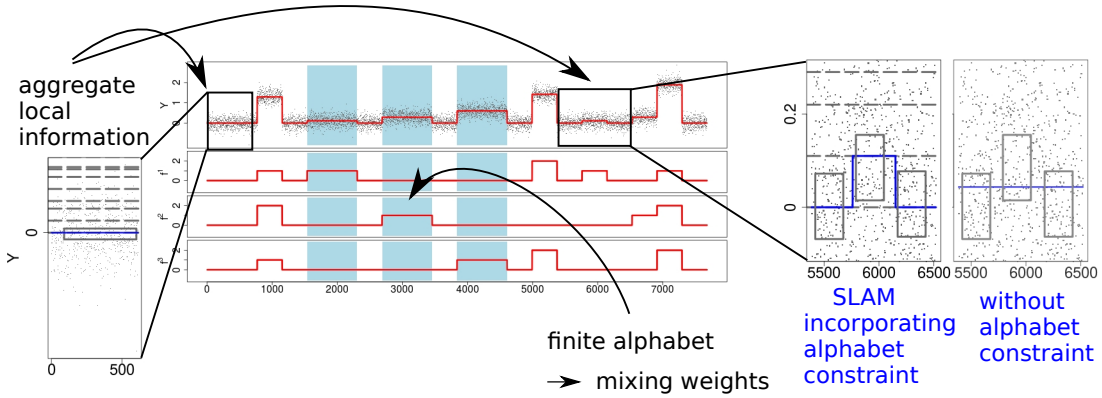

Figure 1.8: Illustration of SLAM.

fashion, that is, allocating local information on all different intervals (scales) simultaneously, see e.g., (Siegmund and Yakir, 2000; Dümbgen and Spokoiny, 2001; Davies and Kovac, 2001; Dümbgen and Walther, 2008; Frick et al., 2014). This is illustrated in Figure 1.8.

Let $\boldsymbol{g}|_{[x_i,x_j]} \equiv g_{ij}$ denote that $\boldsymbol{g}$ is constant on some interval $[x_i, x_j]$ with function value g_{ij}. In order to allocate local information on a single interval $[x_i, x_j] \subset [0, 1)$, we consider for some given (test) value $g_{ij} \in \mathbb{R}$ the local hypothesis testing problem

$$H_0 : \boldsymbol{g}|_{[x_i,x_j]} \equiv g_{ij} \quad \text{vs.} \quad H_1 : \boldsymbol{g}|_{[x_i,x_j]} \not\equiv g_{ij}. \tag{1.14}$$

A natural test-statistic for this testing problem is the log-likelihood ratio test statistic

$$T_i^j(Y_i, \ldots, Y_j, g_{ij}) = \frac{(\sum_{l=i}^j Y_l - g_{ij})^2}{2\sigma^2(j - i + 1)}. \tag{1.15}$$

We then combine the local testing problems in (1.14) and define in our context the multiscale statistic T_n for some candidate function g (which may depend on Y) as

$$T_n(Y, g) := \max_{\substack{1\le i\le j\le n \\ g|_{[x_i,x_j]}\equiv g_{ij}}} \frac{|\sum_{l=i}^j Y_l - g_{ij}|}{\sigma\sqrt{j - i + 1}} - pen(j - i + 1), \tag{1.16}$$

with *pen*alty terms $pen(j - i + 1) := \sqrt{2\,(\ln(n/(j - i + 1)) + 1)}$. The maximum in (1.16) is understood to be taken only over those intervals $[x_i, x_j]$ on which g is constant with value $g_{ij} = g(x_i)$. The calibration term $pen(\cdot)$ serves as a balancing of different scales in a way that the maximum in (1.16) is equally likely attained on all scales, see (Dümbgen and Spokoiny, 2001; Frick et al., 2014). Other scale penalizations can be employed as well, see e.g. (Walther, 2010), but, for the ease of brevity, will not be discussed here. Note that, as the multiscale statistic in (1.16) is defined as the maximum of the local test statistics in (1.15) (up to the penalization term), a test function g is *accepted* (that is, $T_n(Y, g) \le q$ for some threshold q depending on the significance level) if and only if all local tests *accept* on intervals where g is constant. The function values of g determine the local testing problems (the value g_{ij} in

(1.14)) on the single scales $[x_i, x_j]$. The penalization term adjusts the thresholds (levels) of the different local tests.

Recall that a test can always be inverted into a confidence statement and vice versa. Thus, the local tests of the multiscale test in (1.16) can be inverted into local confidence statements. More precisely, with the notation $\bar{Y}_i^j := \sum_{l=i}^j Y_l/(j-i+1)$, the statistic $T_n(Y, g)$ in (1.16) has the following geometric interpretation:

$$T_n(Y, g) \le q \;\Leftrightarrow g_{ij} \in B(i, j)\ \forall 1 \le i \le j \le n \text{ with } g|_{[x_i, x_j]} \equiv g_{ij}, \tag{1.17}$$

for $q \in \mathbb{R}$, with intervals

$$B(i, j) := \left[\overline{Y}_i^j - \frac{q + pen(j-i+1)}{\sqrt{j-i+1}/\sigma}, \overline{Y}_i^j + \frac{q + pen(j-i+1)}{\sqrt{j-i+1}/\sigma}\right]. \tag{1.18}$$

The boxes $B(i, j)$ correspond to local confidence intervals for the underlying signal $g|_{[x_i, x_j]}$ on the intervals $[x_i, x_j]$. This is illustrated in Figure 1.8, where the gray boxes in the zoom-in correspond to confidence intervals $B(i, j)$ on the interval $[x_i, x_j]$. For g to be accepted (that is $T_n(Y, g) \le q$) it must be covered by $[x_i, x_j] \times B(i, j)$ whenever it is constant on $[x_i, x_j]$.

In the following we will make use of the fact that the distribution of $T_n(Y, \boldsymbol{g})$, with $\boldsymbol{g}$ the true signal from the SBSR model (1.3), can be bounded from above with that of $T_n := T_n(\epsilon, 0)$, with ϵ as in (1.3). It is known that $T_n \overset{\mathcal{D}}{\Rightarrow} L(\mathbb{B}) < \infty$ a.s. as $n \to \infty$, a certain functional of the Brownian motion $\mathbb{B}$, see (Dümbgen and Spokoiny, 2001; Dümbgen et al., 2006). Note that the distribution of $T_n(\epsilon, 0)$ does not depend on the (unknown) $\boldsymbol{f}$ and $\boldsymbol{\omega}$ anymore. As this distribution is not explicitly accessible and to be more accurate for small n ($\le$ 5000 say) the finite sample distribution of T_n can be easily obtained by Monte Carlo simulations. From this one obtains $q_n(\alpha)$, $\alpha \in (0, 1)$, the $(1-\alpha)$-quantile of T_n. We then obtain

$$\inf_{\boldsymbol{g} \in \mathcal{M}_{\boldsymbol{m}}} \mathbf{P}\left(T_n(Y, \boldsymbol{g}) \le q_n(\alpha)\right) \ge 1 - \alpha. \tag{1.19}$$

Hence, for the intervals in (1.18) with $q = q_n(\alpha)$ it follows that for all $\boldsymbol{g} \in \mathcal{M}_{\boldsymbol{m}}$

$$\mathbf{P}\left(g_{ij} \in B(i, j)\ \forall 1 \le i \le j \le n \text{ with } \boldsymbol{g}|_{[x_i, x_j]} \equiv g_{ij}\right) \ge 1 - \alpha. \tag{1.20}$$

We use the notation $B(i, j)$ for both, the intervals in (1.18) and the boxes $[i, j] \times B(i, j)$.

Inference about the weights

We will now use the system of boxes $\mathfrak{B} := \{B(i, j) : 1 \le i \le j \le n\}$ from (1.18) with $q = q_n(\alpha)$ as in (1.19) to construct a confidence region $C_{1-\alpha}$ for $\boldsymbol{\omega}$ such that (1.13) holds, which ensures

$$\inf_{\boldsymbol{g} \in \mathcal{M}_{\boldsymbol{m}}^{\delta, \lambda}} \mathbf{P}\left(\boldsymbol{\omega} \in C_{1-\alpha}\right) \ge 1 - \alpha. \tag{1.21}$$

To this end, separability in (1.9) is crucial. It ensures that the weights $\boldsymbol{\omega}_i$ are present somewhere in the signal $\boldsymbol{g}$ (see Figure 1.8). Thus, the boxes $\mathfrak{B}$ capture (local) information about $\boldsymbol{\omega}_i$. More precisely, we will show that any $B^\star \in \mathfrak{B}^m$ (denoted as the space of $\boldsymbol{m}$-boxes) which corresponds to a separable region directly provides a confidence set $C^\star_{1-\alpha} = B^\star$ for $\boldsymbol{\omega}$. However, as the underlying signal $\boldsymbol{f}$ is unknown and hence, it is unknown where exactly the signal is separable, $B^\star$ cannot be determined directly. Therefore, we will construct a covering $\mathfrak{B}^\star \subset \mathfrak{B}^m$ with $B^\star \in \mathfrak{B}^\star$ (conditioned on $T_n(Y, \boldsymbol{g})$) such that the resulting confidence set

$$C_{1-\alpha} := \bigcup_{B \in \mathfrak{B}^\star} B \tag{1.22}$$

has minimal volume (up to a log-factor) (see Section 3.4). The construction of $\mathfrak{B}^\star$ is done by applying certain reduction rules on the set $\mathfrak{B}^{\boldsymbol{m}}$ reducing it to a smaller set $\mathfrak{B}^\star \subset \mathfrak{B}^{\boldsymbol{m}}$ with $B^\star \in \mathfrak{B}^\star$. This is summarized in the CRW (Confidence Region for the Weights) algorithm in Figure 3.1, which constitutes the first part of SLAM. In Example 1.2.1 for $\alpha = 0.1$ this gives $C_{0.9} = [0.00, 0.33] \times [0.07, 0.41] \times [0.39, 0.71]$ as a confidence box for $\boldsymbol{\omega} = (\boldsymbol{\omega}_1, \boldsymbol{\omega}_2, \boldsymbol{\omega}_3)^\top$ which covers the true value $\boldsymbol{\omega} = (0.11, 0.29, 0.60)^\top$ in this case. SLAM now estimates $\boldsymbol{\omega}$ by

$$\hat{\omega} := \operatorname*{argmax}_{\omega \in C_{1-\alpha}} AS\,B(\omega). \tag{1.23}$$

(1.23) can be computed with linear programming (see Theorem 5.1.1). Alternatively, for a finite sample size n, as the boxes $B(i, j)$ from (1.18) are constructed in a symmetric way, for $C_{1-\alpha} =: [\underline{\omega}_1, \overline{\omega}_1] \times \ldots \times [\underline{\omega}_{\boldsymbol{m}}, \overline{\omega}_{\boldsymbol{m}}]$ one may as well simply estimate $\boldsymbol{\omega}$ by

$$\hat{\omega} := \frac{1}{\sum_{i=1}^{\boldsymbol{m}} (\underline{\omega}_i + \overline{\omega}_i)} (\underline{\omega}_1 + \overline{\omega}_1, \ldots, \underline{\omega}_{\boldsymbol{m}} + \overline{\omega}_{\boldsymbol{m}}). \tag{1.24}$$

In Example 1.2.1 (1.24) gives for $\alpha = 0.1$ $\hat{\omega} = (0.17, 0.25, 0.58)^\top$.

On the one hand, when being interested in confidence statements, the threshold q in (1.17) and (1.18), respectively, is chosen as the $(1 - \alpha)$-quantile of the statistic T_n as in (1.19). On the other hand, when being interested in estimation, q and α, respectively, can be seen as tuning parameters. It turns out that specific (optimal) choices will lead to (almost) optimal estimation rates. Thus, for all following considerations, define α_n and β_n via

$$\alpha_n := \exp(-c_1 \ln^2(n)), \quad q_n(\beta_n) := c_3\, q_n(\alpha_n) + c_4, \tag{1.25}$$

with $q_n(\alpha_n), q_n(\beta_n)$ the $(1 - \alpha_n)$- and $(1 - \beta_n)$-quantiles of T_n as in (1.19), for some constants $c_1 = c_1(\delta), c_3, c_4 = c_4(\lambda)$, to be specified later in (3.13). Both, $q_n(\alpha_n)$ and $q_n(\beta_n)$, grow with rate $O(\delta \ln(n)/\sigma)$ (see proof of Theorem 3.4.2). Then, in addition to uniform coverage in (1.21), for $\alpha = \alpha_n$ in (1.25) we show in Corollary 3.4.3 that the confidence region $C_{1-\alpha_n}$ from (1.22) covers the unknown weight vector $\boldsymbol{\omega}$ with maximal distance shrinking of order $\ln(n)/\sqrt{n}$ with

probability tending to one at a superpolynomial rate, that is

$$\mathbf{P}\left(\overline{\operatorname{dist}}(\boldsymbol{\omega}, C_{1-\alpha_n}(Y)) < c_2 \frac{\ln(n)}{\sqrt{n}}\right) \geq 1 - \exp(-c_1 \ln^2(n))$$

for all $n \geq N^\star$, for some constants $c_1 = c_1(\delta), c_2 = c_2(\delta, \lambda)$ (see (3.13)) and some explicit $N^\star = N^\star(\lambda, \delta) \in \mathbb{N}$ (see (3.14) and (3.15)), where for $D \subset \mathbb{R}^{\boldsymbol{m}}$ and $d \in \mathbb{R}^{\boldsymbol{m}}$

$$\overline{\operatorname{dist}}(d, D) := \sup_{\tilde{d} \in D} \left\| d - \tilde{d} \right\|_\infty . \tag{1.26}$$

Inference about the source functions

Once the mixing weights $\boldsymbol{\omega}$ have been estimated by $\hat{\omega}$, SLAM estimates $\boldsymbol{f}$ in two steps. First, the number of c.p.'s $K(\boldsymbol{g})$ of $\boldsymbol{g} = \boldsymbol{f}\boldsymbol{\omega} \in \mathcal{M}_{\boldsymbol{m}}^{\delta,\lambda}$ is estimated by solving the constrained optimization problem

$$\hat{K} := \min_{g \in \mathcal{M}_{\boldsymbol{m}}(\mathfrak{A}, \hat{\omega})} K(g) \quad \text{s.t.} \quad T_n(Y, g) \leq q_n(\beta). \tag{1.27}$$

This means that SLAM chooses $\hat{f}$ as parsimonious as possible (with as few jumps as possible), while still fulfilling the multiscale constraint $T_n(Y, \hat{f}\hat{\omega}) \leq q_n(\beta)$. This multiscale constraint, on the r.h.s. of (1.27), is the same as for $C_{1-\alpha}(Y)$ in (1.22), but with a possibly different confidence level $1 - \beta$. Finally, we estimate $\boldsymbol{f}^1, \ldots, \boldsymbol{f}^{\boldsymbol{m}}$ as the constrained maximum likelihood estimator

$$\hat{f} = (\hat{f}^1, \ldots, \hat{f}^m)^\top := \operatorname*{argmax}_{f \in \mathcal{H}(\beta)} \sum_{i=1}^{n} \ln\left(\phi_{f\hat{\omega}(x_i)}(Y_i)\right), \tag{1.28}$$

where ϕ_μ denotes the density of the normal distribution with mean μ and variance σ^2 and

$$\mathcal{H}(\beta) := \left\{ f \in \mathcal{S}(\mathfrak{A})^{\boldsymbol{m}} : T_n\left(Y, f\hat{\omega}\right) \leq q_n(\beta) \text{ and } K\left(f\hat{\omega}\right) = \hat{K} \right\}. \tag{1.29}$$

Note that this procedure even increases the detection power for $\boldsymbol{g}$ itself as it explicitly takes into account the finite alphabet for the estimation of the c.p.'s. This is illustrated in Figure 1.8. The zoom-in on the right shows a region where the true underlying signal has a small jump. However, without the finite alphabet constraint, one can find a constant signal (the blue line in the right version of the zoom-in) which is covered by all confidence boxes (for sake of clarity only three of them are plotted). SLAM, however, explicitly takes into account the finite alphabet, which implies that (after having estimated $\boldsymbol{\omega}$) only finitely many function values for $\boldsymbol{g}$ are possible. As there is no constant signal, which only takes one of these values and is covered by the confidence boxes $B(i, j)$, SLAM detects this jump.

Again, choosing the confidence levels α and β in an optimal way, with $\alpha = \alpha_n$ and $\beta = \beta_n$ as in (1.25), in Section 3.4 (see Theorem 3.4.2) we show that with probability at least $1 - \alpha_n$, for n large enough, the SLAM estimator $\hat{f}$ in (1.28) estimates for all $i = 1, \ldots, \boldsymbol{m}$

1. the respective number of c.p.'s $K(\boldsymbol{f}^i)$ correctly,

2. all c.p. locations with rate $\ln^2(n)/n$ simultaneously, and

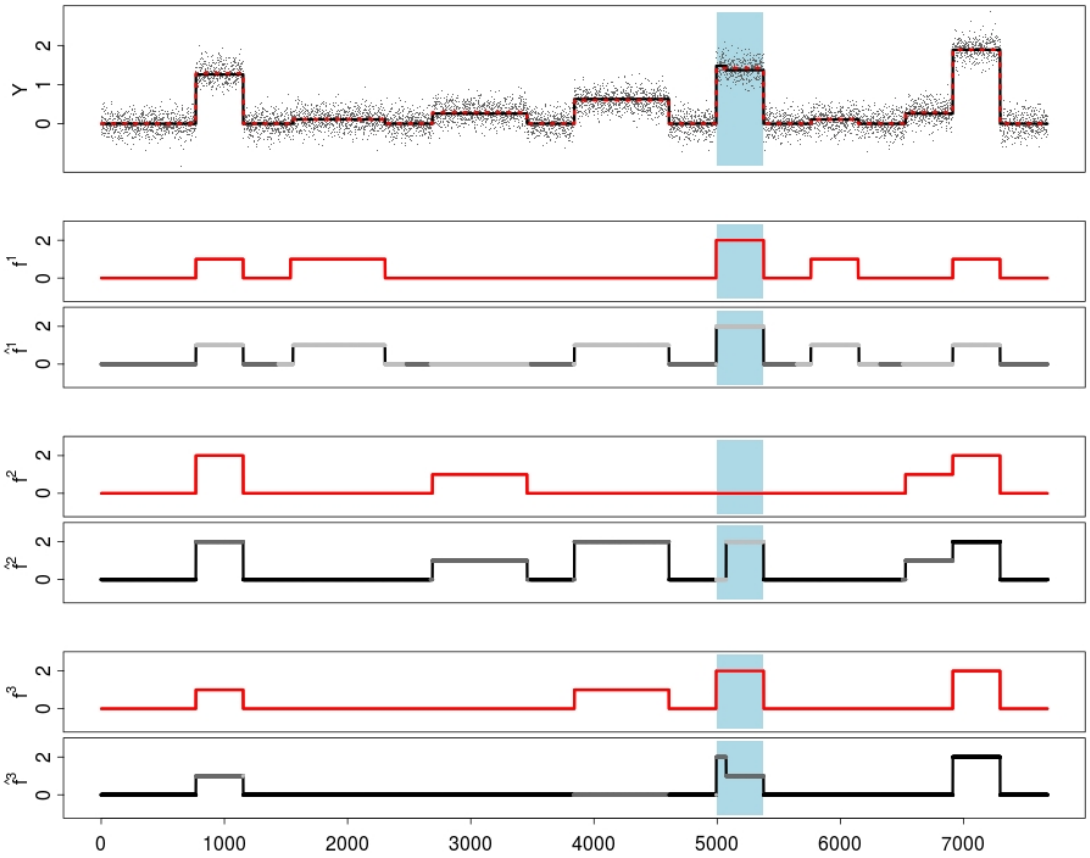

Figure 1.9: First row: $\boldsymbol{g}$ (red dotted line), $\hat{g}$ (black line) with $\hat{\omega} = (0.11, 0.26, 0.63)^\top$, and data Y (gray) from Example 1.2.1. Subsequent rows: $\boldsymbol{f}^i$ (red line) and SLAM's estimate $\hat{f}^i$ (gray/black line) for $q_n(\alpha) = 0.2$ and $q_n(\beta) = 2.1$. Gray shades of $\hat{f}^i$ indicate the confidence for the given segment (recall $\mathfrak{A} = \{0, 1, 2\}$): a maximal deviation of two (light gray), one (gray), and no deviation (black) at confidence level $\beta = 0.01$. The blue area displays a constant region of $\boldsymbol{g}$ where $\hat{g}$ includes a (wrong) jump and its effect on estimation of the sources.

3. the function values of $\boldsymbol{f}^i$ exactly (up to the uncertainty in the c.p. locations).

Obviously, the rate in 2. is optimal up to possible log-factors as the sampling rate is $1/n$. From Theorem 3.4.2 it follows further (see Remark 3.4.4) that the minimax detection rates are even achieved (again up to possible log-factors) when $\delta, \lambda \to 0$ (as $n \to \infty$). Further, in Theorem 3.3.1 we show that a slight modification $\tilde{\mathcal{H}}(\beta)$ of $\mathcal{H}(\beta)$ in (1.29) constitutes an asymptotically uniform (for given ASB δ and minimal scale λ) multivariate confidence band for $\boldsymbol{f}$.

To illustrate, Figure 1.9 depicts SLAM's estimates of the mixture $\hat{g} = \hat{f}\hat{\omega}$, with $\hat{\omega} = (0.11, 0.26, 0.63)^\top$, and the source functions $\hat{f}^1$, $\hat{f}^2$, $\hat{f}^3$ from (1.28) with Y as in Example 1.2.1, $\beta = 0.01$ (corresponding to $q_n(\beta) = 2.1$), and an automatic choice of α, the Minial Valid Threshold (MVT)-selection method explained in Section 3.5. In order to visualize $\tilde{\mathcal{H}}(\beta)$, we illustrate the provided confidence in gray scale encoding the projections of $\tilde{\mathcal{H}}(\beta)$.

SLAM is also applicable in the non-blind case, where the mixing weights $\boldsymbol{\omega}$ are known. Then, the sources $\boldsymbol{f}$ may directly be estimated as in (1.27) and (1.28) with $\hat{\omega}$ replaced by $\boldsymbol{\omega}$. This yields the same (almost) optimal estimation rates for the sources $\boldsymbol{f}$, see Remark 3.4.5. Note

that the non-blind setting is equivalent to estimation of step-functions for a known (finite) set of possible function values. This is an interesting task on its own, which has received only few attention in the literature so far and is covered by this thesis as well.
The performance of SLAM is investigated in a simulation study in Section 6.1. We first investigate accuracy of $\hat{\omega}$ and the confidence region $C_{1-\alpha}(Y)$ as in (1.24) and (1.22). We found always higher coverage of $C_{1-\alpha}(Y)$ than the nominal confidence level $1-\alpha$. In line with this, $\hat{\omega}$ appeared to be very stable under the choice of α. Second, we investigate SLAM's estimate $\hat{f}$. A major conclusion is that if $\boldsymbol{g}$ is not well estimated in a certain region, this typically will influence the quality of the estimates of $\boldsymbol{f}^i$ in this region but not beyond (see the marked light-blue region in Figure 1.9 where the estimator $\hat{g}$ includes a wrong jump in a constant region of $\boldsymbol{g}$ but this error does not propagate serially). This may be explained by the flexible c.p. model $\mathcal{M}_{\boldsymbol{m}}$ together with the multiscale nature of SLAM, which locally "repairs" estimation errors.

Model selection

When the number of source components $\boldsymbol{m}$ is known the multiscale method SLAM, as introduced above, is able to recover $\boldsymbol{\omega}$ and $\boldsymbol{f}$ at optimal (up to log-factors) rate of convergence. However, in many practical situations $\boldsymbol{m}$ is unknown or only approximately known. In the following, we introduce a selection procedure for $\boldsymbol{m}$.

Example 1.3.1. Figure 1.10 shows realizations of the SBSR model for a binary alphabet $\mathfrak{A} = \{0,1\}$, $n = 1,421$, and standard deviation $\sigma = 0.06$. The left part of Figure 1.10 shows an example with $\boldsymbol{m} = 3$ source functions $\boldsymbol{f}^1, \boldsymbol{f}^2, \boldsymbol{f}^3$ and mixing weights $\boldsymbol{\omega} = (0.08, 0.12, 0.8)^\top$ and the right part with $\boldsymbol{m} = 2$ and $\boldsymbol{\omega} = (0.15, 0.85)^\top$. The aim is to reconstruct from the observations Y (displayed as gray dots in top row) the unknown number of sources $\boldsymbol{m}$ and based on this the unknown source functions $\boldsymbol{f}^i$ (displayed as red solid lines in row 2) and their corresponding mixing weights $\boldsymbol{\omega}$. Note that the true underlying regression functions (red lines in top row), with $\boldsymbol{m} = 3$ (left) and $\boldsymbol{m} = 2$ (right), respectively, are very similar in this example.

The proposed selector $\hat{m}$ is based on the same multiscale statistic T_n (1.16) as in SLAM. For given $\boldsymbol{m} = m$ SLAM yields conditional confidence sets $C^m_{1-\alpha}$ for $\boldsymbol{\omega}$. Increasing m, increases the number of model parameters and yields a better data fit. Thus, for a fixed confidence level α we propose to select the smallest m such that the corresponding confidence set $C^m_{1-\alpha}$ from SLAM is non-empty, that is, the multiscale constraint can be fulfilled with just m sources.
This procedure automatically yields lower confidence bounds for $\boldsymbol{m}$ (see Theorem 3.6.4), i.e., statistical error guarantees for the minimal "model dimension", a task which is in general difficult to obtain. For instance, in the example of the right part of Figure 1.10, even if the significance level α is chosen as small as 1%, the lower confidence bound equals the true number of sources $\hat{m}_{0.99} = 2$, which means that with 99% confidence the observations Y (gray dots in first line of Figure 1.10 (right)) come from at least two sources. In the example from the left part of Figure 1.10, where the underlying mixture $\boldsymbol{g}$ with $\boldsymbol{m} = 3$ is very close to the one from the right side which comes from just two sources, one finds that $\hat{m}_{0.9} = 2$. This means that with 90% confidence it can only be guaranteed that the mixture comes from at least two sources (although

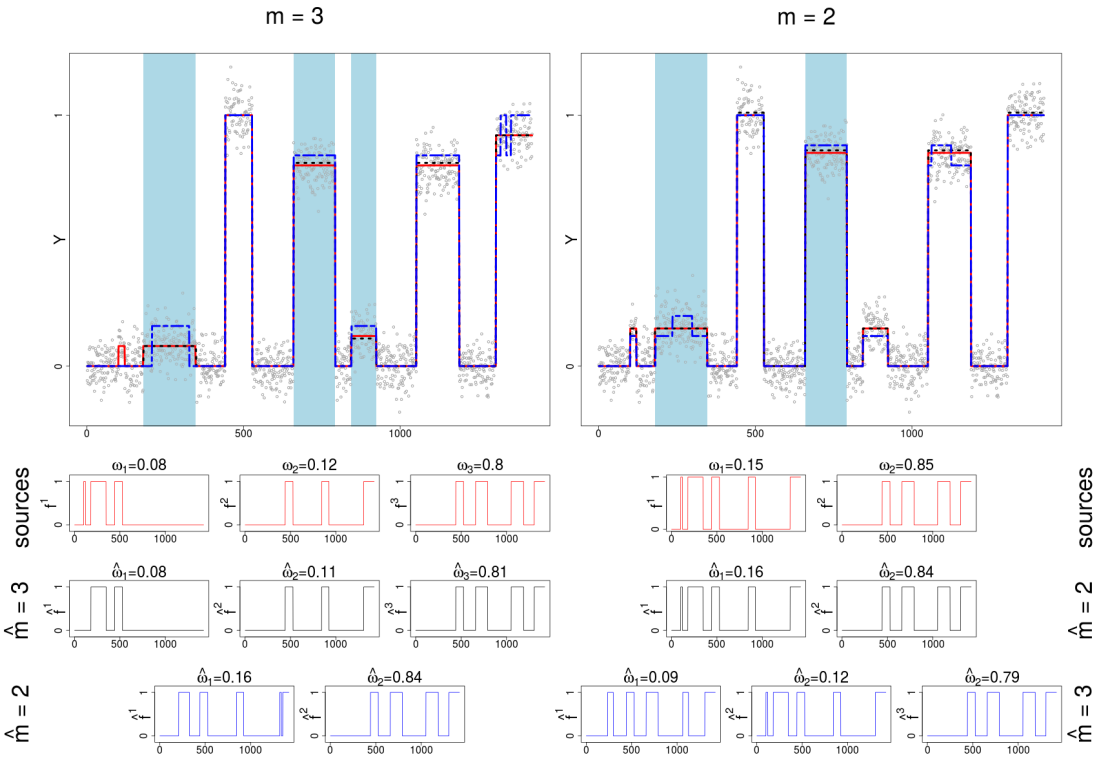

Figure 1.10: Observations Y (gray dots in top rows) according to SBSR model (1.3), $\sigma = 0.06$, $n = 1,421$, with true signal $\boldsymbol{g}$ (solid red line in top rows). Separable regions (see (1.9)) are marked blue. Left: $\boldsymbol{m} = 3$, $\boldsymbol{\omega} = (0.08, 0.12, 0.8)^\top$, and $\boldsymbol{f} = (\boldsymbol{f}^1, \boldsymbol{f}^2, \boldsymbol{f}^3)$ (solid red lines in row 2). The estimator from Theorem 3.6.11 yields $\hat{m} = 3$, $\hat{\omega} = (0.08, 0.11, 0.81)^\top$, and the black lines for sources (row 3) and mixture (top row). With $\hat{m}_{0.9} = 2$ the corresponding estimate is shown as blue line for sources (row 4) and mixture (top row) with $\hat{\omega} = (0.16, 0.84)^\top$. Right: $\boldsymbol{m} = 2$, $\boldsymbol{\omega} = (0.15, 0.85)^\top$, and $\boldsymbol{f} = (\boldsymbol{f}^1, \boldsymbol{f}^2)$ (solid red lines in row 2). The estimator from Theorem 3.6.11 yields $\hat{m} = 2$, $\hat{\omega} = (0.16, 0.84)^\top$, and the black lines for sources (row 3) and mixture (top row). With $\hat{m} = 3$ the corresponding estimate is shown as blue line for sources (row 4) and mixture (top row) with $\hat{\omega} = (0.09, 0.12, 0.79)^\top$.

it actually comes from three). Similar as for SLAM, if the confidence level $1 - \alpha = 1 - \alpha_n$ is chosen appropriately, with $q(\alpha_n) = c(\lambda, \delta, \sigma)\sqrt{n}$ as in Definition 3.6.8, the proposed selector $\hat{m} = \hat{m}_{1-\alpha_n}$ converges exponentially fast to the true $\boldsymbol{m}$, see Theorem 3.6.9. For this estimator, in both examples of Figure 1.10, the true number of sources is estimated correctly. Based on this selection procedure we derive asymptotically optimal (up to log-factors) estimation procedures and confidence statements for $\boldsymbol{\omega}$ and $\boldsymbol{f}$ when $\boldsymbol{m}$ is unknown, using $\hat{m}$ as a plug-in estimator for SLAM (see Theorem 3.6.11 and 3.6.12).

In the left example of Figure 1.10 the corresponding estimate yields $\hat{\omega} = (0.08, 0.11, 0.81)^\top$ and the black lines in row 3 for the sources. One can see that the sources are recovered very accurately, only missing a small jump in the beginning of the signal. The corresponding estimates for number of sources equal to the 90% lower confidence bound $\hat{m}_{0.9} = 2$ yields $\hat{\omega} = (0.16, 0.84)^\top$ and the blue lines in row 4. This estimate is still very reasonable, in the sense that it combines the first two sources to a single source function, similar as in the right

example of Figure 1.10. To compensate for the misspecified number of sources, the estimator introduces some additional wrong jumps. Analogously in the right example of Figure 1.10 (with $\boldsymbol{m} = 2$), if the number of sources is misspecified as $\hat{m} = 3$ SLAM (blue lines in row 4) inserts additional wrong jumps. In Section 6.2 we report on simulation results for the SLAM selector. They indicate that it outperforms standard methods like the AIC and BIC procedure, which, in contrast to our method, do not give any statistical guarantees.

1.3.3 Multivariate FABS

For the MABS model (1.6) the main contribution of this thesis is to derive an estimator which (almost) attains minimax prediction and estimation rates, where we assume the number of sources $\boldsymbol{m}$, the alphabet $\mathfrak{A}$, and the noise variance σ^2 to be fixed. The aim is to study the influence of all quantities on recovery as $n, M \to \infty$. Again, in order to guarantee identifiability δ-separability is employed. Note that increasing M makes inference on $\boldsymbol{F}$ in (1.6) easier (we observe more mixtures of the same sources) while inference on $\boldsymbol{\omega}$ more difficult (the dimension of $\boldsymbol{\omega}$ and thus the number of parameters to be estimated increases with M). In contrast, increasing n makes inference on $\boldsymbol{F}$ more difficult (the dimension of $\boldsymbol{F}$ and thus the number of parameters to be estimated increases with n) while inference on $\boldsymbol{\omega}$ easier (we observe more samples from the the same mixture matrix $\boldsymbol{\omega}$). In Corollary 4.1.4 we show that the minimax rate for the prediction error is of the form

$$\frac{\sigma^2 m}{n} + \frac{\sigma e^{-c\frac{M}{\sigma^2}}}{n\sqrt{M}} \lesssim \inf_{\hat{\theta}} \sup_{\boldsymbol{F},\boldsymbol{\omega}} \mathrm{E}_{\boldsymbol{F}\boldsymbol{\omega}} \left(\frac{\left\| \hat{\theta} - \boldsymbol{F}\boldsymbol{\omega} \right\|^2}{nM} \right) \lesssim \frac{\sigma^2 m}{n} + \frac{\sigma e^{-c'\frac{M}{\sigma^2}}}{n\sqrt{M}}, \tag{1.30}$$

whenever $\ln(n)/M \to 0$, $M/n \to 0$, and that the least squares estimator (LSE) achieves this rate. Here $\lesssim$ and $\gtrsim$ denote inequalities up to a universal constant which does not depend on any model parameters and $c, c' = c'(\boldsymbol{m}, \mathfrak{A}) > 0$ are positive constants. A major consequence of (1.30) is that when $M \gg \ln(n)$ the unknown design matrix $\boldsymbol{F}$ in the linear model (1.6) does not play much of a role for the prediction error. Exact recovery results as in (1.10) allow to relate the prediction error $\left\| \hat{\theta} - \boldsymbol{F}\boldsymbol{\omega} \right\|$ in (1.30) to the estimation error via the metric $d\left((\boldsymbol{F}, \boldsymbol{\omega}), (F, \omega)\right) = (\sqrt{M}/m)\, \mathbb{1}_{\boldsymbol{F} \neq F} + \max_{i=1,\dots,m} \|\boldsymbol{\omega}_i - \omega_i\|$. In Theorem 4.2.3 we show that

$$\sigma^2 c_1 + \frac{\sigma}{\sqrt{M}} c_2 e^{-c\frac{M}{\sigma^2}} \lesssim \inf_{\hat{F},\hat{\omega}} \sup_{\boldsymbol{F},\boldsymbol{\omega}} \mathrm{E}_{\boldsymbol{F}\boldsymbol{\omega}} \left(\frac{d\left((\boldsymbol{F}, \boldsymbol{\omega}), (\hat{F}, \hat{\omega})\right)^2}{M} \right) \lesssim \sigma^2 c_1' + \frac{\sigma}{\sqrt{M}} c_2' e^{-c'\frac{M}{\sigma^2}}, \tag{1.31}$$

whenever $\ln(n)/M \to 0$, $M/n \to 0$, with $c_1 = c_1(m, n, \mathfrak{A}), c_2 = c_2(m, n, \mathfrak{A}), c_1' = c_1'(m, \mathfrak{A}), c_2' = c_2'(m, \mathfrak{A}) > 0$ positive constants (and $c_1, c_2 \in o(1)$ as $n \to \infty$), and this rate is achieved by the LSE. A major consequence of (1.31) is that also for the estimation error if $M \gg \ln(n)$ the unknown $\boldsymbol{F}$ in (1.6) does not play much of a role.

Our theoretical findings show that the LSE achieves optimal rates, both for the prediction error and for the estimation error. Unfortunately, we are not aware of any polynomial time algorithm for exact computation of the LSE. Pananjady et al. (2016) have shown that the LSE for a similar

```
al <- c(0,1)
sources <- rbind(rep(al, each = 100), rep(al[2:1], each = 100))
omega <- c(0.2, 0.8)
y <- as.numeric(omega %*% sources + 0.5 * rnorm(dim(sources)[2]))
estimate <- slamSelect(y, al, lambda = 0.2, delta = 0.1)
confBound <- slamSelect(y, al, lambda = 0.2, delta = 0.1, alpha = 0.1)
est <- slamR(y = y, al = al, m = length(omega), lambda = 0.2, confreg =
TRUE, confband = TRUE, alpha = 0.1, beta = 0.01)
confReg <- attr(est, "confReg")
confBand <- attr(est, "confBand")
```

Figure 1.11: Illustration of function `slamSelect` and `slamR` in R-package `slamR`.

problem (see Section 5.2 for details) is NP-hard to compute. We conjecture that this is the case here, too. In Section 5.2 we propose a simple iterative Lloyd's algorithm to approximate the LSE. Simulations in Section 6.3 suggest similar rates as for the LSE.

1.4 Algorithms and implementation

SLAM For given number of sources m, SLAM's estimate for ω as in the SBSR model (1.3) can be computed with polynomial complexity $O(n^{2m+1})$, see (1.23) and Algorithm CRW in Figure 3.1. Using dynamic programming, the final estimate of sources f as in (1.3) can then be computed with a complexity ranging from $O(n)$ and $O(n^2)$ depending on the final solution. The SLAM selector for the number of sources m can be computed in $O(n^{2\hat{m}+1})$ time. As $\hat{m} \leq m$ in most simulations (see Section 6.2), in practice, the overall complexity of SLAM does usually not increase when m is unknown. Details are given in Section 5.1. An R-package including an implementation of SLAM is available[2]. Its two main functions are `slamSelect` and `slamR`. The former performs model selection for the number of sources m with the estimator $\hat{m}$ (see Definition 3.6.8) and, given an (estimated) number of sources, the latter estimates the mixing weights ω and the sources f with the SLAM procedure. `slamSelect` takes as input the numeric observations `y`, the alphabet `al`, a minimal scale `lambda`, and a minimal ASB `delta`. If, in addition, a confidence level α is specified, the corresponding $1-\alpha$ lower confidence bound is computed. An example is given in Figure 1.11. `slamR` takes as input the numeric observations `y`, the alphabet `al`, the true or estimated (with `slamSelect`) number of sources `m`, and a minimal scale `lambda`. The threshold parameter $q(\alpha)$ for estimating the mixing weights is chosen according to the MVT-selection method explained in Section 3.5. If `confreg == TRUE` and `alpha` is specified, the $1-\alpha$ confidence region $C_{1-\alpha}$ in (1.22) for the mixing weights ω is computed. If `confband == TRUE` and `beta` is specified, the $1-\beta$ confidence band $\tilde{\mathcal{H}}(\beta)$ in (1.29) for the sources f is computed. An example is given in Figure 1.11.

[2]R package available at `http://www.stochastik.math.uni-goettingen.de/slamR`

Clustering algorithm In Section 5.2 a clustering algorithm (see Figure 5.1) which approximates the LSE in the MABS model (1.6) is proposed. It successively updates an estimate for matrices $\boldsymbol{F}$ and $\boldsymbol{\omega}$. Given an estimate $\hat{F}$ the LS solution for $\boldsymbol{\omega}$ can be formulated as a convex optimization problem, where standard solvers exist. On the other hand, given an estimate $\hat{\omega}$, the LS solution for $\boldsymbol{F}$ can be obtained by clustering with given centers $\{e\hat{\omega} \ : e \in \mathfrak{A}^{\boldsymbol{m}}\}$. We found that the algorithm terminates very quickly, usually after less than 10 iterations.

1.5 Literature survey: contrasted and compared

Finite alphabet blind separation A rigorous statistical modeling, methodology, and theory for the FABS problem was entirely lacking, to best of our knowledge, prior to this work. We are not aware of any other work which provides a characterization of identifiability for FABS and estimates (and confidence statements) in the SBSR and MABS model, respectively, in such a rigorous and general way. However, some specific instances of FABS have been considered. For the binary alphabet $\mathfrak{A} = \{-1, 1\}$ FABS has been considered in (Talwar et al., 1996; Pajunen, 1997; Diamantaras and Chassioti, 2000; Diamantaras, 2006; Gu et al., 2010). Diamantaras (2006) also considers a general finite alphabet but only for complex weights. Thus, he only works with a two-dimensional signal. The separability condition (1.9) (see Section 2.1.2) is mainly motivated by results of Diamantaras (2006). Equally spaced alphabets, i.e., $\{a_1, \ldots, a_k\} = \{a_0, a_0 + T, a_0 + 2T, \ldots, a_0 + kT\}$ are considered in (Diamantaras and Papadimitriou, 2009; Rostami et al., 2011). Diamantaras (2008) only considers the case $\boldsymbol{m} = 2$. Here we treat arbitrary alphabets $\mathfrak{A} = \{a_1, \ldots, a_k\} \subset \mathbb{R}$ and number of sources $\boldsymbol{m} \in \mathbb{N}$. Moreover, some authors (Pajunen, 1997; Diamantaras and Papadimitriou, 2009; Rostami et al., 2011) assume a specific distribution on the alphabet, e.g., uniform. Separability only assumes some specific combinations of alphabet values (which are minimal conditions in a sense) to be present in the signal, hence such a specific distribution is not needed.

A related problem is non-negative matrix factorization (NMF) (Lee and Seung, 1999; Donoho and Stodden, 2004; Arora et al., 2012; Bittorf et al., 2012), where one assumes a multivariate signal $Y = \boldsymbol{F}\boldsymbol{\omega} + Z \in \mathbb{R}^{n \times M}$ as in (1.6), but with $\boldsymbol{F}$ and $\boldsymbol{\omega}$ both non-negative (without any alphabet restriction on the sources). In contrast to NMF, the additional finite alphabet restriction imposed here, leads to a model structure more related to a classification problem. NMF with both $\boldsymbol{F}$ and $\boldsymbol{\omega}$ (and possibly also Y) having entries in a known finite set has been considered for example in (Li, 2005). While NMF shares a structural similarity with the MABS model in (1.6), it is fundamentally different to the SBSR model (1.3). A crucial assumption in NMF is that $m \ll \min(n, M)$, which obviously does not hold in the SBSR model where $M = 1$. Indeed, techniques and algorithms for NMF are very different from the ones derived here for the SBSR model, as our multiscale methodology explicitly takes advantage of the one dimensional (i.e., ordered) c.p. structure under the finite alphabet assumption.

The δ-separability condition from Section 1.3.1 is similar in nature to identifiability conditions for NMF (Donoho and Stodden, 2004; Arora et al., 2012), from where the notation *separable* originates. However, proofs are very different. Whereas in NMF they are build on geometrical

considerations, in FABS they are build on combinatorics. In order to ensure identifiability in NMF, the "α-robust simplicial" condition on the mixing matrix $\boldsymbol{\omega} \in \mathbb{R}_+^{m \times M}$ (see e.g., (Bittorf et al., 2012, Definition 2.1)) and the "separability" condition on the source matrix $\boldsymbol{F} \in \mathbb{R}_+^{n \times m}$ (see e.g. (Bittorf et al., 2012, Definition 2.2)) are well established. There, the "δ-robust simplicial" condition assumes that the mixing vectors $\boldsymbol{\omega}_{1\cdot}, \ldots, \boldsymbol{\omega}_{m\cdot} \in \mathbb{R}_+^M$ constitute vertices of an m-simplex with minimal diameter (distance between any vertex and the convex hull of the remaining vertices) δ. This means that different source values $\boldsymbol{F}_{i\cdot} \in \mathbb{R}^m$ are mapped to different mixture values $\boldsymbol{F}_{i\cdot}\boldsymbol{\omega} \in \mathbb{R}_+^M$ by the mixing matrix $\boldsymbol{\omega} \in \mathbb{R}_+^{m \times M}$. This condition is analog to the condition $ASB(\boldsymbol{\omega}) \geq \delta$ in (1.8), which ensures that different source values $e \in \mathfrak{A}^m$ are mapped to different mixture values $e\boldsymbol{\omega} \in \mathbb{R}$ via the mixing weights $\boldsymbol{\omega} \in \Omega_m$, with minimal distance δ between different mixture values. The "separability" condition in NMF is essentially the same as in (1.9). In both models (NMF and FABS) separability ensures a certain variability of the sources in order to guarantee identifiability of the mixing matrix and vector, respectively, from their mixture. However, whereas in NMF separability only yields identifiability if $M \geq m$, in FABS separability always yields identifiability even for a single linear mixtures ($M = 1$), as it explicitly explores the finite alphabet.

Another related problem is Independent Component Analysis (ICA) (see e.g., (Comon, 1994; Belkin et al., 2013; Arora et al., 2015)), which is based on the stochastic independence of the different sources (assumed to be random). Here we do not make any independence assumption on the different sources. We rather treat them as deterministic and fixed, making ICA not accessible to our problem. Moreover, in contrast to the SBSR model, ICA is not applicable for single linear mixtures ($M = 1$), as the error terms of the single sources then sum up to a single error term and ICA would treat this as one observation. ICA for underdetermined multiple linear mixture models, i.e., $1 < m < M$, is treated in (Lee et al., 1999).

Some BSS methods assume second-order stationary (SOS) processes for the sources, see (Tong et al., 1991; Belouchrani et al., 1997). Other BSS methods assume a certain sparsity of the mixing matrix (Spielman et al., 2012) or sparse representations (SR) (Abrard et al., 2001; Bofill and Zibulevsky, 2001; Yilmaz and Rickard, 2004; Li et al., 2006). We stress, that FABS does not make any sparsity assumption in the usual sense, where many coefficients are assumed to be zero. Conceptually related is blind deconvolution (see e.g., (Yellin and Porat, 1993; Li et al., 2003; Diamantaras and Papadimitriou, 2011)), however, the convolution model makes analysis and identifiability severely different. Also related is statistical seriation where $\boldsymbol{F}$ in (1.6) is a permutation matrix which needs to be estimated, see (Flammarion et al., 2016).

Change point regression The estimation of step functions, with unknown number and location of c.p.'s is a widely discussed problems, see e.g., (Tukey, 1961; Carlstein et al., 1994; Olshen et al., 2004; Fearnhead, 2006; Friedrich et al., 2008; Tibshirani and Wang, 2008; Spokoiny, 2009; Harchaoui and Lévy-Leduc, 2010; Jeng et al., 2010; Killick et al., 2012; Zhang and Siegmund, 2012; Niu and Zhang, 2012; Siegmund, 2013; Frick et al., 2014; Matteson and James, 2014; Fryzlewicz, 2014; Du et al., 2015). However, to best of our knowledge the combination with a BSS problem as in the SBSR model (1.3) has not been considered before.

Minimization of the ℓ_0 norm using dynamic programming, which has a long history in c.p. analysis (see e.g., (Bai and Perron, 1998; Fearnhead, 2006; Friedrich et al., 2008; Killick et al., 2012)), for segment estimation under a multiscale constraint has been introduced in (Boysen et al., 2009) (see also (Davies et al., 2012) and (Frick et al., 2014)) and here we extend this to mixtures of segment signals and in particular to a finite alphabet restriction.
To best of our knowledge, the way the problem of clonal separation is treated here is new, see, however, (Yau et al., 2011; Carter et al., 2012; Liu et al., 2013; Roth et al., 2014; Ha et al., 2014; Ding et al., 2014). Methods suggested there all rely on specific prior information about the sources $\boldsymbol{f}$ and cannot be applied to the general SBSR model. Moreover, most of them treat the problem from a Bayesian perspective.

Model selection Estimation of $\boldsymbol{m}$ in the SBSR model can be considered as a model-selection problem, for which many well established procedures exist, in general. The most popular ones include the Akaike Information Criterion (AIC) (Akaike, 1974) and the Bayesian Information Criterion (BIC) (Schwarz, 1978). For a discussion of other criteria see e.g., (Claeskens and Hjort, 2008). However, the regularity conditions (which allow a Taylor expansion of the likelihood) needed for the theoretical justification of the BIC and AIC criterion (see (Schwarz, 1978; Burnham, 2004)) are not satisfied in the SBSR model (see Section 6.2.1 for details and simulations). Moreover, these procedures do not explore the specific structure of FABS and, in particular, they do not provide any statistical guarantees for the selected number of components. Note that already for $\boldsymbol{m} = 1$ this becomes apparent as then the problem boils down to c.p. estimation, where determining the number of jumps is also recognized as a model selection step and these criteria are well known to fail, see (Zhang and Siegmund, 2007, 2012).
Model selection for the number of sources, as it is considered in this thesis for the SBSR model, has also been considered for other BSS problems. A maximum likelihood procedure for estimating the number of sources in ICA is, for instance, considered in (Penny et al., 2001). They argue that, whereas usually model selection with maximum likelihood leads to an overestimation of model parameters (i.e. overestimation of $\boldsymbol{m}$), this is not the case for ICA. This is because for ICA adding more sources will at some point decrease the likelihood as the independence condition will be violated if too many sources are added. Such an approach cannot be transferred to the SBSR model as no probabilistic assumption is made on the sources, in particular no independence assumption. Heuristic approachs for estimating the number of sources in NMF are given in (Brunet et al., 2004; Kim and Park, 2008). As they use a randomized initialization in their iterative NMF algorithm, each run will result in a different factorization. They propose to compute for different number of sources several realizations and choose the m where the factorizations were most stable. As SLAM does not include a random component, this heuristic approach cannot be used for estimating $\boldsymbol{m}$ in this context. A Bayesian approach for estimating the number of sources in NMF is considered in (Schmidt et al., 2009). There are also some heuristic approaches for estimating the number of sources for methods which are build on sparse representations (SR), see e.g., (Bofill and Zibulevsky, 2001; Yilmaz and Rickard, 2004; Li et al., 2006). However, all these approaches explore the particular sparseness

assumption and the fact that several mixtures are observed, which is both not the case in the SBSR model.

Linear models with unknown design Most related to the work on the multivariate linear model (1.6) in this thesis is (Pananjady et al., 2017), who consider model (1.6) with $\boldsymbol{F}$ being unknown up to a permutation matrix. They derive minimax prediction rates for this model and show that the LSE obtains the optimal rates (up to log-factors). They also consider the case where $\boldsymbol{F}$ is unknown up to a selection matrix (i.e. not every row of $\boldsymbol{F}$ necessarily appears in the data Y and some rows might be selected several times). One can rewrite (1.6) in an analog way, to obtain a MABS model as in (1.6) where the design matrix equals $\boldsymbol{F} = \boldsymbol{\Pi}A$, with $\boldsymbol{\Pi}$ an unknown selection matrix and A being the matrix where the rows constitute of all different combinations of alphabet values. Thus, one can consider (1.6) as a special case of the model considered in (Pananjady et al., 2017). Pananjady et al. (2017) derive minimax prediction rates of the form

$$\inf_{\hat{\theta}} \sup_{\boldsymbol{\Pi}A\boldsymbol{\omega}} \mathrm{E}_{\boldsymbol{\Pi}A\boldsymbol{\omega}} \left(\frac{1}{nM} \left\| \hat{\theta} - \boldsymbol{\Pi}A\boldsymbol{\omega} \right\|^2 \right) \approx \frac{\sigma^2 m}{n} + \frac{\sigma^2 \left(\ln(n)\right)}{M}, \tag{1.32}$$

where the log-term only appears in their upper bound. In our situation, where we assume a specific finite alphabet for the design matrix, thus a specific matrix A, the second term in the minimax rate becomes exponential in M instead of parametric. The rate (1.32) is obtained in (Pananjady et al., 2017) by treating the whole matrix $\boldsymbol{\Pi}A$ as unknown. Here we explicitly exploit a specific structure of A and thus obtain a faster rate. Note that, just as in our setting (see (1.30)), Pananjady et al. (2017) obtain with (1.32) that whenever $\ln(n) \gg M$ the unknown permutation Π does not play much of a role for the prediction error. Another major difference is that Pananjady et al. (2017) do not impose any identifiability conditions on $\boldsymbol{F} = \boldsymbol{\Pi}A$ and $\boldsymbol{\omega}$ in (1.6). Thus, in contrast to results of this thesis, they do not obtain any bounds for the estimation error. By regularizing the model in an appropriate way, we obtain the minimax estimation rate for $M \to \infty$ for $\boldsymbol{F}$ and $\boldsymbol{\omega}$ up to constants and show that it is achieved by the LSE.

Pananjady et al. (2016) already considered a similar problem as Pananjady et al. (2017) but with $M = 1$ (not general $M \geq 1$ as in (1.6)) and for permutation matrices $\boldsymbol{\Pi}$ only (not for selection matrices as in MABS). There they assumed a random design A with Gaussian entries, in contrast to MABS where A is a specific fixed matrix. They focus on the estimation of the unknown permutation $\boldsymbol{\Pi}$ (and not on joint estimation of $\boldsymbol{\omega}$ and $\boldsymbol{\Pi}$ as in this work) and give a sharp condition on the signal to noise ratio $\|\boldsymbol{\omega}\| / \sigma$ and the number of observations n under which it is possible to exactly recover the permutation $\boldsymbol{\Pi}$ and they show that the LSE recovers $\boldsymbol{\Pi}$ whenever this is possible. Marques et al. (2009) consider a similar model as Pananjady et al. (2017) in the context of object recognition, where $m = 3$ and $M = 2$. There $m = 3$ corresponds to the dimension of an object, $M = 2$ to the dimension of a photo of this object, and the unknown mixture matrix $\boldsymbol{\omega}$ to an unknown camera perspective. They also focus on recovery of the unknown permutation $\boldsymbol{\Pi}$. Their results basically require that sufficiently many of the n permutations are known in advance. Unnikrishnan et al. (2015) study a similar model as Pananjady et al. (2016) but mainly focus on the noiseless case. They also consider a random

design for A (in contrast to MABS) with i.i.d. entries drawn from a continuous distribution. They focus on recovery of $\boldsymbol{\omega}$ (not on $\boldsymbol{\Pi}$) and show that whenever $n > 2m$ with probability one $\boldsymbol{\omega}$ can be recovered from the (noiseless) observations Y.

1.6 Summary

The following summarizes the main contributions of this thesis.

- We introduce **statistical models for Finite Alphabet Blind Separation (FABS)**. A problem, which appears in many different areas, like digital communications and cancer genetics, but for which rigorous theory was almost entirely lacking prior to this work.
- We are the first to provide a complete **characterization of identifiability** for FABS, also for the case where the number of source components $\boldsymbol{m}$ is unknown.
- In a c.p. regression setting, as, e.g., in cancer genetics, we obtain confidence statements and the SLAM-estimators with (up to log-factors) **optimal rates for all quantities**.
- In particular, we show with a **data example from cancer genetics** that SLAM provides accurately estimates for the number of clonal components, their relative proportion, and their CNA profiles, something which has not been obtainable prior to now.
- We provide **software**, the R package `slamR`, with an efficient implementation of SLAM.
- We study multivariate FABS, as, e.g., in digital communications. We derive **minimax rates** when number of observations (length of signal) n and mixtures (receivers) M tend to infinity. This reveals that signals are recovered exactly by an order of $\ln(n)$ receivers.
- In a broader sense, this thesis reveals that finite alphabet structures can significantly improve statistical efficiency and recoverability and may be seen as a **new type of sparsity**.

CHAPTER 2

Identifiability and model-regularization

2.1 Identifiability

In the following we analyze identifiability of the weights $\boldsymbol{\omega}$ and the sources $\boldsymbol{f}$ from the mixture $\boldsymbol{g}$ in FABS (1.1). First, we consider the situation where the number of source components $\boldsymbol{m}$ is given. Second, the case where $\boldsymbol{m}$ is unknown is treated. To this end, note that a serial structure of sources $\boldsymbol{f}$, e.g., a c.p.-structure as in the SBSR model, is irrelevant for identifiability. Thus, in this chapter the sources $\boldsymbol{f}$ are w.l.o.g. considered as a matrix with elements in the finite alphabet $\mathfrak{A}$. Moreover, note that multiple observed values leave the identification problem invariant, i.e., do not contribute further to identifiability. Hence, w.l.o.g. all observations $\boldsymbol{g}_1, \ldots, \boldsymbol{g}_n$ are assumed to be pairwise different. Note, that this implies $n \leq k^{\boldsymbol{m}} = |\mathfrak{A}^{\boldsymbol{m}}|$.

Definition 2.1.1 (Identifiable mixtures)**.** Consider the FABS model (1.1) with M mixtures, n observations, and a given number of source components $\boldsymbol{m}$. A pair $(\boldsymbol{\omega}, \boldsymbol{f})$ of weights $\boldsymbol{\omega} \in \Omega_{\boldsymbol{m},M}$ and sources $\boldsymbol{f} \in \mathfrak{A}^{n\times\boldsymbol{m}}$ is identifiable from its mixture $\boldsymbol{g} := \boldsymbol{f}\boldsymbol{\omega}$, if there exists exactly one $(\omega, f) \in \Omega_{\boldsymbol{m},M} \times \mathfrak{A}^{n\times\boldsymbol{m}}$ such that $\boldsymbol{g} = f\omega$.

Example 2.1.2. To illustrate the problem and notation, consider a simple example of FABS, where $\boldsymbol{m} = 2$, $M = 1$, and the alphabet is binary with $\mathfrak{A} = \{0, 1\}$. That means we consider mixing vectors $\boldsymbol{\omega} = (\boldsymbol{\omega}_1, \boldsymbol{\omega}_2)$ with $\boldsymbol{\omega}_1, \boldsymbol{\omega}_2 \in \mathbb{R}_+$ and $\boldsymbol{\omega}_1 + \boldsymbol{\omega}_2 = 1$ and two different sources $\boldsymbol{f}_{\cdot 1} = (\boldsymbol{f}_{11}, \ldots, \boldsymbol{f}_{n1})$, $\boldsymbol{f}_{\cdot 2} = (\boldsymbol{f}_{12}, \ldots, \boldsymbol{f}_{n2})$ with $\boldsymbol{f}_{ij} \in \{0, 1\}$ for $i = 1, 2$ and $j = 1, \ldots, n$. The question we would like to answer is, under which conditions on $\boldsymbol{\omega}$ and $\boldsymbol{f}$ is $(\boldsymbol{\omega}, \boldsymbol{f})$ uniquely determined via $\boldsymbol{g} := \boldsymbol{f}\boldsymbol{\omega}$. For a given observation $\boldsymbol{g}_j$ the underlying source vector $\boldsymbol{f}_{j\cdot} = (\boldsymbol{f}_{j1}, \boldsymbol{f}_{j2})$ equals one of the four different values

$$(0, 0), (1, 0), (0, 1), (1, 1) \tag{2.1}$$

and hence,

$$\boldsymbol{g}_j \in \{0, \boldsymbol{\omega}_1, \boldsymbol{\omega}_2, 1\}. \tag{2.2}$$

Clearly, if any two of the four values in the set on the r.h.s. of (2.2) coincide, then two different source values in (2.1) lead to the same mixture value for $\boldsymbol{g}_j$ and hence the sources are not identifiable, i.e., they cannot be distinguished. Consequently, a necessary condition for identifiability

is that all values in the r.h.s. of (2.2) are different, which is equivalent to

$$\omega_1 \neq \omega_2 \quad \text{and} \quad 0 < \omega_1, \omega_2 < 1. \tag{2.3}$$

In other words, it is necessary that the alphabet values in $\mathfrak{A}^{\boldsymbol{m}}$ are well separated via the mixing weights $\boldsymbol{\omega}$. For arbitrary alphabets and number of sources this is characterized by the necessary condition that $ASB(\boldsymbol{\omega}) = ASB(\boldsymbol{\omega}, \mathfrak{A}) > 0$ as in (1.8). Further, we may assume w.l.o.g. that $\omega_1 < \omega_2$, i.e., we denote that source as $\boldsymbol{f}_{1\cdot}$ which comes with the smaller weight. (2.3) alone, however, is necessary but not sufficient for identifiability. For instance, if $\boldsymbol{f}_{\cdot 1} = \boldsymbol{f}_{\cdot 2}$ then $\boldsymbol{g}_j \in \{0, 1\}$ and hence, $\boldsymbol{\omega}$ is not identifiable from $\boldsymbol{g}$. In this simple example, it is easy to check that a necessary and sufficient variability of $\boldsymbol{f}_{\cdot 1}$ and $\boldsymbol{f}_{\cdot 1}$ is that $\boldsymbol{f}$ either takes the value $(1, 0)$ (i.e., $\boldsymbol{g}_j = \boldsymbol{\omega}_1$ for some $j = 1, \ldots, n$) or $(0, 1)$ (i.e., $\boldsymbol{g}_j = \boldsymbol{\omega}_2$ for some $j = 1, \ldots, n$) as by (2.3) and $\boldsymbol{\omega}_1 + \boldsymbol{\omega}_2 = 1$ it always follows that $0 < \omega_1 < 1/2 < \omega_2 = 1 - \omega_1 < 1$. In other words, it is necessary and sufficient that $\boldsymbol{\omega}_i \in \mathrm{imag}(\boldsymbol{g})$, which coincides with separability in (1.9).

2.1.1 Combinatorial characterisation of identifiability

The following theorem characterized identifiability in the FABS as a purely combinatorial issue. To this end, let $S^n_{\boldsymbol{m}}$ be the collection of injective maps from $\{1, \ldots, \boldsymbol{m}\}$ to $\{1, \ldots, n\}$, i.e., for $\rho \in S^n_{\boldsymbol{m}}$ the vector $(\boldsymbol{g}_{\rho(1)}, \ldots, \boldsymbol{g}_{\rho(\boldsymbol{m})})$ corresponds to a selection of elements from $\{\boldsymbol{g}_1, \ldots, \boldsymbol{g}_n\}$ (recall that they are assumed to be pairwise different).

Theorem 2.1.3. *Consider the FABS model (1.1) for M mixtures, n observations, and given number of source components $\boldsymbol{m}$, with $\boldsymbol{g} = (\boldsymbol{g}_1, \ldots, \boldsymbol{g}_n)^\top = \boldsymbol{f}\boldsymbol{\omega}$ and $(\boldsymbol{\omega}, \boldsymbol{f}) \in \Omega_{\boldsymbol{m},M} \times \mathfrak{A}^{n \times \boldsymbol{m}}$. Let $E \in \mathfrak{A}^{\boldsymbol{m} \times \boldsymbol{m}}$ be an arbitrary but fixed invertible $\boldsymbol{m} \times \boldsymbol{m}$ matrix with elements in $\mathfrak{A}$. Assume that $ASB(\boldsymbol{\omega}) > 0$ and*
***A 1.** there exists $\rho \in S^n_{\boldsymbol{m}}$ such that $(\boldsymbol{f}_{\rho(r)1}, \ldots, \boldsymbol{f}_{\rho(r)\boldsymbol{m}})^\top_{1 \leq r \leq \boldsymbol{m}} = E$.*
Then $(\boldsymbol{\omega}, \boldsymbol{f})$ is identifiable if and only if
***A 2.** there exists exactly one $\sigma \in S^n_{\boldsymbol{m}}$ such that for $\omega := E^{-1}(\boldsymbol{g}_{\sigma(1)}, \ldots, \boldsymbol{g}_{\sigma(\boldsymbol{m})})^\top$*

$$\omega \in \Omega_{\boldsymbol{m},M} \quad \text{and} \quad \{\boldsymbol{g}_1, \ldots, \boldsymbol{g}_n\} \in \{a\omega : \ a \in \mathfrak{A}^{\boldsymbol{m}}\}, \tag{2.4}$$

i.e., ω is a valid mixing weight and can reproduce all observations.

Theorem 2.1.3 yields that, for a fixed invertible matrix $E \in \mathfrak{A}^{\boldsymbol{m} \times \boldsymbol{m}}$, if the sources $\boldsymbol{f}$ are restricted to those where the rows of E appear *somewhere* in the rows of $\boldsymbol{f}$, i.e., $E_{1\cdot}, \ldots, E_{\boldsymbol{m}\cdot} \in \mathrm{imag}(\boldsymbol{f})$, then identifiability reduced to the combinatorial issue A2. Put it differently, if one restricts to the submodel invoked by A1 (where the submodel depends on the matrix E), identifiability can be easily determined via checking for all different collections $\sigma \in \mathcal{S}^n_{\boldsymbol{m}}$ whether the corresponding rows of $\boldsymbol{g}$ can be assigned to rows of E in a unique way as in A2.
Note that A1 can easily be simplified to the assumption that $\boldsymbol{f}$ has full rank, that is $\mathrm{rank}(\boldsymbol{f}) = \boldsymbol{m}$. To see this, note that there are only finitely many invertible matrices $E \in \mathfrak{A}^{n \times \boldsymbol{m}}$. Thus,

in order to check identifiability under assumption $\text{rank}(\boldsymbol{f}) = \boldsymbol{m}$, one can check A2 for any invertible $E \in \mathfrak{A}^{n\times\boldsymbol{m}}$. Indeed, $\text{rank}(\boldsymbol{f}) = \boldsymbol{m}$ is an almost minimal condition for identifiability. By simple linear algebra, it is easy to check that $\text{rank}(\boldsymbol{f}) < \dim(\text{span}(\Omega_{\boldsymbol{m},1})) = \boldsymbol{m} - 1$ implies that for any $\boldsymbol{\omega} \in \Omega_{\boldsymbol{m},M}$ exists an $\omega \neq \boldsymbol{\omega} \in \Omega_{\boldsymbol{m},M}$ such that $\boldsymbol{\omega}\boldsymbol{f} = \omega\boldsymbol{f}$, i.e., $(\boldsymbol{\omega}, \boldsymbol{f})$ is not identifiable. For arbitrary mixing weights (see Section 2.4.1), which not necessarily sum up to one, $\text{rank}(\boldsymbol{f}) = \boldsymbol{m}$ is even necessary. Further, note that if all $k^{\boldsymbol{m}}$ possible different values are observed, that is $\text{imag}(\boldsymbol{g}) = \{\boldsymbol{g}_1, \ldots, \boldsymbol{g}_n\} = \{e\boldsymbol{\omega} : e \in \mathfrak{A}^{\boldsymbol{m}}\}$, A1 holds for any $E \in \mathfrak{A}^{n\times\boldsymbol{m}}$.
Theorem 2.1.3 yields that if, for a specific matrix $E \in \mathfrak{A}^{n\times\boldsymbol{m}}$, A2 always holds, then A1 (for this specific E) provides a sufficient identifiability condition. It turns out (see Section 2.1.2) that this is the case when E is the identity matrix. Then, A1 equals separability as in (1.9). The following example shows that this is not true in general. That is, not for any choice of E A2 always holds and thus, not for all E A1 is sufficient for identifiability. In particular, the following example shows that $\text{rank}(\boldsymbol{f}) = \boldsymbol{m}$ is not sufficient for identifiability.

Example 2.1.4. With the notation of Theorem 2.1.3 let $n = \boldsymbol{m} = 3$, $M = 1$, and $\mathfrak{A} = \left\{0, 1, 21/(6 + \sqrt{15}), 6\right\}$. Consider mixing weights $\boldsymbol{\omega}^\top = \left((6 - \sqrt{15})/30, (6 + \sqrt{15})/30, 0.6\right)$ and sources $\boldsymbol{f} = E = \text{diag}(6, 21/(6 + \sqrt{15}), 1)$. Then ρ in A1 is the identity map and $\boldsymbol{g} = \boldsymbol{f}\boldsymbol{\omega} = \left((6 - \sqrt{15})/5, 0.7, 0.6\right)^\top$. For $\sigma : (1, 2, 3) \mapsto (3, 1, 2)$ we find that $E^{-1}\left(\boldsymbol{g}_{\sigma(1)}, \boldsymbol{g}_{\sigma(2)}, \boldsymbol{g}_{\sigma(3)}\right)^\top = (0.1, 0.2, 0.7)^\top =: \tilde{\boldsymbol{\omega}}$, which is a valid mixing weight. Hence, $(\boldsymbol{\omega}, \boldsymbol{f})$ is not identifiable.

2.1.2 Separability

The following theorem shows that separability, that is, A1 with E the identity matrix, is sufficient for identifiability. Moreover, the proof gives an explicit construction of the unique $(\boldsymbol{\omega}, \boldsymbol{f})$ from $\boldsymbol{g}$ in $O(n)$ time (see Figure 2.2).

Theorem 2.1.5 (Separability)**.** *Consider the FABS model (1.1) for M mixtures, n observations, and given number of source components $\boldsymbol{m}$, with $\boldsymbol{g} = (\boldsymbol{g}_1, \ldots, \boldsymbol{g}_n)^\top = \boldsymbol{f}\boldsymbol{\omega}$ and $(\boldsymbol{\omega}, \boldsymbol{f}) \in \Omega_{\boldsymbol{m},M} \times \mathfrak{A}^{n\times\boldsymbol{m}}$. Furthermore, assume that $AS\,B(\boldsymbol{\omega}) > 0$ and*
***A 3.** there exists $\rho \in S_{\boldsymbol{m}}^n$ such that*

$$\left(\boldsymbol{f}_{\rho(r)1}, \ldots, \boldsymbol{f}_{\rho(r)\boldsymbol{m}}\right)_{1\leq r\leq\boldsymbol{m}} = I_{\boldsymbol{m}\times\boldsymbol{m}},$$

where $I_{\boldsymbol{m}\times\boldsymbol{m}}$ denotes the $\boldsymbol{m} \times \boldsymbol{m}$ identity matrix.
Then $(\boldsymbol{\omega}, \boldsymbol{f})$ is identifiable.

Note that separability in A3 only requires that the unit vectors are attained *somewhere* by the sources $\boldsymbol{f} = (\boldsymbol{f}_{1\cdot}, \ldots, \boldsymbol{f}_{n\cdot})^\top$ (or equivalently that the mixing weights $\boldsymbol{\omega}_i$ appear *somewhere* in the mixture $\boldsymbol{g} = (\boldsymbol{g}_1, \ldots, \boldsymbol{g}_n)^\top$) and does not specify the location. Figure 2.1 summarizes relations between A1 - A3 in a diagram.

Remark 2.1.6 (Relaxing separability).

a) Note that A3 is equivalent to $\boldsymbol{\omega}_1, \ldots, \boldsymbol{\omega}_{\boldsymbol{m}} \in \text{imag}(\boldsymbol{g})$ as in (1.9). As the mixing weights sum up to one, i.e., $\sum_{i=1}^{\boldsymbol{m}} \boldsymbol{\omega}_i = 1$, when the number of sources is $\boldsymbol{m}$ is known, A3 can be

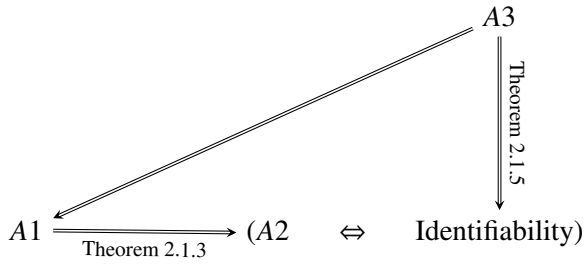

Figure 2.1: Relation between A1, A2, and A3 of Theorem 2.1.3 and 2.1.5.

replaced by the weaker condition $\boldsymbol{\omega}_1, \ldots, \boldsymbol{\omega}_{\boldsymbol{m}-1} \in \operatorname{imag}(\boldsymbol{g})$. This is not true when $\boldsymbol{m}$ is unknown.

b) In A3 the entries 0 and 1 of the identity matrix correspond to the smallest and second smallest alphabet value, respectively (recall $\mathfrak{A} = \{0, 1, a_3, \ldots, a_k\}$ as in (1.7)). It is easy to check that 0 can be replaces by the largest alphabet value a_k and 1 by the second largest alphabet value a_{k-1}.

Remark 2.1.7 (Separability is almost necessary). For arbitrary alphabets $\mathfrak{A}$ and number of sources $\boldsymbol{m}$, Theorem 2.1.5 yields that separability in A3 (together with the necessary condition $ASB(\boldsymbol{\omega}) > 0$) is *sufficient* for identifiability in FABS (1.1). Moreover, for the binary alphabet $\mathfrak{A} = \{0, 1\}$ and $\boldsymbol{m} = 2$ sources, separability is *necessary* for identifiability (recall Example 2.1.2). In that sense, without specifying alphabet and number of sources, separability is sufficient and necessary for identifiability.

Input: $\boldsymbol{g}_1, \ldots, \boldsymbol{g}_n$ and $\mathfrak{A}$
  $r = 1$
  $\mathfrak{G} \leftarrow \{\boldsymbol{g}_1, \ldots, \boldsymbol{g}_n\} \setminus \{(0, \ldots, 0)\}$
  $\boldsymbol{\omega}_1 \leftarrow \operatorname{argmin}\{\|x\| : \ x \in \mathfrak{G}\}$
  $\mathfrak{G} \leftarrow \mathfrak{G} \setminus \{a(\boldsymbol{\omega}_1, 1 - \boldsymbol{\omega}_1)^\top : \ a \in \mathfrak{A}^2\}$
  while $\mathfrak{G} \neq \emptyset$ **do**
    $r = r + 1$
    $\boldsymbol{\omega}_r \leftarrow \operatorname{argmin}\{\|x\| : \ x \in \mathfrak{G}\}$
    $\mathfrak{G} \leftarrow \mathfrak{G} \setminus \{a(\boldsymbol{\omega}_1, \ldots, \boldsymbol{\omega}_r, 1 - \boldsymbol{\omega}_1 - \ldots - \boldsymbol{\omega}_r)^\top : \ a \in \mathfrak{A}^{r+1}\}$
  end while
  $\boldsymbol{m} \leftarrow r$
  return $\boldsymbol{m}$ and $\boldsymbol{\omega}_1, \ldots, \boldsymbol{\omega}_{\boldsymbol{m}}$

Figure 2.2: Algorithm for weight identification in FABS (1.1), with $\mathfrak{A}$ as in (1.7), under separability assumptions A3 and $ASB(\boldsymbol{\omega}) > 0$.

A formal proof of Theorem 2.1.5 is given in Section A.1. In the following the idea of the proof is illustrated via an explicit recovery algorithm for $\boldsymbol{\omega}$. This generalizes an algorithm of Diamantaras and Chassioti (2000) for the binary alphabet $\Omega = \{-1, 1\}$ to a general finite alphabet. For simplicity, assume that $M = 1$. As A3 is equivalent to (1.9), in order to identify $\boldsymbol{\omega}$ from $\boldsymbol{g}$ it suffices to determine those observations $\boldsymbol{g}_j$ which correspond to mixing weights

$\boldsymbol{\omega}_i$. To this end, consider the ordered observations $\boldsymbol{g}_{(1)} < \ldots < \boldsymbol{g}_{(n)}$. As $AS\,B(\boldsymbol{\omega}) > 0$, each observation $\boldsymbol{g}_j$ corresponds to a unique vector in $\mathfrak{A}^{\boldsymbol{m}}$ with

$$\{\boldsymbol{\omega}_1, \ldots, \boldsymbol{\omega}_{\boldsymbol{m}}\} \subset \{\boldsymbol{g}_1, \ldots, \boldsymbol{g}_n\} \subset \{e\boldsymbol{\omega} : \ e \in \mathfrak{A}^{\boldsymbol{m}}\}. \tag{2.5}$$

Clearly, the smallest possible value in the set on the r.h.s. of (2.5) is 0, which corresponds to $e = (0, \ldots, 0)$, where all sources take the smallest alphabet value, 0. Similar, the second smallest value in the set on the r.h.s. of (2.5) is $\boldsymbol{\omega}_1$, which corresponds to $e = (1, 0, \ldots, 0)$, where all sources take the smallest alphabet value, 0, but only the source with the smallest mixing weight $\boldsymbol{f}^1$ takes the second smallest alphabet value, 1. Thus, $\boldsymbol{\omega}_1$ is identified as

$$\boldsymbol{\omega}_1 = \begin{cases} \boldsymbol{g}_{(2)} & \text{if } \boldsymbol{g}_{(1)} = 0 \\ \boldsymbol{g}_{(1)} & \text{oterweise} \end{cases}. \tag{2.6}$$

With $\boldsymbol{\omega}_1$ the set $\{e(\boldsymbol{\omega}_1, 1-\boldsymbol{\omega}_1)^\top : \ e \in \mathfrak{A}^2\}$ can be computed. As the weights sum up to one, this is a subset of $\{e\boldsymbol{\omega} : \ e \in \mathfrak{A}^{\boldsymbol{m}}\}$ and the smallest value in $\{e\boldsymbol{\omega} : \ e \in \mathfrak{A}^{\boldsymbol{m}}\} \backslash \{e(\boldsymbol{\omega}_1, 1-\boldsymbol{\omega}_1)^\top : \ e \in \mathfrak{A}^2\}$ equals $\boldsymbol{\omega}_2$. Thus, it follows from (2.5) that

$$\boldsymbol{\omega}_2 = \min\left(\{\boldsymbol{g}_1, \ldots, \boldsymbol{g}_n\} \setminus \left\{e(\boldsymbol{\omega}_1, 1-\boldsymbol{\omega}_1)^\top : \ e \in \mathfrak{A}^2\right\}\right). \tag{2.7}$$

That way, all $\boldsymbol{\omega}_i$'s can successively be identified and, as $AS\,B(\boldsymbol{\omega}) > 0$, $\boldsymbol{f}$ can be identified. This algorithm is summarized in Figure 2.2.

Unknown number of source components

Note that the algorithm in Figure 2.2 does not require $\boldsymbol{m}$ to be known. Indeed, Theorem 2.1.5 still holds when $\boldsymbol{m}$ is unknown, which is a direct consequence of its proof.

Definition 2.1.8 (Identifiable mixtures for unknown $\boldsymbol{m}$)**.** Consider the FABS model (1.1) with M mixtures and n observations. A pair $(\boldsymbol{\omega}, \boldsymbol{f}) \in \bigcup_{m\geq 2} \Omega_{m,M} \times \mathfrak{A}^{n\times m}$ is identifiable from its mixture $\boldsymbol{g} := \boldsymbol{f}\boldsymbol{\omega}$, if there exists exactly one $(\omega, f) \in \bigcup_{m\geq 2} \Omega_{m,M} \times \mathfrak{A}^{n\times m}$ such that $\boldsymbol{g} = f\omega$.

Theorem 2.1.9. *Consider the FABS model (1.1) for M mixtures and n observations, with $(\boldsymbol{\omega}, \boldsymbol{f}) \in \bigcup_{m\geq 2} \Omega_{m,M} \times \mathfrak{A}^{n\times m}$. If $AS\,B(\boldsymbol{\omega}) > 0$ and $\boldsymbol{f}$ is separable as in A3, then $(\boldsymbol{\omega}, \boldsymbol{f})$ is identifiable.*

Theorem 2.1.9 yields that for

$$\mathcal{M}_m^0 := \{f\omega : \omega \in \Omega_{m,M}, \ AS\,B(\omega) > 0 \text{ and } f \in \mathfrak{A}^{n\times \boldsymbol{m}} \text{ separable}\} \tag{2.8}$$

the following mapping is well defined

$$\mathfrak{m} : \bigcup_{m\geq 2} \mathcal{M}_m^0 \ \to \ \mathbb{N} \text{ s.t. } \mathfrak{m}(g) = m \iff g \in \mathcal{M}_m^0. \tag{2.9}$$

2.2 Exact and stable recovery

Recall that in $\Omega_{\boldsymbol{m},M}$ (see (1.2)) the row-ordering is fixed via $\|\boldsymbol{\omega}_{1\cdot}\| < \ldots < \|\boldsymbol{\omega}_{\boldsymbol{m}\cdot}\|$. To regularize this condition, for $\boldsymbol{\omega} \in \Omega_{\boldsymbol{m},M}$ define analog to the ASB in (1.8) the *weights separation boundary*

$$WSB(\boldsymbol{\omega}) = WSB(\boldsymbol{\omega}, \mathfrak{A}) := \frac{1 + \boldsymbol{m}a_k}{2} \min_{i=2,\ldots,\boldsymbol{m}} \left(\|\boldsymbol{\omega}_{i\cdot}\| - \|\boldsymbol{\omega}_{i-1\cdot}\|\right). \tag{2.10}$$

Definition 2.2.1 (δ-separable)**.** Consider FABS (1.1) with M mixtures and n observations. A pair $(\boldsymbol{\omega}, \boldsymbol{f}) \in \bigcup_{m\geq 2} \Omega_{m,M} \times \mathfrak{A}^{n\times m}$ is *δ-separable* if

1. $ASB(\boldsymbol{\omega}), WSB(\boldsymbol{\omega}) \geq \delta$ as in (1.8) and (2.10) and
2. $\boldsymbol{f}$ fulfills the separability condition A3.

For the following considerations we define the space of δ-separable mixing weights as

$$\Omega^{\delta}_{\boldsymbol{m},M} := \{\omega \in \Omega_{\boldsymbol{m},M} : \ ASB(\omega), WSB(\omega) \geq \delta\} \ \text{ and } \ \Omega^{\delta}_{\boldsymbol{m}} := \Omega^{\delta}_{\boldsymbol{m},1}. \tag{2.11}$$

Remark 2.2.2 (WSB). Note that for all $\boldsymbol{\omega} \in \Omega_{\boldsymbol{m},M}$ in (1.2) it holds that $WSB(\boldsymbol{\omega}) > 0$. Note further that for a single mixture $M = 1$ it holds that $ASB(\boldsymbol{\omega}) < WSB(\boldsymbol{\omega})$ and hence, in Definition 2.2.1 and (2.11) the condition $WSB(\boldsymbol{\omega}) \geq \delta$ can be dropped whenever $M = 1$.

The following theorem goes beyond identifiability. It shows how the parameter δ in (2.11) regularizes FABS. Again, first the results for known number of sources $\boldsymbol{m}$ is given.

Theorem 2.2.3 (Exact recovery)**.** *Consider the FABS model (1.1) for M mixtures, n observations, and given number of sources $\boldsymbol{m}$. Let $\epsilon, \delta > 0$ be such that $\epsilon < \delta/(1 + \boldsymbol{m}a_k)$ and $(\boldsymbol{\omega}, \boldsymbol{f}), (\omega, f) \in \Omega_{\boldsymbol{m},M} \times \mathfrak{A}^{n\times \boldsymbol{m}}$ both δ-separable as in Definition 2.2.1 with*

$$\max_{j=1,\ldots,n} \left\|(\boldsymbol{f}\boldsymbol{\omega})_{j\cdot} - (f\omega)_{j\cdot}\right\| < \epsilon,$$

1. *then* $\max_{i=1,\ldots,\boldsymbol{m}} \|\boldsymbol{\omega}_{i\cdot} - \omega_{i\cdot}\| < \epsilon$ *and*
2. $\boldsymbol{f} = f$.

In words, whenever two δ-separable mixtures are close, then the corresponding sources are equal and the corresponding mixing weights are also close.

Remark 2.2.4 (Converse exact recovery). Note that the converse direction of Theorem 2.2.3 also holds up to a $\boldsymbol{m}a_k$ factor. More precisely, for any $\epsilon > 0$ and $(\boldsymbol{\omega}, \boldsymbol{f}), (\omega, f) \in \Omega_{\boldsymbol{m},M} \times \mathfrak{A}^{n\times \boldsymbol{m}}$, if $\max_{i=1,\ldots,\boldsymbol{m}} \|\boldsymbol{\omega}_{i\cdot} - \omega_{i\cdot}\| < \epsilon$ and $\boldsymbol{f} = f$, then $\max_{j=1,\ldots,n} \left\|(\boldsymbol{f}\boldsymbol{\omega})_{j\cdot} - (f\omega)_{j\cdot}\right\| < \boldsymbol{m}a_k\epsilon$. This follows directly from the triangle inequality.

Next, an exact recovery result for unknown number of sources $\boldsymbol{m}$ is given. In particular, this shows exact recovery of $\mathfrak{m}(\boldsymbol{f}\boldsymbol{\omega})$ in an ϵ-neighborhood of $\boldsymbol{f}\boldsymbol{\omega}$ when $(\boldsymbol{f}, \boldsymbol{\omega})$ is δ-separable. The theorem considers the case $M = 1$ as in the SBSR model (1.3). When $M > 1$, one can adapt the proof of Theorem 2.2.5 accordingly, however, at the price of being less sharp for the case $M = 1$ (see Remark 2.3.11).

Theorem 2.2.5 (Exact recovery for unknown $\boldsymbol{m}$)**.** *Consider the FABS model (1.1) for a single mixtures $M = 1$ and n observations. Let $\epsilon, \delta > 0$ be such that $0 < \epsilon < \delta^{3/2} \,/\, (\sqrt{3}a_k)$ and $(\boldsymbol{\omega}, \boldsymbol{f}), (\omega, f) \in \bigcup_{m\geq 2} \Omega_m \times \mathfrak{A}^{n\times m}$ both δ-separable as in Definition 2.2.1 with*

$$\max_{j=1,\dots,n} \left|(\boldsymbol{f\omega})_j - (f\omega)_j\right| < \epsilon, \tag{2.12}$$

1. *then $\mathfrak{m}(\boldsymbol{f\omega}) = \mathfrak{m}(f\omega)$,*
2. *$\max_{i=1,\dots,\boldsymbol{m}} |\boldsymbol{\omega}_i - \omega_i| < \epsilon$, and*
3. *$\boldsymbol{f} = f$.*

Theorem 2.2.5 yields that as soon as two δ-separable mixtures $\boldsymbol{f\omega}, f\omega$, each having arbitrary number of sources $\mathfrak{m}(\boldsymbol{f\omega})$ and $\mathfrak{m}(f\omega)$, respectively, are closer than $\delta^{3/2}/(\sqrt{3}a_k)$ in sup norm, their underlying sources (including the number of sources) equal. In particular, the threshold value $\delta^{3/2}/(\sqrt{3}a_k)$ only depends on δ but not on the true number of sources of $\boldsymbol{f\omega}$ and $f\omega$. This is in contrast to the corresponding exact recovery result for known number of sources $\mathfrak{m}(\boldsymbol{f\omega}) = \mathfrak{m}(f\omega) = \boldsymbol{m}$ in Theorem 2.2.3, where the corresponding threshold is $\delta/(1 + \boldsymbol{m}a_k)$.

Remark 2.2.6. The condition on the mixtures $\boldsymbol{f\omega}$ and $f\omega$ in Theorem 2.2.5, where the number of sources is unknown, is strictly stronger than in Theorem 2.2.3, where the number of sources $\boldsymbol{m}$ is known. It is shown later in Theorem 2.3.10 that whenever Ω_m^δ in (2.11) is non-empty, then $\delta \leq 2/(m(m+1))$. Thus, as $a_k \geq 1$ and $m \geq 2$ (when $m = 1$ the result is trivial),

$$\frac{\delta^{3/2}}{\sqrt{3}a_k} \leq \delta\sqrt{\frac{2}{3a_k^2 m(m+1)}} \leq \frac{\delta}{1+ma_k}\sqrt{\frac{2(1+m)^2}{3m(m+1)}} \leq \frac{\delta}{1+ma_k}. \tag{2.13}$$

In summary, the price to pay for $\boldsymbol{m}$ not known is an additional shrinkage of the order $\sqrt{\delta}$ in which $\boldsymbol{g}$ can be perturbed while $\boldsymbol{f}$ and $\boldsymbol{m}$ remain exactly recoverable and $\boldsymbol{\omega}$ within an $\delta^{3/2}$-neighborhood.

Example 2.2.7 (Exact recovery)**.** Consider FABS for a single mixture $M = 1$ and a binary alphabet $\mathfrak{A} = \{0, 1\}$, where one wants to guarantee exact recovery of sources in an ϵ-neighborhood, i.e., that for two mixtures $g = f\omega, \boldsymbol{g} = \boldsymbol{f\omega}$

$$\max_{j=1,\dots,n} \left|\boldsymbol{g}_j - g_j\right| \leq \epsilon \quad \Rightarrow \quad f = \boldsymbol{f}. \tag{2.14}$$

First, consider the situation where the number of sources is known and fixed, say $\mathfrak{m}(g) = \mathfrak{m}(\boldsymbol{g}) = m$. Then, Theorem 2.2.3 yields that for (2.14) to hold it suffices that $(\boldsymbol{\omega}, \boldsymbol{f})$ and (ω, f) are $(1 + m)\epsilon$-separable, meaning that $f, \boldsymbol{f}$ are separable as in A3 and $ASB(\omega), ASB(\boldsymbol{\omega}) \geq (1 + m)\epsilon$ as in (1.8), that is, $\omega, \boldsymbol{\omega} \in \Omega_{\boldsymbol{m}}^{(1+m)\epsilon}$ as in (2.11). Figure 2.3 illustrates the space $\Omega_m^{(1+m)\epsilon}$ for two sources ($m = 2$) $\Omega_2^{3\epsilon}$ (the union of the red and blue area in the left figure) and for three sources ($m = 3$) $\Omega_3^{4\epsilon}$ (the union of the red and blue area in the right figure) for $\epsilon = 0.0074$. Note that as $\sum_{i=1}^m \boldsymbol{\omega}_i = 1$ we consider Ω_m as a subset of $\mathbb{R}^{m-1}$. The black lines in Figure 2.3 display non-identifiable ω in Ω_2 and Ω_3 as in (1.2), that is where $ASB(\omega) = 0$. In $\Omega_m^{(1+m)\epsilon}$

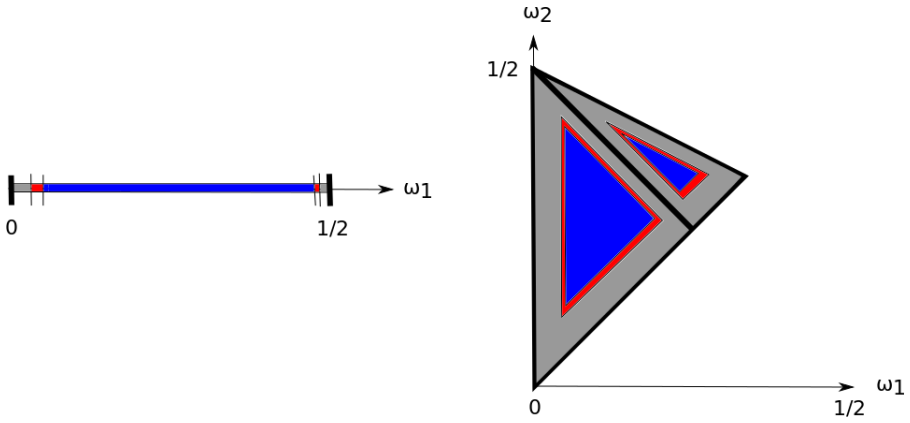

Figure 2.3: Space of possible mixing weights for two Ω_2 (left) and three Ω_3 (right) sources. For a binary alphabet $\mathfrak{A} = \{0, 1\}$ the black lines indicate the non-identifiable region, where $ASB(\omega) = 0$, i.e., $\omega \notin \cup_{\delta>0}\Omega^{\delta}$. The blue region shows the set of mixing weights $\Omega^{0.05}$ which fulfill (2.14) for $\epsilon = 0.0074$ when the number of sources is unknown and arbitrary. The union of the red and the blue region shows the set of mixing weights $\Omega_2^{0.02}$ (left) and $\Omega_3^{0.03}$ (right) which fulfill (2.14) for $\epsilon = 0.0074$ when $m = 2$ (left) and $m = 3$ (right), respectively, is known and fixed.

a $(1 + m)\epsilon$ neighborhood of these non-identifiable regions is removed, illustrated in as gray regions in Figure 2.3. In particular, as m gets larger, the diameter of the gray area in Figure 2.3 increases, reflecting the higher complexity introduced by additional sources. If m gets too large (for fixed ϵ) the gray region covers all possible mixing weights in Ω_m meaning that (2.14) cannot be guaranteed for any mixing weights.

Second, consider the situation where the number of sources is unknown and arbitrary. Then Theorem 2.2.5 yields that for (2.14) to hold it suffices that $(\boldsymbol{\omega}, \boldsymbol{f})$ and (ω, f) are $(\sqrt{3}\epsilon)^{2/3}$-separable, meaning that $f, \boldsymbol{f}$ are separable as in A3 and $ASB(\omega), ASB(\boldsymbol{\omega}) \geq (\sqrt{3}\epsilon)^{2/3}$ as in (1.8), that is, $\omega, \boldsymbol{\omega} \in \Omega_{\boldsymbol{m}}^{(\sqrt{3}\epsilon)^{2/3}}$ as in (2.11). Figure 2.3 illustrates the space $\Omega_2^{(\sqrt{3}\epsilon)^{2/3}} \cup \Omega_3^{(\sqrt{3}\epsilon)^{2/3}}$ (the blue area in Figure 2.3) for $\epsilon = 0.0074$. Note that it is completely surrounded by the red region, meaning that if the number of sources is unknown, the conditions on the parameter space for (2.14) to hold become more restrictive. As the number of sources increases, the difference between the blue and the red area in Figure 2.3 gets smaller. The red region in Figure 2.3 precisely shows those mixing weights for which (2.14) fails when the number of sources is unknown.

2.3 Restrictiveness of separability

In all following considerations, δ-separability in Definition 2.2.1 is fundamental for inferring $\boldsymbol{m}, \boldsymbol{\omega}$, and $\boldsymbol{f}$ from noisy observations in the SBSR model (1.3) and MABS model (1.6), respectively. In the following restrictiveness of this assumption is discussed. To this end, a specific stochastic model for $\boldsymbol{\omega}, \boldsymbol{f}$ has to be considered. Here, the mixing weights $\boldsymbol{\omega}$ are considered as uniformly distributed on $\Omega_{\boldsymbol{m},M}$ (for known number of sources) and $\bigcup_{m\geq 2}\Omega_m$ (for unknown number of sources), respectively. See Remark 2.3.13 for a specification of the latter. For the

sources $\boldsymbol{f}$ Markov processes, including iid sequences, are considered, as e.g., in (Diamantaras and Papadimitriou, 2009; Yau et al., 2011; Rostami et al., 2011).

2.3.1 Separability of stochastic processes

In this subsection it is shortly discuss how likely it is for the separability condition A3 to be satisfied when $(\boldsymbol{f}_{j1}, \dots, \boldsymbol{f}_{j\boldsymbol{m}})_j$ is a stochastic process. Therefore, define the hitting times

$$\mathfrak{T}^r := \min\left\{j \in \mathbb{N} : \left(\boldsymbol{f}_{j1}, \dots, \boldsymbol{f}_{j\boldsymbol{m}}\right) = e^r\right\}, \tag{2.15}$$

for $r = 1, \dots, \boldsymbol{m}$ with e^r the r-th unit vector, and stopping time $\mathfrak{T} := \max_{r=1,\dots,\boldsymbol{m}} \mathfrak{T}^r$. Then it follows that

$$\begin{aligned}\mathbf{P}(\boldsymbol{f} \text{ is separable}) &= \mathbf{P}\left(\exists\, \rho \in S_{\boldsymbol{m}}^n : \left(\boldsymbol{f}_{\rho(r)1}, \dots, \boldsymbol{f}_{\rho(r)\boldsymbol{m}}\right) = e_r,\ r = 1, \dots, \boldsymbol{m}\right) \\ &= \mathbf{P}(\mathfrak{T} \le n) \ge 1 - \sum_{r=1}^{\boldsymbol{m}} \mathbf{P}(\mathfrak{T}^r > n)\,.\end{aligned} \tag{2.16}$$

Note that this bound only depends on the distributions of the hitting times $\mathfrak{T}^r$, which are often explicitly known or good estimates exist. The following theorem shows that the probability in (2.16) converges exponentially fast to one, when $\boldsymbol{f}$ constitutes a Markov process.

Theorem 2.3.1. *Consider the FABS model (1.1) for M mixtures, n observations, and given number of sources $\boldsymbol{m}$. Assume that the source signals $(\boldsymbol{f}_{j1}, \dots, \boldsymbol{f}_{j\boldsymbol{m}})_j$ constitute an irreducible Markov process on the finite state space $\mathfrak{A}^{\boldsymbol{m}}$, with transition matrix $P = (p_{ij})_{1 \le i,j \le k^{\boldsymbol{m}}}$, where we identify the first $\boldsymbol{m}$ states of $\mathfrak{A}^{\boldsymbol{m}}$ with the unit vectors $e^1, \dots, e^{\boldsymbol{m}} \in \mathbb{R}^{\boldsymbol{m}}$. Let $N \in \mathbb{N}$ be such that $P^N > 0$, $Q_r := (p_{ij})_{1 \le i, j \ne r \le k^{\boldsymbol{m}}}$ for $r = 1, \dots, \boldsymbol{m}$, and $c := \max_{1 \le r \le \boldsymbol{m}} \left\|Q_r^N \mathbf{1}\right\|_\infty$. Then $c < 1$ and*

$$\boldsymbol{P}(\boldsymbol{f} \textit{ is separable}) \ge 1 - \boldsymbol{m} c^{\lfloor \frac{n}{N} \rfloor} \ge 1 - \boldsymbol{m} c^{\frac{n-N}{N}}. \tag{2.17}$$

Example 2.3.2 (Bernoulli Model)**.** Consider FABS with a binary alphabet $\mathfrak{A} = \{0, 1\}$ and two sources $\boldsymbol{m} = 2$. If the two sources $\boldsymbol{f}_{j1}$ and $\boldsymbol{f}_{j2}$ are independent and identically distributed for all $j = 1, \dots, n$ with $\mathbf{P}(\boldsymbol{f}_{ji} = 0) = p \in (0, 1)$ and $\mathbf{P}(\boldsymbol{f}_{ji} = 1) = 1 - p =: q$ for $i = 1, 2$ and $j = 1, \dots, n$, then $(\boldsymbol{f}_{j1}, \boldsymbol{f}_{j2})_j$ constitutes an irreducible Markov process on the state space $\{(1, 0), (0, 1), (0, 0), (1, 1)\}$. Hence, in Theorem 2.3.1

$$P = \begin{pmatrix} pq & pq & p^2 & q^2 \\ pq & pq & p^2 & q^2 \\ pq & pq & p^2 & q^2 \\ pq & pq & p^2 & q^2 \end{pmatrix} > 0, \quad Q_1 = Q_2 = \begin{pmatrix} pq & p^2 & q^2 \\ pq & p^2 & q^2 \\ pq & p^2 & q^2 \end{pmatrix},$$

with $N = 1$, and $c = qp + p^2 + q^2 = 1 - pq$. Thus, Theorem 2.3.1 yields $\mathbf{P}(\boldsymbol{f} \text{ is separable}) \ge 1 - 2(1 - pq)^n$.

2.3.2 Alphabet separation boundary

Next, the condition $ASB(\boldsymbol{\omega}) \geq \delta$ in Definition 2.2.1 is considered. To this end, define for the given alphabet $\mathfrak{A}$ in (1.7) and $m \in \mathbb{N}$ the first and second alphabet differences as

$$\Delta\mathfrak{A}^m := \{e_1 - e_2 : e_1 \neq e_2 \in \mathfrak{A}^m\}, \quad \Delta^2\mathfrak{A}^m := \{e_1 - e_2 : e_1 \neq e_2 \in \Delta\mathfrak{A}^m\} \tag{2.18}$$

and note that

$$ASB(\boldsymbol{\omega}) = 0 \quad \Leftrightarrow \quad \boldsymbol{\omega} \in \bigcup_{d \in \Delta\mathfrak{A}^m} d^{\perp}, \tag{2.19}$$

where $d^{\perp}$ denotes the kernel of the map $d : \mathbb{R}^{m\times M} \to \mathbb{R}^M,\ x \mapsto dx$. $d^{\perp}$ is an $M(m-1)$-dimensional linear subspace of $\mathbb{R}^{m\times M}$ and $\Omega_{m,M}$ is a subset of the affine subspace

$$\begin{pmatrix} 1 & 0 & \dots & 0 & 0 \\ 0 & 1 & \dots & 0 & 0 \\ & & \ddots & & \\ 0 & 0 & \dots & 1 & 0 \\ 0 & 0 & \dots & 0 & 1 \end{pmatrix} + \begin{pmatrix} 1 & 1 & \dots & 1 & 1 \\ 1 & 1 & \dots & 1 & 1 \\ & & \ddots & & \\ 1 & 1 & \dots & 1 & 1 \\ 1 & 1 & \dots & 1 & 1 \end{pmatrix}^{\perp}. \tag{2.20}$$

Therefore, $d^{\perp}$ and $\Omega_{m,M}$ are either disjoint or they intersect in a subset of dimension $M(m-2)$, implying that

$$\bigcup_{\delta>0} \Omega_{m,M}^{\delta} = \{\omega \in \Omega_{m,M} :\ ASB(\omega) > 0\}$$

has Lebesgue measure one, where $\Omega_{m,M}$ is considered as a subset of $\mathbb{R}^{(m-1)\times M}$ (recall that $\sum_{i=1}^m \omega_{ij} = 1$ in $\Omega_{m,M}$ for all $j = 1, \dots, M$). This yields the following theorem. To this end, we denote $\boldsymbol{\omega}$ as uniformly distributed on $\Omega_{m,M}$ if for the Lebesgue measure λ on $\mathbb{R}^{(m-1)\times M}$ and a Borel set $A \subset \Omega_{m,M} \subset \mathbb{R}^{(m-1)\times M}$ it holds that $\mathbf{P}(\boldsymbol{\omega} \in A) = \lambda(A)/\lambda(\Omega_{m,M})$.

Theorem 2.3.3. *If $\boldsymbol{\omega}$ is uniformly distributed on the simplex $\Omega_{m,M}$ in (1.2), then for any finite alphabet $\mathfrak{A}$*

$$\boldsymbol{P}(ASB(\boldsymbol{\omega}) > 0) = \boldsymbol{P}\left(\boldsymbol{\omega} \in \bigcup_{\delta>0} \Omega_{m,M}^{\delta}\right) = 1.$$

In particular, Theorem 2.3.3 shows that, for separable sources $\boldsymbol{f}$, $(\boldsymbol{\omega}, \boldsymbol{f})$ is identifiable with probability one. In the statistical settings of the SBSR model (1.3) and the MABS model (1.6) δ-separability is required, for a fixed $\delta > 0$. The following theorem considers the case $M = 1$ and shows that δ-separability is not very restrictive when δ is small. To this end define

$$\Delta\mathfrak{A}_{\min} := \min_{x\in\Delta\mathfrak{A}^1} |x|, \quad \Delta^2\mathfrak{A}_{\min} := \min_{x\in\Delta^2\mathfrak{A}^1} |x|. \tag{2.21}$$

For example, for an equidistant alphabet $\mathfrak{A} = \{0, 1, \dots, k\}$ it holds that $\Delta\mathfrak{A}_{\min} = \Delta^2\mathfrak{A}_{\min} = 1$.

Theorem 2.3.4. *If $\boldsymbol{\omega}$ is uniformly distributed on Ω_m in (1.2) and $\mathfrak{A}$, $0 < \delta < \Delta\mathfrak{A}_{\min}$, then*

$$\boldsymbol{P}(AS\,B(\boldsymbol{\omega}) \geq \delta) = \boldsymbol{P}(\boldsymbol{\omega} \in \Omega_m^{\delta}) \geq 1 - \frac{k^{2m}\, m^2(m-1)}{\sqrt{2}\,\Delta^2\mathfrak{A}_{\min}}\,\delta.$$

Theorem 2.3.4 is stated for single mixtures ($M = 1$). It is easy to check that $AS\,B(\boldsymbol{\omega})$ for $\boldsymbol{\omega}$ uniformly distributed on $\Omega_{m,M}$ is monotone increasing in M, in the sense that for a fixed $x > 0$ it holds that $\mathbf{P}(AS\,B(\boldsymbol{\omega}) > x)$ increases with M. Thus, Theorem 2.3.4 also holds when $M > 1$. However, when M increases the bound on the r.h.s. of Theorem 2.3.4 becomes less sharp. The following theorem shows that $AS\,B(\boldsymbol{\omega})$ increases with rate $\sqrt{M}$. To this end, define the constants (for fixed alphabet $\mathfrak{A}$ and number of sources $\boldsymbol{m}$)

$$c = c(m, \mathfrak{A}) \coloneqq \frac{\sqrt{2}\,\Delta^2\mathfrak{A}_{\min}}{\sqrt{3}k^{2m}\, m^2(m-1)}, \quad C = C(m, \mathfrak{A}) \coloneqq \frac{\sqrt{2}(1 + ma_k)}{\sqrt{m(m-1)}}. \tag{2.22}$$

Theorem 2.3.5. *If $\boldsymbol{\omega}$ is uniformly distributed on $\Omega_{m,M}$ in (1.2), then for c, C as in (2.22) it holds almost surely that*

$$c < \liminf_{M\to\infty} \frac{AS\,B(\boldsymbol{\omega})}{\sqrt{M}} \leq \limsup_{M\to\infty} \frac{AS\,B(\boldsymbol{\omega})}{\sqrt{M}} < C.$$

Theorem 2.3.4 shows that for uniformly distributed $\boldsymbol{\omega} \in \Omega_{\boldsymbol{m}}$ the probability of $AS\,B(\boldsymbol{\omega}) \geq \delta$ is at least of order $1 - O(\delta)$. The following theorem shows that $\mathbf{P}(AS\,B(\boldsymbol{\omega}) < \delta)$ is, indeed, a polynomial in δ of order $\boldsymbol{m} - 1$.

Theorem 2.3.6. *If $\boldsymbol{\omega}$ is uniformly distributed on $\Omega_{\boldsymbol{m}}$ in (1.2), then there exist constants $c_i = c_i(\mathfrak{A}, \boldsymbol{m})$, $i = 1, \ldots, \boldsymbol{m} - 1$, such that*

$$\boldsymbol{P}(AS\,B(\boldsymbol{\omega}) < \delta) = c_1\delta + c_2\delta^2 + \ldots + c_{\boldsymbol{m}-1}\delta^{\boldsymbol{m}-1}.$$

In the following, the constants $c_1, \ldots, c_{\boldsymbol{m}-1}$ in Theorem 2.3.6 are computed explicitly for some examples and sharpness of the bound in Theorem 2.3.4 is explored.

Example 2.3.7 (Binary alphabet and two sources)**.** Consider FABS for a binary $\mathfrak{A} = \{0, 1\}$, a single mixture $M = 1$, and $\boldsymbol{m} = 2$ sources. For $\boldsymbol{\omega} \in \Omega_2$

$$AS\,B(\boldsymbol{\omega}) = \min(\boldsymbol{\omega}_1, \boldsymbol{\omega}_2 - \boldsymbol{\omega}_1) = \min(\boldsymbol{\omega}_1, 1 - 2\boldsymbol{\omega}_1).$$

Hence, Ω_2 corresponds to the interval $[0, 1/2]$ and Ω_2^{δ} to $[\delta, (1-\delta)/2]$ (cf. Figure 2.3, left) , which implies

$$\mathbf{P}(AS\,B(\boldsymbol{\omega}) \geq \delta) = (1 - 3\delta)_+,$$

where $(x)_+ \coloneqq \max(x, 0)$. The bound in Theorem 2.3.4 for $k = 2$, $\boldsymbol{m} = 2$, and $\Delta^2\mathfrak{A}_{\min} = 1$ only yields $\mathbf{P}(AS\,B(\boldsymbol{\omega}) \geq \delta) \geq 1 - 45.3\delta$. One reason for this gap is that in the proof of Theorem 2.3.4 the number of hyperplanes $d^{\perp}$ with $d \in \Delta\mathfrak{A}^m$ as in (2.19) which intersect $\Omega_{\boldsymbol{m}}$ is bounded by half the number of elements in $\Delta\mathfrak{A}^{\boldsymbol{m}}$, namely $k^{2\boldsymbol{m}}/2$. In this example $k^{2\boldsymbol{m}}/2 = 8$. However,

the actual number of intersecting hyperplanes is just 2.

Example 2.3.8 (Binary alphabet and three sources)**.** Consider FABS for a binary $\mathfrak{A} = \{0, 1\}$, a single mixture $M = 1$, and $\boldsymbol{m} = 3$ sources. For $\boldsymbol{\omega} \in \Omega_3$

$$\begin{aligned} AS\,B(\boldsymbol{\omega}) &= \min(\omega_1, \omega_2 - \omega_1, \omega_3 - \omega_2, |\omega_3 - \omega_1 - \omega_2|) \\ &= \min(\omega_1, \omega_2 - \omega_1, 1 - \omega_1 - 2\omega_2, |1 - 2\omega_1 - 2\omega_2|). \end{aligned}$$

Hence, Ω_3 and Ω_3^δ correspond to the two dimensional sets in Figure 2.3 (right). Let λ denote the Lebesgue measure in $\mathbb{R}^2$, then from Figure 2.3 (right) it follows that $\lambda(\Omega_3) = \frac{1}{12}$ and

$$\begin{aligned} \lambda(\Omega_3^\delta) &= \left(\int_\delta^{\frac{1-3\delta}{4}} \int_{\omega_1+\delta}^{\frac{1-\delta-2\omega_1}{2}} d\omega_2 d\omega_1 + \int_{2\delta}^{\frac{1-\delta}{4}} \int_{\frac{1+\delta-2\omega_1}{2}}^{\frac{1-\delta-\omega_1}{2}} d\omega_2 d\omega_1 + \int_{\frac{1-\delta}{4}}^{\frac{1-3\delta}{3}} \int_{\omega_1+\delta}^{\frac{1-\delta-\omega_1}{2}} d\omega_2 d\omega_1 \right)_+ \\ &= \left(\frac{1}{12} - \frac{5}{4}\delta + \frac{11}{4}\delta^2 \right)_+ . \end{aligned}$$

Thus, if $\boldsymbol{\omega}$ is uniformly distributed on Ω_3

$$\mathbf{P}(AS\,B(\boldsymbol{\omega}) > \delta) = (1 - 15\delta + 33\delta^2)_+.$$

For $k = 2$, $\boldsymbol{m} = 3$, and $\Delta^2\mathfrak{A}_{\min} = 1$, as in this example, Theorem 2.3.4 only yields $\mathbf{P}(AS\,B(\boldsymbol{\omega}) > \delta) \geq 1 - 814.6\delta$. As in example Example 2.3.7, replacing $k^{2\boldsymbol{m}}/2 = 32$ in the bound of Theorem 2.3.4 by the actual number of intersecting hyperplanes (which in this case is 4) results in a sharper bound.

Example 2.3.7 and 2.3.8 motivate to further bound the number of $d \in \Delta\mathfrak{A}^{\boldsymbol{m}}$ such that $d^\perp \cap \Omega^{\boldsymbol{m}} \neq \emptyset$, which is done in the following example for an equidistant alphabet.

Example 2.3.9 (General equidistant alphabets)**.** Assume an equidistant alphabet $\mathfrak{A} = \{0, 1, \ldots, k-1\}$. Then in (2.21)

$$\Delta\mathfrak{A}^m = \{-(k-1), \ldots, -1, 0, 1, \ldots, (k-1)\}^m \backslash \{(0, \ldots, 0)^\top\},$$

and in particular $\#\Delta\mathfrak{A}^m = (2k-1)^m - 1$. Further, for all $\boldsymbol{\omega} \in \Omega_m$ and $d \in \Delta\mathfrak{A}^m$ such that $d_1, \ldots, d_{m-1} \geq 0$ and $d_m > 0$ (or $d_1, \ldots, d_{m-1} \leq 0$ and $d_m < 0$) it follows that $|\langle \boldsymbol{\omega}, d \rangle| > 1/m$, which implies that $\boldsymbol{\omega} \notin d^\perp$. Consequently,

$$\#\{d \in \Delta\mathfrak{A}^m : d^\perp \cap \Omega_m \neq \emptyset\} \leq (2k-1)^m - 1 - 2k^{m-1}(k-1).$$

Thus, it follows from (the proof of) Theorem 2.3.4 that if $\boldsymbol{\omega}$ is uniformly distributed on Ω_m, then for any $\delta < 1$

$$\mathbf{P}(AS\,B(\boldsymbol{\omega}) > \delta) \geq 1 - \frac{\left((2k-1)^m - 1 - 2k^{m-1}(k-1)\right) m^2(m-1)}{\sqrt{2}}\,\delta.$$

For the setting of Example 2.3.7 with $k = 2$ and $m = 2$ this gives $\mathbf{P}(AS\,B(\boldsymbol{\omega}) > \delta) \geq 1 - 11.3\,\delta$

and for the setting of Example 2.3.8 with $k = 2$ and $m = 3$ this gives $\mathbf{P}(AS\,B(\boldsymbol{\omega}) > \delta) \geq 1 - 229\,\delta$, which both improve the bound from Theorem 2.3.4 for general alphabets.

2.3.3 Known vs. unknown number of sources

In Section 2.3.1 and 2.3.2 restrictiveness of δ-separability in FABS was considered for known number of sources $\boldsymbol{m}$. This subsection considers unknown $\boldsymbol{m}$. We restrict to single mixtures $M = 1$ as in the SBSR model (1.3).

First, note that in the definition of Ω_m^δ in (2.11) m and δ are related. On the one hand, for given $\delta > 0$, Ω_m^δ is nonempty (i.e., there exist $\omega \in \Omega_m$ with $AS\,B(\omega) \geq \delta$) only up to a certain maximal $m \in \mathbb{N}$ and, on the other hand, for given $m \in \mathbb{N}$, δ must be chosen sufficiently small for Ω_m^δ to be nonempty. Put it differently, the ASB δ implicitly gives a bound on the maximal number of source components which can be identified. An explicit bound is given as follows.

Theorem 2.3.10. *For any alphabet $\mathfrak{A}$ as in (1.7) and $m \in \mathbb{N}$ it holds that*

$$\max_{\omega\in\Omega_m} AS\,B(\omega) \leq \min\left(\frac{2\min_{j=1,\dots,k-1}(a_{j+1} - a_j)}{m(m+1)}, \frac{a_k}{k^m - 1}\right) \leq \min\left(\frac{2}{m(m+1)}, \frac{a_k}{k^m - 1}\right).$$

Remark 2.3.11 (ASB-bound for general M). In Lemma A.1.2 in the appendix we derive the bound

$$\max_{\omega\in\Omega_{m,M}} AS\,B(\omega) \leq \frac{\sqrt{M}(1 + ma_k)}{\sqrt{2m(m+1)}},$$

which is valid for any number of mixtures M (not just for $M = 1$ as in Theorem 2.3.10). However, whereas the bound in Theorem 2.3.10 decreases with m, the general bound in Lemma A.1.2 is (for large m) constant in m and thus, for the specific case of a single linear mixture $M = 1$ trivial. However, this is not true when M gets large. For instance, in Lemma A.1.4 we show that for the special case where $M/m \in \mathbb{N}$

$$\max_{\omega\in\Omega_{m,M}} AS\,B(\omega) \geq 0.2\Delta\mathfrak{A}_{\min}\sqrt{M/m},$$

which shows that for general M the maximal ASB decreases with m at most of order $1/\sqrt{m}$ and not of order $1/m^2$ as in Theorem 2.3.10 for $M = 1$.

Note that in Theorem 2.3.10 it depends on the specific alphabet and the number of sources m which of the two terms in the minimum on the right hand side is attained. While the second term, which is exponential in m, depends on the diameter of the alphabet, the first term, which is quadratic in m, is independent of the specific alphabet $\mathfrak{A}$. For a given alphabet $\mathfrak{A}$ and a given number of sources $\boldsymbol{m}$ one can compute $\max_{\omega\in\Omega_m} AS\,B(\omega)$ with linear programming (see Section 5.1). Figure 2.4 shows $\max_{\omega\in\Omega_m} AS\,B(\omega, \mathfrak{A})$ and the upper bound from Theorem 2.3.10 for different alphabets and number of sources. It shows that for equidistant alphabet $\mathfrak{A} = \{0, 1, \dots, k\}$ the bound in Theorem 2.3.10 is sharp. However, for non-equidistant alphabet, e.g., $\mathfrak{A} = \{0, 1, 1.1, 1.5, a_k\}$, for $a_k = 2, \dots, 10$ as in Figure 2.4, it is not sharp, in general.

In particular, Theorem 2.3.10 shows that if $\boldsymbol{\omega}$ is uniformly distributed on $\Omega_{\boldsymbol{m}}$ then for any $\delta > 0$

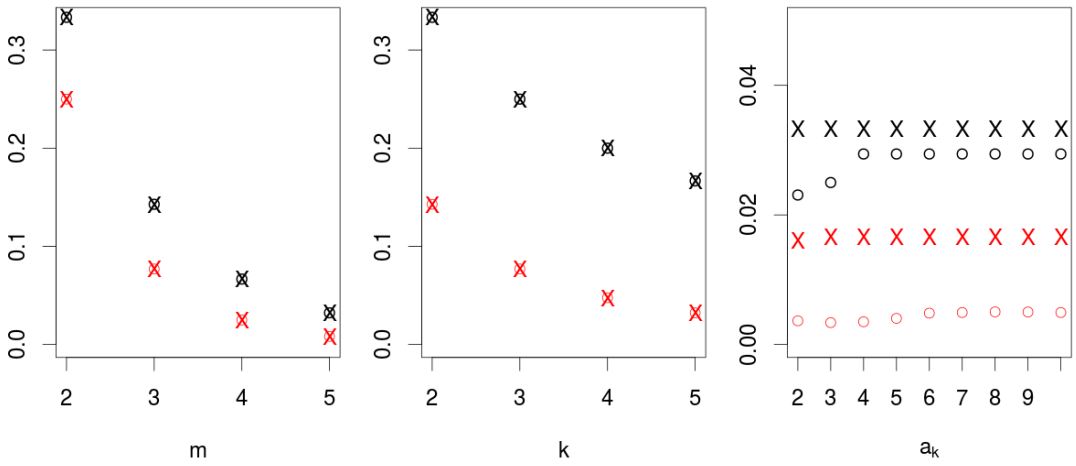

Figure 2.4: Exact value for $\max_{\omega\in\Omega_m} AS\,B(\omega,\mathfrak{A})$ (cirels) and upper bound from Theorem 2.3.10 (crosses). Left: $\mathfrak{A} = \{0,1\}$ (black) and $\mathfrak{A} = \{0,1,2\}$ (red), for $m = 2,\ldots,5$. Middel: $m = 2$ (black) and $m = 3$ (red), with $\mathfrak{A} = \{0,1,\ldots,k-1\}$, for $k = 2,\ldots,5$. Left: $m = 2$ (black) and $m = 3$ (red), with $\mathfrak{A} = \{0,1,1.1,1.5,a_k\}$, for $a_k = 2,\ldots,10$.

it holds true that $\mathbf{P}(AS\,B(\boldsymbol{\omega}) \geq \delta) \to 0$ as $\boldsymbol{m} \to \infty$. So in particular, when $\boldsymbol{m}$ is unknown, in order to achieve identifiability, it is necessary that $\boldsymbol{m}$ is reasonably small with high probability. The following theorem shows that if $\boldsymbol{\omega}$ is distributed on $\Omega = \bigcup_{m=2}^{\infty}\Omega_m$ such that $\mathbf{P}(\boldsymbol{m} = m)$ is proportional to the relative size of $\Omega_m \subset \mathbb{R}^{m-1}$ and $\boldsymbol{\omega}|\{\boldsymbol{m} = m\}$ is uniformly distributed on Ω_m, then $\mathbf{P}\left(AS\,B(\boldsymbol{\omega}) \geq \delta\right) = \sum_{m=2}^{\infty}\mathbf{P}\left(AS\,B(\boldsymbol{\omega}) \geq \delta|\boldsymbol{m} = m\right)\mathbf{P}\left(\boldsymbol{m} = m\right)$ is of order $1 - O(\delta)$.

Theorem 2.3.12. *If $\boldsymbol{\omega}$ is uniformly distributed on $\Omega = \bigcup_{m=2}^{\infty}\Omega_m$ in (1.2), as in Remark 2.3.13, and $0 < \delta < \Delta\mathfrak{A}_{\min}$, then*

$$\boldsymbol{P}(AS\,B(\boldsymbol{\omega}) \geq \delta) \geq 1 - \frac{k^3}{\sqrt{2}\Delta^2\mathfrak{A}}\frac{2I_1(2k) + kI_2(2k)}{I_1(2) - 1}\,\delta,$$

where $I_1(\cdot)$ and $I_2(\cdot)$ denote the modified Bessel functions of the first and second kind.

The terms $I_1(2k)$ and $I_2(2k)$ in the constant of the lower bound in Theorem 2.3.12 increase exponentially in k. Thus, analog as for $\boldsymbol{m}$ itself, in order to achieve identifiability for unknown $\boldsymbol{m}$, the size of the alphabet k should be small (relative to the noise variance with $k \lesssim \ln(1/\sigma)$).

Remark 2.3.13 (Uniform distribution on Ω). The uniform distribution on the disjoint union $\Omega = \bigcup_{m=2}^{\infty}\Omega_m$ in Theorem 2.3.12 is to be understood as follows. $S \subset \Omega$ is measurable if and only if $S \cap \Omega_m$ is Borel measurable in $\mathbb{R}^{m-1}$ for all $m \geq 2$, where Ω_m is considered as a subset of $\mathbb{R}^{m-1}$. Let λ^m be the Lebesgue measure on $\mathbb{R}^m$, then, as $\sum_{m=2}^{\infty}\lambda^{m-1}(\Omega_m) < \infty$ (see proof of Theorem 2.3.12), one can define a uniform distribution on Ω as

$$\mu(S) := \frac{\sum_{m=2}^{\infty}\lambda^{m-1}(S \cap \Omega_m)}{\sum_{m=2}^{\infty}\lambda^{m-1}(\Omega_m)} \quad \text{for any measurable } S \subset \Omega.$$

Finally, we can combine Theorem 2.3.12, 2.3.10, and 2.3.1 to get the following corollary.

Corollary 2.3.14 (Probability of δ-separability)**.** *For a given alphabet $\mathfrak{A}$ let $0 < \delta < \Delta\mathfrak{A}_{\min}$. If*

$\boldsymbol{\omega}$ is uniformly distributed on $\Omega = \bigcup_{m=2}^{\infty} \Omega_m$ and $\{\boldsymbol{f}_j\}_{j=1,\ldots,n}$ constitute an irreducible Markov process independent of $\boldsymbol{\omega}$, then there exists a constant $c = c(\delta) < 1$ and $N = N(\delta) \in \mathbb{N}$, which both only depend on the transition probabilities of $\boldsymbol{f}$, such that

$$\boldsymbol{P}\left((\boldsymbol{\omega}, \boldsymbol{f}) \text{ is } \delta\text{-separable }\right) \geq 1 - \sqrt{\frac{2}{\delta}}\, c^{\frac{n-N}{N}} - \frac{k^3}{\sqrt{2}\Delta^2 \mathfrak{A}} \frac{2I_1(2k) + kI_2(2k)}{I_1(2) - 1}\, \delta.$$

2.4 Extensions

In the following a few extensions of identifiability for FABS are considered.

2.4.1 Arbitrary mixing weights

So far, we assumed the mixing weights to be positive and to sum up to one. This assumption is motivated from the application in cancer genetics, where the mixing weights correspond to physical mixing proportions. However, in some other applications this assumption is not satisfied. For instance, in digital communications the mixing weights correspond to the channel response which can be negative (see e.g., (Proakis, 2007)). In the following separability is extended for arbitrary mixing weights and single mixtures $M = 1$.

To this end, note that if the alphabet $\mathfrak{A} = \{a_1, a_2, \ldots, a_{k-1}, a_k\}$ with $a_1 < a_2 < \ldots < a_{k-1} < a_k$ is symmetric, i.e., $a_{l+1} - a_l = a_{k-l+1} - a_{k-l}$ for $l = 1, \ldots, k-1$, then w.l.o.g. one can rescale the alphabet such that

$$\mathfrak{A} = \begin{cases} \{-a_{k^\star}, \ldots, -a_1, a_1, \ldots, a_{k^\star}\}, & k^\star := k/2 \text{ if } k \text{ even} \\ \{-a_{k^\star}, \ldots, -a_1, 0, a_1, \ldots, a_{k^\star}\}, & k^\star := (k-1)/2 \text{ if } k \text{ odd} \end{cases}.$$

In particular, $\boldsymbol{f}^i \in \mathfrak{A}^n$ implies $-\boldsymbol{f}^i \in \mathfrak{A}^n$ and thus, for arbitrary (possibly negative) mixing weights and sources $\boldsymbol{f} \in \mathfrak{A}^{n \times \boldsymbol{m}}$

$$\sum_{i=1}^{\boldsymbol{m}} \boldsymbol{f}^i \boldsymbol{\omega}_i = \sum_{\substack{i=1 \\ \boldsymbol{\omega}_i > 0}}^{\boldsymbol{m}} \boldsymbol{f}^1 \left|\boldsymbol{\omega}_i\right| + \sum_{\substack{i=1 \\ \boldsymbol{\omega}_i < 0}}^{\boldsymbol{m}} -\boldsymbol{f}^1 \left|\boldsymbol{\omega}_i\right| = \sum_{i=1}^{\boldsymbol{m}} f^i \left|\boldsymbol{\omega}_i\right|$$

with $f^i = \boldsymbol{f}^i$ if $\boldsymbol{\omega}_i > 0$, $f^i = -\boldsymbol{f}^i$ if $\boldsymbol{\omega}_i \leq 0$, and $f \in \mathfrak{A}^{n \times \boldsymbol{m}}$. Consequently, for symmetric alphabets, one can restrict to positive weights (as in Theorem 2.1.5). Therefore, in the following theorem, we only consider non-symmetric alphabet with $a_2 - a_1 \neq a_k - a_{k-1}$.[1] For given

[1] In (Behr and Munk, 2017a, Theorem 7.1) this assumption was missing.

$m, s \in \mathbb{N}$ with $s \leq m$ and $a, b, c \in \mathbb{R}$ define the matrix

$$A^s(a,b,c) := \left(\begin{array}{ccccc|cccc} b & b & b & \dots & b & c & c & \dots & c \\ \hline a & b & b & \dots & b & c & c & \dots & c \\ b & a & b & \dots & b & c & c & \dots & c \\ & & \ddots & & & & & \vdots & \\ b & b & b & \dots & a & c & c & \dots & c \\ \hline c & c & c & \dots & c & a & b & \dots & b \\ c & c & c & \dots & c & b & a & \dots & b \\ & & & \vdots & & & & \ddots & \\ c & c & c & \dots & c & b & b & \dots & a \end{array}\right) \in \mathbb{R}^{(m+1)\times m}, \tag{2.23}$$

with

$$(A^s(a,b,c))_{ij} = \begin{cases} a & \text{if } i = j \\ c & \text{if } i \leq s < j \text{ or } j \leq s < i \\ b & \text{otherwise} \end{cases}.$$

Theorem 2.4.1 (Separability for arbitrary mixing weights)**.** *Consider the FABS model (1.1) for a single mixtures $M = 1$, n observations, and given number of sources $\boldsymbol{m}$, with general mixing weights $\boldsymbol{\omega} \in \{x \in \mathbb{R}^{\boldsymbol{m}} : x_1 < \ldots < x_{\boldsymbol{m}}\}$ and sources $\boldsymbol{f} \in \mathfrak{A}^{n\times \boldsymbol{m}}$ for the finite alphabet $\mathfrak{A} = \{a_1, a_2, \ldots, a_{k-1}, a_k\}$ with $a_1 < \ldots < a_k$ and $a_2 - a_1 \neq a_k - a_{k-1}$.*
Assume that $ASB(\boldsymbol{\omega}) > 0$ and let $s \in \{0, \ldots, \boldsymbol{m}\}$ be such that $\boldsymbol{\omega}_s \leq 0 < \boldsymbol{\omega}_{s+1}$ (with $\boldsymbol{\omega}_0 := 0$ and $\boldsymbol{\omega}_{\boldsymbol{m}+1} := 1$). If there exists $\rho \in S^n_{2(\boldsymbol{m}+1)}$ such that

$$\left(\boldsymbol{f}_{\rho(r)1}, \ldots, \boldsymbol{f}_{\rho(r)\boldsymbol{m}}\right)_{1\leq r\leq 2(\boldsymbol{m}+1)} = \begin{pmatrix} A^s(a_2, a_1, a_k) \\ A^s(a_{k-1}, a_k, a_1) \end{pmatrix} \tag{2.24}$$

then $(\boldsymbol{\omega}, \boldsymbol{f})$ is identifiable.

Recall that for positive mixing weights the separability condition A3 in Theorem 2.1.5 had a very simple interpretation, namely, that each of the single mixing weights $\boldsymbol{\omega}_i$ appears somewhere in the mixture $\boldsymbol{g}$, see (1.9). The interpretation of (2.24) is somewhat more difficult, but similar. In the case of probability mixing weights $\boldsymbol{\omega} \in \Omega_{\boldsymbol{m}}$ as in (1.2) both, the sum and the absolute sum of the mixing weights are fixed via $\sum_{i=1}^{\boldsymbol{m}} \boldsymbol{\omega}_i = \sum_{i=1}^{\boldsymbol{m}} |\boldsymbol{\omega}_i| = 1$ and this determines the scaling factor of the mixing weights in the mixture $\boldsymbol{g}$. Now, for general mixing weights $\boldsymbol{\omega} \in \{x \in \mathbb{R}^{\boldsymbol{m}} : x_1 < \ldots < x_{\boldsymbol{m}}\}$ as in Theorem 2.4.1 both, the sum and the absolute sum (or equivalently the sum of the negative mixing weights and the sum of the positive mixing weights) are unknown and thus, additional conditions to determined these unknown scaling parameters are needed. These correspond to the first rows of $A^s(a_2, a_1, a_k)$ and $A^s(a_{k-1}, a_k, a_1)$ in (2.23), respectively. They ensure that the smallest possible mixture value (which corresponds to the first row of $A^s(a_2, a_1, a_k)$) and the largest possible mixture value (which corresponds to the

first row of $A^s(a_{k-1}, a_k, a_1)$) are observed and thus determine these scaling factors. Analog to the identity matrix in A3 of Theorem 2.1.5, the last $\boldsymbol{m}$ rows of $A^s(a_2, a_1, a_k)$ and $A^s(a_{k-1}, a_k, a_1)$ in (2.23) ensure that the mixing weights $\boldsymbol{\omega}_i$ appear somewhere in the mixture $\boldsymbol{g}$ without the influence of the others. However, the unknown sign of $\boldsymbol{\omega}_i$ yields the additional unambiguity of a mixture value being increased either by increasing a source with a positive weight or by decreasing a source with a negative weight.
Note that from Theorem 2.4.1 it follows directly that Theorem 2.3.1 holds with $\boldsymbol{m}$ replaced by $2\boldsymbol{m} + 2$, when we allow for arbitrary mixing weights.

2.4.2 Unknown alphabet

The fundamental assumption in FABS is the given finite alphabet $\mathfrak{A}$ for the sources $\boldsymbol{f}$, which allows to explore the combinatorial structure to identify $\boldsymbol{\omega}$ and $\boldsymbol{f}$ from its mixture. The following theorem shows that for $\boldsymbol{m} = 2$ and $M = 1$ knowledge of existence of a finite source alphabet can still yield identifiability even if the alphabet is unknown.
To this end, for a set $\mathfrak{A} := \{a_1, \ldots, a_k\} \subset \mathbb{R}$ with $a_1 < \ldots < a_k$ define the *odds separation boundary*

$$OSB(\mathfrak{A}) := \min_{2 \le l, l' \le k-1} \left| \frac{a_2 - a_1}{a_k - a_{k-1}} - \frac{a_{l+1} - a_1}{a_k - a_{k-l'}} \right|, \tag{2.25}$$

with the convention that $\min(\emptyset) = \infty$, and the matrix

$$A(\mathfrak{A}) := \begin{pmatrix} a_1 & a_1 & a_1 & \ldots & a_1 & a_2 & a_3 & \ldots & a_k \\ a_1 & a_2 & a_3 & \ldots & a_k & a_k & a_k & \ldots & a_k \end{pmatrix}^\top. \tag{2.26}$$

Theorem 2.4.2 (Identifiability for unknown alphabet)**.** *For $n \in \mathbb{N}$ let $\boldsymbol{\omega} \in \Omega_2$ and $\boldsymbol{f} \in \mathbb{R}^{2\times n}$. Define $\mathfrak{A} = \{a_1, a_2, \ldots, a_k\} := \{\boldsymbol{f}_{ij} : \ i = 1, 2 \ j = 1, \ldots, n\}$ with $a_1 < \ldots < a_k$.*
If $ASB(\boldsymbol{\omega}, \mathfrak{A}) > 0$ in (1.8), $OSB(\mathfrak{A}) > 0$ in (2.25), and there exists $\rho \in S^n_{2k-1}$ such that

$$\left(\boldsymbol{f}_{\rho(r)1}, \boldsymbol{f}_{\rho(r)2}\right)_{1 \le r \le (2k-1)} = A(\mathfrak{A}), \tag{2.27}$$

then $(\boldsymbol{\omega}, \boldsymbol{f})$ is identifiable from $\boldsymbol{g} = \boldsymbol{f}\boldsymbol{\omega}$.

The identifiability conditions in Theorem 2.4.2 are analog to separability in Theorem 2.1.5. The condition $ASB(\boldsymbol{\omega}, \mathfrak{A}) > 0$ ensures that, once the alphabet $\mathfrak{A}$ and the mixing weights $\boldsymbol{\omega}$ are identified, $\boldsymbol{f}$ is identifiable from $\boldsymbol{g}$, i.e., it ensures that different source values lead to different mixtures values, which is necessary for identifiability. The second condition, $OSB(\mathfrak{A}) > 0$, is a condition on the (unknown) alphabet $\mathfrak{A}$. It ensures that $\mathfrak{A}$ does not exhibit a certain symmetry such that the order statistic of $\boldsymbol{g}_j$ allows to reconstruct the weights $\boldsymbol{\omega}$ without knowledge of $\mathfrak{A}$. For instance, for any equidistant alphabet $\mathfrak{A} = \{a_0 + L, a_0 + 2L, \ldots, a_0 + kL\}$ with diameter L of size $k \ge 3$ it holds that $OSB(\mathfrak{A}) = 0$. On the other hand, if the alphabet is drawn uniformly on some bounded subset of $\mathbb{R}^k$, then $OSB(\mathfrak{A}) > 0$ almost surely. Condition (2.24) is analog to A3 (and (2.24)) as it requires *some* specific alphabet values to appear somewhere in the sources $\boldsymbol{f}$.

Remark 2.4.3. The condition $OSB(\mathfrak{A}) > 0$ in Theorem 2.4.2 can be replaced by the weaker

condition that for every $2 \leq l, l' \leq k-1$ at least one of the following holds

$$\left| \frac{a_2 - a_1}{a_k - a_{k-1}} - \frac{a_{l+1} - a_1}{a_k - a_{k-l'}} \right| > 0, \quad \max\left(\frac{a_k - a_{k-l'}}{a_k - a_{k-1}}, \frac{a_{l+1} - a_1}{a_2 - a_1} \right) > \frac{1 - \omega_1}{\omega_1}.$$

Remark 2.4.4 (Infinite alphabets). Another direction to relax the assumption of a known finite alphabet in FABS, is to assume a known, but infinite alphabet. Clearly, $AS\,B(\boldsymbol{\omega}) > 0$ remains necessary for identifiability. This condition, however, becomes significantly more restrictive when the size of the alphabet increases. For example, for any infinite alphabet with a limit point, in particular, any bounded infinite alphabet, it follows immediately that $AS\,B(\boldsymbol{\omega}) = 0$ for any $\boldsymbol{\omega} \in \Omega$. But also for the unbounded infinite alphabet $\mathfrak{A} = \mathbb{N}$ there exists no $\boldsymbol{\omega} \in \Omega$ with $AS\,B(\boldsymbol{\omega}) > 0$. To see this, fix some $m \geq 2$ and $\boldsymbol{\omega} \in \Omega_m$ and w.l.o.g. assume that $\omega_1 \in \mathbb{Q}$, i.e., $\omega_1 = n/d$ with $n, d \in \mathbb{N}$ and $d > n$. Then, $\tilde{d} := (d-n)d \in \mathbb{N}$, $n \cdot d \in \mathbb{N}$, and

$$AS\,B(\boldsymbol{\omega}) \leq \left| \left(\tilde{d}\omega_1 + 0 \cdot (1 - \omega_1) \right) - (0 \cdot \omega_1 + nd\,(1 - \omega_1)) \right| = 0.$$

Hence, finiteness of the alphabet $\mathfrak{A}$ is somewhat fundamental for identifiability in FABS.

CHAPTER 3

Multiscale segmentation of single mixtures

In this chapter the SBSR model (1.3) is considered with underlying separable mixture $\boldsymbol{g} \in \mathcal{M}_{\boldsymbol{m}}^{\delta,\lambda}$ as in (1.11) for given minimal ASB $\delta > 0$ and minimal scale[1] $\lambda \geq 1/n$. First, a known number of sources $\boldsymbol{m}$ is assumed. Model selection for unknown $\boldsymbol{m}$ is considered in Section 3.6.

For simplicity, in (1.3) it is assumed that $\boldsymbol{g}$ is sampled equidistantly at $x_j = (j-1)/n$, $j = 1, \ldots, n$ and that all functions are defined on the domain $[0, 1)$. Extensions to more general domains $\subseteq \mathbb{R}$ and sampling designs are straightforward under suitable assumptions (see e.g., (Boysen et al., 2009)) but will be suppressed to ease notation. Further, for sake of brevity, in (1.3) it is assumed that the variance σ^2 is known, otherwise one may pre-estimate it $\sqrt{n}$-consistently by standard methods, see e.g., (Müller and Stadtmüller, 1987; Hall et al., 1990; Dette et al., 1998; Davies and Kovac, 2001).

3.1 Confidence region for the weights

Let Y and $\boldsymbol{g} = \boldsymbol{f}\boldsymbol{\omega} \in \mathcal{M}_{\boldsymbol{m}}^{\delta,\lambda}$ be as in the SBSR model (1.3). Our starting point for the recovery of the weights $\boldsymbol{\omega}$ and the sources $\boldsymbol{f}$ is the construction of proper confidence sets for $\boldsymbol{\omega}$ which is also of statistical relevance by its own as the source functions are unknown which hinders direct inversion of a confidence set for $\boldsymbol{g}$. Consider the system of boxes $\mathfrak{B} = \mathfrak{B}^\lambda = \{B(i, j) : 1 \leq i \leq j \leq n,\ j - i + 1 \geq n\lambda\}$ from (1.18) with $q = q_n(\alpha)$ as in (1.19) for some given $\alpha \in (0, 1)$, as described in Section 1.3. As the underlying sources $\boldsymbol{f}$ are assumed to be separable (see (1.12)) there exist intervals $[x_{i_r^\star}, x_{j_r^\star}] \subset (0, 1]$ with $x_{j_r^\star} - x_{i_r^\star} \geq \lambda$, for $r = 1, \ldots, \boldsymbol{m}$, such that

$$\boldsymbol{f}|_{[x_{i_r^\star}, x_{j_r^\star}]} \equiv e^r, \tag{3.1}$$

with e^r the r-th unit vector. Assume for the moment that these intervals would be known and let $B^\star := B(i_1^\star, j_1^\star) \times \ldots \times B(i_{\boldsymbol{m}}^\star, j_{\boldsymbol{m}}^\star) \in \mathfrak{B}^{\boldsymbol{m}}$ be the corresponding $\boldsymbol{m}$-box. Then a $(1-\alpha)$-confidence region for $\boldsymbol{\omega}$ is given as

$$C_{1-\alpha}(i_1^\star, j_1^\star, ..., i_m^\star, j_m^\star) := B^\star. \tag{3.2}$$

[1] The assumption $\lambda \geq 1/n$ ensures that each function value of $\boldsymbol{g}$ is represented by at least one sampling point $\boldsymbol{g}(x_j)$. This is necessary for separability of $(\boldsymbol{f}(x_1), \ldots, \boldsymbol{f}(x_n))^\top$.

To see that (3.2) is, indeed, a $(1-\alpha)$-confidence region for $\boldsymbol{\omega}$, note that

$$\left\{\boldsymbol{\omega} \in C_{1-\alpha}(i_1^\star, j_1^\star, ..., i_{\boldsymbol{m}}^\star, j_{\boldsymbol{m}}^\star)\right\} \supset \bigcap_{1\le r\le \boldsymbol{m}} \left\{\boldsymbol{g}|_{[x_{i_r^\star}, x_{j_r^\star}]} \equiv \boldsymbol{\omega}_r \in B(i_r^\star, j_r^\star)\right\}$$

and

$$\{T_n(Y,\boldsymbol{g}) \le q_n(\alpha)\} = \bigcap_{\substack{1\le i\le j\le n \\ \boldsymbol{g}|_{[x_i,x_j]}\equiv \boldsymbol{g}_{ij}}} \left\{\boldsymbol{g}_{ij} \in B(i,j)\right\}.$$

This implies that

$$\left\{\boldsymbol{\omega} \in C_{1-\alpha}(i_1^\star, j_1^\star, ..., i_{\boldsymbol{m}}^\star, j_{\boldsymbol{m}}^\star)\right\} \supset \{T_n(Y,\boldsymbol{g}) \le q_n(\alpha)\} \tag{3.3}$$

and therefore it holds uniformly in $\boldsymbol{g} \in \mathcal{M}_{\boldsymbol{m}}^{\delta,\lambda}$ that

$$\mathbf{P}\left(\boldsymbol{\omega} \in C_{1-\alpha}(i_1^\star, j_1^\star, ..., i_m^\star, j_m^\star)\right) \ge \mathbf{P}\left(T_n(Y,\boldsymbol{g}) \le q_n(\alpha)\right) \ge 1-\alpha. \tag{3.4}$$

Of course, as the source functions $\boldsymbol{f}$ are unknown, intervals $[x_{i_r^\star}, x_{j_r^\star}]$ which satisfy (3.1) are not available immediately and thus, one cannot construct the $\boldsymbol{m}$-box $B^\star$ required for (3.2) directly. For this reason, we will describe a strategy to obtain a sub-system of $\boldsymbol{m}$-boxes, i.e., a subset $\mathfrak{B}^\star \subset \mathfrak{B}^{\boldsymbol{m}}$, which covers $B^\star$ conditioned on $\{T_n(Y,\boldsymbol{g}) \le q_n(\alpha)\}$ almost surely. To this end, observe that for any random set $C^\star(Y) \subset \mathbb{R}^{\boldsymbol{m}}$ with

$$\mathbf{P}\left(C^\star(Y) \supset C_{1-\alpha}(i_1^\star, j_1^\star, \ldots, i_{\boldsymbol{m}}^\star, j_{\boldsymbol{m}}^\star)\middle| T_n(Y,\boldsymbol{g}) \le q_n(\alpha)\right) = 1 \tag{3.5}$$

(3.3) and (3.4) imply $\mathbf{P}(\boldsymbol{\omega} \in C^\star(Y)) \ge 1-\alpha$. We then define $C_{1-\alpha}$ as in (1.22). To this end, $\mathfrak{B}^\star$ is constructed such that the diameter of the resulting $C_{1-\alpha}$ is of order $\ln(n)/\sqrt{n}$ (see Corollary 3.4.3). The construction will be done explicitly by an algorithm which relies on the application of certain reduction rules (R1, R2, R3) to $\mathfrak{B}^{\boldsymbol{m}}$ to be described in the following.

Let $\mathrm{proj}_r : \mathfrak{B}^{\boldsymbol{m}} \to \mathfrak{B}$, for $r = 1, \ldots, \boldsymbol{m}$, denote the r-th projection (i.e., $\mathrm{proj}_r(B_1 \times \ldots \times B_{\boldsymbol{m}}) := B_r$) and define the set of boxes on which any signal fulfilling the multiscale constraint is non constant (nc) as

$$\mathfrak{B}_{\mathrm{nc}} := \{B(i,j) \in \mathfrak{B} : \exists [s,t], [u,v] \subset [i,j] \text{ with } B(s,t) \cap B(u,v) = \emptyset\}. \tag{3.6}$$

R 1. Delete $B \in \mathfrak{B}^{\boldsymbol{m}}$ if there exists an $r \in \{1, \ldots, \boldsymbol{m}\}$ such that $\mathrm{proj}_r(B) \in \mathfrak{B}_{\mathrm{nc}}$ as in (3.6).

The reasoning behind R1 is as follows. $\boldsymbol{g}|_{[x_{i_r^\star}, x_{j_r^\star}]}$ is constant for $r = 1, \ldots, \boldsymbol{m}$ as $\boldsymbol{f}^1, \ldots, \boldsymbol{f}^{\boldsymbol{m}}$ are constant on $[x_{i_r^\star}, x_{j_r^\star}]$. Consequently, all $\boldsymbol{m}$-boxes that include a box $B(i,j) \in \mathfrak{B}$ such that $\boldsymbol{g}$ cannot be constant on $[x_i, x_j]$ (conditioned on $T_n(Y,\boldsymbol{g}) \le q_n(\alpha)$) can be deleted in order to preserve coverage of $B^\star$. Let $[x_i, x_j]$ be an interval on which $\boldsymbol{g}$ is constant (say $\boldsymbol{g}|_{[x_i,x_j]} \equiv c$) and assume that there exist intervals $[s,t], [u,v] \subset [i,j]$ such that $B(s,t) \cap B(u,v) = \emptyset$. Then by construction of the boxes $B(s,t)$ and $B(u,v)$, $T_n(Y,\boldsymbol{g}) \le q_n(\alpha)$ implies that $c \in B(s,t)$ and $c \in B(u,v)$, which contradicts $B(s,t) \cap B(u,v) = \emptyset$. In other words, $\mathfrak{B}_{\mathrm{nc}}$ (nc $\hat{=}$ non constant)

in (3.6) includes all boxes $B(i,j)$ such that all function $g \in \mathcal{M}_{\boldsymbol{m}}^{\delta,\lambda}$ which fulfill the multiscale constraint $T_n(Y,g) \le q_n(\alpha)$ cannot be constant on $[x_i, x_j]$.

R 2. Delete $B \in \mathfrak{B}^{\boldsymbol{m}}$, with $[\underline{b}_r, \overline{b}_r] := \mathrm{proj}_r(B)$ if at least one of the following holds true.

1. $\overline{b}_1 \le 0$ or $\underline{b}_1 \ge \frac{1}{\boldsymbol{m}}$,
2. $\overline{b}_r \le \underline{b}_{r-1}$ or $\underline{b}_r \ge (1 - \sum_{i=1}^{r-1} \underline{b}_i)/(\boldsymbol{m} - r + 1)$ for any $r = 2, \dots, \boldsymbol{m}$,
3. $\sum_{r=1}^{\boldsymbol{m}} \overline{b}_r < 1$.

R2 1. comes from the fact that $0 < \boldsymbol{\omega}_1 < 1/\boldsymbol{m}$, R2 2. from $\boldsymbol{\omega}_{r-1} < \boldsymbol{\omega}_r < (1 - \sum_{i=1}^{r-1} \boldsymbol{\omega}_i)/(\boldsymbol{m} - r + 1)$, and R2 3. from $\sum_{j=1}^{m} \boldsymbol{\omega}_i = 1$.
In what follows, define for $k = 1, \dots, n$

$$\mathcal{J}_k = \mathcal{J}_k^{\lambda} := \{[i,j] : k \in [i,j], j - i + 1 \ge n\lambda, \text{ and } B(i,j) \notin \mathfrak{B}_{\mathrm{nc}}\}. \tag{3.7}$$

R 3. Delete $B \in \mathfrak{B}^{\boldsymbol{m}}$, if there exists a $k \in \{1, \dots, n\}$ such that for all $[i,j] \in \mathcal{J}_k$

$$\Big[\max_{i \le u \le v \le j} \underline{b}_{uv}, \min_{i \le u \le v \le j} \overline{b}_{uv}\Big] \cap \Big\{e\omega : \ e \in \mathfrak{A}^{\boldsymbol{m}} \text{ and } \omega \in B\Big\} \tag{3.8}$$

is empty, with $[\underline{b}_{uv}, \overline{b}_{uv}] := B(u,v) \in \mathfrak{B}^0$.

Conditioning on $T_n(Y, \boldsymbol{g}) \le q_n(\alpha)$ implies $\boldsymbol{\omega} \in B^\star$, and, in particular, that there exists an $\omega \in B^\star$ such that $\mathrm{imag}(\boldsymbol{g}) := \{\boldsymbol{g}(x_1), \dots, \boldsymbol{g}(x_n)\} \subset \{e\omega : \ e \in \mathfrak{A}^{\boldsymbol{m}}\}$. Moreover, for every $k \in \{1, \dots, n\}$ there exists an interval $[x_i, x_j]$ where $\boldsymbol{g}$ is constant with $\boldsymbol{g}|_{[x_i,x_j]} \equiv \boldsymbol{g}(x_k) \in \mathrm{imag}(\boldsymbol{g})$ and $x_j - x_i \ge \lambda$. So, $T_n(Y, \boldsymbol{g}) \le q_n(\alpha)$ implies $\boldsymbol{g}(x_k) \in B(u,v)$ for all $[u,v] \subset [i,j]$ and, therefore, for $B = B^\star$ (3.8) is not empty (conditioned on $T_n(Y, \boldsymbol{g}) \le q_n(\alpha)$).
R1 - R3 is summarized in Algorithm CRW (Confidence Region for the Weights) in Figure 3.1.

Input: Y, $\boldsymbol{m}$, $\mathfrak{A}$, α, λ
$\overline{\mathfrak{B}} \leftarrow \{B(i,j) \in \mathfrak{B} \setminus \mathfrak{B}_{\mathrm{nc}} : j - i + 1 \ge \lambda n\}$ ▹ see R1
$\mathfrak{B}^\star \leftarrow \{[\underline{b}, \overline{b}] \in \overline{\mathfrak{B}} : \overline{b} > 0 \text{ and } \underline{b} < 1/\boldsymbol{m}\}$ ▹ see R2
for i=2... $\boldsymbol{m}$ **do**
  $\mathfrak{B}^\star \leftarrow \Big\{[\underline{b}_1, \overline{b}_1] \times ... \times [\underline{b}_i, \overline{b}_i] \in \mathfrak{B}^\star \times \overline{\mathfrak{B}} : \overline{b}_i > \underline{b}_{i-1} \text{ and } \underline{b}_i < (1 - \sum_{r=1}^{i-1} \underline{b}_r)/(\boldsymbol{m} - i + 1)\Big\}$
end for
$\mathfrak{B}^\star \leftarrow \Big\{[\underline{b}_1, \overline{b}_1] \times ... \times [\underline{b}_{\boldsymbol{m}}, \overline{b}_{\boldsymbol{m}}] \in \mathfrak{B}^\star : \sum_r \overline{b}_j \ge 1\Big\}$
$\mathfrak{B}^\star \leftarrow$ R3 applied to $\mathfrak{B}^\star$
return $C_{1-\alpha} := \bigcup_{B \in \mathfrak{B}^\star} B$

Figure 3.1: Algorithm CRW for construction of confidence regions for the mixing weights $\boldsymbol{\omega}$ in the SBSR model.

Remark 3.1.1 (Noninformative $\boldsymbol{m}$-box). If $\mathfrak{B}^\star = \emptyset$, we formally may set $C_{1-\alpha} := \Omega_{\boldsymbol{m}}$, the trivial confidence region. As $\{\mathfrak{B}^\star = \emptyset\} \subset \{T_n(Y, \boldsymbol{g}) > q_n(\alpha)\}$, the probability that this happens can be bounded from above by α. This is, in general, only a very rough bound. Simulations show that $\mathfrak{B}^\star = \emptyset$ is hardly ever the case when α is reasonably small. For instance, in $10,000$

simulations of Example 1.2.1 with $n = 1280$, $\sigma = 0.1$, $\alpha = 0.1$ it did not happen once. Of course, when $\alpha \nearrow 1$ (for fixed sample size n), $\mathfrak{B}^\star = \emptyset$ finally, as no mixture $\boldsymbol{g}$ can fulfill the multiscale constrained $T_n(Y, \boldsymbol{g}) \leq q$ for arbitrarily small q.

Remark 3.1.2 (Shape of $C_{1-\alpha}$). The previous construction of the confidence set $C_{1-\alpha}$ does not ensure that the confidence set is of $\boldsymbol{m}$-box form

$$[\underline{\omega}_1, \overline{\omega}_1] \times \ldots \times [\underline{\omega}_{\boldsymbol{m}}, \overline{\omega}_{\boldsymbol{m}}]. \tag{3.9}$$

In general it is a union of $\boldsymbol{m}$-boxes. However, we can always take the smallest covering $\boldsymbol{m}$-box of $C_{1-\alpha}$, given by

$$\left[\inf_{\tilde{\omega} \in C_{1-\alpha}} \tilde{\omega}_1, \sup_{\tilde{\omega} \in C_{1-\alpha}} \tilde{\omega}_1\right] \times \ldots \times \left[\inf_{\tilde{\omega} \in C_{1-\alpha}} \tilde{\omega}_{\boldsymbol{m}}, \sup_{\tilde{\omega} \in C_{1-\alpha}} \tilde{\omega}_{\boldsymbol{m}}\right], \tag{3.10}$$

in order to get a confidence set as in (3.9). Note that $\overline{\operatorname{dist}}(\boldsymbol{\omega}, C_{1-\alpha}) =: d$ remains the same when we replace $C_{1-\alpha}$ by (3.10). To see this, consider $\hat{C} := \boldsymbol{\omega} + [-d, d]^{\boldsymbol{m}}$, which is a covering $\boldsymbol{m}$-box of $C_{1-\alpha}$, so in particular $\hat{C}$ covers (3.10), with $\overline{\operatorname{dist}}(\boldsymbol{\omega}, \hat{C}) = d$.

Summing up, we have now constructed a confidence set $C_{1-\alpha}$ for the mixing vector $\boldsymbol{\omega}$ in the SBSR model. Given $C_{1-\alpha}$ SLAM estimates $\boldsymbol{\omega}$ as in (1.23). From this, in the next section we derive estimators for the sources $\boldsymbol{f}^1, \ldots, \boldsymbol{f}^{\boldsymbol{m}}$.

3.2 Estimation of source functions

SLAM estimates $\boldsymbol{f} = (\boldsymbol{f}^1, \ldots, \boldsymbol{f}^{\boldsymbol{m}})$ by solving the constraint optimization problem (1.28), which admits a solution if and only if

$$\min_{f \in \mathcal{S}(\mathfrak{A})^{\boldsymbol{m}}} T_n(Y, f\hat{\omega}(\alpha)) \leq q_n(\beta). \tag{3.11}$$

(3.11) cannot be guaranteed in general, but the following theorem shows that if α, β are chosen as in (1.25) it holds asymptotically with probability one, independently of the specific choice of $\hat{\omega} \in C_{1-\alpha}(Y)$ in (1.23) or (1.24).

Theorem 3.2.1. *Consider the SBSR model with $\boldsymbol{g} \in \mathcal{M}^{\delta,\lambda}_{\boldsymbol{m}}$. For $\alpha \in (0,1)$ let $C_{1-\alpha}(Y)$ be as in (1.22). Then for any estimator $\hat{\omega} = \hat{\omega}(Y) \in C_{1-\alpha}(Y)$ and c_3, c_4 as in (3.13)*

$$\boldsymbol{P}\left(\min_{f \in \mathcal{S}(\mathfrak{A})^{\boldsymbol{m}}_{\lambda/3}} T_n(Y, f\hat{\omega}) \leq c_3\, q_n(\alpha) + c_4 \,\middle|\, T_n(Y, \boldsymbol{g}) \leq q_n(\alpha)\right) = 1.$$

For finite n simulations show that violation of (3.11) is hardly ever the case. For instance, in $10,000$ simulation runs of Example 1.2.1 with $\alpha = \beta = 0.1$ it did not happen once. Therefore, in practice, failure of (3.11) might rather indicate that the model assumption is not correct (e.g., due to outliers) and could be treated by preprocessing of the data. Another strategy can be to decrease β and hence the constraint in (3.11) as for $\beta > \beta'$ it holds that $q_n(\beta') > q_n(\beta)$.

Remark 3.2.2 (Incorporating identifiability conditions in SLAM). The separability condition $e^1, \dots, e^m \in \{\boldsymbol{f}(x_1), \dots, \boldsymbol{f}(x_n)\}$ in (1.12) could be incorporated in the estimator (1.28), which provides a further restriction on $\mathcal{H}(\beta)$ in (1.29). This may yield a finite sample improvement of SLAM, however, at the expense of being less robust if separability is violated (see Section 6.1.5 for a simulation study of SLAM when separability is violated).

3.3 Confidence bands for the source functions

The SLAM estimation procedure in (1.28) leads to asymptotically uniform confidence bands for the source functions $\boldsymbol{f}^1, \dots, \boldsymbol{f}^m$. To this end, let $\tilde{T}_n$ be as in (1.16), but with $pen(j-i+1)$ replaced by

$$pen(j-i+1) + c_2 \sqrt{\frac{(j-i+1)\ln(n)^2}{\sigma^2 n}}, \tag{3.12}$$

with c_2 as in (3.13), and let $\tilde{\mathcal{H}}(\beta)$ be as in (1.29) but with T_n replaced by $\tilde{T}_n$. Then $\tilde{\mathcal{H}}(\beta)$ constitutes an asymptotically uniform confidence band as the following theorem shows.

Theorem 3.3.1. *Consider the SBSR model and let $\hat{\omega}$ be the SLAM estimator from (1.23) for $\alpha = \alpha_n$ as in (1.25). Then $\tilde{\mathcal{H}}(\beta)$ as in (1.29) with T_n replaced by $\tilde{T}_n$ provides an asymptotically uniform confidence region for the sources $\boldsymbol{f}$,*

$$\lim_{n \longrightarrow \infty} \inf_{\boldsymbol{g} \in \mathcal{M}_{\boldsymbol{m}}^{\delta,\lambda}} \boldsymbol{P}\left((\boldsymbol{f}^1, ..., \boldsymbol{f}^{\boldsymbol{m}}) \in \tilde{\mathcal{H}}(\beta)\right) \geq 1 - \beta.$$

Remark 3.3.2. The additional term in the penalty in (3.12) accounts for the estimation error of $\hat{\omega}$ and enlarges the confidence bands $\tilde{\mathcal{H}}(\beta)$. Note that at first glance it seems counter intuitive that decreasing δ decreases this term (see the dependence of c_2 on δ in (3.13)) and hence, makes the confidence band smaller. However, note that just as in Theorem 2.2.3, the smaller δ, the smaller the bound ϵ on the approximation error of $\boldsymbol{g}$. This approximation error directly relates to the approximation error of $\boldsymbol{\omega}$, for which the additional term in (3.12) accounts for. Thus, the influence of increasing δ is hidden in the limit $n \to \infty$. As a consequence, the size of the confidence band is mainly influenced by the minimal scale λ, its dependence on δ is negligible. We stress, however, that a small $ASB(\boldsymbol{\omega})$ with $\delta \leq ASB(\boldsymbol{\omega})$ will, of course, lead to wider confidence bands, as confidence bands for $\boldsymbol{f}$ are in one-to-one correspondence to confidence bands for $\boldsymbol{g}$ and a small $ASB(\boldsymbol{\omega}) \sim ASB(\hat{\omega})$ allows for a larger variation of f within a neighborhood of g.

3.4 Consistency and rates

In the following, we investigate further theoretical properties of SLAM. As in Theorem 3.3.1 our results will be stated uniformly over the space $\mathcal{M}_{\boldsymbol{m}}^{\delta,\lambda}$ in (1.11), i.e., for a given minimal

length λ of the constant parts of the mixture $\boldsymbol{g}$ and a given minimal ASB δ. Define the constants

$$\begin{aligned} c_1 &:= \frac{\delta^2}{2312\ \sigma^2 \boldsymbol{m}^2 a_k^2}, \quad c_2 := \frac{8/3\delta + 24\sqrt{2\sigma^2 \ln(9e/\lambda)}}{\sqrt{\lambda}}, \\ c_3 &:= 1 + \sqrt{\frac{4}{3}}\boldsymbol{m}a_k, \quad c_4 := \sqrt{\frac{4}{3}}\boldsymbol{m}a_k \sqrt{2\ln(e/\lambda)}. \end{aligned} \tag{3.13}$$

Further, let $N^\star \in \mathbb{N}$ be the smallest integer, s.t.

$$\begin{aligned} \delta\sqrt{\ln(N^\star)} \geq \max\Bigg(& \frac{27\sigma^2 \boldsymbol{m}a_k \sqrt{2\ln(e/\lambda)}}{\sqrt{\ln(N^\star)}(\sqrt{N^\star\lambda} - \boldsymbol{m}\sigma a_k)}, \ 8\sigma\sqrt{\frac{2\ln(eN^\star/\ln(N^\star)^2)}{\ln(N^\star)}}, \\ & \frac{60\sqrt{3}\sigma\boldsymbol{m}a_k\sqrt{2\ln(2/\lambda)}}{\sqrt{\ln(N^\star)}}\Bigg) \end{aligned} \tag{3.14}$$

and

$$\lambda\frac{N^\star}{\ln(N^\star)^2} \geq \max\left(\boldsymbol{m}a_k(3 + 68\frac{\sigma}{\delta}\sqrt{\ln(9e/\lambda)}),\ \frac{27a_k}{\delta + 9\sigma\sqrt{2\ln(9e/\lambda)}}\right)^2. \tag{3.15}$$

Remark 3.4.1 (Behavior of $N^\star$). Note that the left-hand side in (3.14) and (3.15) is increasing and the right-hand side decreasing (or constant) in $N^\star$. For fixed λ and $\delta \searrow 0$, (3.14) dominates the behavior of $N^\star$ as it is essentially of the form $\delta\sqrt{\ln(N^\star)} \geq c$, whereas (3.15) is of the form $\delta\sqrt{N^\star}/\ln(N^\star) \geq c$. Conversely, for fixed δ and $\lambda \searrow 0$, (3.15) dominates the behavior of $N^\star$ as it is essentially of the form $\lambda N^\star/(\ln(\lambda^{-1})\ln(N^\star)^2) \geq c$ whereas (3.14) is of the form $\lambda N^\star \ln(N^\star)^2/\ln(\lambda^{-1}) \geq c$.

Theorem 3.4.2. *Consider the SBSR model with $g \in \mathcal{M}_{\boldsymbol{m}}^{\delta,\lambda}$. Let $\hat{\omega}$ and $\hat{f} = (\hat{f}^1, \ldots, \hat{f}^{\boldsymbol{m}})$ be the SLAM estimators from (1.23) and (1.28), respectively, with $\alpha = \alpha_n$ and $\beta = \beta_n$ as in (1.25). Further, let $\hat{\tau}^i$ and τ^i be the vectors of all c.p. locations of $\hat{f}^i$ and f^i, respectively, for $i = 1, \ldots, \boldsymbol{m}$. Then for all $n > N^\star$ in (3.14) and (3.15) and for all $i = 1, \ldots, \boldsymbol{m}$*

1. $K(\hat{f}^i) = K(\boldsymbol{f}^i)$,
2. $\max_j |\hat{\tau}^i_j - \tau^i_j| \leq 2\frac{\ln^2(n)}{n}$,
3. $\max_j \left|\hat{f}^i|_{[\hat{\tau}_j, \hat{\tau}_{j+1})} - \boldsymbol{f}^i|_{[\tau_j, \tau_{j+1})}\right| = 0$, *and*
4. $|\hat{\omega}_i - \boldsymbol{\omega}_i| \leq c_2\frac{\ln(n)}{\sqrt{n}}$

with probability at least $1 - \exp(-c_1\ln^2(n))$, with c_1 and c_2 as in (3.13).

From the proof of Theorem 3.4.2 it also follows that assertions 1. - 4. hold for any $\hat{\omega} \in C_{1-\alpha}(Y) \cap \Omega_{\boldsymbol{m}}^\delta$ and we obtain the following.

Corollary 3.4.3. *Consider the SBSR model with $\boldsymbol{g} \in \mathcal{M}_{\boldsymbol{m}}^{\delta,\lambda}$. Let $C_{1-\alpha}(Y)$ be as in (1.22) and α_n as in (1.25). Further, let $\overline{\text{dist}}$ be is as in (1.26). Then for all $n > N^\star$ in (3.14) and (3.15)*

$$\overline{\text{dist}}(\boldsymbol{\omega}, C_{1-\alpha_n}(Y) \cap \Omega_{\boldsymbol{m}}^\delta) < c_2\frac{\ln(n)}{\sqrt{n}}$$

with probability at least $1 - \exp(-c_1 \ln^2(n))$*, with* c_1 *and* c_2 *as in (3.13).*

Remark 3.4.4 (SLAM (almost) attains minimax rates).

a) (c.p. locations) Theorem 3.4.2 states that we can recover the c.p. locations of $\boldsymbol{f}^i$ in probability with rate $\ln^2(n)/n$. Obviously, the estimation rate of the c.p. locations is bounded from below by the sampling rate $1/n$. Consequently, the rate of Theorem 3.4.2 differs from the optimal rate only by a $\ln^2(n)$ factor.

b) (Weights) By the one-to-one correspondence between the weights and the function values of $\boldsymbol{g}$ the weights' detection rate $\ln(n)/\sqrt{n}$ immediately follows from the box height in (1.18) with $q_n(\alpha_n) \in O(\ln(n))$ and coincides with the optimal rate $O(1/\sqrt{n})$ up to a $\ln(n)$ term.

c) (Dependence on λ) The minimal scale λ in Theorem 3.4.2 may depend on n, i.e., $\lambda = \lambda_n$. In order to ensure consistency of SLAM's estimates $\hat{\omega}$ and $(\hat{f}^1, \ldots, \hat{f}^m)$, Theorem 3.4.2 requires that (3.14) and (3.15) holds (for a sufficiently large $N^\star$) and that $c_2 \ln(n)/\sqrt{n} \to 0$, as $n \to \infty$. By Remark 3.4.1 this is fulfilled whenever $\lambda^{-1} \ln(\lambda^{-1}) \in o(n/\ln^2(n))$. This means that the statements 1. - 4. in Theorem 3.4.2 hold true asymptotically with probability one as the minimal scale λ_n of successive jumps in a sequence of mixtures $\boldsymbol{g}_n$ does not asymptotically vanish as fast as of order $\ln^3(n)/n$. We stress that no method can recover finer details of a bump signal (including the mixture $\boldsymbol{g}$) below its detection boundary which is of the order $\ln(n)/n$, i.e., SLAM achieves this minimax detection rate up to a $\ln^2(n)$ factor, see (Dümbgen and Walther, 2008; Frick et al., 2014).

d) (Dependence on δ) Just as the minimal scale λ, the minimal ASB δ in Theorem 3.4.2 may depend on n as well, i.e., $\delta = \delta_n$. SLAM's estimates remain consistent whenever $\delta^{-1} \in o\Big(\sqrt{\ln(n)}\Big)$, i.e., the statements 1. - 4. in Theorem 3.4.2 hold true asymptotically with probability one if the minimal ASB δ_n in a sequence of mixtures $\boldsymbol{g}_n$ does not decrease as fast as of order $1/\sqrt{\ln(n)}$. We stress that no method can recover smaller jump heights of the mixture $\boldsymbol{g}$ below its minimax detection rate, which is $1/\ln(n)$. To see this, note that statement 2. in Theorem 3.4.2 provides asymptotic detection power one for $2\ln(n)^2$ i.i.d. observations with mean δ_n (recall that the ASB corresponds to the minimal possible jump height of the mixture $\boldsymbol{g}$). Hence, SLAM achieves the minimax rate up to a $\sqrt{\ln(n)}$ factor.

Remark 3.4.5 (SLAM for known $\boldsymbol{\omega}$). If $\boldsymbol{\omega}$ is known in the SBSR model, the second part of SLAM can be used separately. We may then directly solve (1.27) without pre-estimating $\boldsymbol{\omega}$, i.e. we simply replace $\hat{\omega}$ by $\boldsymbol{\omega}$. Then, Theorem 3.3.1 is still valid for $\tilde{\mathcal{H}}(\beta)$ replaced by $\mathcal{H}(\beta)$. Further, a careful modification of the proof of Theorem 3.4.2 shows that the assertions in Theorem 3.4.2 hold for a possibly smaller $N^\star$ in (3.14) and (3.15) and for $\alpha_n = \exp(-c_1 \ln(n)^2)$ replaced by β_n (recall that $q_n(\beta_n) > q_n(\alpha_n)$ in (1.25) and hence, $\beta_n < \alpha_n$). We stress that the finite alphabet assumption is still required and the corresponding identifiability assumption $ASB(\boldsymbol{\omega}) \geq \delta$ must be valid.

3.5 Selection of the threshold parameter

On the one hand, for given α and β SLAM yields confidence statements for the weights $\boldsymbol{\omega}$ and the source functions $\boldsymbol{f}$ at level $1-\alpha$ and $1-\beta$, respectively. This suggests the choice of these parameters as confidence levels. On the other hand, when estimation of $\boldsymbol{\omega}$ and $\boldsymbol{f}$ is targeted $q_n(\alpha)$ and $q_n(\beta)$ can be seen as tuning parameters for the estimates $\hat{\omega}$ and $\hat{f}$. In particular, Theorem 3.4.2 yields that the particular choice $q_n(\alpha) = q_n(\alpha_n)$ and $q_n(\beta) = q_n(\beta_n)$ as in (1.25) lead to asymptotically optimal rate of convergence. Although, simulations in Section 6.1.3 suggest that SLAM's estimates are quite stable for a range of α's and β's, for finite sample size n, a fine tuning of these parameters improves estimation accuracy, of course. In the following, a possible strategy for this is suggested. First, $q_n(\alpha)$ for tuning the estimate $\hat{\omega}_q := \hat{\omega}(Y, q)$ is discussed. Recall that for estimating $\boldsymbol{\omega}$, $q_n(\beta)$ is not required.

Theorem 3.4.2 yields $\ln(n)/\sqrt{n}$-consistency of $\hat{\omega}$ when $q_n(\alpha) = q_n(\alpha_n)$ with α_n as in (1.25), independently of the specific choice of $\hat{\omega} \in C_{1-\alpha_n} \cap \Omega^{\delta}_{\boldsymbol{m}}$. Further, for α' (and $q_n(\alpha')$, respectively) with $\alpha' \geq \alpha_n$ (and $q_n(\alpha') \leq q_n(\alpha_n)$, respectively) $C_{1-\alpha'} \subseteq C_{1-\alpha_n}$ whenever $\mathfrak{B}^\star = \mathfrak{B}^\star_{q_n(\alpha')} \neq \emptyset$ in (1.22). Thus, choosing the threshold q, for a sufficiently rich discrete set $Q = \{q_1, q_2, \ldots, q_N = q_n(\alpha_n)\}$, as the *minimal valid threshold (MVT)*

$$q^\star := \min\left(q \in Q : \bigcup_{B \in \mathfrak{B}^\star_q} B \cap \Omega^{\delta}_{\boldsymbol{m}} \neq \emptyset \right)$$

guarantees the convergence rates of Theorem 3.4.2 for the corresponding estimate $\hat{\omega}(Y, q^\star)$. In practice, $Q = \{-1.0, -0.9, ..., 1.9, 2.0\}$ was found to be a sufficiently rich candidate set.

It remains to select $q_n(\beta)$ (and β, respectively), which is required additionally for $\hat{f}$, recall (1.28) and (1.29). Theorem 3.4.2 suggests to choose $q_n(\beta) = q_n(\beta_n)$ with β_n as in (1.25), i.e., $q_n(\beta) \to \infty$ with rate $O(\log(n))$. For finite n, there exist several methods for selection of $q_n(\beta)$ in c.p. regression (see e.g., (Zhang and Siegmund, 2007)), which might be used here as well. However, due to the high stability of $\hat{f}$ in q (see Section 6.1.3) we simply suggest to choose $\beta = 0.1$, which we have used here for our data analysis. This choice controls the probability of overestimating the number of jumps in $\boldsymbol{g}$, $\mathbf{P}(K(\hat{g}) > K(\boldsymbol{g})) \leq 0.1$ asymptotically. In general, it depends on the application. A large $q_n(\beta)$ (hence small β) has been selected in the application example in Chapter 7 to remove spurious changes in the signal which appear biologically not as of much relevance.

3.6 Model selection

So far, we have assumed that the number of sources $\boldsymbol{m}$ in the SBSR model (1.3) is given. In the following, we want to study the situation where $\boldsymbol{m}$ is unknown, i.e., we consider model selection for the SBSR model. To this end, define

$$\mathcal{M} := \bigcup_{m=1}^{\infty} \mathcal{M}_m. \tag{3.16}$$

Theorem 2.2.5 shows that δ-separability guarantees identifiability and regularizes the SBSR model via the parameter δ, even when the number of sources is unknown. Therefore, we define the set of δ-separable mixtures with minimal scale λ and arbitrary number of components as

$$\mathcal{M}^{\delta,\lambda} := \bigcup_{m\in\mathbb{N}} \mathcal{M}_m^{\delta,\lambda}, \tag{3.17}$$

with $\mathcal{M}_m^{\delta,\lambda}$ as in (1.11). Note that, Theorem 2.3.10 implies

$$\mathcal{M}^{\delta,\lambda} = \bigcup_{m=1}^{m_{\max}} \mathcal{M}_m^{\delta,\lambda}$$

in (3.17) with $m_{\max} = m_{\max}(\delta) < \min\left(\sqrt{2/\delta}, \ln(a_k/\delta + 1)/\ln(k)\right)$. Thus, although in principle we allow for an arbitrary number of source components $m \in \mathbb{N}$, a fixed minimal ASB $\delta > 0$ implicitly restricts to finitely many models $m \in \{1, \dots, m_{\max}(\delta)\}$, where $m_{\max}(\delta) \nearrow \infty$ as $\delta \searrow 0$. Similar, separability for a minimal scale λ yields an upper bound on m, namely $m \leq \lambda^{-1}$, as A3 requires at least m regions each of minimal size λ with specific distinct values for g and f.

In the following, we will introduce a selection procedure for $\boldsymbol{m}$ based on the confidence sets $C_{1-\alpha}(Y) = C_{1-\alpha}(Y, \boldsymbol{m}, \lambda)$ for $\boldsymbol{\omega}$ from Section 3.1 (see Algorithm CRW in Figure 3.1). Recall that we can associate each significant level α with the corresponding quantile of T_n as in (1.16) and thus we use the notation $C_q(Y, \boldsymbol{m}, \lambda) := C_{1-\alpha(q)}(Y, \boldsymbol{m}, \lambda)$. Recall that $C_q(Y, \boldsymbol{m}, \lambda)$ was constructed in such a way that whenever there exists a $g = f\omega \in \mathcal{M}_{\boldsymbol{m}}^{\delta,\lambda}$ such that $T_n(Y, g) \leq q$, then $\omega \in C_q(Y, \boldsymbol{m}, \lambda) \cap \Omega_{\boldsymbol{m}}^{\delta}$ (recall (1.13)) and, simultaneously, whenever $\omega \in C_q(Y, \boldsymbol{m}, \lambda) \cap \Omega_{\boldsymbol{m}}^{\delta}$ (and the true underlying mixture $\boldsymbol{g}$ fulfills $T_n(Y, \boldsymbol{g}) \leq q$), then there exists a $g \in \mathcal{M}_{\boldsymbol{m}}^{\lambda/3}(\omega)$ such that $T_n(Y, g) \leq c_3 q + c_4$ (recall Theorem 3.2.1). More precisely, for given $\lambda, \delta > 0$ and $m \geq 2$ define

$$C_q^m = C_q^m(\lambda, \delta) := C_q(Y, m, \lambda) \cap \Omega_m^{\delta}, \tag{3.18}$$

with $C_q(Y, m, \lambda)$ as in Algorithm CRW in Figure 3.1 and Ω_m^{δ} as in (2.11). Then it follows from (1.13) that for every fixed $\omega \in \Omega_m^{\delta}$

$$\bigcup_{g\in\mathcal{M}_m^{\delta,\lambda}(\omega)} \{T_n(Y, g) \leq q\} \subset \{\omega \in C_q^m\} \tag{3.19}$$

and from Theorem 3.2.1 that

$$\{\omega \in C_q^m\} \cap \{T_n(Y, \boldsymbol{g}) \leq q\} \subset \bigcup_{g\in\mathcal{M}_m^{\delta,\lambda/3}(\omega)} \{T_n(Y, g) \leq q'\}, \tag{3.20}$$

with $q' := c_3 q + c_4$ and c_3, c_4 as in (3.13).

Remark 3.6.1. For $m = 1$ it is easy to check that

$$C_q^1(Y) := \begin{cases} \{1\} & \text{if } \inf_{f\in\mathcal{S}(\mathfrak{N})_\lambda} T_n(Y, f) \leq q \\ \emptyset & \text{otherwise} \end{cases} \tag{3.21}$$

satisfies (3.19) and (3.20).

Note that, without any prior information on both, λ and δ, if a given ω explains the data Y at a certain confidence level, one can always increase the number of sources m by either adding arbitrarily small additional weights or by splitting up weights while choosing the corresponding source function arbitrarily similar, in order to get mixing weights of higher dimension which still explain Y equally well. Therefore, we estimate the number of source functions as the smallest number m, such that there exist mixing weights (and, hence, corresponding source functions) of dimension m which can explain the data Y at a prespecified confidence level. This procedure automatically bounds the probability of underestimating the number of source components. The following definition specifies this estimator more formally.

Definition 3.6.2. For given $\lambda, \delta > 0$ let $\{C_q^m(Y)\}_{m\in\mathbb{N}} = \{C_q^m(Y,\lambda,\delta)\}_{m\in\mathbb{N}}$ be as in (3.18) for $m \geq 2$ and as in Remark 3.6.1 for $m = 1$. Define the estimator for the number of sources as

$$\hat{m}(q) = \hat{m}(q,\lambda,\delta) := \min\left(m \geq 1 \text{ s.t. } C_q^m \neq \emptyset\right), \tag{3.22}$$

with the convention that $\min(\emptyset) = \infty$.

Remark 3.6.3 (Dependence on λ and δ). The estimator $\hat{m}(q)$ in Definition 3.6.2 depends on both, a minimal scale λ and ASB δ. To remove this dependence, one may as well consider the estimator $\lim_{\delta\searrow 0}\hat{m}(q, 1/n, \delta)$. Note that a minimal scale of $1/n$, i.e., for each constant piece of $\boldsymbol{g}$ there is at least one observation, is necessary, as otherwise separability as in A3 is not guaranteed for the underlying signal of Y. We will see in the following (see Theorem 3.6.4) that in order to bound the probability of overestimation preknowledge on λ and δ is not necessary. However, to bound the probability of underestimation, and hence, to obtain consistency, (for any estimator) prior information on λ and δ is necessarily required, as argued above.

3.6.1 Lower confidence bounds for m

Note that (3.19) implies

$$\{\hat{m}(q) > \boldsymbol{m}\} = \{C_q^{\boldsymbol{m}} = \emptyset\} \subset \{\boldsymbol{\omega} \notin C_q^{\boldsymbol{m}}\} \subset \{T_n(Y,\boldsymbol{g}) > q\}. \tag{3.23}$$

From (3.23) it follows directly that when q is chosen to be the $(1-\alpha)$-quantile $q_{1-\alpha}$ of the statistic T_n in (1.16) then

$$\hat{m}_{1-\alpha} := \hat{m}(q_{1-\alpha}) \tag{3.24}$$

in (3.22) constitutes a $1-\alpha$ lower confidence bound for the underlying number of source components $\boldsymbol{m}$.

Theorem 3.6.4. *Assume the SBSR model (1.3). Then for $\alpha \in (0,1)$ and $\hat{m}_{1-\alpha}$ as in (3.24)*

$$\inf_{\lambda\geq 1/n,\delta>0}\ \inf_{\boldsymbol{g}\in\mathcal{M}^{\delta,\lambda}} \boldsymbol{P}(\hat{m}_{1-\alpha} \leq \boldsymbol{m}) \geq 1-\alpha.$$

Remark 3.6.5. For fixed sample size n, (3.19) implies $\lim_{q\to\infty} \hat{m}(q) = 1$. This is in accordance with Theorem 3.6.4, where for $\alpha \to 0$ the corresponding quantile $q_{1-\alpha}$ of T_n tends to infinity and, hence, $\hat{m}_{1-\alpha} \to 1$ as $\alpha \to 0$.

3.6.2 Model selection consistency

In Section 3.6.1 we have seen that condition (3.19) yields a bound for the error to overestimate $\boldsymbol{m}$. Analogously, condition (3.20) yields a bound for the underestimation error. Combing both, leads to an explicit exponential bound (which depends on q) for the probability that $\hat{m}(q) \neq \boldsymbol{m}$. This bound is fundamental for the following results.

Theorem 3.6.6. *For $\lambda, \delta > 0$ assume the SBSR model (1.3) with $\boldsymbol{g} \in \mathcal{M}^{\delta,\lambda}$. Then for $\hat{m}(q)$ as in (3.22)*

$$\boldsymbol{P}\left(\hat{m}(q) \neq \boldsymbol{m}\right) \leq \alpha_n(q) + \beta_n(q), \tag{3.25}$$

with $\alpha_n(q) := \boldsymbol{P}\left(T_n(Y, \boldsymbol{g}) > q\right)$ and

$$\beta_n(q) := 1 - \left(1 - 4\exp\left(-\left(\frac{\sqrt{n\lambda/12}\delta^{3/2}}{\sqrt{6}a_k\sigma} - \frac{1}{\sqrt{2}}\left(c_3 q + c_4 + \sqrt{2\ln(12e/\lambda)}\right)\right)_+^2\right)\right)^{12/\lambda}.$$

Theorem 3.6.6 yields consistency of $\hat{m}(q)$ for a wide range of $q = q_n \nearrow \infty$, as the following theorem shows.

Theorem 3.6.7. *For given $\lambda, \delta > 0$ assume the SBSR model (1.3) with $\boldsymbol{g} \in \mathcal{M}^{\lambda,\delta}$. If $q_n \to \infty$ and $\limsup q_n/\sqrt{n} \leq \sqrt{\lambda}\delta^2/(24\sqrt{2}a_k^2\sigma)$ for $n \to \infty$, then $\hat{m}(q_n)$ in (3.22) is uniformly consistent over $\mathcal{M}^{\delta,\lambda}$, that is,*

$$\inf_{\boldsymbol{g}\in\mathcal{M}^{\delta,\lambda}} \boldsymbol{P}\left(\hat{m}(q_n) = \boldsymbol{m}\right) \to 1, \quad \text{for } n \to \infty.$$

Moreover, for a specific (optimal) choice of q this gives an exponential rate of convergence for $\hat{m}(q)$ in (3.22).

Definition 3.6.8. For given $\lambda, \delta > 0$ let $\hat{m}(q)$ be as in (3.22), $q_{\min} := \min\{q \in \mathbb{R} : \hat{m}(q) < \infty\}$, and $q_n = q_n(\lambda, \delta) := \max\left(q_{\min},\ c\sqrt{n}\right)$, with $c = c(\lambda, \delta, \sigma) := \sqrt{\lambda}\delta^2/(24\sqrt{2}a_k^2\sigma)$. Define the *SLAM selector*

$$\hat{m} := \hat{m}(q_n).$$

Theorem 3.6.9. *For given $\lambda, \delta > 0$ assume the SBSR model (1.3), with $\boldsymbol{g} \in \mathcal{M}^{\delta,\lambda}$. Then for $\hat{m}$ and c as in Definition 3.6.8*

$$\boldsymbol{P}\left(\hat{m}(q_n) = \boldsymbol{m}\right) \geq 1 - \exp\left(-c^2 n/8\right) + O\left(\exp\left(-4c^2 n\right)\right).$$

Remark 3.6.10 (Dependence on λ and δ (continued)). When the minimal scale λ and the minimal ASB δ in Theorem 3.6.9 depend on n, i.e., $\lambda = \lambda_n$ and $\delta = \delta_n$, in order to provide model selection consistency as $\lambda_n, \delta_n \searrow 0$, the proof of Theorem 3.6.9 yields

$$\frac{\lambda_n\delta_n^3}{\sigma^2}\, n - \frac{1}{\delta_n}\ln(\lambda_n^{-1}) \to \infty \quad \text{and} \quad \frac{\lambda_n\delta_n^4}{\sigma^2}\, n \to \infty, \qquad \text{with } n \to \infty. \tag{3.26}$$

For fixed δ this is fulfilled when $\lambda_n^{-1} \in O(n/\ln(n))$. This means that the estimator $\hat{m}$ in Theorem 3.6.9 is even consistent when the minimal scale λ_n of successive jumps in a sequence of mixtures $\boldsymbol{g}_n$ does not asymptotically vanish as fast as of order $\ln(n)/n$, which equals the minimax detection rate (Dümbgen and Walther, 2008; Frick et al., 2014) (recall Remark 3.4.4) .
For fixed λ (3.26) is fulfilled when $\delta_n^{-1} \in o\left(n^{1/4}\right)$. This means that the estimator $\hat{m}$ in Theorem 3.6.9 is consistent when the minimal ASB δ_n in a sequence of mixtures $\boldsymbol{g}_n$ does not asymptotically vanish as fast as of order $n^{-1/4}$. Partly, this rate arises from the exact recovery bound given in Theorem 2.2.5, which differs from the corresponding bound for known $\boldsymbol{m}$ of Theorem 2.2.3 by a $\sqrt{\delta}$-factor. i.e., compared to the case where $\boldsymbol{m}$ is known, one has to improve the approximation of $\boldsymbol{g}$ by a $\sqrt{\delta}$-factor in order to get exact recovery of $\boldsymbol{f}$. It is an open issue whether this bound in Theorem 2.2.5 is sharp, i.e., whether there exist sequences of mixtures $g, \tilde{g} \in \mathcal{M}^{\delta_n}$ with $\|g - \tilde{g}\|_\infty \in O\left(\delta_n^{3/2}\right)$ and $\mathfrak{m}(g) \neq \mathfrak{m}(\tilde{g})$. Note that this may even depend on the specific alphabet. The remaining $\sqrt{\delta}$-factor arises from a possible increase of the multiscale statistic for $\hat{\omega} \in C_{1-\alpha}$ by an $\boldsymbol{m}$-factor, see Theorem 3.2.1 and the dependence of c_3 on $\boldsymbol{m}$. When $\boldsymbol{m}$ is fixed and known, this only appears in the constants for $\delta_n \to 0$. However, when $\boldsymbol{m}$ is unknown, it may, increase with n, i.e., $\boldsymbol{m} = \boldsymbol{m}_n \to \infty$ as $\delta_n \to 0$, with $\boldsymbol{m}_n \leq \sqrt{1/\delta_n}$ (see Theorem 2.3.10). This results in a decrease of the maximal δ_n^{-1}-rate by an additional $\sqrt{n}$-factor.

3.6.3 Inference on $\boldsymbol{\omega}$ and $\boldsymbol{f}$ for unknown $\boldsymbol{m}$

To estimate $\boldsymbol{\omega}$ and $\boldsymbol{f}$ in the SBSR model (1.3) when the number of sources $\boldsymbol{m}$ is unknown, one can replace the true number of sources $\boldsymbol{m}$ in the SLAM estimates $\hat{\omega}$ and $\hat{f}$ from Section 3.1 and 3.2 with the estimate $\hat{m}$ from Definition 3.6.8. Combining Theorem 3.4.2 and Theorem 3.6.9 yields that this does change the estimation precision by such a small amount that this will only enter the constants of its risk but not its rate of convergence. More precisely, we get the following theorem.

Theorem 3.6.11. *For given $\lambda, \delta > 0$ assume the SBSR model (1.3) with $\boldsymbol{g} \in \mathcal{M}^{\delta,\lambda}$. Let $\hat{\omega}(m)$ and $\hat{f}(m)$ be the SLAM estimators as in Theorem 3.4.2, $\hat{m}$ the SLAM model selector as in Definition 3.6.8, and $\hat{\omega} = \hat{\omega}(\hat{m})$, $\hat{f} = \hat{f}(\hat{m})$. Further, let $\hat{\tau}^i$ and τ^i be the vectors of all c.p. locations of $\hat{f}^i$ and $\boldsymbol{f}^i$, respectively. Then with probability at least*

$$1 - \exp(-c_1 \ln^2(n)) + O\left(\exp\left(-\frac{c^2}{8}n\right)\right),$$

1. $\hat{m} = \mathfrak{m}(\boldsymbol{g})$

and for all $i = 1, \ldots, \hat{m}$

2. $K(\hat{f}^i) = K(\boldsymbol{f}^i)$,
3. $\max_j |\hat{\tau}_j^i - \tau_j^i| \leq 2\frac{\ln^2(n)}{n}$,
4. $\max_j \left|\hat{f}^i|_{[\hat{\tau}_j, \hat{\tau}_{j+1})} - \boldsymbol{f}^i|_{[\tau_j, \tau_{j+1})}\right| = 0$, *and*
5. $|\hat{\omega}_i - \boldsymbol{\omega}_i| \leq c_2 \frac{\ln(n)}{\sqrt{n}}$,

with c_1, c_2 as in (3.13) and c as in Definition 3.6.8.

Comparing Theorem 3.4.2 and 3.6.11 shows that inferring $\boldsymbol{\omega}$ and $\boldsymbol{f}$ does not become significantly more difficult when $\boldsymbol{m}$ is unknown. The probability that $\boldsymbol{\omega}$ and $\boldsymbol{f}$ are estimated with an optimal rate (up to log-factors) increases for unknown $\boldsymbol{m}$ only by an additional $O\left(\exp\left(-\frac{c^2}{8}n\right)\right)$ term, with c as in Definition 3.6.8, and thus the overall rate of convergence remains the same. The only difference appears in the constants. Whereas the dependence on λ is unchanged and still optimal (up to log-factors), the dependence on δ becomes more restrictive.
Analog to Theorem 3.6.11 one can use the SLAM selector $\hat{m}$ from Definition 3.6.8 in order to derive asymptotically uniform (for given λ and δ) confidence statements for $\boldsymbol{\omega}$ and $\boldsymbol{f}$.

Theorem 3.6.12. *For given $\lambda, \delta > 0$ assume the SBSR model (1.3) with $\boldsymbol{g} \in \mathcal{M}^{\delta,\lambda}$. Let $\{C_{1-\alpha}(Y, \lambda, m)\}_{m\in\mathbb{N}}$ be the SLAM confidence sets for $\boldsymbol{\omega}$ from Section 3.1, $\tilde{H}(\beta) = \tilde{H}(\beta, Y, m)$ the confidence regions for $\boldsymbol{f}$ as in Theorem 3.3.1, and $\hat{m}$ as in Definition 3.6.8. Then for any $\alpha, \beta \in (0, 1)$ and α_n as in (1.25) it holds that*

1. $\lim_{n\to\infty} \inf_{\boldsymbol{g}\in\mathcal{M}^{\delta,\lambda}} \boldsymbol{P}(\boldsymbol{\omega} \in C_{1-\alpha}(Y, \lambda, \hat{m}) \geq 1 - \alpha,$
2. $\inf_{\boldsymbol{g}\in\mathcal{M}^{\delta,\lambda}} \boldsymbol{P}\left(\sup_{\tilde{\omega}\in C_{1-\alpha_n}(Y,\lambda,\hat{m})\cap\Omega^{\delta}_{\hat{m}}} \|\boldsymbol{\omega} - \tilde{\omega}\|_\infty \geq c_2 \frac{\ln(n)}{\sqrt{n}}\right) \leq \exp(-c_1 \ln^2(n)) + O\left(\exp\left(-\frac{c^2}{8}n\right)\right),$
3. $\lim_{n\to\infty} \inf_{\boldsymbol{g}\in\mathcal{M}^{\delta,\lambda}} \boldsymbol{P}(\boldsymbol{f} \in \tilde{\mathcal{H}}(\beta, Y, \hat{m})) \geq 1 - \beta,$

with c_1, c_2 as in (3.13) and c as in Definition 3.6.8.

CHAPTER 4

Minimax rates for multiple mixtures

In the following the MABS model (1.6) is considered and minimax rates for fixed number of sources $\boldsymbol{m} = m$ and both, the sample size n and the number of mixtures M, tending to infinity are derived. To this end, the unknown finite alphabet design matrix $F \in \mathfrak{A}^{n\times m}$ in (1.6) is rewritten as a product of an unknown selection matrix Π and a known design matrix A with rows consisting of all different alphabet combinations in $\mathfrak{A}^m$. This highlights the combinatorial structure of estimating F in (1.6). Fix a finite alphabet $\mathfrak{A} = \{0, 1, a_3, \ldots, a_k\}$ as in (1.7) and $n, m, M \in \mathbb{N}$ with $K \coloneqq k^m$. Then the MABS model (1.6) is equivalent to

$$Y = \boldsymbol{\Pi} A\boldsymbol{\omega} + Z, \tag{4.1}$$

with an unknown selection matrix

$$\boldsymbol{\Pi} \in \{0, 1\}^{n\times K}, \quad \sum_{j=1}^{n} \boldsymbol{\Pi}_{ij} = 1 \ \forall i = 1, \ldots, n, \tag{4.2}$$

and known finite alphabet design matrix

$$A \coloneqq \begin{pmatrix} 0 & 0 & 0 & \ldots & 0 & 0 & 0 \\ 0 & 0 & 0 & \ldots & 0 & 0 & 1 \\ 0 & 0 & 0 & \ldots & 0 & 0 & a_3 \\ & & & \vdots & & & \\ 0 & 0 & 0 & \ldots & 0 & 0 & a_k \\ 0 & 0 & 0 & \ldots & 0 & 1 & 0 \\ & & & \vdots & & & \\ a_k & a_k & a_k & \ldots & a_k & a_k & a_k \end{pmatrix} \in \{0, 1, a_3, \ldots, a_k\}^{K\times m}, \tag{4.3}$$

where the rows of A constitute all different vectors in $\mathfrak{A}^m = \{0, 1, a_3, \ldots, a_k\}^m$. Further, the mixing matrix $\boldsymbol{\omega} \in \Omega_{m,M}$ is unknown as well and we assume i.i.d. normal noise $Z_{ij} \sim \mathcal{N}(0, \sigma^2)$, $i = 1, \ldots, n$, $j = 1, \ldots, M$, with known variance σ^2. As before, δ-separability from Definition 2.2.1 is assumed to regularize the model (4.1). Here, $(\Pi, \boldsymbol{\omega})$ in (4.1) is denoted as δ-separable, if $(\Pi A, \boldsymbol{\omega})$ is δ-separable as in Definition 2.2.1. Further, analog to λ in (1.12), a second parameter which regularizes separability of $\boldsymbol{\Pi}$ is introduced. To this end, ΠA is denoted as Λ-*separable*,

if the i-th unit vector e^i appears in ΠA at least Λ times for each $i = 1, \dots, m$. That is

$$\#\left\{j \in \{1, \dots, n\} : \ (\Pi A)_{j\cdot} = e^i\right\} \geq \Lambda \quad \text{for all } i = 1, \dots, m. \tag{4.4}$$

In summary, for A as in (4.3) we consider the parameter space

$$\mathcal{N}^{\delta,\Lambda} = \mathcal{N}^{\delta,\Lambda}_{n,M,m} := \left\{\Pi A\omega : \ \omega \in \Omega^{\delta}_{m,M}, \ \Pi \text{ as in (4.2) and (4.4)} \right\}.$$

4.1 Minimax rates for prediction error

The following theorem gives a lower bound on the minimax prediction error in the MABS model (4.1).

Theorem 4.1.1 (Lower bound)**.** *Consider the MABS model (4.1) with parameter space $\mathcal{N}^{\delta,\Lambda}$. Further, assume that $M/m, n/m \in \mathbb{N}$ and $\sigma/\sqrt{8} < \delta \leq \sqrt{M}(\Delta\mathfrak{A}_{\min})^2(45a_k m)^{-1}$ and $\Lambda \leq n/m$. Then*

$$\inf_{\hat{\theta}} \sup_{\boldsymbol{\Pi} A\boldsymbol{\omega} \in \mathcal{N}^{\delta,\Lambda}} \mathrm{E}_{\boldsymbol{\Pi} A\boldsymbol{\omega}} \left(\left\| \hat{\theta} - \boldsymbol{\Pi} A\boldsymbol{\omega} \right\|^2 \right) \geq 0.4M \left(\frac{1}{(m-1)\sigma^2} + \frac{72m^5 a_k^2}{(\Delta\mathfrak{A}_{\min})^2 n} \right)^{-1} + \frac{1}{2}\sigma\delta e^{-\frac{\delta^2}{8\sigma^2}}.$$

The next theorem gives an upper bound on the minimax prediction error. If δ and Λ are chosen appropriately, it almost (up to the dependency on m and $\mathfrak{A}$ in the exponential term) coincides with the lower bound from Theorem 4.1.1 (see Corollary 4.1.4). This upper bound is achieved by the LSE $\hat{\theta} \in \operatorname{argmin}_{\tilde{\theta} \in \mathcal{N}^{\delta,\Lambda}} \left\| Y - \tilde{\theta} \right\|^2$.

Remark 4.1.2 (LSE).

a) (Existence) The LSE $\hat{\theta}$ exists, that is the minimum in $\min_{\tilde{\theta} \in \mathcal{N}^{\delta,\Lambda}} \left\| Y - \tilde{\theta} \right\|^2$ is attained. To see this, note that

$$\mathcal{N}^{\delta,\Lambda} = \bigcup_{\Pi \ \Lambda\text{-separable}} \left\{\Pi A\omega : \ \omega \in \Omega^{\delta}_{m,M}\right\} \tag{4.5}$$

is a finite union of closed, bounded in $[0, a_k]^{n\times M}$, hence, compact sets.

b) (Uniqueness) $\hat{\theta}$ is not always unique, but the upper bound in Theorem 4.1.3 holds for any minimizer. A counterexample is the following. Let $n = m = 2$, $M = 1$, $\Lambda = 1$, $\mathfrak{A} = \{0, 1, 2\}$, and $\delta = 0.01$. By separability, $\hat{\Pi} A$ is restricted to the identity matrix. Thus

$$\operatorname*{argmin}_{\tilde{\theta} \in \mathcal{N}^{\delta,\Lambda}} \left\| Y - \tilde{\theta} \right\|^2 = \operatorname*{argmin}_{\omega \in \Omega^{\delta}_{2,1}} \|Y - \omega\|^2 = \operatorname*{argmin}_{\omega \in \Omega^{\delta}_{2,1}} \omega_1^2 - (1 + Y_1 + Y_2)\omega_1,$$

with $\omega_1 = 1 - \omega_2$. Simple calculations give that $\Omega^{\delta}_{2,1} = \{(\omega_1, 1-\omega_1)^\top : \ \omega_1 \in [0.1, 3/10] \cup [11/30, 0.45]\}$. If the observations Y_1, Y_2 are such that $(1 + Y_1 + Y_2)/2 = 1/3$, it is easy to check that $\operatorname{argmin}_{\omega \in \Omega^{\delta}_{2,1}} \omega_1^2 - (1 + Y_1 + Y_2)\omega_1 = \{(3/10, 7/10)^\top, (11/30, 19/30)^\top\}$.

c) (Computation) We are not aware of an efficient implementation of the LSE and we speculate that this is an NP-hard problem in general (see the discussion in Section 5.2). In Section 5.2 an iterative Lloyd's algorithm for its approximation is proposed.

Theorem 4.1.3 (Upper bound)**.** *Let $Y = \mathbf{\Pi} A\boldsymbol{\omega} + Z$ with $\mathbf{\Pi} A\boldsymbol{\omega} \in \mathcal{N}^{\delta,\Lambda}$ be as in the MABS model (4.1) and let $\hat{\theta} \in \operatorname{argmin}_{\tilde{\theta}\in\mathcal{N}^{\delta,\Lambda}} \left\|Y - \tilde{\theta}\right\|^2$ be the LSE. Then*

$$\sup_{\mathbf{\Pi} A\boldsymbol{\omega}\in\mathcal{N}^{\delta}} \mathrm{E}_{\mathbf{\Pi} A\boldsymbol{\omega}}\left(\left\|\hat{\theta} - \mathbf{\Pi} A\boldsymbol{\omega}\right\|^2\right) \leq 4\sigma^2 mM + 12\sigma n^2 k^m m^{7/2} a_k^3 \frac{M^{5/2}}{\sqrt{\Lambda}\delta} e^{-\frac{\Lambda\delta^2}{8(mM+1)(1+ma_k)^2\sigma^2}}.$$

Let throughout the following $\gtrsim$ and $\lesssim$ denote inequalities up to a universal constant which does not depend on any model parameters. Further, for some constants $c_1, c_2 > 0$ as in Corollary 4.1.4 assume that

$$M \geq \frac{144\sigma^2 m^3 a_k^3}{c_2 c_1^2}\left(2\ln(n) + 2\ln(M) + \ln\left(a_k^3 m^{7/3} k^m\right)\right) \text{ and } n \geq \min\left(\frac{m^6 a_k^2 \sigma^2}{(\Delta\mathfrak{N}_{\min})^2}, c_2 mM\right). \quad (4.6)$$

Note that (4.6) holds finally whenever $\ln(n)/M \to 0$ and $M/n \to 0$.

Corollary 4.1.4 (Minimax prediction rate)**.** *For some constants $c_1, c_2 > 0$ consider the MABS model (4.1) with parameter space $\mathcal{N}^{\delta,\Lambda}$ for $\delta = c_1\sqrt{M}$ and $\Lambda = c_2 M$. Further, assume that $\sigma/\sqrt{8M} < c_1 < (\Delta\mathfrak{N}_{\min})^2(45a_k m)^{-1}$ and $c_2 \geq 1/M$. Then whenever (4.6) holds*

$$\inf_{\hat{\theta}} \sup_{\mathbf{\Pi} A\boldsymbol{\omega}\in\mathcal{N}^{\delta,\Lambda}} \mathrm{E}_{\mathbf{\Pi} A\boldsymbol{\omega}}\left(\frac{1}{nM}\left\|\hat{\theta} - \mathbf{\Pi} A\boldsymbol{\omega}\right\|^2\right) \gtrsim \frac{\sigma^2 m}{n} + \frac{\sigma c_1}{n\sqrt{M}}\, e^{-\frac{c_1^2}{8}\frac{M}{\sigma^2}},$$

$$\inf_{\hat{\theta}} \sup_{\mathbf{\Pi} A\boldsymbol{\omega}\in\mathcal{N}^{\delta,\Lambda}} \mathrm{E}_{\mathbf{\Pi} A\boldsymbol{\omega}}\left(\frac{1}{nM}\left\|\hat{\theta} - \mathbf{\Pi} A\boldsymbol{\omega}\right\|^2\right) \lesssim \frac{\sigma^2 m}{n} + \frac{\sigma}{\sqrt{c_2} c_1 n\sqrt{M}}\, e^{-\frac{c_2 c_1^2}{16m^3(1+a_k)^2}\frac{M}{\sigma^2}}$$

and the LSE achieves the second inequality.

Remark 4.1.5. Note that the assumption $\delta = c_1\sqrt{M}$ and $\Lambda = c_2 M$ for some constants c_1, c_2 in Corollary 4.1.4 is not very restrictive. When $\boldsymbol{\omega}$ is uniformly distributed, Theorem 2.3.5 yields for $\delta = AS\,B(\boldsymbol{\omega})$ that $\delta/\sqrt{M} \geq c_1$ for some constant c_1 asymptotically with probability one as $M \to \infty$. Further, by Theorem 2.3.1, when ΠA is chosen uniformly, for Λ as in (4.4) $\Lambda/M \geq c_2$ for any $c_2 > 0$ asymptotically with probability one as $n/M \to \infty$.

Corollary 4.1.4 nicely shows the specific tradeoff between n and M regarding the prediction error of $\mathbf{\Pi} A\boldsymbol{\omega}$. The dependence on M vanishes exponentially fast (as long as $\ln(n)/M \to 0$ and $M/n \to 0$). For sufficiently large M the prediction rate is dominated by its first term, which is parametric in n. Thus, as long as $\ln(n)/M \to 0$ and $M/n \to 0$ the unknown permutation $\mathbf{\Pi}$ in the linear model (4.1) does not play much of a role.

4.2 Estimation error

The proof of Theorem 4.1.3 yields as a corollary the following upper bound on the maximal classification error $\mathbf{P}\left(\hat{\Pi} \neq \mathbf{\Pi}\right)$ for the LSE.

Corollary 4.2.1 (Upper bound on classification error)**.** *For some constants $c_1, c_2 > 0$ consider the MABS model (4.1) with parameter space $\mathcal{N}^{\delta,\Lambda}$ for $\delta = c_1\sqrt{M}$ and $\Lambda = c_2 M$. Further, assume that $\sigma/\sqrt{8M} < c_1 < (\Delta\mathfrak{N}_{\min})^2(45a_k m)^{-1}$ and $c_2 \geq 1/M$. Let $\hat{\theta} = \hat{\Pi}A\hat{\omega} \in \operatorname{argmin}_{\tilde{\theta}\in\mathcal{N}^{\delta,\Lambda}} \left\|Y - \tilde{\theta}\right\|^2$ be the LSE. Then whenever (4.6) holds*

$$\sup_{\boldsymbol{\Pi}A\boldsymbol{\omega}\in\mathcal{N}^{\delta,\Lambda}} \boldsymbol{P}_{\boldsymbol{\Pi}A\boldsymbol{\omega}}\left(\hat{\Pi} \neq \boldsymbol{\Pi}\right) \lesssim \frac{\sigma}{\sqrt{c_2}c_1 n\sqrt{M}}\, e^{-\frac{c_2c_1^2}{16m^3(1+a_k)^2}\frac{M}{\sigma^2}}. \tag{4.7}$$

In order to derive lower bounds for the maximal estimation error, one can combine Corollary 4.1.4 with Theorem 2.2.3. To this end, for $(\boldsymbol{\Pi}, \boldsymbol{\omega})$ and (Π, ω) as in (4.1) define the metric

$$d\left((\boldsymbol{\Pi}, \boldsymbol{\omega}), (\Pi, \omega)\right) = \frac{\sqrt{M}}{m}\, \mathbb{1}_{\boldsymbol{\Pi}\neq\Pi} + \max_{i=1,\dots,m} \|\boldsymbol{\omega}_i - \omega_i\|. \tag{4.8}$$

The metric in (4.8) combines the classification error of $\hat{\Pi} \neq \boldsymbol{\Pi}$ with the estimation error $\|\boldsymbol{\omega}_i - \hat{\omega}_i\|$. Note that the scaling factor $\sqrt{M}$ naturally arises from the dimensionality of $\|\boldsymbol{\omega}_i - \hat{\omega}_i\|$. The metrics $d\left((\boldsymbol{\Pi}, \boldsymbol{\omega}), (\Pi, \omega)\right)$ and $\|\boldsymbol{\Pi}A\boldsymbol{\omega} - \Pi A\omega\|$ are locally equivalent on $\mathcal{N}^{\delta}$ as the following theorem shows.

Theorem 4.2.2. *Let $\Pi A\omega, \Pi' A\omega' \in \mathcal{N}^{\delta}$ then*

1. *$d\left((\Pi, \omega), (\Pi', \omega')\right) \geq \|\Pi A\omega - \Pi' A\omega'\|/(\sqrt{n}ma_k)$ and*
2. *if $\|\Pi A\omega - \Pi' A\omega'\| \leq \delta/(1 + ma_k)$, then $d\left((\Pi, \omega), (\Pi', \omega')\right) \leq \|\Pi A\omega - \Pi' A\omega'\|$.*

The following theorem shows that the LSE is not only asymptotically minimax rate optimal for the prediction error as in Corollary 4.1.4, but also asymptotically for $M \to \infty$ minimax rate optimal for the estimation error in terms of the metric d in (4.8) .

Theorem 4.2.3 (Minimax estimation rate)**.** *For some constants $c_1, c_2 > 0$ consider the MABS model (4.1) with parameter space $\mathcal{N}^{\delta,\Lambda}$ for $\delta = c_1\sqrt{M}$ and $\Lambda = c_2 M$. Further, assume that $\sigma/\sqrt{8M} < c_1 < (\Delta\mathfrak{N}_{\min})^2(45a_k m)^{-1}$ and $c_2 \geq 1/M$. Then whenever (4.6) holds*

$$\inf_{\hat{\Pi},\hat{\omega}} \sup_{\boldsymbol{\Pi},\boldsymbol{\omega}} \mathrm{E}_{\boldsymbol{\Pi}A\boldsymbol{\omega}}\left(d\left((\boldsymbol{\Pi}, \boldsymbol{\omega}), (\hat{\Pi}, \hat{\omega})\right)^2\right) \gtrsim \sigma^2 M\, \frac{1}{nma_k^2} + \sigma\sqrt{M}\frac{c_1}{nm^2a_k^2}\, e^{-\frac{c_1^2}{8}\frac{M}{\sigma^2}},$$

$$\inf_{\hat{\Pi},\hat{\omega}} \sup_{\boldsymbol{\Pi},\boldsymbol{\omega}} \mathrm{E}_{\boldsymbol{\Pi}A\boldsymbol{\omega}}\left(d\left((\boldsymbol{\Pi}, \boldsymbol{\omega}), (\hat{\Pi}, \hat{\omega})\right)^2\right) \lesssim \sigma^2 M\, \frac{m^3a_k^2}{c_1^2} + \sigma\sqrt{M}\, \frac{m^2a_k^2}{\sqrt{c_2}c_1^3}\, e^{-\frac{c_2c_1^2}{16m^3(1+a_k)^2}\frac{M}{\sigma^2}}$$

and the LSE achieves the second inequality.

Again, Theorem 4.2.3 shows that when M is sufficiently large, increasing M further does not influence the estimation rate in terms of $d(\cdot,\cdot)^2/M$. Moreover, for M large enough, the minimax estimation rate of $d(\cdot,\cdot)^2/M$ does not increase with n, although the dimension of $\boldsymbol{\Pi}$ and $\hat{\Pi}$, respectively, increase with n. Thus, if $\ln(n) \ll M$ the unknown permutation Π in the linear model (4.1) does not play much of a role for the estimation rate.

CHAPTER 5

Implementation

5.1 Multiscale methods

The SLAM estimators and confidence statements for given number of sources $\boldsymbol{m}$ from Chapter 3 are implemented in two steps. In the first step, for a given $\alpha \in (0,1)$ a confidence region for the mixing weights $\boldsymbol{\omega}$ is computed as in Algorithm CRW (see Figure 3.1). To this end, each of the $n^{2\boldsymbol{m}}$ $\boldsymbol{m}$-boxes in $\mathfrak{B}^{\boldsymbol{m}} = \{B(i,j) : 1 \le i \le j \le n\}^{\boldsymbol{m}}$ needs to be examined with the reduction rules R1 - R3 for validity as a candidate box for the intervals $[i_1^\star, j_1^\star] \times \ldots \times [i_{\boldsymbol{m}}^\star, j_{\boldsymbol{m}}^\star]$. The reduction rule R1 can be applied to all the n^2 boxes in $\mathfrak{B}$ separately, which, using dynamic programming, amounts to a total complexity of $O(n^2)$. For a single candidate box in $\mathfrak{B}^{\boldsymbol{m}}$ the complexity of applying reduction rule R2 is $O(1)$ and of R3 is $O(n)$. For the latter, note that a candidate box $B \in \mathfrak{B}^{\boldsymbol{m}}$ is accepted by R3, if the $O(n)$ intervals $\{[i,j] \in \mathcal{J}_k^\lambda : \ j - i + 1 = n\lambda\}$ for which $\left[\max_{i \le u \le v \le j} \underline{b}_{uv}, \min_{i \le u \le v \le j} \overline{b}_{uv}\right] \cap \left\{e\omega : \ e \in \mathfrak{U}^{\boldsymbol{m}} \text{ and } \omega \in B\right\}$ is non-empty cover all points $1, \ldots, n$. This yields the overall complexity $O\left(n^{2\boldsymbol{m}+1}\right)$[1]. There are, however, important pruning steps, which can lead to a considerably smaller complexity.

First, note that it suffices to consider $\boldsymbol{m}$-boxes which are maximal elements with respect to the partial order of inclusion, i.e., for $B^1 = [\underline{b}_1^1, \overline{b}_1^1] \times \ldots \times [\underline{b}_{\boldsymbol{m}}^1, \overline{b}_{\boldsymbol{m}}^1]$, $B^2 = [\underline{b}_1^2, \overline{b}_1^2] \times \ldots \times [\underline{b}_{\boldsymbol{m}}^2, \overline{b}_{\boldsymbol{m}}^2]$

$$B^1 \preccurlyeq B^2 \Leftrightarrow [\underline{b}_i^1, \overline{b}_i^1] \subseteq [\underline{b}_i^2, \overline{b}_i^2] \quad \text{for all } i = 1, \ldots, \boldsymbol{m},$$

where an element a of a partially ordered set P is maximal if there is no element b in P such that $b > a$. To see this, assume that an $\boldsymbol{m}$-box B is not deleted by the reduction rule R3 in the second last line of Algorithm CRW, then an $\boldsymbol{m}$-box $B' \in \mathfrak{B}^{\boldsymbol{m}}$ with $B' \prec B$ does not influence the confidence region $C_{1-\alpha}$ (see last line of Algorithm CRW), as $A^{-1}B' \subset A^{-1}B$. Conversely, if an $\boldsymbol{m}$-box B is deleted by the reduction rule R3 in the second last line of Algorithm CRW, then an $\boldsymbol{m}$-box $B' \in \mathfrak{B}^{\boldsymbol{m}}$ with $B' \prec B$ will be deleted by R3 as well, such that B' does not need to be considered either.

Second, note that the parameter $\boldsymbol{\omega}$ which is inferred in Algorithm CRW is global and hence, one can restrict to observations on a subinterval $[x_i, x_j] \subset [0,1)$ as long as $\boldsymbol{g}|_{[x_i,x_j]}$ is δ-separable. The explicit complexity of Algorithm CRW depends on the finial solution $\hat{f}$ itself. Depending on the final $\hat{f}$, the above mentioned pruning steps yield a complexity between $O(n^{\boldsymbol{m}+1})$ and

[1] In (Behr et al., 2017) the additional n-factor from applying reduction rule R3 was missing.

$O(n^{2m+1})$. With linear programming (see Theorem 5.1.1), $\hat{\omega}$ is then computed as in (1.23). In the second step, for a given $\beta \in (0,1)$ and given $\hat{\omega}$ SLAM solves the constrained optimization problem (1.28). Note that $\hat{f}^1, \dots, \hat{f}^m$ are the unique functions such that $\sum_{i=1}^m \hat{\omega}_i \hat{f}^i = \hat{g}$ for

$$\hat{g} := \operatorname*{argmax}_{\tilde{g} \in \mathfrak{H}(\beta)} \sum_{i=1}^{n} \phi_{\tilde{g}(x_i)}(Y_i), \tag{5.1}$$

with

$$\mathfrak{H}(\beta) := \left\{ \tilde{g} \in \mathcal{S}(\{e\hat{\omega} : e \in \mathfrak{A}^m\}) : T_n(Y, \tilde{g}) \leq q_n(\beta) \text{ and } K(\tilde{g}) = \hat{K} \right\} \tag{5.2}$$

and $\hat{K}$ as in (1.27). Frick et al. (2014) provide a pruned dynamic programming algorithm to efficiently solve (5.1) without the restriction that $\hat{g}$ can only attain values in $\{e\hat{\omega} : e \in \mathfrak{A}^m\}$ as it is the case here. To extend their algorithm to this case, it is necessary for a finite set $\mathfrak{L} = \{l_1, \dots, l_k\}$ of possible function values to check finiteness of their *minimal cost* $d^\star_{[i,j]} = \min_{\theta \in \mathbb{R}} d_{[i,j]}$ (see (Frick et al., 2014, eq. 30)) with $\mathbb{R}$ replaced by $\mathfrak{L}$. In (Frick et al., 2014) finiteness of $d^\star_{[i,j]} = \min_{\theta \in \mathbb{R}} d_{[i,j]}$ is examined by the relation

$$\min_{\theta \in \mathbb{R}} d_{[i,j]} = \infty \quad \Leftrightarrow \quad \max_{i \leq u \leq v \leq j} \underline{b}_{uv} > \min_{i \leq u \leq v \leq j} \overline{b}_{uv}, \tag{5.3}$$

with $\{B(i,j) = [\underline{b}_{ij}, \overline{b}_{ij}] : 1 \leq i \leq j \leq n\}$ as in (1.18). Let L be any number such that $L > \max(\mathfrak{L})$ and define $Q(i,j) =$

$$\left[\underline{q}_{ij}, \overline{q}_{ij}\right] := \begin{cases} [\max(\mathfrak{L} \cap B(i,j)), \min(\mathfrak{L} \cap B(i,j))] & \text{if } \mathfrak{L} \cap B(i,j) \neq \emptyset, \\ [L, L] & \text{else.} \end{cases} \tag{5.4}$$

Then as in (5.3) it holds that

$$\min_{\theta \in \mathfrak{L}} d_{[i,j]} = \infty \quad \Leftrightarrow \quad \max_{i \leq u \leq v \leq j} \underline{q}_{uv} > \min_{i \leq u \leq v \leq j} \overline{q}_{uv}, \tag{5.5}$$

which allows to adapt the dynamic program from Frick et al. (2014). This modifications, however, do not change the complexity of their algorithm, which depends on the final solution $\hat{g}$ and is between $O(n)$ and $O(n^2)$. Here, significant speed up can be achieved by restricting the system of intervals in T_n and $\mathfrak{B}$, respectively, to a smaller subsystem, e.g. intervals of dyadic length, which for example reveals the complexity of the dynamic program as $O(n \ln(n))$.

SLAM selector In the following we discuss computational issues of the estimator $\hat{m}(q)$ in (3.22). In order to compute $\hat{m}(q)$ one has to compute successively $C_q^1, C_q^2, \dots$ until one of the sets C_q^m is nonempty, where $C_q^m = C_q(Y, \lambda, m) \cap \Omega_m^\delta$ with $C_q(Y, \lambda, m)$ the confidence sets for $\boldsymbol{\omega}$ for given number of sources from Section 3.1. As discussed above, the computation of $C_q(Y, \lambda, m)$ has a complexity between $O\left(n^{m+1}\right)$ and $O\left(n^{2m+1}\right)$ depending on the true underlying signal. Thus, the overall complexity of the computation of $C_q(Y, \lambda, 1), C_q(Y, \lambda, 2), \dots, C_q(Y, \lambda, \hat{m})$ can be done in $O\left(n^{2\hat{m}(q)+1}\right)$ time. As the computation cost of intersecting $C_q(Y, \lambda, m)$ and Ω_m^δ does not depend on n and as $\hat{m}(q)$ hardly ever overestimated $\boldsymbol{m}$ (see Section 6.2) the overall com-

plexity for the computation of $\hat{m}(q)$ is, in practice, between $O\left(n^{m+1}\right)$ and $O\left(n^{2m+1}\right)$. Checking emptiness of $C_q(Y, \lambda, m) \cap \Omega_m^\delta$ can be done with a mixed-integer linear program (MILP) as the following theorem shows. To this end, note that

$$C_{q,\lambda} \cap \Omega_m^\delta \neq \emptyset \quad \Leftrightarrow \quad \max_{\omega \in C_{q,\lambda} \cap \Omega_m} ASB(\omega) \geq \delta.$$

Theorem 5.1.1. *The optimization problem*

$$\max_{\substack{\omega \in \Omega_m \\ a_i \leq \omega_i \leq b_i \text{ for } i=1,\ldots,m}} ASB(\omega, \mathfrak{A}), \tag{5.6}$$

with constants $a_1 \leq b_1, \ldots, a_m \leq b_m$ can be formulated as a MILP

$$\begin{aligned} &\max \quad c^\top x \quad \text{s.t.} \\ &\quad Ax \geq b, \\ &\quad \text{int} \quad x_i \quad i = m+2, \ldots, m+D+1, \end{aligned} \tag{5.7}$$

with vector of variables $x = (\omega, \delta, B) \in \mathbb{R}^{m+1} \times \{0,1\}^D$, objective function coefficients $c = (0, \ldots, 0, 1, 0, \ldots, 0) \in \mathbb{R}^{m+1} \times \{0,1\}^D$, a matrix of constraint coefficients $A \in \mathbb{R}^{(3(D+m)+2) \times (D+m+1)}$, and a vector of values for the right-hand sides of the constraints $b \in \mathbb{R}^{(3(D+m)+2)}$.

Remark 5.1.2 (Minimization). By definition of the ASB, clearly, $\min_{\omega \in \Omega_m} ASB(\omega, \mathfrak{A}) = 0$ for all finite alphabets $\mathfrak{A}$ and number of source components m. With additional boundary restrictions, i.e.,

$$\min_{\substack{\omega \in \Omega_m \\ a_i \leq \omega_i \leq b_i \text{ for } i=1,\ldots,m}} ASB(\omega, \mathfrak{A}) \tag{5.8}$$

this does not hold in general. It is clear from the proof of Theorem 5.1.1 that (5.8) is solved by the same MILP as (5.6) with max replaced by min.

5.2 Clustering based algorithm

In Chapter 4 we have seen that the LSE attains (almost) optimal rates for both, the maximal prediction error and the maximal estimation error (in terms of the metric d in (4.8)). Unfortunately, we are not aware of any polynomial time algorithm for its exact computation. To this end, note that in (4.5) for $\Pi \neq \Pi'$, both Λ-separable, Theorem 2.2.3 implies that the corresponding two sets in the union in (4.5) are disjoint. Thus, computation of the LSE amounts to minimization over exponentially many (in n) disjoint, compact sets. Pananjady et al. (2016) have shown that exact computation of the LSE is NP-hard in general, for the MABS model (4.1) with $M = 1$, but for arbitrary design A (not the specific form in (4.3)) and restricted to permutation matrices Π (not the bigger class of selection matrices). Although, their results do not directly apply to our setting, it is near at hand that exact computation of the LSE for the MABS model (4.1) is also not feasible.

Input: Y, A, t, m
$\hat{\omega}^1 \leftarrow$ uniform random choice
$\hat{\Pi}_{j\cdot}A \leftarrow \operatorname{argmin}_{a\in\mathfrak{A}^m} \left\|Y_j - a\hat{\omega}^1\right\|$ for $j = 1, \ldots, n$
$\hat{\omega}^2 \leftarrow \operatorname{argmin}_{\omega} \left\|Y - \hat{\Pi}A\omega\right\|^2$
while $\max_{1\le i\le m,\ 1\le j\le n} \left|\hat{\omega}^1_{ij} - \hat{\omega}^2_{ij}\right| > t$ **do**
  $\hat{\omega}^1 \leftarrow \hat{\omega}^2$
  $\hat{\Pi}_{j\cdot}A \leftarrow \operatorname{argmin}_{a\in\mathfrak{A}^m} \left\|Y_j - a\hat{\omega}^2\right\|$ for $j = 1, \ldots, n$
  $\hat{\omega}^2 \leftarrow \operatorname{argmin}_{\omega} \left\|Y - \hat{\Pi}A\omega\right\|^2$
end while
Return: $\hat{\omega}^1$ and $\hat{\Pi}$.

Figure 5.1: Lloyd's algorithm for approximation of the LSE in the ABSS model.

Therefore, in the following a Lloyd's algorithm for its approximation is proposed. To ensure minimax optimality in $\mathcal{N}^{\delta,\Lambda}$ the LSE depends on the regularization parameters (δ, Λ). For computational purposes consider now the unrestricted case $\delta = \Lambda = 0$. Then, on the one hand, given the selection Π computation of the unrestricted LSE corresponds to a convex optimization problem, which can be solved easily with standard techniques, see e.g. (Van den Meersche et al., 2009). Note that the condition $0 < \|\omega_{1\cdot}\| < \ldots < \|\omega_{m\cdot}\|$ in (1.2) can be neglected in this optimization step, as for any permutation matrix P it holds that $\|Y - \Pi A\omega\| = \left\|Y - \Pi AP^{-1}P\omega\right\|$ and hence, one can reorder the columns of $\hat{\omega}$ and the rows of $\hat{\Pi}A$ subsequently. On the other hand, given the mixture matrix ω computation of the LSE corresponds to a simple LS clustering with known centers $A\omega \in \mathbb{R}^{K\times M}$. Therefore, an iterative Lloyd's algorithm (see e.g., (Lu and Zhou, 2016)) which starts with a random $\hat{\omega}$ and successively updates $\hat{\Pi}$ and $\hat{\omega}$ can be employed, see Figure 5.1 for details. Note that this algorithm may as well be applied to the more general setting of an arbitrary design A with unknown selection matrix Π as in (Pananjady et al., 2017). Clearly, in each step of the Lloyd's algorithm $\left\|Y - \hat{\Pi}A\hat{\omega}\right\|^2$ decreases and thus, converges to a local minimum of $(\omega, \Pi) \mapsto \|Y - \Pi A\omega\|^2$. In order to reach the global minimum, we propose to compute K realizations of the algorithm in Figure 5.1 (for several random initial values for $\hat{\omega}$) and chose the one which minimizes $(\omega, \Pi) \mapsto \|Y - \Pi A\omega\|^2$. In practice, $t = 0.001$ (see Figure 5.1) and $K = 3$ worked well, usually terminating within 10 iterations. For instance, computation in R for $n = M = 1,000$, $m = 3$, $\mathfrak{A} = \{0, 1\}$ takes about 5 seconds on a desktop computer with intel core i7 processor.

CHAPTER 6

Simulations

6.1 SLAM

In the following, the influence of all parameters and the underlying signal on the performance of the SLAM estimator for known number of sources $\boldsymbol{m}$ from Chapter 3 is investigated empirically. Performance measures are the mean absolute error, MAE, for $\hat{\omega}$ and the mean absolute integrated error, MIAE, for $\hat{f}$. Further, we report the centered mean, Mean$(\hat{K}) - K$, the centered median, Med$(\hat{K}) - K$, of the number of c.p.'s of $\hat{f}$, the frequency of correctly estimated number of c.p.'s for the single source functions $\boldsymbol{f}^i$, Mean$(\hat{K} = K)_i$, and for the whole source function vector $\boldsymbol{f}$, Mean$(\hat{K} = K)$. To investigate the accuracy of the c.p. locations of the single estimated source functions $\hat{f}^1, \ldots, \hat{f}^m$ we report the mean of $\max_i \min_j \left|\tau_i - \hat{\tau}_j\right|$ and $\max_j \min_i \left|\tau_i - \hat{\tau}_j\right|$, where τ and $\hat{\tau}$ denotes the vector of c.p. locations of the true signal and the estimate, respectively. Furthermore, we report common segmentation evaluation measures for the single estimated source functions $\hat{f}^1, \ldots, \hat{f}^m$, namely the entropy-based V-measure, V_1, with balancing parameter 1 of Rosenberg and Hirschberg (2007) and the false positive sensitive location error, FPSLE, and the false negative sensitive location error, FNSLE, of Futschik et al. (2014). The V-measure, taking values in $[0, 1]$, measures whether given clusters include the correct data points of the corresponding class. Larger values indicate higher accuracy, 1 corresponding to a perfect segmentation. The FPSLE and the FNSLE capture the average distance between true and estimated segmentation boundaries, with FPSLE being larger if a spurious split is included, while FNSLE getting larger if a true boundary is not detected (see (Futschik et al., 2014) for details). To investigate the performance of the confidence region $C_{1-\alpha}$ for $\boldsymbol{\omega}$ we use $\overline{\mathrm{dist}}(\boldsymbol{\omega}, C_{1-\alpha})$ from (1.26), the mean coverage Mean$(\boldsymbol{\omega} \in C_{1-\alpha})$, and the diameters $\overline{\omega}_i - \underline{\omega}_i$, where $C_{1-\alpha} = [\overline{\omega}_1, \underline{\omega}_1] \times \ldots \times [\overline{\omega}_{\boldsymbol{m}}, \underline{\omega}_{\boldsymbol{m}}]$. Further, we report the mean coverage of the confidence band $\tilde{\mathcal{H}}(\beta)$, i.e. Mean$(\boldsymbol{f} \in \tilde{\mathcal{H}}(\beta))$. In order to reduce computation time, we only considered intervals of dyadic length as explained in Section 5.1, possibly at expense of detection power. Simulation runs were always $10,000$.

6.1.1 Number of source functions m

In order to illustrate the influence of the number of source functions $\boldsymbol{m}$ on the performance of SLAM we vary $\boldsymbol{m} = 2, \ldots, 5$ while keeping the other parameters in the SBSR model fixed. We investigate a binary alphabet $\mathfrak{A} = \{0, 1\}$ and set $\boldsymbol{f}^i = \mathbb{1}_{[(i-1)/5, i/5)}$ for $i = 1, \ldots, 5$, simple bump

functions (see Figure 6.3). For each $\boldsymbol{m} \in \{2,3,4,5\}$ $\boldsymbol{\omega}$ is chosen such that $ASB(\boldsymbol{\omega}) = 0.02$ in (1.8) (see Table 6.1). For $\sigma = \delta = 0.02$, $n = 1,000$, and $\alpha = \beta = 0.1$ $\hat{\omega}$, $C_{0.9}$, $\hat{f}^1, \ldots, \hat{f}^m$, and $\tilde{\mathcal{H}}(0.1)$ are computed for each $\boldsymbol{m} \in \{2,3,4,5\}$, incorporating prior knowledge $\lambda \geq 0.025$ (see Algorithm CRW in Figure 3.1), with true minimal scale $\lambda = 0.05$. The results are displayed in Table 6.2. A major finding is that as the number of possible mixture values equals $k^{\boldsymbol{m}}$, the complexity of the SBSR model grows exponentially in $\boldsymbol{m}$ such that demixing becomes substantially more difficult with increasing $\boldsymbol{m}$.

	$\boldsymbol{m} = 2$	$\boldsymbol{m} = 3$	$\boldsymbol{m} = 4$	$\boldsymbol{m} = 5$
$\boldsymbol{\omega}$	$(0.02, 0.98)$	$(0.02, 0.04, 0.94)$	$(0.04, 0.06, 0.12, 0.78)$	$(0.06, 0.08, 0.12, 0.16, 0.58)$

Table 6.1: Weight vector $\boldsymbol{\omega}$ for $\boldsymbol{m} = 2,3,4,5$ such that the $ASB(\boldsymbol{\omega}) = 0.02$.

	$\boldsymbol{m} = 2$	$\boldsymbol{m} = 3$	$\boldsymbol{m} = 4$	$\boldsymbol{m} = 5$
MAE($\hat{\omega}$) $[10^{-4}]$	$(1,1)$	$(11,18,24)$	$(90,154,62,69)$	$(91,68,81,196,54)$
$\overline{\text{dist}}(\boldsymbol{\omega}, C_{1-\alpha})$ $[10^{-3}]$	11	23	63	54
Mean($\boldsymbol{\omega} \in C_{1-\alpha}$) [%]	100	99.99	99.96	100
$\overline{\boldsymbol{\omega}}_i - \underline{\boldsymbol{\omega}}_i$ $[10^{-3}]$	$(21,21)$	$(37,33,23)$	$(68,93,35,23)$	$(40,55,84,63,23)$
MIAE($\hat{f}^i$) $[10^{-3}]$	$(0.2,0.0)$	$(26,9,0.0)$	$(115,103,67,0.0)$	$(315,317,49,183,0.0)$
Mean($\hat{K}$) $- K$	$(0,0)$	$(0.22,-0.03,0)$	$(3.7,2.6,-0.6,0)$	$(2.75,2.28,0.75,-1.61,0)$
Med($\hat{K}$) $- K$	$(0,0)$	$(0,0,0)$	$(4,2,0,0)$	$(2,2,0,-2,0)$
Mean($\hat{K} = K)_i$ [%]	$(99.8,99.8)$	$(88.5,98,100)$	$(15.9,31,69.4,100)$	$(7.1,30.4,63.8,12,99.9)$
Mean($\hat{K} = K$) [%]	99.8	87.2	15.8	1
$\max_i \min_j \lvert\tau_i - \hat{\tau}_j\rvert$	$(0.37,0.02)$	$(33.82,4.77,0.00)$	$(245.49,95.75,2.52,0.00)$	$(374.38,208.32,40.12,7.41,0.02)$
$\max_j \min_i \lvert\tau_i - \hat{\tau}_j\rvert$	$(0.03,0.00)$	$(18.59,12.53,0.000)$	$(9.61,18.66,126.33,0.00)$	$(83.09,117.17,61.13,348.89,0.00)$
V_1 [%]	$(99.9,100)$	$(88.3,96.2,100)$	$(60.9,83.4,68.6,100)$	$(37.5,54.1,82.8,12.6,100)$
FPSLE	$(0.07,0.00)$	$(8.98,6.05,0.00)$	$(51.52,21.36,78.23,0.00)$	$(110.3,92.21,34.98,216.82,0.00)$
FNSLE	$(0.3,0.02)$	$(24.04,3.22,0.00)$	$(168.04,45.09,62.15,0.00)$	$(205.75,137.64,41.29,90.02,0.02)$
Mean($\boldsymbol{f} \in \tilde{\mathcal{H}}(\beta)$) [%]	99.93	99.49	98.77	91.08

Table 6.2: Performance of SLAM for $\boldsymbol{m} \in \{2,\ldots,5\}$, for a binary alphabet $\mathfrak{A} = \{0,1\}$, sources $\boldsymbol{f}^i = \mathbb{1}_{[(i-1)/5, i/5)}$ for $i = 1,\ldots,5$, and $\boldsymbol{\omega}$ as in Table 6.1.

6.1.2 Number of alphabet values k

To illustrate the influence of the number of alphabet values k we consider three different alphabets $\mathfrak{A}_k = \{0,\ldots,k\}$ for $k = 2,3,4$. For $\boldsymbol{m} = 2$ we set

$$\boldsymbol{f}^1 = \sum_{i=0}^{15} (i \mod k)\, \mathbb{1}_{[i,i+1)/16}, \quad \boldsymbol{f}^2 = \sum_{i=0}^{[15/k]} (i \mod k)\, \mathbb{1}_{k[i,i+1)/16}, \tag{6.1}$$

step functions taking successively every alphabet value in $\mathfrak{A}^2$ (see Figure 6.1). Further, we set $\boldsymbol{\omega} = (0.02, 0.98)$ such that $ASB(\boldsymbol{\omega}) = 0.02$ for $k = 2,3,4$. For $\sigma = 0.05$, $n = 1,056$, and $\alpha = \beta = 0.1$ we compute $\hat{\omega}$, $C_{0.9}$, $\hat{f}^1, \ldots, \hat{f}^m$, and $\tilde{\mathcal{H}}(0.1)$ for each $k = 2,3,4$, incorporating prior knowledge $\lambda \geq 1/32$, with truth $\lambda = 1/16$. The results are displayed in Table 6.3. From this we find that an increasing k does not influence SLAM's performance for $\hat{\omega}$ and $C_{1-\alpha}$ too much. However, the model complexity $k^{\boldsymbol{m}}$ increases polynomially (for $m = 2$ as in Table 6.3 quadratically) in k, reflected in a decrease of SLAM's performance for the estimate of the source functions $\hat{f}$.

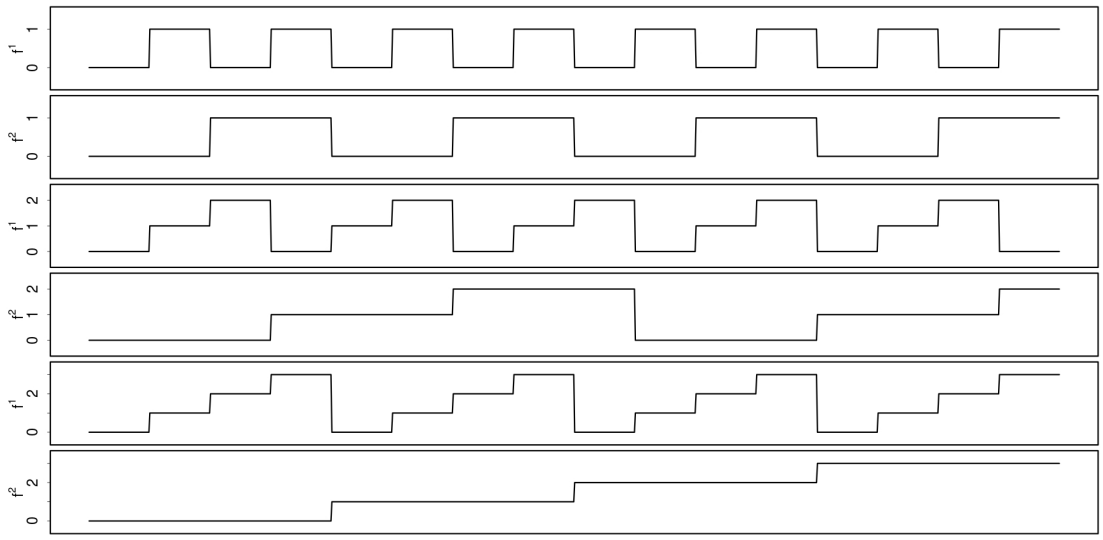

Figure 6.1: $\boldsymbol{f}^1$ and $\boldsymbol{f}^2$ from (6.1) for $\mathfrak{A} = \{0,1\}, \{0,1,2\}$, and $\{0,1,2,3\}$ (from top to bottom).

	$k=2$	$k=3$	$k=4$
$\mathrm{MAE}(\hat{\omega})$ $[10^{-3}]$	$(19, 12)$	$(18, 12)$	$(15, 11)$
$\overline{\mathrm{dist}}(\boldsymbol{\omega}, C_{1-\alpha})$ $[10^{-3}]$	51	51	47
$\mathrm{Mean}(\boldsymbol{\omega} \in C_{1-\alpha})$ [%]	100	100	100
$\overline{\omega}_i - \underline{\omega}_i$ $[10^{-3}]$	$(71, 71)$	$(71, 71)$	$(67, 67)$
$\mathrm{MIAE}(\hat{f}^i)$ $[10^{-2}]$	$(29, 0)$	$(49, 0)$	$(60, 0)$
$\mathrm{Mean}(\hat{K}) - K$	$(-6.65, 0)$	$(-7.42, 0)$	$(-7.04, 0)$
$\mathrm{Med}(\hat{K}) - K$	$(-6, 0)$	$(-7, 0)$	$(-7, 0)$
$\mathrm{Mean}(\hat{K} = K)_i$ [%]	$(0.39, 99.99)$	$(0, 100)$	$(0, 100)$
$\mathrm{Mean}(\hat{K} = K)$ [%]	0.39	0	0
$\max_i \min_j \lvert\tau_i - \hat{\tau}_j\rvert$	$(17.5, 0.0)$	$(22.0, 0.0)$	$(23.31, 0.00)$
$\max_j \min_i \lvert\tau_i - \hat{\tau}_j\rvert$	$(96.0, 0.0)$	$(134.4, 0.0)$	$(79.8, 0.0)$
V_1 [%]	$(81.7, 100)$	$(78, 100)$	$(81.5, 100)$
FPSLE	$(0.4, 0.0)$	$(58.3, 0.0)$	$(37.2, 0.0)$
FNSLE	$(25.7, 0.0)$	$(29.3, 0.0)$	$(25.2, 0.0)$
$\mathrm{Mean}(f \in \tilde{\mathcal{H}}(\beta))$ [%]	94.60	98.49	98.60

Table 6.3: Performance of SLAM for $\mathfrak{A} = \{0, \ldots, k\}$, $k = 2, \ldots, 4$, for two sources $\boldsymbol{m} = 2$ as in Figure 6.1 and $\boldsymbol{\omega} = (0.02, 0.98)$.

6.1.3 Confidence levels α and β

We illustrate the influence of the confidence levels α and β on SLAM's performance with $\boldsymbol{f}$ and $\boldsymbol{\omega}$ as in Example 1.2.1, i.e. $\boldsymbol{m} = 3$, $\mathfrak{A} = \{0, 1, 2\}$, $\boldsymbol{\omega} = (0.11, 0.29, 0.6)$, and $\boldsymbol{f}$ as displayed in Figure 1.4. For $\sigma = 0.02, 0.05, 0.1$ and $n = 1,280$ we compute $\hat{\omega}$, $C_{1-\alpha}$, $\hat{f}^1, \ldots, \hat{f}^m$, and $\tilde{\mathcal{H}}(\beta)$ for each $(\alpha, \beta) \in \{0.01, 0.05, 0.1\}^2$, incorporating prior knowledge $\lambda \geq 0.025$ with truth $\lambda = 0.05$. Results are displayed in Table 6.4 and Table 6.5.

$\sigma = 0.02$			
	$\alpha = 0.01$	$\alpha = 0.05$	$\alpha = 0.1$
MAE($\hat{\omega}$) [10^{-3}]	(2, 2, 2)	(1, 1, 1)	(1, 1, 1)
$\overline{\text{dist}}(\boldsymbol{\omega}, C_{1-\alpha})$ [10^{-3}]	29	25	24
Mean($\boldsymbol{\omega} \in C_{1-\alpha}$) [%]	100	100	100
$\overline{\omega}_i - \underline{\omega}_i$ [10^{-3}]	(48, 46, 44)	(43, 42, 42)	(42, 42, 42)
$\sigma = 0.05$			
	$\alpha = 0.01$	$\alpha = 0.05$	$\alpha = 0.1$
MAE($\hat{\omega}$) [10^{-3}]	(22, 7, 16)	(23, 7, 16)	(22, 7, 16)
$\overline{\text{dist}}(\boldsymbol{\omega}, C_{1-\alpha})$ [10^{-3}]	109	105	102
Mean($\boldsymbol{\omega} \in C_{1-\alpha}$) [%]	100	100	99
$\overline{\omega}_i - \underline{\omega}_i$ [10^{-3}]	(168, 123, 115)	(160, 112, 106)	(155, 107, 102)
$\sigma = 0.1$			
	$\alpha = 0.01$	$\alpha = 0.05$	$\alpha = 0.1$
MAE($\hat{\omega}$) [10^{-3}]	(59, 51, 13)	(45, 48, 13)	(32, 43, 18)
$\overline{\text{dist}}(\boldsymbol{\omega}, C_{1-\alpha})$ [10^{-3}]	231	218	210
Mean($\boldsymbol{\omega} \in C_{1-\alpha}$) [%]	100	100	100
$\overline{\omega}_i - \underline{\omega}_i$ [10^{-3}]	(329, 344, 282)	(305, 323, 226)	(276, 312, 212)

Table 6.4: Performance of SLAM's confidence set $C_{1-\alpha}$ and estimate $\hat{\omega}$ for the mixing $\boldsymbol{\omega}$ as in Example 1.2.1 with $\sigma = 0.02, 0.05, 0.1$ and $n = 1,280$ for $\alpha = 0.01, 0.05, 0.1$.

These illustrate that SLAM's estimate $\hat{\omega}$ for the mixing weights is very stable under the choice of α. The diameters $\overline{\text{dist}}(\boldsymbol{\omega}, C_{1-\alpha})$ and $\overline{\omega}_i - \underline{\omega}_i$, respectively decrease slightly with increasing α, as expected. Further, we found that the coverage Mean($\boldsymbol{\omega} \in C_{1-\alpha}$) is always bigger than the nominal coverage $1 - \alpha$ indicating the conservative nature of the first inequality in (3.4). With increasing β the multiscale constraint in (1.27) becomes stricter leading to an increase of $\hat{K}$. However, as Table 6.5 illustrates, this effect is remarkably small, resulting also in a high stability of $\hat{f}$ with respect to α and β. In contrast to the uniform coverage of the confidence region $C_{1-\alpha}$ for $\boldsymbol{\omega}$ for finite n (recall (1.21)), this holds only asymptotically for the confidence band $\tilde{\mathcal{H}}(\beta)$ (see Theorem 3.3.1). This is reflected in Table 6.5, where with increasing σ the coverage Mean($\boldsymbol{f} \in \tilde{\mathcal{H}}(\beta)$) can be smaller than the nominal $1 - \beta$. Nevertheless, the coverage of the single source functions remains reasonably high even for large σ (see Table 6.5). In summary, we draw from Table 6.4 and 6.5 a high stability of SLAM in the tuning parameters α and β, for both, the estimation error and the confidence statements, respectively.

$\sigma = 0.02$			
	$\boldsymbol{f}^1$	$\boldsymbol{f}^2$	$\boldsymbol{f}^3$
MIAE($\hat{f}^i$) [10^{-4}]	$\begin{pmatrix}0&2&10\\0&2&10\\0&2&10\end{pmatrix}$	$\begin{pmatrix}6&3&11\\9&5&12\\11&7&13\end{pmatrix}$	$\begin{pmatrix}3&1&4\\5&2&4\\6&3&5\end{pmatrix}$
Med($\hat{K}$) − K	$\begin{pmatrix}0&0&0\\0&0&0\\0&0&0\end{pmatrix}$	$\begin{pmatrix}0&0&0\\0&0&0\\0&0&0\end{pmatrix}$	$\begin{pmatrix}0&0&0\\0&0&0\\0&0&0\end{pmatrix}$
Mean($\hat{K} = K)_i$ [%]	$\begin{pmatrix}100&100&100\\100&100&100\\100&100&100\end{pmatrix}$	$\begin{pmatrix}98&100&100\\97&99&99\\96&98&99\end{pmatrix}$	$\begin{pmatrix}99&100&100\\98&99&99\\97&99&99\end{pmatrix}$
Mean($\hat{K} = K$) [%]	$\begin{pmatrix}98&99&100\\97&99&99\\96&98&99\end{pmatrix}$		
V_1 [%]	$\begin{pmatrix}100&100&100\\100&100&100\\100&100&100\end{pmatrix}$	$\begin{pmatrix}100&100&100\\100&100&100\\100&100&100\end{pmatrix}$	$\begin{pmatrix}100&100&100\\100&100&100\\100&100&100\end{pmatrix}$
Mean($\boldsymbol{f} \in \tilde{\mathcal{H}}(\beta)$) [%]	$\begin{pmatrix}95.8&93.3&92.3\\99.0&97.7&97.0\\99.2&98.6&98.1\end{pmatrix}$		
Mean($\boldsymbol{f}^i \in \tilde{\mathcal{H}}(\beta)_i$) [%]	$\begin{pmatrix}99.90&99.74&99.34\\99.94&99.78&99.64\\99.90&99.70&99.68\end{pmatrix}$	$\begin{pmatrix}99.84&99.60&99.38\\99.92&99.84&99.74\\99.90&99.82&99.74\end{pmatrix}$	$\begin{pmatrix}96.68&95.46&94.92\\99.18&98.34&98.10\\99.42&99.02&98.64\end{pmatrix}$
$\sigma = 0.05$			
	$\boldsymbol{f}^1$	$\boldsymbol{f}^2$	$\boldsymbol{f}^3$
MIAE($\hat{f}^i$) [10^{-3}]	$\begin{pmatrix}6&7&8\\6&8&9\\6&8&9\end{pmatrix}$	$\begin{pmatrix}160&161&160\\164&165&164\\160&161&161\end{pmatrix}$	$\begin{pmatrix}80&80&80\\82&83&82\\80&80&80\end{pmatrix}$
Med($\hat{K}$) − K	$\begin{pmatrix}0&0&0\\0&0&0\\0&0&0\end{pmatrix}$	$\begin{pmatrix}2&2&2\\2&2&2\\2&2&2\end{pmatrix}$	$\begin{pmatrix}-2&-2&-2\\-2&-2&-2\\-2&-2&-2\end{pmatrix}$
Mean($\hat{K} = K)_i$ [%]	$\begin{pmatrix}96&90&85\\93&86&80\\93&85&80\end{pmatrix}$	$\begin{pmatrix}21&19&17\\19&16&15\\21&19&17\end{pmatrix}$	$\begin{pmatrix}24&25&27\\21&23&24\\24&25&26\end{pmatrix}$
Mean($\hat{K} = K$) [%]	$\begin{pmatrix}19&16&14\\17&14&12\\19&16&14\end{pmatrix}$		
V_1 [%]	$\begin{pmatrix}99&99&99\\99&99&99\\99&99&99\end{pmatrix}$	$\begin{pmatrix}92&92&92\\92&92&92\\92&92&92\end{pmatrix}$	$\begin{pmatrix}91&91&91\\91&91&91\\91&91&91\end{pmatrix}$
Mean($\boldsymbol{f} \in \tilde{\mathcal{H}}(\beta)$) [%]	$\begin{pmatrix}83.1&76.7&74.0\\81.3&75.6&73.4\\81.7&76.4&74.5\end{pmatrix}$		
Mean($\boldsymbol{f}^i \in \tilde{\mathcal{H}}(\beta)_i$) [%]	$\begin{pmatrix}100&100&100\\100&100&99.98\\100&100&99.98\end{pmatrix}$	$\begin{pmatrix}89.34&84.78&82.82\\86.60&83.04&83.18\\87.24&84.16&83.18\end{pmatrix}$	$\begin{pmatrix}85.80&80.56&78.34\\83.14&78.48&77.14\\83.58&79.48&78.16\end{pmatrix}$
$\sigma = 0.1$			
	$\boldsymbol{f}^1$	$\boldsymbol{f}^2$	$\boldsymbol{f}^3$
MIAE($\hat{f}^i$) [10^{-3}]	$\begin{pmatrix}327&327&327\\297&296&296\\255&254&253\end{pmatrix}$	$\begin{pmatrix}245&246&246\\233&234&234\\231&232&232\end{pmatrix}$	$\begin{pmatrix}90&91&91\\67&68&68\\75&76&76\end{pmatrix}$
Med($\hat{K}$) − K	$\begin{pmatrix}2&3&3\\1&2&2\\1&1&1\end{pmatrix}$	$\begin{pmatrix}1&1&1\\0&0&0\\0&0&0\end{pmatrix}$	$\begin{pmatrix}0&0&0\\0&0&0\\0&0&0\end{pmatrix}$
Mean($\hat{K} = K)_i$ [%]	$\begin{pmatrix}12&9&7\\22&19&17\\36&32&29\end{pmatrix}$	$\begin{pmatrix}15&12&11\\24&22&21\\35&33&32\end{pmatrix}$	$\begin{pmatrix}44&37&34\\62&53&49\\59&52&48\end{pmatrix}$
Mean($\hat{K} = K$) [%]	$\begin{pmatrix}4&2&1\\7&5&4\\8&7&6\end{pmatrix}$		
V_1 [%]	$\begin{pmatrix}85&85&85\\86&86&86\\88&87&87\end{pmatrix}$	$\begin{pmatrix}74&74&75\\73&74&74\\75&76&76\end{pmatrix}$	$\begin{pmatrix}95&95&95\\97&97&97\\96&96&96\end{pmatrix}$
Mean($\boldsymbol{f} \in \tilde{\mathcal{H}}(\beta)$) [%]	$\begin{pmatrix}60.7&58.6&55.7\\71.0&63.5&63.2\\80.2&71.0&66.9\end{pmatrix}$		
Mean($\boldsymbol{f}^i \in \tilde{\mathcal{H}}(\beta)_i$) [%]	$\begin{pmatrix}90.4&89.6&89.3\\99.0&98.8&98.8\\99.7&99.6&99.6\end{pmatrix}$	$\begin{pmatrix}96.7&91.5&86.0\\97.8&95.0&94.3\\97.9&95.2&92.9\end{pmatrix}$	$\begin{pmatrix}72.8&74.6&77.0\\83.5&80.2&79.4\\90.1&86.2&85.6\end{pmatrix}$

Table 6.5: Performance of SLAM's confidence region $\tilde{\mathcal{H}}(\beta)$ and estimate $\hat{f}$ for sources $\boldsymbol{f}$ as in Example 1.2.1 with $\sigma = 0.02, 0.05, 0.1$ and $n = 1,280$ for $(\alpha,\beta) \in \{0.01, 0.05, 0.1\}^2$. In the displayed matrices α increases within a column and β increases within a row.

6.1.4 Prior information on minimal scale λ

In the previous simulations we always included prior information on the minimal scale λ (see Algorithm CRW in Figure 3.1). In the following we demonstrate the influence of this prior information on SLAM's performance in Example 1.2.1, i.e. $\boldsymbol{m} = 3$, $\mathfrak{A} = \{0, 1, 2\}$, $\boldsymbol{\omega} = (0.11, 0.29, 0.6)$, and $\boldsymbol{f}$ as displayed in Figure 1.4. For $\sigma = 0.02$, $n = 1,280$, and $\alpha = \beta = 0.1$ we compute $\hat{\omega}$, $C_{0.9}$, $\hat{f}^1, \ldots, \hat{f}^m$, and $\tilde{\mathcal{H}}(0.1)$ under prior knowledge $\lambda \geq 0.05$, 0.04, 0.025, 0.015, 0.005 (with truth $\lambda = 0.05$). The results in Table 6.6 in the supplement show a certain stability for a wide range of prior information on λ. Only when the prior assumptions on λ is of order 0.1λ (or smaller) SLAM's performance gets significantly worse.

Prior knowledge $\lambda \geq$	0.05	0.04	0.025	0.015	0.005
MAE($\hat{\omega}$) $[10^{-3}]$	(6, 5, 3)	(2, 2, 1)	(2, 2, 1)	(5, 5, 6)	(159, 126, 186)
$\overline{\text{dist}}(\boldsymbol{\omega}, C_{1-\alpha})$ $[10^{-3}]$	17	23	23	37	123
Mean($\boldsymbol{\omega} \in C_{1-\alpha}$) [%]	100	100	100	100	100
$\overline{\omega}_i - \underline{\omega}_i$ $[10^{-3}]$	(24, 25, 25)	(42, 42, 42)	(42, 42, 42)	(65, 64, 63)	(183, 171, 144)
MIAE($\hat{f}^i$) $[10^{-3}]$	(3, 13, 6)	(1, 4, 2)	(1, 4, 2)	(1, 23, 11)	(40, 175, 88)
Mean($\hat{K}$) $- K$	(0.1, 0.2, 0.0)	(0.1, 0.1, 0.0)	(0.1, 0.1, 0.0)	(0.0, 0.3, −0.1)	(2.4, 2.5, −0.2)
Med($\hat{K}$) $- K$	(0, 0, 0)	(0, 0, 0)	(0, 0, 0)	(0, 0, 0)	(0, −2, −2)
Mean($\hat{K} = K)_i$ [%]	(99, 93, 97)	(100, 98, 99)	(100, 98, 99)	(99, 87, 93)	(54, 24, 16)
Mean($\hat{K} = K$) [%]	93	98	98	86	6
$\max_i \min_j \lvert\tau_i - \hat{\tau}_j\rvert$ $[10^{-1}]$	(13, 148, 4)	(6, 40, 2)	(6, 40, 2)	(7, 299, 9)	(508, 1794, 122)
$\max_j \min_i \lvert\tau_i - \hat{\tau}_j\rvert$ $[10^{-1}]$	(2, 41, 50)	(1, 11, 15)	(1, 11, 15)	(1, 45, 91)	(223, 331, 1343)
V_1 [%]	(100, 99, 100)	(100, 100, 100)	(100, 100, 100)	(100, 98, 99)	(96, 89, 91)
FPSLE $[10^{-2}]$	(16, 246, 167)	(8, 67, 51)	(8, 67, 51)	(5, 398, 304)	(708, 1994, 4491)
FNSLE $[10^{-2}]$	(34, 407, 41)	(17, 113, 14)	(17, 113, 14)	(16, 785, 71)	(1610, 5786, 1168)
Mean($\boldsymbol{f} \in \tilde{\mathcal{H}}(\beta)$) [%]	96.01	98.96	98.95	94.78	56.65

Table 6.6: Performance of SLAM for weights $\boldsymbol{\omega}$ and sources $\boldsymbol{f}$ as in Example 1.2.1 with $\sigma = 0.02, 0.05, 0.1$ and $n = 1,280$ with prior knowledge $\lambda \geq 0.05, 0.04, 0.025, 0.015, 0.005$.

6.1.5 Robustness of SLAM

Finally, SLAM's robustness against violations of model assumptions is analyzed.

Robustness against non-identifiability

Throughout this work, we assume δ-separability of the underlying parameters $(\boldsymbol{\omega}, \boldsymbol{f})$, i.e., $ASB(\boldsymbol{\omega}) \geq \delta$ and $\boldsymbol{f}$ separable as in A3, in order to ensure identifiability. In the following we briefly investigate SLAM's behavior if these conditions are close to be, or even violated.

Alphabet separation boundary δ We start with the identifiability condition on $\boldsymbol{\omega}$, namely $ASB(\boldsymbol{\omega}) \geq \delta$ (1.8). We reconsider Example 1.2.1, i.e. $\boldsymbol{m} = 3$, $\mathfrak{A} = \{0, 1, 2\}$, and $\boldsymbol{f}$ as displayed in Figure 1.4, but with $\boldsymbol{\omega}$ chosen randomly, uniformly distributed on Ω_3. For $\sigma = 0.05$, $n = 1,280$, and $\alpha = \beta = 0.1$ we compute $\hat{\omega}$, $C_{1-\alpha}$, $\hat{f}^1, \hat{f}^2, \hat{f}^3$, and $\tilde{\mathcal{H}}(\beta)$, incorporating prior knowledge $\lambda \geq 0.025$, with truth $\lambda = 0.05$. Consequently, for each run we get a different $\boldsymbol{\omega}$ and $ASB(\boldsymbol{\omega})$, respectively. We found that SLAM's performance of $\hat{\omega}$ and $C_{1-\alpha}$, respectively, is not much influenced by $ASB(\boldsymbol{\omega})$ (see Table 6.7, where the average mean squared error of $\hat{\omega}$ and $\overline{\text{dist}}(\boldsymbol{\omega}, C_{1-\alpha})$ remain stable when $ASB(\boldsymbol{\omega})$ becomes small). The situation changes of course, when it comes to estimation of $\boldsymbol{f}$ itself. $ASB(\boldsymbol{\omega}) = 0$ in (1.8) implies non-identifiability of $\boldsymbol{f}$,

i.e., it is not possible to recover $\boldsymbol{f}$ uniquely. Therefore, it is expected that small $ASB(\boldsymbol{\omega})$ will lead to a bad performance of any estimator of $\boldsymbol{f}$. This is also reflected in Theorem 3.4.2 where δ, with $ASB(\boldsymbol{\omega}) \geq \delta$, appears as a "conditioning number" of the SBSR model. The results in Table 6.8 confirm the strong influence of $ASB(\boldsymbol{\omega})$ on the performance of SLAM's estimate for $\boldsymbol{f}$. However, as SLAM does not only give an estimate of $\boldsymbol{f}$ but also a confidence band $\tilde{\mathcal{H}}(\beta)$ this (unavoidable) uncertainty is also reflected in its coverage. To illustrate this define a local version of $ASB(\boldsymbol{\omega})$ as

$$ASB_x(\boldsymbol{\omega}) := \min_{e \neq \boldsymbol{f}(x) \in \mathfrak{A}^{\boldsymbol{m}}} |e\boldsymbol{\omega} - f(x)\boldsymbol{\omega}|\,. \tag{6.2}$$

Intuitively, $ASB_x(\boldsymbol{\omega})$ determines the difficulty to discriminate between the source functions at a certain location $x \in [0,1)$. Now, define the local size of $\tilde{\mathcal{H}}(\beta)$ as $|\tilde{\mathcal{H}}_x(\beta)| := \#\{e \in \mathfrak{A}^{\boldsymbol{m}} : \exists \boldsymbol{f} \in \tilde{\mathcal{H}}(\beta) \text{ s.t. } \boldsymbol{f}(x) = e\}$. Table 6.8 shows that the uncertainty in $|\tilde{\mathcal{H}}_x(\beta)|$ increases in non-identifiable regions, i.e., when $ASB_x(\boldsymbol{\omega})$ is small.

	$\text{MAE}(\hat{\omega})$ $[10^{-3}]$	$\overline{\text{dist}}(\omega, C_{1-\alpha})$ $[10^{-3}]$
$0 \leq ASB \leq 0.0001$	$(6,4,5)$	29
$0.0001 \leq ASB \leq 0.01$	$(7,4,7)$	34
$0.01 \leq ASB \leq 0.02$	$(4,4,4)$	30
$0.02 \leq ASB \leq 0.03$	$(4,4,4)$	29
$0.03 \leq ASB \leq 0.04$	$(4,3,4)$	31
$0.04 \leq ASB \leq 0.05$	$(4,3,4)$	31
$0.05 \leq ASB \leq 0.06$	$(4,3,5)$	31
$0.06 \leq ASB \leq 0.07$	$(3,3,4)$	31

Table 6.7: Performance of SLAM for sources $\boldsymbol{f}$ as in Example 1.2.1 with $\sigma = 0.05$, $n = 1,280$ for $\boldsymbol{\omega}$ uniformly distributed on Ω_3 conditioned on different ranges for the ASB (2.19).

	$\text{MIAE}(\hat{f}^i)$ $[10^{-4}]$	$\lvert\tilde{\mathcal{H}}_x(0.1)\rvert$		
		mean	median	
$0 \leq ASB \leq 0.0001$	$(1916, 1067, 483)$	2.71	3	$0 \leq ASB_x \leq 0.001$
$0.0001 \leq ASB \leq 0.01$	$(1536, 923, 354)$	2.68	3	$0.001 \leq ASB_x \leq 0.01$
$0.01 \leq ASB \leq 0.02$	$(671, 474, 147)$	2.67	3	$0.01 \leq ASB_x \leq 0.02$
$0.02 \leq ASB \leq 0.03$	$(236, 164, 40)$	2.66	3	$0.02 \leq ASB_x \leq 0.03$
$0.03 \leq ASB \leq 0.04$	$(96, 37, 7)$	2.53	2	$0.03 \leq ASB_x \leq 0.04$
$0.04 \leq ASB \leq 0.05$	$(100, 7, 2)$	2.49	2	$0.04 \leq ASB_x \leq 0.05$
$0.05 \leq ASB \leq 0.06$	$(42, 1, 0)$	2.36	2	$0.05 \leq ASB_x \leq 0.1$
$0.06 \leq ASB \leq 0.07$	$(16, 4, 0)$	1.97	1	$0.1 \leq ASB_x$

Table 6.8: Performance of SLAM for sources $\boldsymbol{f}$ as in Example 1.2.1 with $\sigma = 0.05$, $n = 1,280$ for $\boldsymbol{\omega}$ uniformly distributed on Ω_3 conditioned on different ranges ASB (left) and ASB_x (right) as in (1.8) and (6.2), respectively.

Violation of separability condition Next, we consider the separability condition in A3. We consider a modification of Example 1.2.1, i.e. $\boldsymbol{m} = 3$, $\mathfrak{A} = \{0,1,2\}$, where we modified the source function $\boldsymbol{f}^1$ in such a way, that it violates the separability condition in A3, see Figure 6.2. For $\sigma = 0.05$, $n = 1,280$, and $\alpha = \beta = 0.1$ we compute $\hat{\omega}$ and $\hat{f}^1, \hat{f}^2, \hat{f}^3$ incorporating

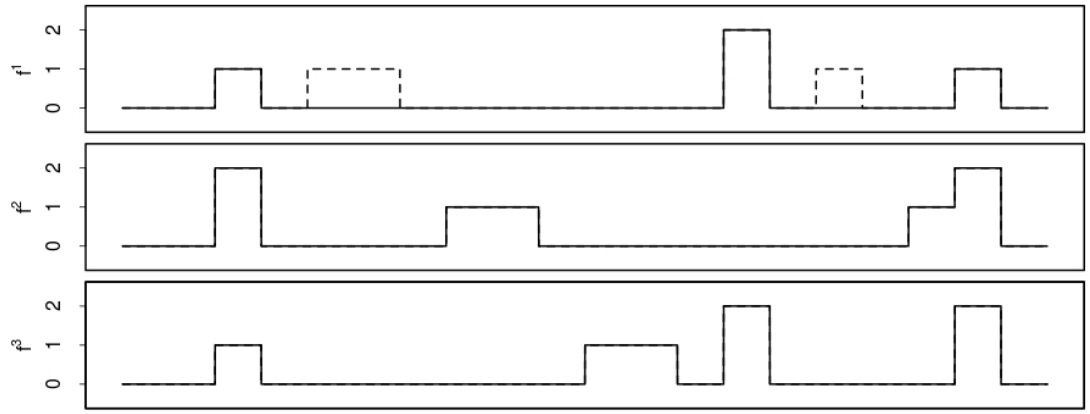

Figure 6.2: Source functions $\boldsymbol{f}$ from Example 1.2.1, where $\boldsymbol{f}^1$ is modified such that $\boldsymbol{f}$ violates the separability condition A3. The dashed lines indicate the removed jumps.

	(1)	(2)	(3)
MAE($\hat{\omega}$) [10^{-3}]	(73, 36, 39)	(43, 58, 16)	(42, 59, 17)
MIAE($\hat{f}^i$) [10^{-3}]	(123, 181, 84)	(447, 435, 137)	(563, 279, 99)
Med($\hat{K}$) − K	(−4, 2, 0)	(4, 1, −2)	(11, 4, −2)
Mean($\hat{K} = K$)$_i$ [%]	(10, 10, 19)	(5, 0, 33)	(2, 1, 4)
V_1 [%]	(71, 85, 96)	(84, 72, 88)	(78, 82, 89)

Table 6.9: Performance of SLAM when model assumptions are violated. (1): Setting as in Example 1.2.1 but with $\boldsymbol{f}$ modified such that it violates the separability condition A3 as in Figure 6.2, for $\sigma = 0.05$, $n = 1,280$, and $\alpha = \beta = 0.1$. (2): Setting as in Example 1.2.1, but with t-distributed errors with 3 degrees of freedom, re-scaled to a standard deviation of $\sigma = 0.05$, for $n = 1,280$, $\alpha = 0.1$, and $q(\beta) = 13.03$. (3): Setting as in Example 1.2.1, but with χ^2-distributed errors with 3 degrees of freedom, re-scaled to a standard deviation of $\sigma = 0.05$, for $n = 1,280$, $\alpha = 0.1$, and $q(\beta) = 3.73$.

prior knowledge $\lambda \geq 0.025$ with truth $\lambda = 0.05$. The results are shown in Table 6.9. The violation of the separability condition A3 leads to non-identifiability of $\boldsymbol{\omega}$, which is naturally reflected in a worse performance of SLAM's estimate of $\boldsymbol{\omega}$. As the condition is violated for $\boldsymbol{f}^1$ (i.e., $\boldsymbol{\omega}_1 \notin \text{imag}(\boldsymbol{g})$ as in (1.9)) this has a particular impact on $\hat{\omega}_1$. The same holds true for $\hat{f}$ itself, where the estimation error of $\hat{\omega}_1$ propagates to a certain degree to the estimation of $\hat{f}^1$. The performance of $\hat{f}^2$ and $\hat{f}^3$, however, is not much influenced.

Violation of normality assumption

In the SBSR model the error distribution is assumed to be Gaussian. In the following, SLAM's performance for t-(heavy tails) and χ^2-(skewed) distributed errors is studied. Again, Example 1.2.1, i.e. $\boldsymbol{m} = 3$, $\mathfrak{N} = \{0, 1, 2\}$, and $\boldsymbol{f}$ as displayed in Figure 1.4 is considered. We add to $\boldsymbol{g}$ now t-distributed and χ^2-distributed errors, respectively, with 3 degrees of freedom, re-scaled to a standard deviation of $\sigma = 0.05$. For $n = 1,280$ and $\alpha = 0.1$ we compute $\hat{\omega}$ and $\hat{f}^1, \hat{f}^2, \hat{f}^3$, incorporating prior knowledge $\lambda \geq 0.025$, with truth $\lambda = 0.05$. We simulated the statistic T_n for t- and χ^2- distributed errors, respectively, and choose $q(\beta)$ to be the corresponding 90%

quantile. For t-distributed errors this gave $q(\beta) = 13.03$ and for χ^2-distributed errors $q(\beta) = 3.73$. The results in Table 6.9 indicate a certain robustness to misspecification of the error distribution, provided the quantiles for T_n are adjusted accordingly.

6.2 SLAM-selector

We consider mixtures of $\boldsymbol{m} = 1, 2, 3, 4, 5$ simple bump functions (see Figure 6.3)

$$f^i = \mathbb{1}_{[(i-1)/5, i/5)}, \qquad \text{for } i = 1, \ldots, 5 \tag{6.3}$$

with value in the binary alphabet $\mathfrak{A} = \{0, 1\}$, i.e., $k = 2$ and $a_2 = 1$, with $\lambda = 1/5$. We choose $\boldsymbol{\omega}$ such that $\delta = 0.02$ as in Table 6.1, the number of observations is $n = 1,000$, with Gaussian error terms $\epsilon_j \sim \mathcal{N}(0, \sigma^2)$ in (1.3) with standard deviations $\sigma = 0.01, 0.02, 0.05, 0.1$, respectively. Figure 6.3 show examples for (true) $\boldsymbol{m} = 4, \sigma = 0.05$ and $\boldsymbol{m} = 3, \sigma = 0.01$, respectively. Note that as $\mathrm{ASB}(\boldsymbol{\omega}) = 0.02$ is fixed, the standard deviation corresponds to the minimal signal to noise ratio (SNR). Each simulation experiment has been repeated $1,000$ times.

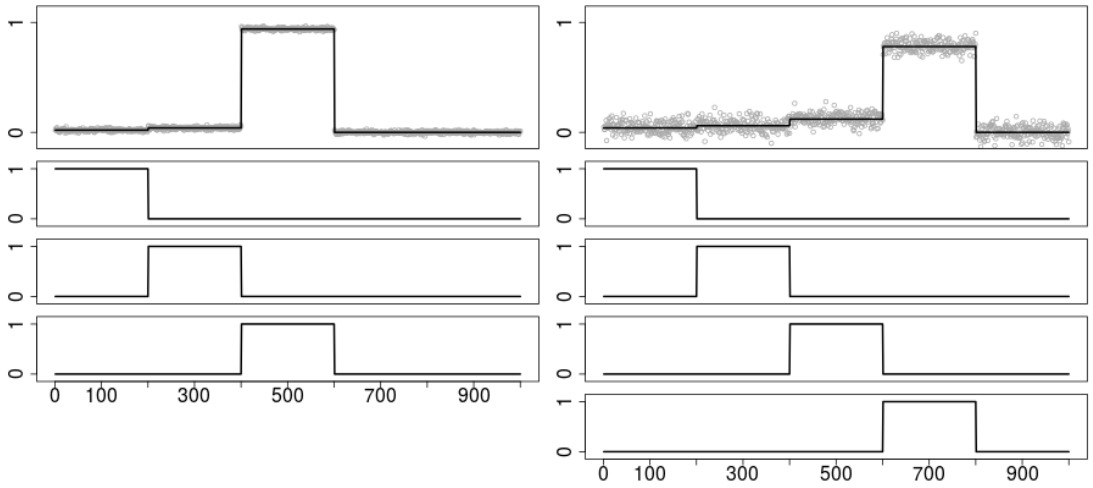

Figure 6.3: Observations Y (gray dots) according to the SBSR model (1.3) for Gaussian noise with $\sigma = 0.01$ (left) and $\sigma = 0.05$ (right), $n = 1,000$, with true underlying signal $\boldsymbol{g}$ (solid line in top row) for $\boldsymbol{m} = 4$ (left) and $\boldsymbol{m} = 4$ (right), $\boldsymbol{\omega} = (0.02, 0.04, 0.94)$ (left) and $\boldsymbol{\omega} = (0.04, 0.06, 0.12, 0.78)$ (right), and $\boldsymbol{f}$ (row 2-5) as in (6.3).

6.2.1 Comparision with AIC, BIC, and LRM

For the SLAM selector of Definition 3.6.8 the first row in Figure 6.4 shows histograms of $\hat{m}$ for $\sigma = 0.01$ (for $\sigma = 0.02, 0.05, 0.1$ see Figure B.2, B.1, and B.3 in the appendix). It shows that the SLAM selector $\hat{m}$ estimates the number of sources $\boldsymbol{m}$ very accurately for reasonable SNR. In particular, $\hat{m}$ rarely overestimates $\boldsymbol{m}$, even when the noise level is very high and $\boldsymbol{m}$ is large. Notably, if $\hat{m}$ underestimates $\boldsymbol{m}$ (because of the high noise level or because $\boldsymbol{m}$ is very large), it rarely underestimates $\boldsymbol{m}$ by more than one. In particular, as discussed in

the following, the SLAM selector performs significantly better than standard methods as the Bayesian information criterion (BIC), Akaike information criterion (AIC), or the local residual method (LRM).

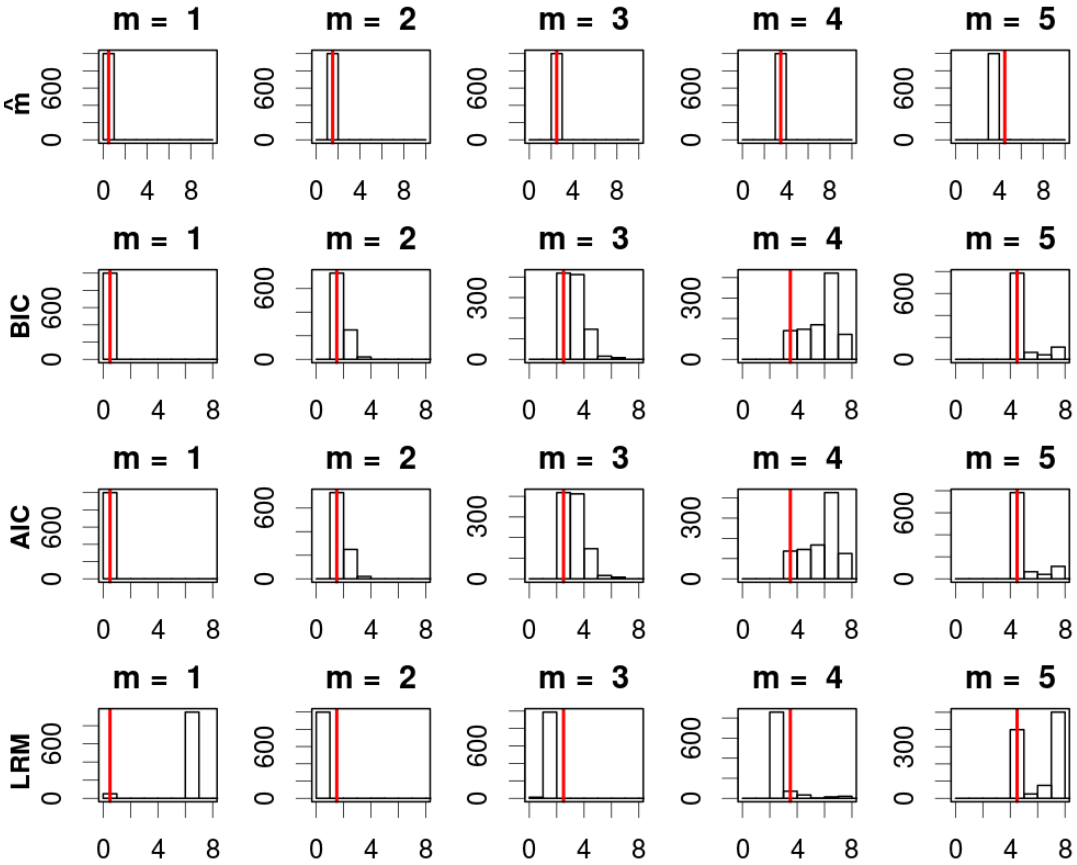

Figure 6.4: Histogram of SLAM selector $\hat{m}$ as in Definition 3.6.8 (top row), $\hat{m}_{\mathrm{BIC}}$ (second row), $\hat{m}_{\mathrm{AIC}}$ (third row) as in (6.6), and $\hat{m}_{\mathrm{LRM}}$ as in (6.7) for $\boldsymbol{\omega}$ as in Table 6.1 and $\boldsymbol{f} = (\boldsymbol{f}^1, \ldots, \boldsymbol{f}^m)$ as in (6.3), with standard deviation $\sigma = 0.01$, $n = 1,000$, for $\boldsymbol{m} = 1, 2, 3, 4, 5$ (from left to right). The red vertical line indicates the true number of source functions $\boldsymbol{m}$.

Bayesian and Akaike Information Criterion Considering estimation of $\boldsymbol{m}$ as a model selection problem, the most prominent selectors are the BIC and the AIC

$$\mathrm{BIC} := -2\ln(\hat{L}) + p\ln(n), \quad \mathrm{AIC} := -2\ln(\hat{L}) + 2p,$$

where $\hat{L}$ denotes the maximized value of the likelihood function and p the dimension of the free parameters to be estimated, in order to select m. Among a finite set of models the model with the lowest BIC and AIC, respectively, is preferred.

For models which satisfy certain regularity conditions the BIC criterion was theoretically justified by Schwarz (1978) via asymptotic expansion of the log-posterior probability. More precisely, Schwarz (1978) showed that for n i.i.d. observations Y from an exponential family with parameter θ belonging to one of a finite set of models $\Theta_1, \ldots, \Theta_M$, where each model is a linear

submanifold of dimension m_i of an Euclidean space, the logarithm of the posterior probability satisfies

$$\ln\left(\mathbf{P}\left(\theta \in \Theta_j \middle| Y\right)\right) = l_n\left(\hat{\theta}_j\right) - \frac{1}{2} m_j \ln(n) + O(1),$$

as $n \to \infty$, where l_n denotes the log-likelihood function and $\hat{\theta}_j$ the maximum likelihood estimator under Θ_j. Note that this result is obtained under very weak assumptions on the prior distribution, whose specific form is hidden in the $O(1)$ remainder term. The crucial assumption in the proof of this result is that the log-likelihood function is twice differentiable w.r.t. the parameter θ around $\hat{\theta}_j$. This assumption, however, is heavily violated in the SBSR model through the discrete nature of the sources $f^1, \dots, f^m$. More precisely, in the SBSR model for fixed number of sources m the parameter space is a disjoint union of several $(m-1)$-simplices Ω_m, which is not a linear submanifold of an Euclidean space. Consequently, we stress that there is no theoretical justification to use the BIC criterion for model selection in the SBSR model. This has been already observed for c.p. regression, see (Zhang and Siegmund, 2007, 2012). However, as the BIC (and AIC) criterion is widely used (often also in situations where the required regularity assumptions are not fulfilled), we will, in the following, compare it with the proposed methods in a simulation study.

As the maximum likelihood estimator (which equals the least squares estimator for Gaussian error) in the model $\mathcal{M}_m$ is not available in general (see Section 5.2), we use SLAM to approximate it. As the observations in the SBSR model are Gaussian and as the mixing weights sum up to one, implying that the number of free parameters corresponds to $\boldsymbol{m}-1$, the BIC and AIC, respectively, in the SBSR model become

$$\mathrm{BIC} = \mathrm{BIC}(\mathcal{M}_m) = \frac{\sum_{j=1}^n \left(y_j - \hat{g}_m(x_j)\right)^2}{\sigma^2} + (m-1)\ln(n), \tag{6.4}$$

$$\mathrm{AIC} = \mathrm{AIC}(\mathcal{M}_m) = \frac{\sum_{j=1}^n \left(y_j - \hat{g}_m(x_j)\right)^2}{\sigma^2} + 2(m-1). \tag{6.5}$$

Thus, the selected number of source functions is

$$\hat{m}_{\mathrm{BIC}} = \operatorname*{argmin}_{1 \le \tilde{m} \le m_{\max}} \mathrm{BIC}(\mathcal{M}_{\tilde{m}}),\ \hat{m}_{\mathrm{AIC}} = \operatorname*{argmin}_{1 \le \tilde{m} \le m_{\max}} \mathrm{AIC}(\mathcal{M}_{\tilde{m}}). \tag{6.6}$$

For $\boldsymbol{f}$ as in (6.3), $\boldsymbol{\omega}$ as in Table 6.1, and Gaussian error terms $\epsilon_j \sim \mathcal{N}(0, \sigma^2)$ in (1.3) with standard deviation $\sigma = 0.01, 0.02, 0.05, 0.1$ we compute the BIC and AIC for $\boldsymbol{m} = 1, 2, 3, 4, 5$ and $m_{\max} = 8$. The second and third rows in Figure 6.4 shows the histogram of $\hat{m}_{\mathrm{BIC}}$ and $\hat{m}_{\mathrm{AIC}}$ for $\sigma = 0.01$ (for $\sigma = 0.02, 0.05, 0.1$ see Figure B.2, B.1, and B.3 in the appendix). Comparing the different rows in Figure 6.4 (and Figure B.2, B.1, and B.1 in the appendix) indicates that the SLAM selector $\hat{m}$ from Definition 3.6.8 outperforms both the BIC and the AIC. While the SLAM selector $\hat{m}$ from Definition 3.6.8 rarely overestimate the number of sources, $\hat{m}_{\mathrm{BIC}}$ and $\hat{m}_{\mathrm{AIC}}$ often largely overestimate $\boldsymbol{m}$. Moreover, the variance of $\hat{m}_{\mathrm{BIC}}$ and $\hat{m}_{\mathrm{AIC}}$ seems to be much higher than the variance of $\hat{m}$. In particular, when the noise level becomes large $\hat{m}_{\mathrm{BIC}}$ and $\hat{m}_{\mathrm{AIC}}$ can produce very unreliable results. This is in contrast to $\hat{m}$, which, even when the noise

level is high and $\boldsymbol{m}$ is large, rarely misspecifies $\boldsymbol{m}$ by more than one. Note, moreover, that the AIC and BIC criterion do not give any statistical guarantees on $\hat{m}_{\mathrm{AIC}}$ and $\hat{m}_{\mathrm{BIC}}$, in contrast to the SLAM selector (recall Theorem 3.6.4).

Local residual method Another simple model selection method, which is often applied in practice, is a LRM. The idea is that for a reasonable estimator $\hat{g}$ in the correct model the residual sum $\sum_{j=1}^{n}\left(y_j - \hat{g}(x_j)\right)^2/n$ is a good estimate of the variance σ^2, which can be estimated very accurately (with $\sqrt{n}$-rate) via local differences estimators, e.g., $\sum_{j=2}^{n}\left(y_j - y_{j-1}\right)^2/(2n)$. More precisely, let $\hat{g}_m$ be the SLAM estimate in model $\mathcal{M}_m$. Then, for a set of models $\{\mathcal{M}_1, \ldots, \mathcal{M}_{m_{\max}}\}$ with $m_{\max} \in \mathbb{N}$ the LRM select $\mathcal{M}_{\hat{m}_{\mathrm{LRM}}}$ with

$$\hat{m}_{\mathrm{LRM}} := \operatorname*{argmin}_{1\leq \tilde{m} \leq m_{\max}} \left| 2\sum_{j=1}^{n}\left(y_j - \hat{g}_{\tilde{m}}(x_j)\right)^2 - \sum_{j=2}^{n}\left(y_j - y_{j-1}\right)^2 \right|. \tag{6.7}$$

For $\boldsymbol{f}$ as in (6.3), $\boldsymbol{\omega}$ as in Table 6.1, and Gaussian error terms $\epsilon_j \sim \mathcal{N}(0, \sigma^2)$ in (1.3) with standard deviation $\sigma = 0.01, 0.02, 0.05, 0.1$ we compute the LRM for $\boldsymbol{m} = 1, 2, 3, 4, 5$ and $m_{\max} = 8$. The bottom row in Figure 6.4 shows the histogram of $\hat{m}_{\mathrm{LRM}}$ for $\sigma = 0.01$ (for $\sigma = 0.02, 0.05, 0.1$ see Figure B.2, B.1, and B.3 in the appendix). It shows that $\hat{m}_{\mathrm{LRM}}$ performs poorly and especially much worse than the SLAM selector.

6.2.2 Lower Confidence Bounds

Theorem 3.6.4 yields that $\hat{m}_{1-\alpha}$ constitutes a $(1-\alpha)$ lower confidence bound for the number of source components $\boldsymbol{m}$. Figure 6.5 shows histograms of $\hat{m}_{1-\alpha}$ for Gaussian error terms $\epsilon_j \sim \mathcal{N}(0, \sigma^2)$ in (1.3) with standard deviation $\sigma = 0.05$ (for $\sigma = 0.01, 0.02, 0.1$ see Figure B.4, B.5, and B.6 in the appendix). The results indicate that the actual coverage of $\hat{m}_{1-\alpha}$ is even higher than the nominal $1-\alpha$. In fact, for $\sigma = 0.01$ in our simulations it did not happen once that $\hat{m}_{1-\alpha} > \boldsymbol{m}$ for $\alpha = 0.05, 0.1, 0.25$, i.e., we obtained an empirical coverage of 100% for $\alpha = 0.05, 0.1, 0.25$. For $\sigma = 0.02, 0.05, 0.1$ the coverage is shown in Table 6.10, showing that also when the variance gets larger the empirical coverage is almost 100% for $\alpha = 0.05, 0.1, 0.25$. Even for $\alpha = 0.25$ the coverage was always higher than 99.4%. Still, $\hat{m}_{1-\alpha}$ for $\alpha = 0.05, 0.1, 0.25$ was close to the true underlying number of components $\boldsymbol{m}$ (see Figure 6.5). Also for the SLAM selector $\hat{m}$ as in Definition 3.6.8 we obtained a very high coverage as displayed Table 6.11. This shows that the SLAM selector is parsimonious (i.e., avoids to many components), in general, and, at the same time, powerful to recover sources very accurately. In practice, this means that one can be very sure that detected components are present in the signal. This can be driven by the overestimation probability α, a small α leads to a more parsimonious result. In practical purposes, one can use it as a screening parameter (see (Frick et al., 2014)). In other words, the parameter q in the estimate $\hat{m}(q)$ enables in applications a trade off between detection power of sources (small q) and control of the overestimation error (large q), where a specific q translates to a bound for the overestimation probability.

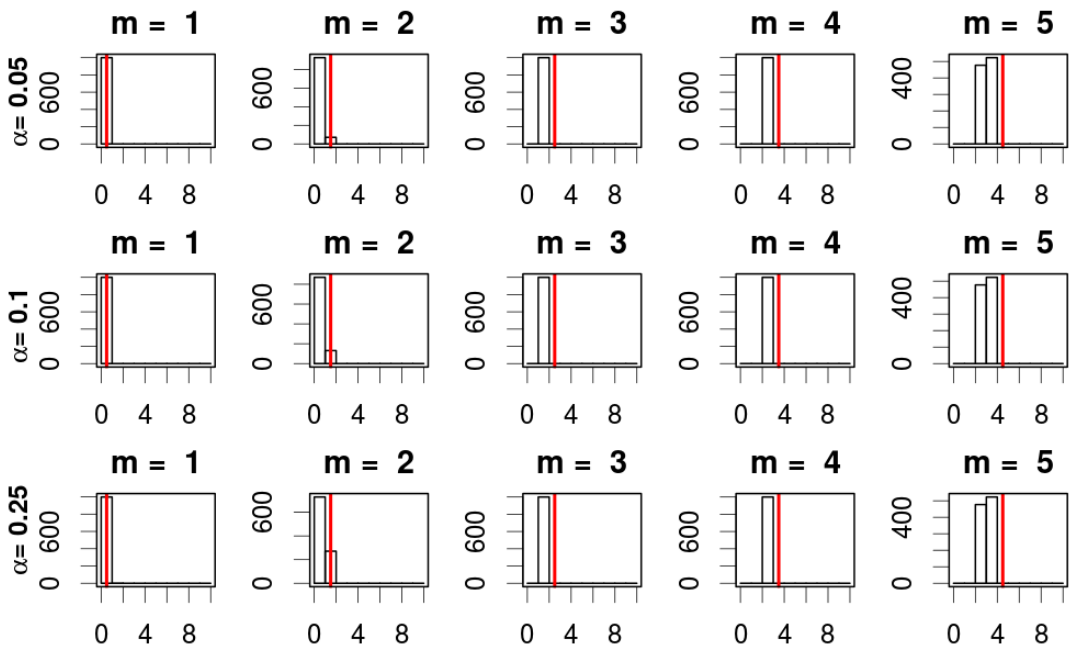

Figure 6.5: Histogram of $\hat{m}_{0.95}, \hat{m}_{0.9}, \hat{m}_{0.75}$ as in Definition 3.6.4 (from top to bottom), for $\boldsymbol{\omega}$ as in Table 6.1 and $\boldsymbol{f} = (\boldsymbol{f}^1, \ldots, \boldsymbol{f}^m)$ as in (6.3), with standard deviation $\sigma = 0.05$, $n = 1,000$, for $\boldsymbol{m} = 1, 2, 3, 4, 5$ (from left to right). The red vertical line indicates the true number of source functions $\boldsymbol{m}$.

σ	0.02	0.05	0.1
$P(\hat{m}_{0.95} > \boldsymbol{m})$	$(0, 0, 0, 0, 0)$	$(0, 0, 0, 0, 0)$	$(0, 0, 0, 0, 0)$
$P(\hat{m}_{0.90} > \boldsymbol{m})$	$(0.001, 0, 0, 0, 0)$	$(0.001, 0, 0, 0, 0)$	$(0, 0, 0, 0, 0)$
$P(\hat{m}_{0.75} > \boldsymbol{m})$	$(0.005, 0, 0, 0, 0)$	$(0.002, 0.001, 0, 0, 0)$	$(0.006, 0, 0, 0, 0)$

Table 6.10: Overestimation probability for $\boldsymbol{m} = (1, \ldots, 5)$ of SLAM selector $\hat{m}_{1-\alpha}$ in (3.24) for $\boldsymbol{\omega}$ as in Table 6.1 and $\boldsymbol{f}$ as in (6.3) with $n = 1,000$.

σ	0.01	0.02	0.05	0.1
$P(\hat{m} > \boldsymbol{m})$	$(0, 0, 0, 0, 0)$	$(0.07, 0, 0, 0.004, 0)$	$(0.079, 0, 0, 0, 0)$	$(0.088, 0, 0, 0, 0)$

Table 6.11: Overestimation probability for $\boldsymbol{m} = (1, \ldots, 5)$ of SLAM selector $\hat{m}$ in Definition 3.6.8 for $\boldsymbol{\omega}$ as in Table 6.1 and $\boldsymbol{f}$ as in (6.3) with $n = 1,000$.

6.3 LS approximation

In the following, the Lloyd's algorithm from Figure 5.1 is explored in a simulation study. In particular, we want to compare its performance with the theoretical findings for the LSE from Chapter 4, which cannot be computed efficiently (see Section 5.2). Corollary 4.1.4 yields that the LSE achieves optimal rates for the maximal prediction error. The maximal prediction error cannot be simulated efficiently, as the maximum may be attained at any $(\boldsymbol{\omega}, \boldsymbol{\Pi})$. Instead, we simulate the Bayes risk with uniform priors for $\boldsymbol{\omega}$ and $\boldsymbol{\Pi}$, respectively. As discussed in Remark 4.1.5, this ensures that $ASB(\boldsymbol{\omega}) \geq c_1 \sqrt{M}$ and $\boldsymbol{\Pi}$ is $c_2 M$-separable, for some constant $c_1, c_2 > 0$

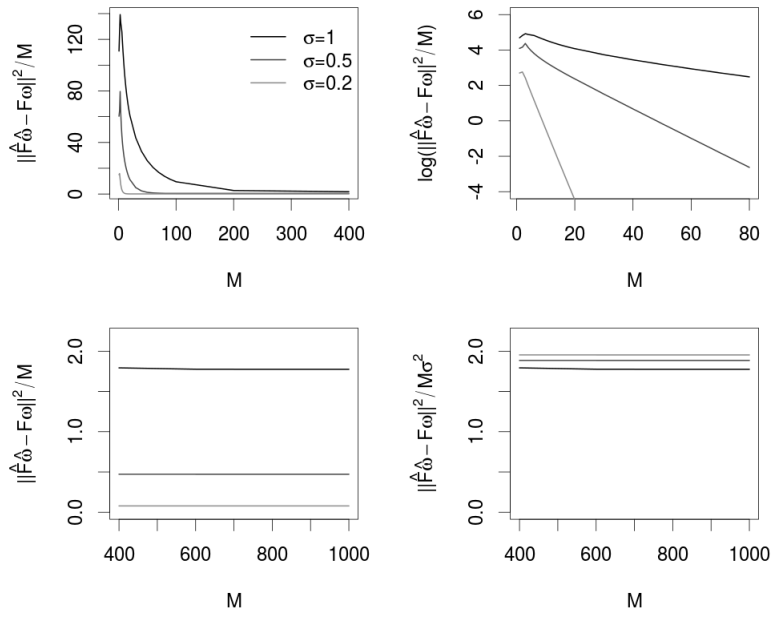

Figure 6.6: Left: Normalized MSE $\mathrm{E}\left(\left\|\hat{\theta} - \Pi A\boldsymbol{\omega}\right\|^2\right)/M$ for the estimator $\hat{\theta} = \hat{\Pi}A\hat{\omega}$ of Figure 5.1 for $m = 3$ sources, a binary alphabet $\mathfrak{A} = \{0, 1\}$, and $n = 500$ observations, for $M \in \{1, \ldots, 1000\}$ and $\sigma = 0.2, 0.5, 1$ (lightgray, darkgray, and black line). Top right: MSE on a logarithmic scale. Bottom right: $\mathrm{E}\left(\left\|\hat{\theta} - \Pi A\boldsymbol{\omega}\right\|^2\right)/(M\sigma^2)$.

asymptotically almost surely[1]. We simulate the estimator $\hat{\theta} = \hat{\Pi}A\hat{\omega}$ of Lloyd's algorithm from Figure 5.1 (see Section 5.2) for $m = 2, 3, 4$ number of sources, alphabets $\mathfrak{A} = \{0, 1\}, \{0, 1, 2, 3\}$, $n = 500, 1000$ number of observations, for $M \in \{1, \ldots, 1000\}$, and standard deviation $\sigma = 0.2, 0.5, 1$. Simulation runs were always $100,000$.

Dependence on σ We simulated the mean squared error (MSE) for the estimator $\hat{\theta} = \hat{\Pi}A\hat{\omega}$ of Lloyd's algorithm from Figure 5.1 for three sources $m = 3$, a binary alphabet $\mathfrak{A} = \{0, 1\}$, $n = 500$ observations, for $M \in \{1, \ldots, 1000\}$ and $\sigma = 0.2, 0.5, 1$. The results are shown in Figure 6.6. For larger variances ($\sigma = 1, 0.5$) the top left plot of Figure 6.6 shows a peak at $M = 3$ and for $M > 3$ an exponential decay to some limiting value. For small variance $\sigma = 0.2$ the exponential decay starts already at $M = 1$. The peak can be explained as follows: When the variance is large, i.e., the signal to noise ratio is small (recall that the alphabet $\mathfrak{A} = \{0, 1\}$ is fixed), the observations Y in (4.1) are likely to lie outside of the parameter space $\mathcal{N} \subset [0, 1]^{n \times M}$. Thus, the Lloyd's algorithm prefers parameters in $\mathcal{N}$ which are close to the boundary of $[0, 1]^{n \times M}$. This corresponds to mixing matrices ω with columns equal to unit vectors, which in general are not close to the true underlying mixing matrix and hence, lead to a larger MSE. However, if $M < m$ such ω have zero alphabet separation boundary $ASB(\omega) = 0$ and in particular, small number of possible mixture values. More precisely, for $M < m$ when

[1] A uniform prior for $\boldsymbol{\omega}$ does not guarantee $WSB(\boldsymbol{\omega}) \geq c_1\sqrt{M}$ asymptotically almost surely. However, this is more of a technical issue, as one can always consider estimation up to permutation matrices P (recall that $\boldsymbol{F}PP^{-1}\boldsymbol{\omega} = \boldsymbol{F}\boldsymbol{\omega}$), that is, one considers the equivalence class $(\boldsymbol{F}, \boldsymbol{\omega}) \sim (\boldsymbol{F}P, P^{-1}\boldsymbol{\omega})$ for any permutation P.

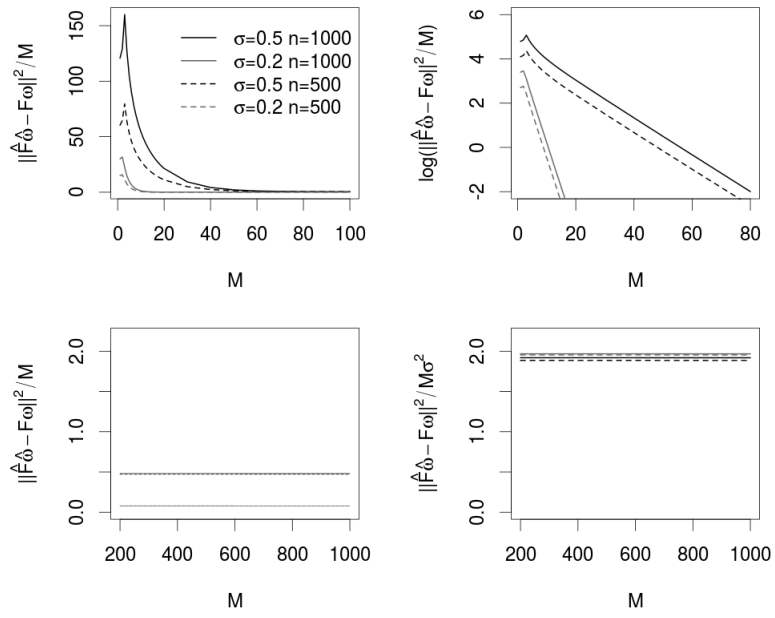

Figure 6.7: Left: Normalized MSE $\mathrm{E}\left(\left\|\hat{\theta} - \Pi A\boldsymbol{\omega}\right\|^2\right)/M$ for the estimator $\hat{\theta} = \hat{\Pi} A\hat{\omega}$ of Lloyd's algorithm from Figure 5.1 for $m = 3$ sources, a binary alphabet $\mathfrak{A} = \{0, 1\}$, for $M \in \{1, \ldots, 1000\}$ and $n = 1000, 500$ (solied and dashed line) observations with $\sigma = 0.2, 0.5$ (gray and black line). Top right: MSE on a logarithmic scale. Bottom right: $\mathrm{E}\left(\left\|\hat{\theta} - \Pi A\boldsymbol{\omega}\right\|^2\right)/(M\sigma^2)$.

the columns of ω are unit vectors and $\tilde{\omega}$ is a different mixing matrix with $AS\,B(\tilde{\omega}) > 0$ then

$$\#\{e\omega : e \in \mathfrak{A}^m\} \leq k^M < k^m = \#\{e\tilde{\omega} : e \in \mathfrak{A}^m\}.$$

Consequently, when $M < m$ mixing matrices ω with columns being unit vectors are not (wrongly) selected by the Lloyd's algorithm and hence, the estimate fits the true underlying parameters better. On the other hand, as the (maximal) number of mixture values k^m does not grow with M, when $M \gg m$ choosing the columns of ω as unit vectors only explores certain small (relatively decreasing with M) areas of the boundary of the parameter space $\mathcal{N}$ and thus does not lead to a better fit of the data, in general. The peak in the MSE at $M = m$ can be misleading: One might think that for $M \approx m$ estimating each column of ω separately from the corresponding column of the data matrix Y leads to a smaller MSE than estimating the whole matrix ω at once from the whole data Y. This is not true in general, which can be seen by the following example. When $M = 1$ estimation of $\omega \in \mathbb{R}^{m\times 1}$ reduces to estimation of its entries $\omega_{11}, \ldots, \omega_{m1}$, as their ordering is determined via the relation $\omega_{11} < \ldots < \omega_{m1}$. However, when $M = 2$ estimating its entries ω_{ij} does not determine ω uniquely from the relation $\|\omega_{1\cdot}\| < \ldots < \|\omega_{m\cdot}\|$. In particular, combining estimates of single columns of ω is not feasible. The top right plot of Figure 6.6 shows the MSE on a logarithmic scale (where we subtracted the limiting value $\lim_{M\to\infty} \mathrm{E}\left(\left\|\hat{\theta} - \Pi A\boldsymbol{\omega}\right\|^2\right)/M$). Its linearity suggests an exponential decay confirming the bounds in Corollary 4.1.4. As in Corollary 4.1.4 the slope in Figure 6.6 (top right) decreases with σ^2 and the intercept does not depend on σ^2. The bottom left plot of Figure 6.6

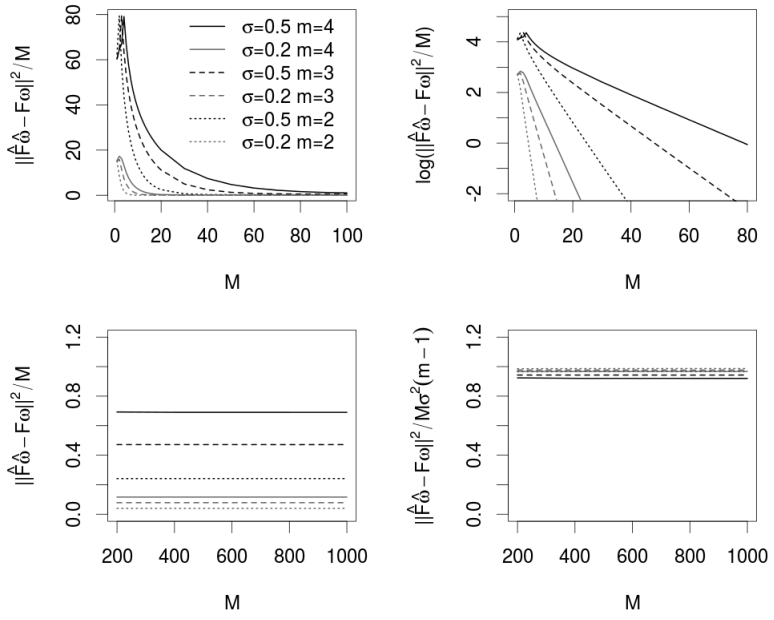

Figure 6.8: Left: Normalized MSE $\mathrm{E}\left(\left\|\hat{\theta} - \Pi A\boldsymbol{\omega}\right\|^2\right)/M$ for the estimator $\hat{\theta} = \hat{\Pi}A\hat{\omega}$ of Lloyd's algorithm from Figure 5.1 for a binary alphabet $\mathfrak{A} = \{0, 1\}$, with $n = 500$ observations for $M \in \{1, \ldots, 1000\}$ and $m = 2, 3, 4$ (dotted, dashed, and solid line) for $\sigma = 0.2, 0.5$ (gray and black line). Top right: MSE on a logarithmic scale. Bottom right: $\mathrm{E}\left(\left\|\hat{\theta} - \Pi A\boldsymbol{\omega}\right\|^2\right)/(M\sigma^2(m-1))$.

shows the limiting value of the MSE. In the bottom right plot of Figure 6.6 one observes that, just as in Corollary 4.1.4, it scales with σ^2.

Dependence on n We simulated the MSE for the estimator $\hat{\theta} = \hat{\Pi}A\hat{\omega}$ of Lloyd's algorithm from Figure 5.1 for three sources $m = 3$, a binary alphabet $\mathfrak{A} = \{0, 1\}$, for $M \in \{1, \ldots, 1000\}$ and $n = 500, 1000$ (and $\sigma = 0.2, 0.5$). The results are shown in Figure 6.7. The top right plot of Figure 6.7 shows the MSE on a logarithmic scale (where we subtracted the limiting value). It clearly shows an exponential decay. As in Corollary 4.1.4 the slope in Figure 6.7 top right does not depend on n and the intercept increases with n. The bottom left plot of Figure 6.7 shows the limiting value of the MSE, just as in Corollary 4.1.4 it does not depend on n.

Dependence on m We simulated the MSE for the estimator $\hat{\theta} = \hat{\Pi}A\hat{\omega}$ of Lloyd's algorithm from Figure 5.1 for a binary alphabet $\mathfrak{A} = \{0, 1\}$, with $n = 500$ observations for $M \in \{1, \ldots, 1000\}$ and $m = 2, 3, 4$ (and $\sigma = 0.2, 0.5$). The results are shown in Figure 6.8. The top right plot of Figure 6.8 shows the MSE on a logarithmic scale (where we subtracted the limiting value). It clearly shows an exponential decay. As in the upper bound of Corollary 4.1.4 the slope in Figure 6.8 top right decreases with m and the intercept does not depend on m. The bottom left plot of Figure 6.8 shows the limiting value of the MSE, just as in Corollary 4.1.4 it increases with m (scaling with $m - 1$). This is in accordance with Corollary 4.1.4 which suggests a limiting constant proportional to m.

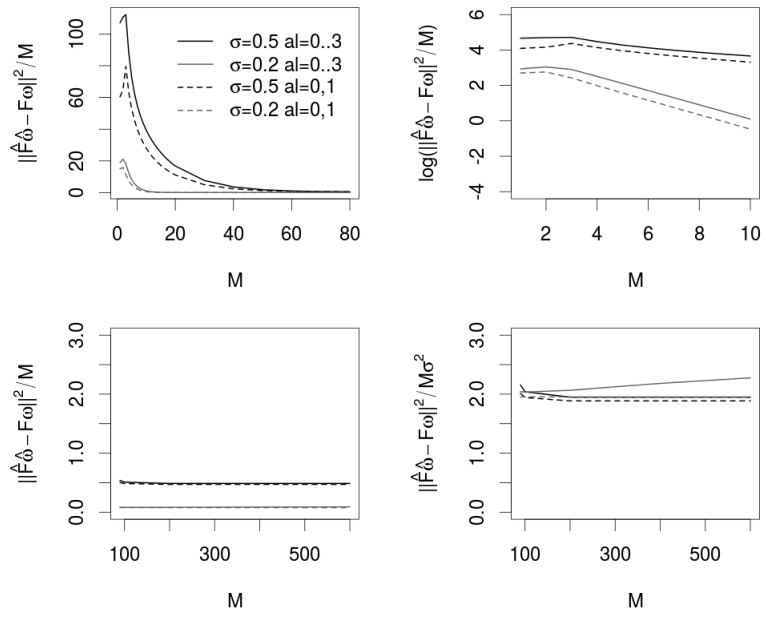

Figure 6.9: Left: Normalized MSE $\mathrm{E}\left(\left\|\hat{\theta} - \Pi A\boldsymbol{\omega}\right\|^2\right)/M$ for the estimator $\hat{\theta} = \hat{\Pi}A\hat{\omega}$ of Lloyd's algorithm from Figure 5.1 for $m = 3$ sources with $n = 500$ observations for $M \in \{1, \ldots, 1000\}$ and alphabets $\mathfrak{A} = \{0, 1\}, \{0, 1, 2, 3\}$ (dashed and solid line) for $\sigma = 0.2, 0.5$ (gray and black line). Top right: MSE on a logarithmic scale. Bottom right: $\mathrm{E}\left(\left\|\hat{\theta} - \Pi A\boldsymbol{\omega}\right\|^2\right)/(M\sigma^2 m)$.

Dependence on $\mathfrak{A}$ We simulated the MSE for the estimator $\hat{\theta} = \hat{\Pi}A\hat{\omega}$ of Lloyd's algorithm from Figure 5.1 for $m = 3$ sources with $n = 500$ observations for $M \in \{1, \ldots, 1000\}$ and alphabets $\mathfrak{A} = \{0, 1\}, \{0, 1, 2, 3\}$ (and $\sigma = 0.2, 0.5$). The results are shown in Figure 6.9. The top right plot of Figure 6.9 shows the MSE on a logarithmic scale (where we subtracted the limiting value). It clearly shows an exponential decay. The slope in Figure 6.9 top right does not depend on the alphabet. This suggests that in Corollary 4.1.4 the additional $(1 + ma_k)^2$ term in the upper bound is not necessary. The intercept in Figure 6.9 top right increases with a_k as in Corollary 4.1.4. The bottom left plot of Figure 6.9 shows the limiting value of the MSE. Just as in Corollary 4.1.4 it does not depend on the alphabet $\mathfrak{A}$.

Estimation error Figure 6.10 shows the simulation results for the estimation error of the estimator $\hat{\theta} = \hat{\Pi}A\hat{\omega}$ of Lloyd's algorithm from Figure 5.1 for the setting of Figure 6.6, i.e., for $m = 3$ sources, a binary alphabet $\mathfrak{A} = \{0, 1\}$, and $n = 500$ observations, for $M \in \{1, \ldots, 1000\}$ and $\sigma = 0.2, 0.5, 1$. Again an exponential decay to some limiting value for $\mathrm{E}\left(d((\hat{\Pi}, \hat{\omega}), (\Pi, \omega))^2\right)/M$, $\mathbf{P}\left(\Pi \neq \hat{\Pi}\right)$, $\mathrm{E}\left(\max_{i=1,\ldots,m} \|\omega_{i\cdot} - \hat{\omega}_{i\cdot}\|^2\right)/M$ and $\mathrm{E}\left(\left\|\Pi A - \hat{\Pi}A\right\|_2^2\right)$ as $M \to \infty$ is observed. Whereas $\mathbf{P}\left(\Pi \neq \hat{\Pi}\right) \to 0$ as $M \to \infty$, the limiting value of $\mathrm{E}\left(\max_{i=1,\ldots,m} \|\omega_{i\cdot} - \hat{\omega}_{i\cdot}\|^2\right)/M$ and, thus, also of $\mathrm{E}\left(d((\hat{\Pi}, \hat{\omega}), (\Pi, \omega))^2\right)/M$, scales with σ^2, which is in accordance with Theorem 4.2.3.

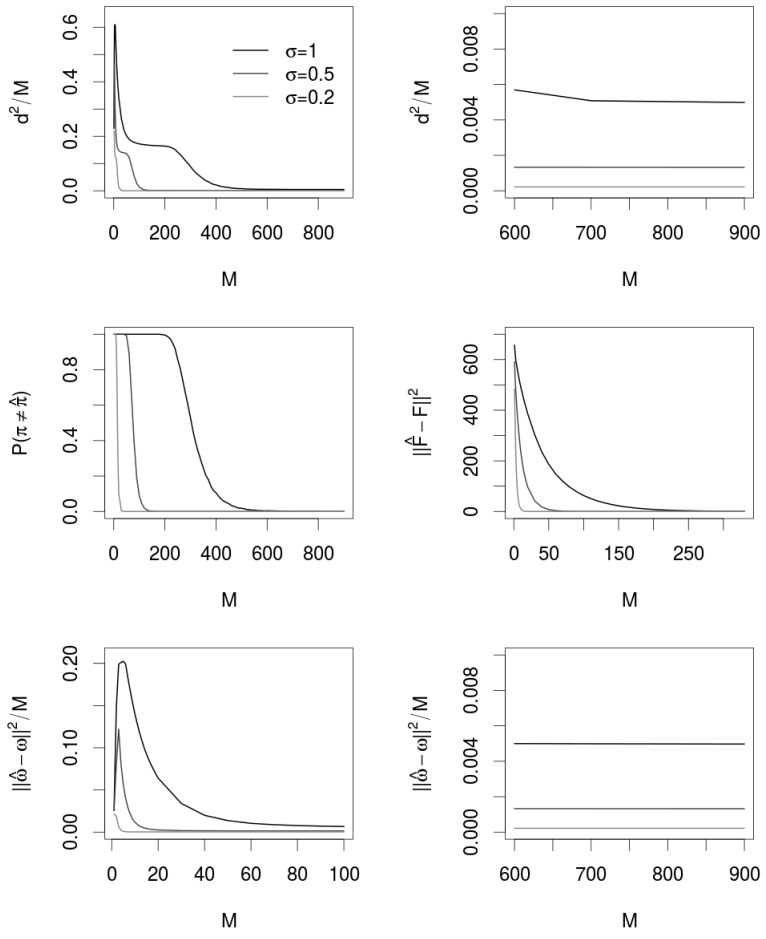

Figure 6.10: From top to bottom: $\mathrm{E}\left(d((\hat{\Pi},\hat{\omega}),(\Pi,\boldsymbol{\omega}))^2\right)/M$ from (4.8); exact recovery probability $\mathbf{P}\left(\Pi \neq \hat{\Pi}\right)$ (left) and $\mathrm{E}\left(\left\|\Pi A - \hat{\Pi}A\right\|_2^2\right)$ (right); and $\mathrm{E}\left(\max_{i=1,\ldots,m}\|\boldsymbol{\omega}_i - \hat{\omega}_i\|^2\right)/M$ for the estimator $\hat{\theta} = \hat{\Pi}A\hat{\omega}$ of Lloyd's algorithm from Figure 5.1 for $m = 3$ sources, a binary alphabet $\mathfrak{A} = \{0,1\}$, and $n = 500$ observations, for $M \in \{1,\ldots,1000\}$ and $\sigma = 0.2, 0.5, 1$ (lightgray, darkgray, and black line).

CHAPTER 7

Applications in cancer genetics

In the following we want to apply the SLAM procedure from Chapter 3 to some real genetic sequencing data from a cancer tumor. Recall from Section 1.1 that a cancer tumor often consists of a few distinct sub-populations , so called clones, of DNA with distinct CN profiles arising from duplication and deletion of genetic material groups. The CN profiles of the underlying clones in a sample measurement correspond to the functions $\boldsymbol{f}^1, \ldots, \boldsymbol{f}^m$, the weights $\omega_1, \ldots, \omega_m$ correspond to their proportion in the tumor, and the measurements correspond to observations Y as in the SBSR model (1.3).
The most common method for tumor DNA profiling is via WGS, which roughly involves the following steps:

1. Tumor cells are isolated, and the pooled DNA is extracted, amplified and fragmented through shearing into single-strand pieces.

2. Sequencing of the single pieces takes place using short "reads" (at time of writing of around 10^2 base-pairs long).

3. Reads are aligned and mapped to a reference genome (or the patient germline genome if available) with the help of a computer.

Although, the observed total reads are discrete (each observation corresponds to an integer number of reads at a certain locus), for a sufficiently high sequencing coverage, as it is the case in our example with around 55 average stretches of DNA mapped to a locus, it is well established to approximate this binomial by a normal variate, see e.g., (Liu et al., 2013).
In the following, SLAM is applied to the cell line LS411, which comes from colorectal cancer and a paired lymphoblastoid cell line. Sequencing was done through a collaboration of Complete Genomics with the Wellcome Trust Center for Human Genetics at the University of Oxford. This data has the special feature of being generated under a designed experiment using radiation of the cell line (*"in vitro"*), designed to produce CNAs that mimic real world CN events. In this case therefore, the mixing weights and sequencing data for the individual clones are known, allowing for validation of SLAM's results, something that is not feasible for patient cancer samples.
The data comes from a mixture of three different types of DNA, relating to a normal (germline) DNA and two different clones. Tumor samples, even from micro-dissection, often contain high proportion of normal cells, which for our purposes are a nuisance, this is known as "stromal

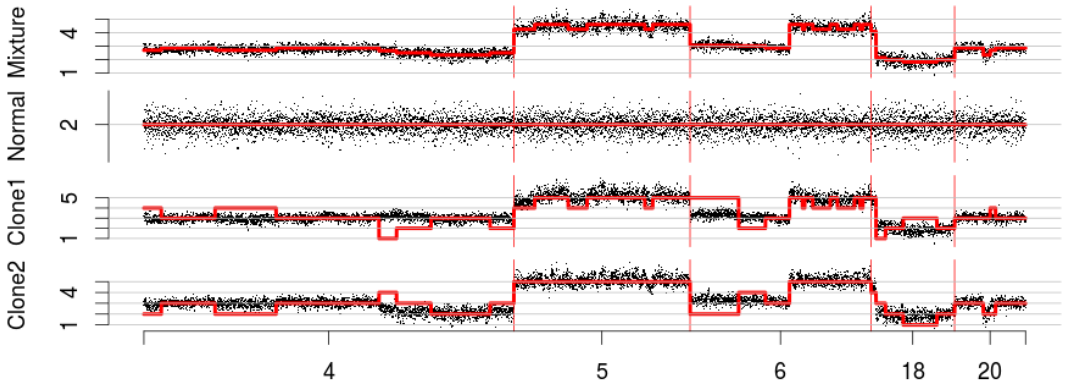

Figure 7.1: As Figure 1.3, but with $q_n(\beta) = 2.2$ corresponding to $\beta = 0.01$.

contamination" of germline genomes in the cancer literature. The true mixing weights in our sample are $\omega^\top = (\omega_{\text{Normal}}, \omega_{\text{Clone1}}, \omega_{\text{Clone2}}) = (0.2, 0.35, 0.45)$.

SLAM will be, in the following, applied only to the mixture data without knowledge of ω and the sequenced individual clones and germline. The latter (which serve as ground truth) will then be used only for validation of SLAM's reconstruction. We restricted attention to regions of chromosome 4, 5, 6, 18 and 20, as detailed below. Figure 1.2 shows the raw data. Sequencing produces some spatial artifacts in the data, and waviness related to the sequencing chemistry and local GC-content, corresponding to the relative frequency of the DNA bases {C, G} relative to {A, T}. This violates the modeling assumptions. To alleviate this we preprocess the data with a smoothing filter using local polynomial kernel regression on normal data, baseline correction, and binning. We used the local polynomial kernel estimator from the R package `KernSmooth`, with bandwidth chosen by visual inspection. We selected the chromosomal regions above as those showing reasonable denoising, and take the average of every 10th data point to make the computation manageable resulting in $n = 7,480$ data points spanning the genome. The resulting data is displayed in Figure 1.3, where we can see that the data is much cleaned in comparison with Figure 1.2 although clearly some artefacts and local drift of the signal remain. For the SLAM procedure we incorporated prior knowledge of constant CN 2 for the normal cells and considered the following separable regions in Algorithm CRW in Figure 3.1: to infer ω_{Normal} we searched for regions where $f^{\text{Normal}} = 2$ and $f^{\text{Clone1}} = f^{\text{Clone2}} = 3$ and to infer ω_{Clone1} we search for regions where $f^{\text{Clone1}} = 3$ and $f^{\text{Clone2}} = f^{\text{Normal}} = 2$. ω_{Clone2} was indirectly inferred via $\omega_{\text{Clone2}} = 1 - \omega_{\text{Clone1}} - \omega_{\text{Normal}}$.

With $\sigma = 0.21$ pre-estimated as in (Davies and Kovac, 2001), SLAM yields the confidence region for $\alpha = 0.1$ $C_{0.9} = [0.00, 0.23] \times [0.30, 0.44] \times [0.37, 0.70]$. With $q_n(\alpha) = -0.15$ selected with the MVT-method from Section 3.5 we obtain $\hat{\omega} = (0.11, 0.36, 0.52)$. Figure 7.1 shows SLAM's estimates for $q_n(\beta) = 2.2$ (which corresponds to $\beta = 0.01$). The top row shows the estimate for total CN $\sum_j \hat{\omega}_j \hat{f}^j$ and rows 2-4 show $\hat{f}^1$, $\hat{f}^2$, and $\hat{f}^3$. We stress that the data for the single clones are only used for validation purposes and do not enter the estimation process. Inspection of Figure 7.1 shows that artifacts and local drifts of the signal result in an overestimation of the number of jumps. However, the overall appearance of the estimated CNA

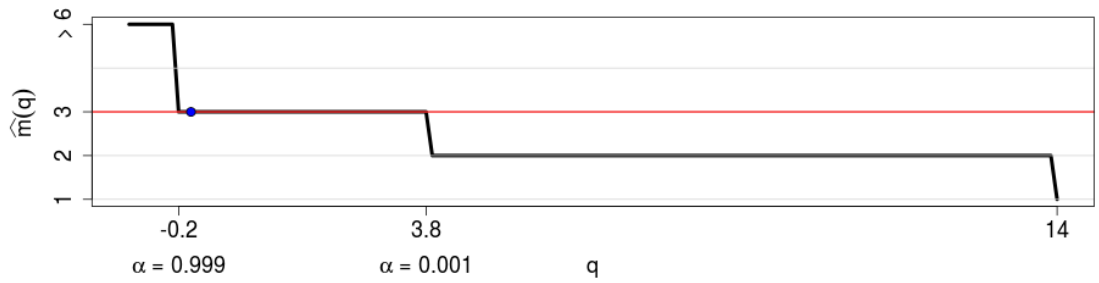

Figure 7.2: Estimated number of source components $\hat{m}(q)$ (y-axis) as in Definition 3.6.2 for different values of q (x-axis), for the WGS-data from Figure 1.3 with true number of source components $\boldsymbol{m} = 3$ (red horizontal line). The blue dot shows the SLAM selector $\hat{m}$ as in Definition 3.6.8.

profile remains quite accurate. This over-fitting effect caused by these artifacts can be avoided by increasing SLAM's tuning parameter $q_n(\beta)$ at the (unavoidable) cost of loosing detection power on small scales (see Figure 1.3, which shows SLAM's estimate for $q_n(\beta) = 20$). In summary, Figure 1.3 and 7.1 show that SLAM can yield highly accurate estimation of the total CNA profile in this example, as well as reasonable CNA profiles and their mixing proportions for the clones.

Estimating the number of clonal components Recall from Section 1.1 that usually in cancer genetics the number of clones is unknown. Therefore, we apply the SLAM selector $\hat{m}(q)$ from Definition 3.6.2 to estimate the number of clonal components in this data example, where $\boldsymbol{m} = 3$. Figure 7.2 displays $\hat{m}(q_{1-\alpha})$ in dependence of the threshold $q_{1-\alpha}$ and the probability α, which corresponds to the error to overestimate $\boldsymbol{m}$, see Theorem 3.6.4. Larger $q_{1-\alpha}$ and hence, smaller α, provide a stronger guarantee in accordance with Figure 7.2. Remarkably, the estimator $\hat{m}(q_{1-\alpha}) = 3$ is stable over the range $\alpha \in (0.001, 0.999)$. This corresponds to the threshold $q \in (-0.2, 3.8)$ in Definition 3.6.2. Finally, the SLAM selector $\hat{m}$ from Definition 3.6.8 yields the correct number of sources $\hat{m} = \boldsymbol{m} = 3$ in this example (see blue dot in Figure 7.2). The BIC and the AIC criterion, however, overestimate the number of sources in this example with $\hat{m}_{\text{BIC}}, \hat{m}_{\text{AIC}} = 7$, in accordance to our simulation results in Section 6.2.1. As Figure 7.3 shows, misspecifying the number of clones as $\hat{m} = 2$, leads to artificial jumps in the sources and mixture, respectively (recall Example 1.3.1). However, the estimate still remains quite reasonable in the sense that it tries to combine the two different clones into a single one.

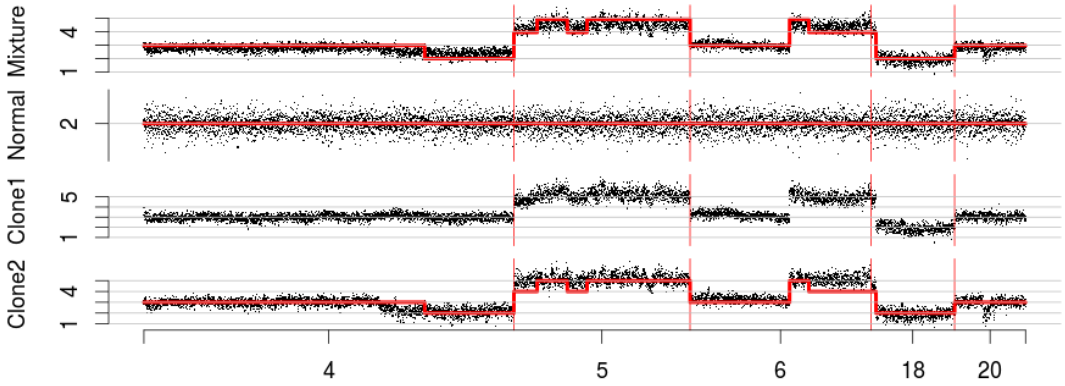

Figure 7.3: As Figure 1.3, but with $\hat{m} = 2$ in SLAM.

CHAPTER 8

Outlook and discussion

This thesis considered a unifying treatment of finite alphabet blind separation (FABS) problems, which, to the best of our knowledge, have not been analyzed in this general and comprehensive form, so far.

In a first step, the identifiability issue was characterized. Separability was introduced and found to regularize FABS via the minimal ASB δ. In particular, it ensures identifiability for arbitrary alphabets $\mathfrak{A}$, number of mixtures M, and number of sources $\boldsymbol{m}$, including the situation where $\boldsymbol{m}$ is unknown.

In a statistical setting, we first considered c.p. regression in the SBSR model (1.3). The multiscale procedure SLAM which estimates the mixing weights $\boldsymbol{\omega}$ and the sources $\boldsymbol{f}$ (including the number of sources components $\boldsymbol{m}$) at (almost) optimal rate of convergence was introduced. Moreover, this procedure yields (asymptotically) honest confidence statements for all quantities (including lower confidence bounds for $\boldsymbol{m}$). Theoretical optimality results were accompanied by a simulation study and a real data example from cancer genetics.

Second, the statistical setting of a multivariate linear model with unknown finite alphabet design was considered. Lower and upper bounds for both, the minimax prediction rate and the minimax estimation rate (in terms of the metric d in (4.8)), were derived. Both are attained by the LSE. In particular, the results reveal that the unknown design does not influence the minimax rates when the number of mixtures M is at least of order $\ln(n)$, where n is the number of observations. This is in strict contrast to the computational issue. Whereas for known design computation of the LSE amounts to a convex optimization problem, for unknown finite alphabet design as in (1.6) it seems to be not feasible, as it amounts to minimization over a disjoint union of exponentially many (in n) (convex) sets. Therefore, we propose a simple Lloyd's algorithm for its approximation. Simulations indicate similar convergence properties as in the theoretical results for the LSE.

In the following we discuss further possible research directions in FABS.

Bayesian FABS This thesis considers FABS in a frequentist setting, where the data Y, in (1.3) and (1.6), has underlying *true* fixed and deterministic mixing weights $\boldsymbol{\omega}$ and sources $\boldsymbol{f}$. Alternatively, one may consider FABS in a Bayesian setting, where $\boldsymbol{\omega}$ and $\boldsymbol{f}$ are themselves random variables. For any Bayesian procedure a prior distribution of the underlying parameters is fundamental. A natural prior distribution for $\boldsymbol{\omega}$ in this setting is a uniform distribution on

$\Omega_{\boldsymbol{m}}$ (for known $\boldsymbol{m}$) and Ω (for unknown $\boldsymbol{m}$), which has been studied in Section 2.3.2 and 2.3.3, respectively. For the sources $\boldsymbol{f}$ a reasonable prior is a Markov process (including i.i.d. sequences), which has been studied in Section 2.3.1. These may be used as a starting point for Bayesian FABS.

SLAM for general error distributions Although, we obtained a certain robustness of SLAM to misspecification of the error distribution in our simulation studies, it is natural to ask how the results of this work can be extended to other types of error distributions than the Gaussian distribution. A natural extension of the Gaussian are sub-Gaussian distributions, where ϵ is sub-Gaussian with scale parameter $\sigma > 0$ if

$$\mathrm{E}\left(e^{t\epsilon}\right) \leq e^{\sigma^2 t^2/2}, \qquad \forall t \in \mathbb{R}. \tag{8.1}$$

The consistency results for SLAM in Theorem 3.4.2 and 3.6.9 rely on a tail bound for the multiscale statistic T_n in (1.16). For the Gaussian case (Sieling, 2013, Corollary 4) yields that for all $n \in \mathbb{N}$ and $q > C$, for some universal constant $C < \infty$, $\mathbf{P}(T_n > q) \leq \exp(-q^2/8)$. When the error terms ϵ_j in (1.3) are only sub-Gaussian with mean zero and variance σ^2, one can use strong Gaussian approximation results (Sakhanenko, 1985) to derive a similar bound.

Theorem 8.0.1. *Let $\boldsymbol{g} \in \mathcal{M}_{\boldsymbol{m}}^{\delta,\lambda}$ for some $\delta, \lambda > 0$ and $\boldsymbol{m} \in \mathbb{N}$ and consider observations $Y_j = \boldsymbol{g}(x_j) + \epsilon_j$, $j = 1, \ldots, n$, from the SBSR model (1.3), but with ϵ_j i.i.d. sub-Gaussian as in (8.1) with mean 0 and variance σ^2. Let $T_n(Y, \boldsymbol{g})$ be as in (1.16). Then, for some universal constants $0 < C, C_1, C_2 < \infty$ it follows for all $q > C$ that*

$$\boldsymbol{P}(T_n(Y, \boldsymbol{g}) > q) \leq \exp(-q^2/32) + (1 + C_2\sqrt{n}) \exp(-C_1 q \sqrt{n\lambda}/4).$$

With Theorem 8.0.1 one can adapt the consistency results for SLAM in Theorem 3.4.2 for the sub-Gaussian case. Defining $q_n(\alpha_n) \coloneqq \delta/(17 m a_k \sigma)\ \ln(n)$ explicitly as in (A.43) one obtains that the assertions of Theorem 3.4.2 still hold true for sub-Gaussian noise, but with probability decreased to $1 - \exp(-q_n(\alpha_n)^2/32) - (1 + C_2\sqrt{n}) \exp(-C_1 q_n(\alpha_n) \sqrt{n\lambda}/4)$ (compared to $1 - \exp(-q_n(\alpha_n)^2/8)$ in the Gaussian case). Note that this still converges superpolynomially fast to one. Analog, the consistency rates for the SLAM selector in Theorem 3.6.9 can be adapted for the sub-Gaussian case, where now $\mathbf{P}(\hat{m} \neq \boldsymbol{m})$ is of rate $O\left(\sqrt{n}\ \exp(-c(\lambda, \delta)\ n)\right)$ (instead of $O\left(\exp(-c(\lambda, \delta)\ n)\right)$ as in the Gaussian case).

A different extension of a Gaussian error distribution is to consider general one-dimensional exponential families. That is, the observations Y_j in (1.3) are assumed to be independently distributed with ν-density $h_{\boldsymbol{g}(x_j)}(z) \coloneqq \exp\left(\boldsymbol{g}(x_j) z - \Psi\left(\boldsymbol{g}(x_j)\right)\right)$, for some σ-finite measure ν on the Borel sets on $\mathbb{R}$ and a cumulant transform Ψ, with the natural parameter space $\Theta = \left\{\theta \in \mathbb{R} : \int_{\mathbb{R}} \exp(\theta z) d\nu(z) < \infty\right\}$. Analog to T_i^j in (1.15) one can consider for the local hypothe-

sis testing problems in (1.14) the log-likelihood ratio statistic

$$T_i^j(Y, g_{ij}) := \log\left(\frac{\sup_{\theta\in\Theta}\Pi_{l=i}^j h_\theta(Y_l)}{\Pi_{l=i}^j h_{g_{ij}}(Y_l)}\right). \tag{8.2}$$

Combining the local statistics in (8.2) in the same way as in (1.16) yields a corresponding multiscale statistic $T_n(Y, g)$. Dümbgen and Spokoiny (2001); Dümbgen et al. (2006); Frick et al. (2014) give several results about this multiscale statistic, its limit distribution, and its geometric interpretation, which leads to the definition of boxes $\mathfrak{B}$ as in (1.18). Combining this with the results of this work yields an extension of SLAM for such distributions. Especially for the case of Poisson and negative binomial distributed Y in (1.3) this might be of particular interest in the context of cancer genetics, as these distributions are often used to model the noise of sequencing data (see (Liu et al., 2013) and references there). Proving consistency results as in Theorem 3.4.2 (and 3.6.11) for general exponential families basically involves three major steps. First, a modulus of continuity for the multiscale statistic $T_n(Y, g)$ (as a function of g) is needed, which boils down to a modulus of continuity of the corresponding cumulant transform Ψ. With this at hand, one can adapt Theorem 3.2.1 which quantifies how the estimation error of $\hat{\omega}$ increases the multiscale statistic T_n and hence, translate an upper bound for $q_n(\beta_n)$ to an upper bound for $q_n(\alpha_n)$. Second, one has to determine the diameters of the boxes in $\mathfrak{B}$, which, in contrast to the Gaussian case, may not always have a closed expression. Finally, a tail bound for the finite sample distribution of T_n is needed, as in Theorem 8.0.1 for the sub-Gaussian case. This gives an explicit upper bound for $\mathbf{P}(T_n(Y, \boldsymbol{g}) > q_n(\alpha_n))$, which translates to a lower bound for the probability that the assertions 1.- 4. in Theorem 3.4.2 hold.

SLAM for median regression Another possible extension of SLAM, without any parametric assumptions on the distribution of Y in (1.3), is to consider median, instead of mean, regression. If in (1.3) the observations Y_j are assumed to be independent with a piecewise constant median $\mathrm{Med}(Y_j) = \sum_{i=1}^m \boldsymbol{\omega}_i \boldsymbol{f}^i(x_j)$, by transforming the problem into a Binomial regression setting (see (Sieling, 2013)), one can derive a multiscale procedure, analog to SLAM, for estimating $\boldsymbol{\omega}$ and $\boldsymbol{f}$ without a specific parametric model.

SLAM for multiple mixtures A natural question to ask is, whether the c.p. regression procedure of SLAM can also be extend for general number of mixtures M (not just for $M = 1$ as in (1.3)). Then, the underlying regression function is a multivariate step function, where in the single components the locations of c.p.'s are the same (because each component comes from the same sources) but the jump sizes can be different (because each component has possibly different mixing weights). It turns out that, while extending the theoretical results for SLAM for arbitrary M is rather straight forward, computationally the problem becomes infeasible when we allow for more than one mixture. The reason for this is that in higher dimensions inversion of the local-log likelihood ratio statistics T_i^j in (1.15) does not result in simple confidence intervals $[\underline{b}_{ij}, \overline{b}_{ij}]$, but rather in high dimensional ellipsoids. For computation of SLAM, with dynamic programming, intersecting local confidence regions efficiently is essential. For

ellipsoids this is computationally not feasible.

SLAM for non-linear mixtures FABS in (1.1) considers *linear* finite alphabet mixtures. One may as well consider non-linear mixtures. Extensions of SLAM would mainly rely on corresponding identifiability results for this case. An example from cancer genetics, where non-linear mixtures of piecewise constant finite alphabet sources occur, is to consider allele frequencies instead of total counts in Chapter 7.

Model selection for multiple mixtures In contrast to the SBSR model for single mixtures $M = 1$, in the MABS model, with arbitrary M, we did not propose a model selection procedure for the number of sources $\boldsymbol{m}$. Note that when $M \geq \boldsymbol{m}$, separability implies $\operatorname{rank}(\Pi A \boldsymbol{\omega}) = \boldsymbol{m}$ and thus, in the noiseless case the number of sources is given by the rank of the mixture. However, this is not the case in a noisy setting, where $\operatorname{rank}(Y) = \min(M, n)$ almost surely. Here, one may employ standard model selection techniques like AIC and BIC to estimate $\boldsymbol{m}$. However, just as in the SBSR model, it might be favorable to derive a refined selection procedure in the MABS model (1.6) which explicitly exploits the finite alphabet structure.

Dependence on $\boldsymbol{m}$ and $\mathfrak{A}$ in minimax rates In the MABS model (1.6) we have considered the minimax rate for fixed number of sources $\boldsymbol{m}$, fixed alphabet $\mathfrak{A}$ and $n, M \to \infty$. The derived lower and upper bounds on the minimax prediction risk in Corollary 4.1.4 coincide up to constants which depend on both, $\mathfrak{A}$ and $\boldsymbol{m}$. If exact constants (depending on $\boldsymbol{m}$ and $\mathfrak{A}$) in the minimax rates were obtained, it could be quantified to which extend one can let $\boldsymbol{m}$ and k grow when compensating with additional mixtures M and observations n.

Estimating weights and sources separately For future research it would also be interesting to study the estimation errors of the mixing matrix $\boldsymbol{\omega}$ and the sources $\boldsymbol{f}$ separately. So far, we have focused on estimating them jointly as in Theorem 3.4.2 for the SBSR model (1.3) and in Corollary 4.1.4 and Theorem 4.2.3 for the MABS model (1.6). It might be possible to estimate one of them while estimation of the other is not feasible. An example where such a situation occurs is multi-reference alignment, see (Bandeira et al., 2017). There, one observes $Y_i = R_i\theta + \sigma^2 Z_i$, where $\theta \in \mathbb{R}^d$ is an unknown parameter, R_i are unknown cyclic shifts, Z_i, $i = 1, \ldots, n$, is i.i.d. standard Gaussian noise, and σ^2 is a known variance. In this setting it is shown in (Bandeira et al., 2017) that the parameter θ can be estimated consistently from Y even when the noise level is so high that it is not possible to estimate the shifts R_i. Analogously, it might be possible to estimate $\boldsymbol{\omega}$ from Y in (1.3) and (1.6), respectively, without estimating $\boldsymbol{f}$.

Statistical guarantees for the Lloyd's algorithm In Chapter 4 it was shown that the LSE is (almost) minimax optimal for the MABS model (4.1). As we cannot compute the LSE exactly in polynomial time, we proposed a Lloyd's algorithm as in Figure 5.1 for its approximation. Simulations indicate a similar performance as the LSE. Recently, Lu and Zhou (2016) gave statistical guarantees for various Lloyd's algorithms. They showed that for sub-Gaussian data

the clustering error becomes exponentially small after an order of $\log(n)$ iterations, with n being the sample size, provided the labels are initialized appropriately. Their results may be applied to our setting to derive theoretical results on the performance of the algorithm in Figure 5.1.

Minimax rates over polynomial time algorithms for MABS A different research direction for the problem that, although, the LSE is (almost) minimax optimal, we cannot compute it efficiently, is to consider the minimax risk restricted to the set of polynomial time estimators, that is

$$\inf_{\hat{\theta}\in\mathcal{P}} \sup_{\mathbf{\Pi} A\boldsymbol{\omega}} \mathrm{E}\left(\left\|\hat{\theta} - \mathbf{\Pi} A\boldsymbol{\omega}\right\|^2\right),$$

with $\mathcal{P} :=$ {estimators which can be computed in polynomial time}. Examples where it has been shown that the minimax rate over polynomial time estimators differs from the minimax rate over all estimators are sparse linear regression (see (Zhang et al., 2014)), sparse principal component analysis (see (Berthet and Rigollet, 2013; Wang et al., 2016)), and pairwise comparison (see (Shah et al., 2016)). It would be interesting to study whether such a gap between polynomial and optimal algorithms exists for the MABS model, too.

APPENDIX A

Proofs

A.1 Proofs of Chapter 2

A.1.1 Proofs of Section 2.1

Proof of Theorem 2.1.3. For $\sigma \in S^n_{\boldsymbol{m}}$ we define $\boldsymbol{g}^\sigma := (\boldsymbol{g}_{\sigma(1)}, \ldots, \boldsymbol{g}_{\sigma(\boldsymbol{m})})$.
"$\Leftarrow$"
By assumption A1 $\boldsymbol{g}^\rho = \boldsymbol{\omega} E$, i.e., $\boldsymbol{g}^\rho E^{-1} = \boldsymbol{\omega}$ and, consequently,

$$\boldsymbol{g}^\rho E^{-1} \in \Omega_{\boldsymbol{m},M} \text{ and } \{\boldsymbol{g}_1, ..., \boldsymbol{g}_n\} \in \left\{(\boldsymbol{g}^\rho E^{-1})a : \ a \in \mathfrak{A}^{\boldsymbol{m}}\right\},$$

which, by assumption A2, is not fulfilled for any other $\sigma \in S^n_{\boldsymbol{m}}$. Thus, $\boldsymbol{\omega}$ is uniquely determined. Moreover, as $ASB(\boldsymbol{\omega}) > 0$, $\boldsymbol{f}$ is uniquely determined as well.
"$\Rightarrow$"
Assume A2 does not hold, i.e., there exists $\sigma \neq \rho \in S^n_{\boldsymbol{m}}$ such that $\omega := \boldsymbol{g}^\sigma E^{-1}$ fulfills

$$\omega \in \Omega_{\boldsymbol{m},M} \text{ and } \{\boldsymbol{g}_1, ..., \boldsymbol{g}_n\} \in \{\omega a : \ a \in \mathfrak{A}^{\boldsymbol{m}}\}.$$

As we assume all observations to be pairwise different, $\omega \neq \boldsymbol{\omega}$ and ω with the corresponding f leads to the same observations $\boldsymbol{g}_1, \ldots, \boldsymbol{g}_n$. Therefore, $(\boldsymbol{\omega}, \boldsymbol{f})$ is not identifiable. □

Proof of Theorem 2.1.5. First, note that by the separability assumption A3

$$\{\boldsymbol{\omega}_1, \ldots, \boldsymbol{\omega}_{\boldsymbol{m}}\} \subset \{\boldsymbol{g}_1, \ldots, \boldsymbol{g}_n\} \subset \{e\boldsymbol{\omega} : \ e \in \mathfrak{A}^{\boldsymbol{m}}\}. \tag{A.1}$$

Define for $r = 1, \ldots, \boldsymbol{m} - 1$

$$\mathfrak{E}_r := \{e \in \mathfrak{A}^{\boldsymbol{m}} : \ e_{r+1} = \ldots = e_{\boldsymbol{m}} = 0\}$$

and notice that for any $e \in \mathfrak{A}^{\boldsymbol{m}} \backslash \mathfrak{E}_r$

$$\|e\boldsymbol{\omega}\|^2 - \|\boldsymbol{\omega}_{r\cdot}\|^2 = \sum_{j=1}^{M} \left(\left(\sum_{i=1}^{\boldsymbol{m}} e_i \boldsymbol{\omega}_{ij} \right)^2 - \boldsymbol{\omega}_{rj}^2 \right).$$

If $e_{r+1} = 0$, then, as $e \in \mathfrak{A}^{\boldsymbol{m}} \backslash \mathfrak{E}_r$, there exists an $i^\star > r + 1$ such that $a_{i^\star} \geq 1$ (recall that we

assume an alphabet as in (1.7)) and hence for any $j = 1, \dots, M$ $\left(\sum_{i=1}^{m} e_i \omega_{ij}\right)^2 \geq \omega_{i^\star j}$. On the other hand, if $e_{r+1} > 0$, then for any $j = 1, \dots, M$ $\left(\sum_{i=1}^{m} e_i \omega_{ij}\right)^2 \geq \omega_{r+1\, j}$ and consequently,

$$\|e\omega\|^2 - \|\omega_{r\cdot}\|^2 \geq \min_{i \geq r+1} \|\omega_{i\cdot}\|^2 - \|\omega_{r\cdot}\|^2 > 0.$$

Thus, we can identify ω_1 as

$$\omega_1 = \operatorname{argmin}\{\|x\| : \ x \in \{g_1, \dots, g_n\} \backslash (0, \dots, 0)\}$$

and, once we have identified $\omega_1, \dots, \omega_r$ for some $r \geq 1$, we can identify

$$\omega_{r+1} = \operatorname{argmin}\left\{\|x\| : \ x \in \{g_1, \dots, g_n\} \setminus \left\{\sum_{i=1}^{r} e_i \omega_i : \ e \in \mathfrak{E}^r\right\}\right\}.$$

Thus, with

$$m = \min\left(r : \ \{g_1, \dots, g_n\} \setminus \left\{\sum_{i=1}^{r} e_i \omega_i : \ e \in \mathfrak{A}^r\right\} = \emptyset\right)$$

we have identified $\omega = (\omega_1, \dots, \omega_m)$ and identifiability of f follows from $AS\,B(\omega) > 0$. □

A.1.2 Proofs of Section 2.2

Proof of Theorem 2.2.3. The separability condition implies that there exists $e^i, \tilde{e}^i \in \mathfrak{A}^m$ for $i = 1, \dots, m$ such that

$$\begin{aligned} \left\|\omega_{i\cdot} - \tilde{e}^i \omega\right\| &< \epsilon, \\ \left\|\omega_{i\cdot} - e^i \omega\right\| &< \epsilon. \end{aligned} \tag{A.2}$$

We start with proving the first assertion by induction for $i = 1, \dots, m$. If either e^1 or $\tilde{e}^1$ equals the unit vector $(1, 0, \dots, 0) \in \mathbb{R}^m$, (A.2) yields

$$\|\omega_{1\cdot} - \omega_{1\cdot}\| < \epsilon. \tag{A.3}$$

If e^1 or $\tilde{e}^1$ equals the zero vector $(0, \dots, 0) \in \mathbb{R}^m$, then $AS\,B(\omega), AS\,B(\omega) \geq \delta$ and (A.2) contradict. So assume that e^1 and $\tilde{e}^1$ both neither equal the first unit vector nor the zero vector and, in particular,

$$e_1^1 \leq 1 \Rightarrow \sum_{i=2}^{m} e_i^1 \geq 1 \tag{A.4}$$

and analog for $\tilde{e}^1$. W.l.o.g. assume that $\|\omega_{1\cdot}\| \geq \|\omega_{1\cdot}\|$. Then

$$\left\|e^1 \omega\right\|^2 = \sum_{j=1}^{M} \left(\sum_{i=1}^{m} e_i^1 \omega_{ij}\right)^2 \geq \min\left(a_2^2 \|\omega_{1\cdot}\|^2, \|\omega_{2\cdot}\|^2\right), \tag{A.5}$$

where the inequality follows from separating into the following cases. If $e_1^1 \geq a_2 > 1$, then

$$\left(\sum_{i=1}^{m} e_i^1 \omega_{ij}\right)^2 \geq (e_1^1)^2 \omega_{1j}^2 \geq a_2^2 \omega_{1j}^2.$$

If $e_1^1 \leq 1$, then by (A.4) $\sum_{i=2}^{m} e_i^1 \geq 1$, that is, $\exists r > 1$ such that $e_r^1 \geq 1$, and

$$\left(\sum_{i=1}^{m} e_i^1 \omega_{ij}\right)^2 \geq (e_r^1)^2 \omega_{rj}^2 \geq \omega_{rj}^2. \tag{A.6}$$

In particular, (A.5) gives

$$\begin{aligned} \left\|e^1 \boldsymbol{\omega}\right\| - \|\boldsymbol{\omega}_{1\cdot}\| &\geq \min\left(a_2 \|\boldsymbol{\omega}_{1\cdot}\| - \|\boldsymbol{\omega}_{1\cdot}\|, \|\boldsymbol{\omega}_{2\cdot}\| - \|\boldsymbol{\omega}_{1\cdot}\|\right) \\ = \min\left(\|(a_2 - 1, 0, \ldots, 0)\boldsymbol{\omega}\|, \|\boldsymbol{\omega}_{2\cdot}\| - \|\boldsymbol{\omega}_{1\cdot}\|\right) &\geq \frac{2\delta}{(1 + \boldsymbol{m} a_k)} > \epsilon \end{aligned} \tag{A.7}$$

and (A.2) gives

$$\left\|e^1 \boldsymbol{\omega}\right\| - \|\boldsymbol{\omega}_{1\cdot}\| \leq \left\|e^1 \boldsymbol{\omega}\right\| - \|\omega_{1\cdot}\| \leq \left\|e^1 \boldsymbol{\omega} - \omega_{1\cdot}\right\| < \epsilon. \tag{A.8}$$

(A.7) and (A.8) contradict, which shows (A.3).

Now assume that

$$\|\boldsymbol{\omega}_{i\cdot} - \omega_{i\cdot}\| < \epsilon \quad \text{for } i = 1, \ldots, r-1 \tag{A.9}$$

and w.l.o.g. assume that

$$\|\boldsymbol{\omega}_{r\cdot}\| \geq \|\omega_{r\cdot}\|. \tag{A.10}$$

First, assume that $\sum_{i=r+1}^{m} e_i^r \geq 1$. Then it follows from (A.2) that

$$\begin{aligned} \|\omega_{r\cdot}\| = \left\|\omega_{r\cdot} - e^r \boldsymbol{\omega} + e^r \boldsymbol{\omega}\right\| \geq \left\|e^r \boldsymbol{\omega}\right\| - \left\|\omega_{r\cdot} - e^r \boldsymbol{\omega}\right\| \geq \left\|e^r \boldsymbol{\omega}\right\| - \epsilon \\ \geq \|\boldsymbol{\omega}_{r+1\cdot}\| - \epsilon \geq \|\boldsymbol{\omega}_{r\cdot}\| + 2\delta/(1 + \boldsymbol{m} a_k) - \epsilon > \|\boldsymbol{\omega}_{r\cdot}\|, \end{aligned} \tag{A.11}$$

where for the third inequality we used an analog argument as in (A.6). (A.11) contradicts (A.10). Thus, it follows that

$$e_{r+1}^r = \ldots = e_{\boldsymbol{m}}^r = 0. \tag{A.12}$$

Further, if $e_r^r = 0$, then

$$\left\|\omega_{r\cdot} - e^r \omega\right\| \leq \left\|\omega_{r\cdot} - e^r \boldsymbol{\omega}\right\| + \left\|e^r \boldsymbol{\omega} - e^r \omega\right\| \leq \left\|\omega_{r\cdot} - e^r \boldsymbol{\omega}\right\| + (r-1) a_k \epsilon \leq (1 + (r-1) a_k)\epsilon < \delta, \tag{A.13}$$

where the second inequality follows from (A.9) and third inequality from (A.2). (A.13) and $AS\,B(\omega) \geq \delta$ contradict. Thus, it follows that

$$e_r^r \geq 1. \tag{A.14}$$

Note that (A.12), (A.14) and (A.2) imply that

$$\begin{aligned}\epsilon &> \left\|\omega_{r\cdot} - e^r\boldsymbol{\omega}\right\| \\ &= \left\|\boldsymbol{\omega}_{r\cdot} - \left(\omega_{r\cdot} - \left((e_r^r - 1)\boldsymbol{\omega}_{r\cdot} + \sum_{i=1}^{r-1} e_i^r\boldsymbol{\omega}_{i\cdot}\right)\right)\right\| \geq \left\|\boldsymbol{\omega}_{r\cdot} - (\omega_{r\cdot} - x)\right\|,\end{aligned} \tag{A.15}$$

with

$$x_j = \begin{cases}\left((e_r^r - 1)\boldsymbol{\omega}_{r\cdot} + \sum_{i=1}^{r-1} e_i^r\boldsymbol{\omega}_{i\cdot}\right)_j & \text{if } \left((e_r^r - 1)\boldsymbol{\omega}_{r\cdot} + \sum_{i=1}^{r-1} e_i^r\boldsymbol{\omega}_{i\cdot}\right)_j \leq \omega_{rj}, \\ \omega_{rj} & \text{otherwise.}\end{cases}$$

As x, ω_r, and $\omega_r - x$ have non-negative entries, it also follows that

$$\|\omega_r\| \geq \|\omega_r - x\|. \tag{A.16}$$

Now, assume that $\sum_{i=1}^{r-1} e_i^r \geq 1$. If $\sum_{i=r+1}^{\boldsymbol{m}} \tilde{e}_i^r \geq 1$ then it follows from (A.2), (A.15), and (A.16) that

$$\begin{aligned}\|\omega_{r+1}\| - \|\omega_r\| &\leq \left\|\tilde{e}^r\omega\right\| - \|\omega_r - x\| \\ &\leq \left\|(\tilde{e}^r\omega - \boldsymbol{\omega}_r) + (\boldsymbol{\omega}_r - (\omega_r - x))\right\| \leq 2\epsilon < 2/(1 + \boldsymbol{m}a_k)\delta,\end{aligned}$$

which contradicts $WSB(\omega) \geq \delta$ and hence, it follows that $\tilde{e}_{r+1}^r = \ldots = \tilde{e}_{\boldsymbol{m}}^r = 0$. Further, if $\tilde{e}_r^r = 0$, then $\tilde{e}_r^r\omega = \sum_{i=1}^{r-1} \tilde{e}_i^r\omega_{i\cdot}$ and

$$\left\|\boldsymbol{\omega}_r - \tilde{e}^r\boldsymbol{\omega}\right\| \leq \left\|\boldsymbol{\omega}_r - \tilde{e}^r\omega\right\| + \left\|\tilde{e}^r\boldsymbol{\omega} - \tilde{e}^r\omega\right\| \leq \epsilon + (r-1)a_k\epsilon < \delta, \tag{A.17}$$

where for the second inequality we used (A.2) and (A.9). (A.17) and $ASB(\boldsymbol{\omega}) \geq \delta$ contradict. Thus it follows that $\tilde{e}_r^r \geq 1$. However, this implies that

$$\begin{aligned}\left\|\boldsymbol{\omega}_r - \tilde{e}^r\omega\right\| &\geq \left\|\sum_{i=1}^{r-1} \tilde{e}_i^r\omega_i + \sum_{i=1}^{r-1} e_i^r\boldsymbol{\omega}_i + (e_r^r - 1)\boldsymbol{\omega}_r + (\tilde{e}_r^r - 1)\omega_r\right\| - \left\|\omega_r - e^r\boldsymbol{\omega}\right\| \\ &\geq \left\|\sum_{i=1}^{r-1} e_i^r\boldsymbol{\omega}_i\right\| - \epsilon \geq \delta - \epsilon > \epsilon,\end{aligned}$$

which contradicts (A.2). Hence, it follows that

$$e_1^r = \ldots = e_{r-1}^r = e_{r+1}^r = \ldots = e_{\boldsymbol{m}}^r = 0 \text{ and } e_r^r \geq 1. \tag{A.18}$$

Thus, by (A.10) and (A.2) it follows that

$$\|\boldsymbol{\omega}_r - \omega_r\| \leq \left\|e_r^r\boldsymbol{\omega}_r - \omega_r\right\| = \|e_r\boldsymbol{\omega} - \omega_r\| \leq \epsilon, \tag{A.19}$$

where for the first inequality we used the fact that for two vectors a, b with $\|a\| \geq \|b\|$ and a

constant $c \geq 1$ it follows that $\|ca - b\| \geq \|a - b\|$. Thus, the first assertion follows by induction. To show the second assertion, assume the contrary, i.e., that there exists $e \neq e' \in \mathfrak{A}^{\boldsymbol{m}}$ such that

$$\epsilon > \left\|e\boldsymbol{\omega} - e'\omega\right\| \geq \left\|e\boldsymbol{\omega} - e'\boldsymbol{\omega}\right\| - \left\|e'\boldsymbol{\omega} - e'\omega\right\|. \tag{A.20}$$

As $AS\,B(\boldsymbol{\omega}) \geq \delta$, it follows that $\|e\boldsymbol{\omega} - e'\boldsymbol{\omega}\| \geq \delta$ and by the first assertion of the theorem, it follows that $\|e'\boldsymbol{\omega} - e'\omega\| \leq \boldsymbol{m}a_k\epsilon$. Therefore (A.20) implies $\epsilon > \delta - \boldsymbol{m}a_k\epsilon$, which is a contradiction. □

Proof of Theorem 2.2.5. W.l.o.g. assume that $m := \mathfrak{m}(f\omega) \leq \mathfrak{m}(\boldsymbol{f}\boldsymbol{\omega}) := \boldsymbol{m}$. It follows from Theorem 2.3.10 (see Remark 2.2.6) that

$$\frac{\delta^{3/2}}{\sqrt{3}a_k} \leq \frac{\delta}{1 + \boldsymbol{m}a_k} \tag{A.21}$$

and thus, one can deduce just as in the proof of Theorem 2.2.3 that

$$|\omega_i - \boldsymbol{\omega}_i| < \epsilon < \frac{\delta^{3/2}}{\sqrt{3}a_k} \quad \text{for all } i = 1, \ldots, m. \tag{A.22}$$

If $m < \boldsymbol{m}$, then

$$\begin{aligned} 1 &= \sum_{i=1}^{m} \omega_i \leq \sum_{i=1}^{m} \boldsymbol{\omega}_i + m\frac{\delta^{3/2}}{\sqrt{3}a_k} \leq 1 - \boldsymbol{\omega}_{\boldsymbol{m}} + m\frac{\delta^{3/2}}{\sqrt{3}a_k} \\ &\leq 1 - \frac{1}{\boldsymbol{m}} + m\frac{\delta^{3/2}}{\sqrt{3}a_k} \leq 1 - \frac{1}{\boldsymbol{m}} + \frac{2^{3/2}}{\sqrt{3}}\frac{\boldsymbol{m} - 1}{(\boldsymbol{m}(\boldsymbol{m}+1))^{3/2}} < 1, \end{aligned}$$

which is a contradiction. Thus, together with (A.22) the first two assertions follow. The last assertion then follows directly from Theorem 2.2.3.

□

A.1.3 Proofs of Section 2.3

Proof of Theorem 2.3.1. Let $\mathfrak{T}^r$ be as in (2.15) and let p_0 be the initial distribution of $(\boldsymbol{f}_{j\cdot})_j$. Define the stopped process

$$\tilde{\boldsymbol{f}}_j^r := \begin{cases} (\boldsymbol{f}_{j1}, \ldots, \boldsymbol{f}_{j\boldsymbol{m}}) & \text{if } j < \mathfrak{T}^r \\ e_r & \text{otherwise,} \end{cases}$$

for $r = 1, \ldots, \boldsymbol{m}$, which is a Markov process as well (see e.g., (Kolokoltsov, 2011, Proposition 4.11.1.)). It is obvious that for the Markov process $(\tilde{\boldsymbol{f}}_j^r)_j$ the state e_r is absorbing and all other states are transient. Moreover, when we reorder the states in $\mathfrak{A}^{\boldsymbol{m}}$ such that e_r is the first state,

the transition matrix of $(\tilde{\boldsymbol{f}}_j^r)_j$ is given by

$$\tilde{P}_r = \begin{pmatrix} 1 & 0 & \dots & 0 \\ p_{2r} & & & \\ & & Q_r & \\ p_{Nr} & & & \end{pmatrix}.$$

The distribution of $\mathfrak{T}^r$ is a discrete phase type distribution (see e.g., (Neuts, 1981, Section 2.2.)), i.e.,

$$\mathbf{P}(\mathfrak{T}^r > n) = p_0 Q_r^n \mathbf{1} \leq \left\| Q_r^n \mathbf{1} \right\|_\infty . \tag{A.23}$$

As $P^N > 0$

$$\tilde{P}_r^N = \begin{pmatrix} 1 & 0 & \dots & 0 \\ s_{2r} & & & \\ \vdots & & Q^N & \\ s_{\boldsymbol{m}r} & & & \end{pmatrix}$$

with $s_{2r}, \dots, s_{\boldsymbol{m}r} > 0$ for $r = 1, \dots, \boldsymbol{m}$. Consequently, all row sums of Q_r^N are smaller than 1, i.e.,

$$c_r := \left\| Q_r^N \mathbf{1} \right\|_\infty < 1 \tag{A.24}$$

and hence $c = \max_{1 \leq r \leq \boldsymbol{m}} c_r < 1$.

Next, we show by induction that $\left\| Q_r^n \mathbf{1} \right\|_\infty \leq c_r^{\lfloor n/N \rfloor}$ for all $n \geq N$. For $n = N$ this holds by definition. So assume that $\left\| Q_r^l \mathbf{1} \right\|_\infty \leq c_r^{\lfloor l/N \rfloor}$ for all $N \leq l \leq n$ and define $A = (a_{ij})_{ij} := Q_r^n$, i.e.,

$$\max_i \sum_j a_{ij} \leq c_r^{\lfloor n/N \rfloor}.$$

If $\lfloor \frac{n}{N} \rfloor = \lfloor \frac{n+1}{N} \rfloor$, then

$$\left\| Q_r^{n+1} \mathbf{1} \right\|_\infty = \| A Q_r \mathbf{1} \|_\infty = \max_i \sum_j \sum_k a_{ik} q_{kj} = \max_i \sum_k a_{ik} \sum_j q_{kj} \leq c_r^{\lfloor \frac{n}{N} \rfloor} = c_r^{\lfloor \frac{n+1}{N} \rfloor},$$

as $\max_i \sum_k a_{ik} \leq c_r^{\lfloor \frac{n}{N} \rfloor}$ and $\sum_j q_{kj} \leq 1$. If $\lfloor \frac{n}{N} \rfloor \neq \lfloor \frac{n+1}{N} \rfloor$, then $\lfloor \frac{n}{N} \rfloor + 1 = \lfloor \frac{n+1}{N} \rfloor$ and $n + 1 = N \left\lfloor \frac{n}{N} \right\rfloor + N$, with $N \lfloor \frac{n}{N} \rfloor =: l \in \{N, \dots, n\}$. Therefore,

$$\left\| Q_r^{n+1} \mathbf{1} \right\|_\infty = \left\| Q_r^l Q_r^N \mathbf{1} \right\|_\infty \leq c_r^{\lfloor \frac{l}{N} \rfloor + 1} = c_r^{\lfloor \frac{n+1}{N} \rfloor}.$$

With (A.23) and (2.16) it follows that

$$1 - \mathbf{P}((\boldsymbol{\omega}, \boldsymbol{f}) \text{ is identifiable}) \leq \boldsymbol{m} c^{\lfloor \frac{n}{N} N \rfloor}$$

Finally, the assertion follows from $\boldsymbol{m} c^{\lfloor \frac{n}{N} \rfloor} / (c^{\frac{n}{N}}) \leq \boldsymbol{m}/c < \infty$. □

Proof of Theorem 2.3.4. In order to proof Theorem 2.3.4, we need to approximate for given

$\delta > 0$ and $m \in \mathbb{N}$ the size of the sets $\Omega_m, \Omega_m^\delta \subset \mathbb{R}^m$. As both have Lebesgue measure zero, we consider the corresponding $(m-1)$-simplex in $\mathbb{R}^{m-1}$

$$\tilde{\Omega}_m := \left\{\omega \in \mathbb{R}^{m-1} : 0 \leq \omega_1 \leq \ldots \leq \omega_{m-1} \leq 1 - \|\omega\|_1\right\}, \tag{A.25}$$

with vertices

$$\tilde{v}_0 = \begin{pmatrix} 0 \\ 0 \\ \vdots \\ 0 \end{pmatrix}, \tilde{v}_1 = \begin{pmatrix} 0 \\ 0 \\ \vdots \\ 1/2 \end{pmatrix}, \quad \ldots, \quad \tilde{v}_{m-2} = \begin{pmatrix} 0 \\ 1/(m-1) \\ \vdots \\ 1/(m-1) \end{pmatrix}, \tilde{v}_{m-1} = \begin{pmatrix} 1/m \\ 1/m \\ \vdots \\ 1/m \end{pmatrix}$$

and

$$\tilde{\Omega}_m^\delta := \left\{\omega \in \tilde{\Omega}_m : AS\,B(\omega_1, \ldots, \omega_{m-1}, 1 - \|\omega\|_1) \geq \delta\right\}.$$

The Lebesgue measure of the simplex $\tilde{\Omega}_m$ is (see e.g., (Stein, 1966))

$$\lambda(\tilde{\Omega}_m) = \left| \frac{1}{(m-1)!} \det \begin{pmatrix} \tilde{v}_1 & \ldots & \tilde{v}_m \\ 1 & \ldots & 1 \end{pmatrix} \right| = \frac{1}{m!(m-1)!}. \tag{A.26}$$

The following lemma gives a bound on the Lebesgue measure of $\tilde{\Omega}_m^\delta$.

Lemma A.1.1. *For a given finite alphabet $\mathfrak{A}$ let $\delta < \Delta\mathfrak{A}_{\min}$. Then*

$$\lambda(\tilde{\Omega}_m \backslash \tilde{\Omega}_m^\delta) \leq \frac{k^{2m} m}{\sqrt{2}\, \Delta^2 \mathfrak{A}_{\min}\, (m-1)!(m-2)!}\, \delta,$$

with $\lambda = \lambda^{m-1}$ the Lebesgue measure on $\mathbb{R}^{m-1}$.

Proof of Lemma A.1.1. Note that

$$\tilde{\Omega}_m \backslash \tilde{\Omega}_m^\delta = \left\{\omega \in \tilde{\Omega}_m : AS\,B(\omega) \leq \delta\right\} = \bigcup_{d \in \Delta\mathfrak{A}^m} \mathfrak{w}_d,$$

with

$$\begin{aligned} \mathfrak{w}_d &:= \left\{\omega \in \tilde{\Omega}_m : |\langle(\omega_1, \ldots, \omega_{m-1}, 1 - \|\omega\|_1), d\rangle| \leq \delta\right\} \\ &= \left\{\omega \in \tilde{\Omega}_m : -\delta - d_m \leq \langle \omega, \tilde{d}\rangle \leq \delta - d_m\right\}, \end{aligned}$$

and $\tilde{d} = (d_1 - d_m, \ldots, d_{m-1} - d_m)$. If $\tilde{d} \equiv 0$, $|d_m| > \Delta\mathfrak{A}_{\min} > \delta$ implies $\lambda^{m-1}(\mathfrak{w}_d) = 0$. Otherwise,

let R be the rotation matrix which maps $\tilde{d}$ to $(\|\tilde{d}\|, 0, \dots, 0)$. Then

$$\begin{aligned}
\lambda^{m-1}(\mathfrak{w}_d) = \lambda^{m-1}(R\mathfrak{w}_d) &= \lambda^{m-1}\left(\left\{\omega \in R\tilde{\Omega}_m : -\delta - d_m \le \langle R^{-1}\omega, \tilde{d}\rangle \le \delta - d_m\right\}\right) \\
&= \lambda^{m-1}\left(\left\{\omega \in R\tilde{\Omega}_m : -\delta - d_m \le \langle \omega, R\tilde{d}\rangle \le \delta - d_m\right\}\right) \\
&= \lambda^{m-1}\left(\left\{\omega \in R\tilde{\Omega}_m : -\delta - d_m \le \|\tilde{d}\|\,\omega_1 \le \delta - d_m\right\}\right) \\
&= \lambda^{m-1}\left(R\tilde{\Omega}_m \bigcap \left\{\omega \in \mathbb{R}^{m-1} : \frac{-\delta - d_m}{\|\tilde{d}\|} \le \omega_1 \le \frac{\delta - d_m}{\|\tilde{d}\|}\right\}\right) \\
&\le \lambda^{m-2}\left(\mathrm{proj}_1(R\tilde{\Omega}_m)\right)\frac{2\delta}{\|\tilde{d}\|} \le \lambda^{m-2}\left(\Delta(R\tilde{\Omega}_m)\right)\frac{2\delta}{\|\tilde{d}\|} \\
&= \lambda^{m-2}\left(\Delta\tilde{\Omega}_m\right)\frac{2\delta}{\|\tilde{d}\|} \le \lambda^{m-2}\left(\Delta\tilde{\Omega}_m\right)\frac{2\delta}{\Delta^2\mathfrak{R}_{\min}},
\end{aligned}$$

where proj_1 denotes the orthogonal projection onto $(1, 0, \dots, 0)^\perp$, i.e., $\mathrm{proj}_1((x_1, \dots, x_{m-1})^\top) = (x_2, \dots, x_{m-1})^\top$ and $\Delta(R\tilde{\Omega}_m)$ denotes the surface area of $R\tilde{\Omega}_m$. The first inequality follows from Cavalieri's principle and the fact that the intersection of a convex set with a hyperplane is smaller than its projection onto the same hyperplane. The second inequality follows from the fact that the orthogonal projection is a contraction and the last inequality follows directly from the definition of $\Delta^2\mathfrak{R}_{\min}$ in (2.21).

It remains to find an upper bound for the Lebesgue measure $\lambda^{m-2}\left(\Delta\tilde{\Omega}_m\right)$ of the surface area of the $m-1$ - simplex $\tilde{\Omega}_m$, which is the union of its facets. To this end, let V_i for $i = 0, \dots, m-1$ denote the Lebesgue measure of the i-th facet of $\tilde{\Omega}_m$, the $m-2$ - simplex with vertices $\tilde{v}_0, \dots, \tilde{v}_{i-1}, \tilde{v}_{i+1}, \dots, \tilde{v}_{m-1}$. Further, let $\mathfrak{G}$ denote the Gramian matrix of $\tilde{v}_1, \dots, \tilde{v}_{m-1}$ with entries

$$(\mathfrak{G})_{ij} = \langle \tilde{v}_i, \tilde{v}_j\rangle = \left(\frac{\min(i,j)}{(i+1)(j+1)}\right)_{ij}, \quad i, j = 1, \dots, m-1$$

and let $\mathfrak{G}^{kl}$ denote the matrix $\mathfrak{G}$ with k-th row and l-th column deleted. Then it follows from (Dörband, 1970) that

$$\begin{aligned}
((m-2)!V_0)^2 &= \sum_{k=1}^{m-1}\sum_{l=1}^{m-1}(-1)^{k+l}\det(\mathfrak{G}^{kl}), \\
((m-2)!V_k)^2 &= \det(\mathfrak{G}^{kk}), \qquad \text{for } k = 1, \dots, m-1.
\end{aligned} \tag{A.27}$$

We have that

$$\det(\mathfrak{G}^{kl}) = \det\left(\left(\frac{\min(i,j)}{(i+1)(j+1)}\right)_{\substack{1\le i\ne k\le m-1\\ 1\le i\ne l\le m-1}}\right) = \frac{k}{m!}\frac{l}{m!}\det\left((\min(i,j))_{\substack{1\le i\ne k\le m-1\\ 1\le i\ne l\le m-1}}\right). \tag{A.28}$$

Next, we show that

$$\det\left((\min(i,j))_{\substack{1\le i\ne k\le m-1\\ 1\le i\ne l\le m-1}}\right) = \begin{cases} 2 & \text{if } k = l \\ 1 & \text{if } k \ne l \end{cases}. \tag{A.29}$$

First, consider the case $k = l$. Then

$$\det\left((\min(i,j))_{1\le i,j\neq k\le m-2}\right) = \det\begin{pmatrix}\begin{pmatrix}1 & 1 & 1 & \dots & & & 1\\ 1 & 2 & 2 & \dots & & & 2\\ & & \ddots & & & & \end{pmatrix}\\ \begin{pmatrix}1 & 2 & \dots & k-1 & k-1 & \dots & k-1\\ 1 & 2 & \dots & k-1 & k+1 & \dots & k+1\\ & & & & & & \vdots\\ 1 & 2 & \dots & k-1 & k+1 & \dots & m-1\end{pmatrix}\end{pmatrix}$$

$$= \det\begin{pmatrix}\begin{pmatrix}1 & 0 & 0 & \dots & & & 0\\ 1 & 1 & 0 & \dots & & & 0\\ & & \ddots & & & & \end{pmatrix}\\ \begin{pmatrix}1 & 1 & \dots & 1 & 0 & \dots & 0\\ 1 & 1 & \dots & 1 & 2 & \dots & 0\\ & & & & & & \vdots\\ 1 & 1 & \dots & 1 & 2 & \dots & 1\end{pmatrix}\end{pmatrix} = 2,$$

where for the second equality we subtracted the i-th column from the $i+1$-th column for $i = 1, \dots, m-2$.

Second, consider the case $k \neq l$. For $m = 2$ (A.29) holds trivially. So assume that (A.29) holds for all $1 \le k, l \le m-1$ for some $m \ge 2$ and let $k \neq l$ be fixed. As the determinant is invariant under transposition, we can assume w.l.o.g. that $k < l$ and, hence, $l > 1$. Then

$$\begin{aligned}
&\det\left((\min(i,j))_{\substack{1\le i\neq k\le m\\ 1\le i\neq l\le m}}\right)\\
&= \det(1_{1\le i\neq k\le m}, \min(2,i)_{1\le i\neq k\le m},\\
&\quad ..., \min(l-1,i)_{1\le i\neq k\le m}, \min(l+1,i)_{1\le i\neq k\le m}, ..., \min(m,i)_{1\le i\neq k\le m})\\
&= \det(1_{0\le i\neq k-1\le m-1}, \min(1,i)_{0\le i\neq k-1\le m-1},\\
&\quad ..., \min(l-2,i)_{0\le i\neq k-1\le m-1}, \min(l,i)_{0\le i\neq k-1\le m-1}, ..., \min(m-1,i)_{0\le i\neq k-1\le m-1})\\
&= \det(\min(1,i)_{1\le i\neq k-1\le m-1},\\
&\quad ..., \min(l-2,i)_{1\le i\neq k-1\le m-1}, \min(l,i)_{1\le i\neq k-1\le m-1}, ..., \min(m-1,i)_{1\le i\neq k-1\le m-1})\\
&\quad = \det\left((\min(i,j))_{\substack{1\le i\neq k\le m-1\\ 1\le i\neq l\le m-1}}\right) = 1,
\end{aligned}$$

where for the second equality we subtracted the first column from the others and for the third equality we evaluate the determinant by its first row, and hence (A.29) follows.

From (A.28) and (A.29) we deduce that

$$\det(\mathfrak{G}^{kl}) = \begin{cases} 2\left(\frac{k}{m!}\right)^2 & \text{if } k = l\\ \frac{k}{m!}\frac{l}{m!} & \text{if } k \neq l\end{cases}$$

and from (A.27) that

$$((m-2)!\ V_0)^2 \le \left(\frac{\sqrt{2}}{m!}\sum_{k=1}^{m-1}(-1)^k k\right)^2 \le \left(\frac{1}{\sqrt{2}(m-1)!}\right)^2,$$
$$((m-2)!\ V_j)^2 = 2\left(\frac{j}{m!}\right)^2, \quad \text{for } j = 1,\dots,m-1$$

and consequently,

$$\lambda^{m-2}\left(\Delta\tilde{\Omega}_m\right) = \sum_{i=0}^{m-1} V_i \le \frac{1}{\sqrt{2}(m-1)!(m-2)!} + \frac{\sqrt{2}}{(m-2)!m!}\sum_{j=1}^{m-1} j = \frac{m}{\sqrt{2}(m-1)!(m-2)!}$$

and

$$\lambda^{m-1}(\mathfrak{w}_d) \le \frac{m\sqrt{2}}{\Delta^2\mathfrak{A}_{\min}(m-1)!(m-2)!}\,\delta.$$

Finally, as $\mathfrak{w}_d = \mathfrak{w}_{-d}$ and $\#\Delta\mathfrak{A}^m \le k^{2m}$, the assertion follows from

$$\lambda(\tilde{\Omega}_m\backslash\tilde{\Omega}_m^\delta) \le \sum_{d\in\Delta\mathfrak{A}^m}\frac{\lambda^{m-1}(\mathfrak{w}_d)}{2} \le \frac{k^{2m}\,\lambda^{m-1}(\mathfrak{w}_d)}{2}.$$

□

From Lemma A.1.1 and (A.26) we deduce that

$$\mathbf{P}(\omega\in\Omega_m^\delta) = 1 - \frac{\lambda(\tilde{\Omega}_m\backslash\tilde{\Omega}_m^\delta)}{\lambda(\tilde{\Omega}_m)} \ge 1 - \frac{k^{2m}\,m^2(m-1)}{\sqrt{2}\,\Delta^2\mathfrak{A}_{\min}}\,\delta,$$

which shows the assertion. □

Proof of Theorem 2.3.5. From Lemma A.1.2 it follows surely that $AS\,B(\boldsymbol{\omega})/\sqrt{M}$ is bounded from above by $(1+ma_k)/\sqrt{2(m(m-1))}$, which shows the inequality on the right hand side. If $M = 1$ and $\boldsymbol{\omega}$ is drawn uniformly, then by Theorem 2.3.4 $\mathbf{P}(AS\,B(\boldsymbol{\omega}) > \delta) \ge 1 - d\,\delta$ with $d = k^{2m}m^2(m-1)/(\sqrt{2}\Delta^2\mathfrak{A}_{\min})$. For arbitrary $M\in\mathbb{N}$, if $\boldsymbol{\omega}$ is drawn uniformly its ASB is bounded by the corresponding ASB's of the single components, i.e., $AS\,B(\boldsymbol{\omega})^2 \ge \sum_{j=1}^M AS\,B(\boldsymbol{\omega}_{\cdot j})^2$, where $AS\,B(\boldsymbol{\omega}_{\cdot j})$, $j = 1,\dots,M$, are independent and identically distributed with

$$\mathrm{E}\left(AS\,B(\boldsymbol{\omega}_{\cdot j})^2\right) \ge \int_0^\infty (1-d\sqrt{x})_+ dx = \frac{1}{3d^2}.$$

Hence, for $c < \frac{1}{\sqrt{3}d}$ it follows from the strong law of large numbers that almost surely

$$\liminf_{M\to\infty}\frac{AS\,B(\boldsymbol{\omega})^2}{M} \ge \liminf_{M\to\infty}\frac{1}{M}\sum_{j=1}^M AS\,B(\boldsymbol{\omega}_{\cdot j})^2 = \mathrm{E}\left(AS\,B(\boldsymbol{\omega}_{\cdot j})^2\right) > c^2,$$

which shows the inequality on the left hand side. □

Proof of Theorem 2.3.6. With the notation of the proof of Lemma A.1.1 we have that

$$\begin{aligned} c(m)\,\mathbf{P}(AS\,B(\boldsymbol{\omega}) < \delta) &= \lambda^{m-1}\left(\bigcup_{d\in\Delta\mathfrak{U}^m} \mathfrak{w}_d\right) \\ &= \sum_{i=1}^{|\Delta\mathfrak{U}^m|} (-1)^{i+1} \sum_{\{d^1,\dots,d^i\}\subset\Delta\mathfrak{U}^m} \lambda^{m-1}\left(\mathfrak{w}_{d^1}\cap\ldots\cap\mathfrak{w}_{d^i}\right), \end{aligned}$$

for some constant $c(m)$ which only depends on m. Moreover,

$$\mathfrak{w}_{d^1}\cap\ldots\cap\mathfrak{w}_{d^i} = \left\{\omega\in\tilde{\Omega}_m \;:\; \langle\tilde{d}^j,\omega\rangle\in[d_m^j\pm\delta] \text{ for } j=1,\dots,i\right\} = \left\{\omega\in\tilde{\Omega}_m \;:\; D\omega\in a\pm\delta\right\},$$

with $\tilde{d}^j := (d_1^j - d_m^j,\dots,d_{m-1}^j - d_m^j)\in\mathbb{R}^{m-1}$, $D := (\tilde{d}^1,\dots,\tilde{d}^i)^\top\in\mathbb{R}^{i\times(m-1)}$, and $a = (d_m^1,\dots,d_m^i)^\top\in\mathbb{R}^i$. Let $r := \operatorname{rank}(D)$ and consider a singular value decomposition $D = U\Sigma V^\star$. Then, as $1\le r\le m-1$ the assertion follows from

$$\begin{aligned} &\lambda^{m-1}\left(\{\omega\in\tilde{\Omega}_m \;:\; D\omega\in a\pm\delta\}\right) = \lambda^{m-1}\left(\{\omega\in V^\star\tilde{\Omega}_m \;:\; \Sigma\omega\in U^\star a\pm\delta\}\right) \\ &= \lambda^{m-1}\left(\{\omega\in V^\star\tilde{\Omega}_m \;:\; \omega_1\in[(U^\star a)_1\pm\delta],\dots,\omega_r\in[(U^\star a)_r\pm\delta]\}\right) = O(\delta^r). \end{aligned}$$

□

Proof of Theorem 2.3.10. First, note that for all $j=1,\dots,k-1$ and $\omega\in\Omega_m$

$$AS\,B(\omega,\mathfrak{U}) \le AS\,B(\omega,\{a_j,a_{j+1}\}) = (a_{j+1}-a_j)AS\,B(\omega,\{0,1\})$$

and hence

$$\max_{\omega\in\Omega_m} AS\,B(\omega,\mathfrak{U}) \le \min_{j=1,\dots,k-1}(a_{j+1}-a_j)\max_{\omega\in\Omega_m} AS\,B(\omega,\{0,1\}). \tag{A.30}$$

Further, $AS\,B(\omega,\{0,1\}) \le \min(\omega_1,\omega_2-\omega_1,\dots,\omega_m-\omega_{m-1})$ and hence $AS\,B(\omega,\{0,1\})$ can be bounded from above by the solution of the optimization problem

$$\begin{aligned} \max_{\omega\in\mathbb{R}^m}\ &\min(\omega_1,\omega_2-\omega_1,\dots,\omega_m-\omega_{m-1}) \quad \text{s.t.} \\ \omega_1+\ldots+\omega_m &= 1 \\ \omega_1 &\ge 0 \\ \omega_i-\omega_{i-1} &\ge 0, \quad i=2,\dots,m. \end{aligned}$$

Applying the coordinate transformation $(\lambda_1,\dots,\lambda_m) = (\omega_1,\omega_2-\omega_1,\dots,\omega_m-\omega_{m-1})$, this can be rewritten as

$$\begin{aligned} \max_{\lambda\in\mathbb{R}^m}\ &\min(\lambda_1,\lambda_2,\dots,\lambda_m) \quad \text{s.t.} \\ m\lambda_1+(m-1)\lambda_2+\ldots+\lambda_m &= 1 \\ \lambda_i &\ge 0, \quad i=1,\dots,m. \end{aligned} \tag{A.31}$$

Note that omitting the positivity constraint in (A.31) does not change its optimal solution and hence coincides with the global maximum of $f:\mathbb{R}^{m-1}\to\mathbb{R}$, $f(\lambda) = \min(\lambda_1,\dots,\lambda_{m-1},1-$

$m\lambda_1 - (m-1)\lambda_2 - \ldots - 2\lambda_{m-1}$), which is attained at

$$\lambda_1 = \ldots = \lambda_{m-1} = 1 - m\lambda_1 - (m-1)\lambda_2 - \ldots - 2\lambda_{m-1},$$

i.e., $\max_{\lambda \in \mathbb{R}^{m-1}} f(\lambda) = 2/(m(m+1))$. Together with (A.30) it follows that

$$\max_{\omega \in \Omega_m} AS\,B(\omega) \leq \frac{2}{m(m+1)} \min_{j=1,\ldots,k-1} (a_{j+1} - a_j).$$

Moreover, as the weights ω sum up to one, it follows for any $e \in \mathfrak{A}^m$ that $e\omega \in [0, a_k]$. Thus, $\max_{\omega \in \Omega_m} AS\,B(\omega)$ must be smaller than the maximum of the minimal distance between k^m points in the interval $[0, a_k]$, which equals $a_k/(k^m - 1)$. Hence, the assertion follows. □

Proof of Theorem 2.3.12. From (A.26) together with an expression for the modified Bessel function of the v-th kind (Abramowitz and Stegun, 1972, equation 9.6.10)

$$I_v(z) = \left(\frac{z}{2}\right)^v \sum_{k=0}^{\infty} \frac{(z/2)^{2k}}{k!\Gamma(k+v+1)} \tag{A.32}$$

one gets

$$\lambda(\tilde{\Omega}) = \sum_{m=2}^{\infty} \lambda(\tilde{\Omega}^m) = \sum_{m \in \mathbb{N}} \frac{1}{m!(m-1)!} = I_1(2) - 1 \approx 0.59,$$

and similar from Lemma A.1.1

$$\begin{aligned}
\lambda(\tilde{\Omega} \backslash \tilde{\Omega}^\delta) &= \sum_{m=2}^{\infty} \lambda(\tilde{\Omega}_m \backslash \tilde{\Omega}_m^\delta) \leq \frac{\delta}{\sqrt{2}\,\Delta^2 \mathfrak{A}_{\min}} \sum_{m=2}^{\infty} \frac{k^{2m} m}{(m-1)!(m-2)!} \\
&= \frac{\delta}{\sqrt{2}\,\Delta^2 \mathfrak{A}_{\min}} \left(\sum_{m=2} \frac{k^{2m}(m-2)}{(m-1)!(m-2)!} + \sum_{m=2}^{\infty} \frac{2k^{2m}}{(m-1)!(m-2)!} \right) \\
&= \frac{\delta}{\sqrt{2}\,\Delta^2 \mathfrak{A}_{\min}} \left(k^6 \sum_{m=0} \frac{k^{2m}}{m!(m+2)!} + 2k^4 \sum_{m=0}^{\infty} \frac{k^{2m}}{m!(m+1)!} \right) \\
&= \frac{\delta}{\sqrt{2}\,\Delta^2 \mathfrak{A}_{\min}} k^3 (2I_1(2k) + kI_2(2k)),
\end{aligned}$$

which shows the assertion. □

A.1.4 Proofs of Section 2.4

Proof of Theorem 2.4.1. W.l.o.g. assume that $(a_2 - a_1)/(a_k - a_{k-1}) < 1$. Otherwise one can multiply all observations by -1, such that the new alphabet becomes $-a_k < \ldots < -a_1$. Further, note that $AS\,B(\boldsymbol{\omega}) > 0$ implies that $\boldsymbol{\omega}_i \neq 0$ for all $i = 1, \ldots, \boldsymbol{m}$. For $\boldsymbol{g} := \boldsymbol{f\omega}$ let $\mathfrak{G} := \{\boldsymbol{g}_1, \ldots, \boldsymbol{g}_n\}$ be the set of the pairwise different observations. (2.24) implies that there exist $i_0, \ldots, i_{\boldsymbol{m}}, j_0, \ldots, j_{\boldsymbol{m}} \in \{1, \ldots, n\}$ such that for $r = 0, \ldots, \boldsymbol{m}$

$$\boldsymbol{g}_{i_r} = A^s(a_2, a_1, a_k)_{r+1.}\,\boldsymbol{\omega}, \quad \boldsymbol{g}_{j_r} = A^s(a_{k-1}, a_k, a_1)_{r+1.}\,\boldsymbol{\omega}.$$

First, note that

$$\min \mathfrak{G} = \boldsymbol{g}_{i_0} = a_k \sum_{\substack{i=1 \\ \omega_i<0}}^{m} \omega_i + a_1 \sum_{\substack{i=1 \\ \omega_i>0}}^{m} \omega_i, \quad \max \mathfrak{G} = \boldsymbol{g}_{j_0} = a_1 \sum_{\substack{i=1 \\ \omega_i<0}}^{m} \omega_i + a_k \sum_{\substack{i=1 \\ \omega_i>0}}^{m} \omega_i$$

and thus

$$\mathfrak{o}_+ := \sum_{\substack{i=1 \\ \omega_i>0}}^{m} \omega_i = \frac{a_k \max \mathfrak{G} - a_1 \min \mathfrak{G}}{a_k^2 - a_1^2}, \quad \mathfrak{o}_- := \sum_{\substack{i=1 \\ \omega_i<0}}^{m} \omega_i = \frac{a_k \min \mathfrak{G} - a_1 \max \mathfrak{G}}{a_k^2 - a_1^2}.$$

If $\mathfrak{o}_- = 0$, all weights are positive and, as $\mathfrak{o}_+$ is identified and thus w.l.o.g. equal to one, Theorem 2.1.5 applies. Thus, assume that $\mathfrak{o}_- < 0$ and define $\mathfrak{G}_0 := \mathfrak{G} \backslash \{\min \mathfrak{G}, \max \mathfrak{G}\}$ and

$$\tilde{m}_0 := \max\{i = 1, \dots, m \text{ s.t. } \omega_i < 0\}, \quad \tilde{m}_0^+ := \tilde{m}_0 + 1,$$

i.e., $\omega_1 < \ldots < \omega_{\tilde{m}_0} < 0 < \omega_{\tilde{m}_0^+} < \ldots < \omega_m$. Second, note that

$$\begin{aligned}
&\min \mathfrak{G}_0 = \min\left(\boldsymbol{g}_{i_{\tilde{m}_0^+}}, \boldsymbol{g}_{j_{\tilde{m}_0}}\right) \\
&= \min\left(a_2 \omega_{\tilde{m}_0^+} + \sum_{i=1}^{\tilde{m}_0} a_k \omega_i + \sum_{i=\tilde{m}_0^+ + 1}^{m} a_1 \omega_i,\ a_{k-1} \omega_{\tilde{m}_0} + \sum_{i=1}^{\tilde{m}_0 - 1} a_k \omega_i + \sum_{i=\tilde{m}_0^+}^{m} a_1 \omega_i\right), \\
&= \min\left(a_2 \omega_{\tilde{m}_0^+} + a_k \mathfrak{o}_- + a_1(\mathfrak{o}_+ - \omega_{\tilde{m}_0^+}),\ a_{k-1} \omega_{\tilde{m}_0} + a_k(\mathfrak{o}_- - \omega_{\tilde{m}_0}) + a_1 \mathfrak{o}_+\right),
\end{aligned}$$

and analog

$$\begin{aligned}
&\max \mathfrak{G}_0 = \max\left(\boldsymbol{g}_{j_{\tilde{m}_0^+}}, \boldsymbol{g}_{i_{\tilde{m}_0}}\right) \\
&= \max\left(a_{k-1} \omega_{\tilde{m}_0^+} + \sum_{i=1}^{\tilde{m}_0} a_1 \omega_i + \sum_{i=\tilde{m}_0^+ + 1}^{m} a_k \omega_i,\ a_2 \omega_{\tilde{m}_0} + \sum_{i=1}^{\tilde{m}_0 - 1} a_1 \omega_i + \sum_{i=\tilde{m}_0^+}^{m} a_k \omega_i\right) \\
&= \max\left(a_{k-1} \omega_{\tilde{m}_0^+} + a_1 \mathfrak{o}_- + a_k(\mathfrak{o}_+ - \omega_{\tilde{m}_0^+}),\ a_2 \omega_{\tilde{m}_0} + a_1(\mathfrak{o}_- - \omega_{\tilde{m}_0}) + a_k \mathfrak{o}_+\right).
\end{aligned}$$

Thus,

$$\begin{aligned}
\frac{\min \mathfrak{G}_0 - a_k \mathfrak{o}_- - a_1 \mathfrak{o}_+}{a_k - a_{k-1}} &= \min\left(\frac{a_2 - a_1}{a_k - a_{k-1}} \omega_{\tilde{m}_0^+}, -\omega_{\tilde{m}_0}\right) \\
\frac{a_k \mathfrak{o}_+ + a_1 \mathfrak{o}_- - \max \mathfrak{G}_0}{a_2 - a_1} &= \min\left(\frac{a_k - a_{k-1}}{a_2 - a_1} \omega_{\tilde{m}_0^+}, -\omega_{\tilde{m}_0}\right).
\end{aligned}$$

Hence, if $(\min \mathfrak{G}_0 - a_k \mathfrak{o}_- - a_1 \mathfrak{o}_+) / (a_k - a_{k-1}) < (a_k \mathfrak{o}_+ + a_1 \mathfrak{o}_- - \max \mathfrak{G}_0) / (a_2 - a_1)$, we find

$$\omega_{\tilde{m}_0^+} = \frac{\min \mathfrak{G}_0 - a_k \mathfrak{o}_- - a_1 \mathfrak{o}_+}{a_2 - a_1}$$

and if $(\min \mathfrak{G}_0 - a_k \mathfrak{v}_- - a_1 \mathfrak{v}_+) / (a_k - a_{k-1}) = (a_k \mathfrak{v}_+ + a_1 \mathfrak{v}_- - \max \mathfrak{G}_0) / (a_2 - a_1)$, that

$$\boldsymbol{\omega}_{\tilde{\boldsymbol{m}}_0} = \frac{\max \mathfrak{G}_0 - a_k \mathfrak{v}_+ - a_1 \mathfrak{v}_-}{a_2 - a_1}.$$

Thus, we have identified the first weight, namely

$$\boldsymbol{\omega}_1^\star := \begin{cases} \boldsymbol{\omega}_{\tilde{\boldsymbol{m}}_0^+} & \text{if } \frac{\min \mathfrak{G}_1 - a_k \mathfrak{v}_- - a_1 \mathfrak{v}_+}{a_k \mathfrak{v}_+ + a_1 \mathfrak{v}_- - \max \mathfrak{G}_1} < \frac{a_k - a_{k-1}}{a_2 - a_1} \\ \boldsymbol{\omega}_{\tilde{\boldsymbol{m}}_0} & \text{otherwise.} \end{cases}$$

Now assume that we have identified l different weights, $\boldsymbol{\omega}_1^\star, \dots, \boldsymbol{\omega}_l^\star$. If $\mathfrak{v}_- = \sum_{i=1, \boldsymbol{\omega}_i^\star < 0}^{l} \boldsymbol{\omega}_i^\star$, all the remaining weights are positive and Theorem 2.1.5 applies. Thus assume that $\mathfrak{v}_- < \sum_{i=1, \boldsymbol{\omega}_i^\star < 0}^{l} \boldsymbol{\omega}_i^\star$ and define $\mathfrak{G}_l := \mathfrak{G}_{l-1} \backslash \mathfrak{R}_{l-1}$, with

$$\mathfrak{R}_{l-1} := \bigcup_{\substack{e', e'' \in \mathfrak{A} \\ e \in \mathfrak{A}^l}} \left\{ e'(\mathfrak{v}_- - \sum_{\substack{i=1 \\ \boldsymbol{\omega}_i^\star < 0}}^{l} \boldsymbol{\omega}_i^\star) + e''(\mathfrak{v}_+ - \sum_{\substack{i=1 \\ \boldsymbol{\omega}_i^\star > 0}}^{l} \boldsymbol{\omega}_i^\star) + (\boldsymbol{\omega}_1^\star, ..., \boldsymbol{\omega}_l^\star) e \right\}$$

and

$$\begin{aligned} \tilde{\boldsymbol{m}}_l &:= \max \left\{ i = 1, ..., \boldsymbol{m} \text{ s.t. } \boldsymbol{\omega}_i < 0 \text{ and } \boldsymbol{\omega}_i \notin \{\boldsymbol{\omega}_1^\star, ..., \boldsymbol{\omega}_l^\star\} \right\}, \\ \tilde{\boldsymbol{m}}_l^+ &:= \min \left\{ i = 1, ..., \boldsymbol{m} \text{ s.t. } \boldsymbol{\omega}_i > \boldsymbol{\omega}_{\tilde{\boldsymbol{m}}_l} \text{ and } \boldsymbol{\omega}_i \notin \{\boldsymbol{\omega}_1^\star, ..., \boldsymbol{\omega}_l^\star\} \right\}. \end{aligned}$$

Note that

$$\min \mathfrak{G}_l = \min \left(\boldsymbol{g}_{i_{\tilde{\boldsymbol{m}}_l^+}}, \boldsymbol{g}_{j_{\tilde{\boldsymbol{m}}_l}} \right), \quad \max \mathfrak{G}_l = \max \left(\boldsymbol{g}_{j_{\tilde{\boldsymbol{m}}_l^+}}, \boldsymbol{g}_{i_{\tilde{\boldsymbol{m}}_l}} \right)$$

and thus

$$\begin{aligned} \frac{\min \mathfrak{G}_l - a_k \mathfrak{v}_- - a_1 \mathfrak{v}_+}{a_k - a_{k-1}} &= \min \left(\frac{a_2 - a_1}{a_k - a_{k-1}} \boldsymbol{\omega}_{\tilde{\boldsymbol{m}}_l^+}, -\boldsymbol{\omega}_{\tilde{\boldsymbol{m}}_l} \right) \\ \frac{a_k \mathfrak{v}_+ + a_1 \mathfrak{v}_- - \max \mathfrak{G}_l}{a_2 - a_1} &= \min \left(\frac{a_k - a_{k-1}}{a_2 - a_1} \boldsymbol{\omega}_{\tilde{\boldsymbol{m}}_l^+}, -\boldsymbol{\omega}_{\tilde{\boldsymbol{m}}_l} \right). \end{aligned}$$

Hence, if $(\min \mathfrak{G}_l - a_k \mathfrak{v}_- - a_1 \mathfrak{v}_+) / (a_k - a_{k-1}) < (a_k \mathfrak{v}_+ + a_1 \mathfrak{v}_- - \max \mathfrak{G}_l) / (a_2 - a_1)$, we find

$$\boldsymbol{\omega}_{\tilde{\boldsymbol{m}}_l^+} = \frac{\min \mathfrak{G}_l - a_k \mathfrak{v}_- - a_1 \mathfrak{v}_+}{a_2 - a_1}$$

and if $(\min \mathfrak{G}_l - a_k \mathfrak{v}_- - a_1 \mathfrak{v}_+) / (a_k - a_{k-1}) = (a_k \mathfrak{v}_+ + a_1 \mathfrak{v}_- - \max \mathfrak{G}_l) / (a_2 - a_1)$, that

$$\boldsymbol{\omega}_{\tilde{\boldsymbol{m}}_l} = \frac{\max \mathfrak{G}_l - a_k \mathfrak{v}_+ - a_1 \mathfrak{v}_-}{a_2 - a_1}.$$

Thus, we have identified the $(l+1)$-th weight as

$$\boldsymbol{\omega}_{l+1}^\star := \begin{cases} \boldsymbol{\omega}_{\tilde{\boldsymbol{m}}_l^+} & \text{if } \frac{\min \mathfrak{G}_l - a_k \mathfrak{v}_- - a_1 \mathfrak{v}_+}{a_k \mathfrak{v}_+ + a_1 \mathfrak{v}_- - \max \mathfrak{G}_l} < \frac{a_k - a_{k-1}}{a_2 - a_1} \\ \boldsymbol{\omega}_{\tilde{\boldsymbol{m}}_l} & \text{otherwise.} \end{cases}$$

By induction, we can identify all weights and thus, by $ASB(\boldsymbol{\omega}) > 0$ the assertion follows. □

Proof of Theorem 2.4.2. W.l.o.g. assume that $\boldsymbol{g}_1 < \ldots < \boldsymbol{g}_n$. Then $\boldsymbol{g}_1 = a_1$ and $\boldsymbol{g}_n = a_k$ and we can assume w.l.o.g. that $a_1 = 0$ and $a_k = 1$ (otherwise one may consider $(\boldsymbol{g}_j - a_1)/(a_k - a_1)$ instead). Thus, $\boldsymbol{g}_2 = a_2\boldsymbol{\omega}_1$ and $1 - \boldsymbol{g}_{n-1} = (1 - a_{k-1})\boldsymbol{\omega}_1$. Assume we have identified $\boldsymbol{\omega}_1 a_2, \ldots, \boldsymbol{\omega}_1 a_{1+l}$ and $\boldsymbol{\omega}_1(1 - a_{k-1}), \ldots, \boldsymbol{\omega}_1(1 - a_{k-l'})$ for some $l, l' \geq 1$. Set $\mathfrak{G} := \{\boldsymbol{g}_1, \ldots, \boldsymbol{g}_n\}$, then

$$r^l := \min\left(\mathfrak{G} \backslash \{\boldsymbol{\omega}_1 a_2, ..., \boldsymbol{\omega}_1 a_{1+l}\}\right) = \min\left(\boldsymbol{\omega}_1 a_{1+l+1}, (1 - \boldsymbol{\omega}_1)a_2\right),$$
$$s^{l'} := \min\left((1 - \mathfrak{G}) \backslash \{\boldsymbol{\omega}_1(1 - a_{k-1}), ..., \boldsymbol{\omega}_1(1 - a_{k-l'})\}\right) = \min\left(\boldsymbol{\omega}_1(1 - a_{k-l'-1}), (1 - \boldsymbol{\omega}_1)(1 - a_{k-1})\right)$$

and

$$\tilde{s}^{l'} := \frac{\boldsymbol{g}_2}{1 - \boldsymbol{g}_{n-1}} s^{l'} = \min\left(\boldsymbol{\omega}_1 \frac{(1 - a_{k-l'-1})a_2}{(1 - a_{k-1})}, (1 - \boldsymbol{\omega}_1)a_2\right).$$

If $r^l = \tilde{s}^{l'}$, it follows from $OSB(\mathfrak{A}) > 0$ that $r^l = (1 - \boldsymbol{\omega}_1)a_2$ and $\boldsymbol{\omega}_1 = \boldsymbol{g}_2/(\boldsymbol{g}_2 + r^l)$, and hence we have identified $\boldsymbol{\omega} = (\boldsymbol{\omega}_1, 1 - \boldsymbol{\omega}_1)^\top$.
If $r^l < \tilde{s}^{l'}$, then $r^l = \boldsymbol{\omega}_1 a_{1+l+1}$ and if $r^l > \tilde{s}^{l'}$, then $s^{l'} = \boldsymbol{\omega}_1(1 - a_{k-l'-1})$. Thus, we have increased either l or l' by one. Note that if $l = k - 1$, then $r^l = (1 - \boldsymbol{\omega}_1)a_2$ and hence, either $r^l = \tilde{s}^{l'}$ (in which case $\boldsymbol{\omega}$ is identified) or $r^l > \tilde{s}^{l'}$ (in which case l' increases). Similar, if $l' = k - 1$, then $s^{l'} = (1 - \boldsymbol{\omega}_1)(1 - a_{k-1})$ and hence, either $r^l = \tilde{s}^{l'}$ (in which case $\boldsymbol{\omega}$ is identified) or $r^l < \tilde{s}^{l'}$ (in which case l increases). Consequently, $r^l = \tilde{s}^{l'}$ finally and $\boldsymbol{\omega}$ is identified.
Now, we show to identify the unknown alphabet, given the mixing weights $\boldsymbol{\omega} = (\boldsymbol{\omega}_1, 1 - \boldsymbol{\omega}_1)^\top$. We have that $a_2 = \boldsymbol{g}_2/\boldsymbol{\omega}_1$. So assume we have identified $a_2, \ldots, a_l$ for some $l \geq 2$. Then

$$\min\left(\mathfrak{G} \backslash \{a\boldsymbol{\omega}_1 + a'(1 - \boldsymbol{\omega}_1) : \ a, a' \in \{0, a_2, \ldots, a_l\}\}\right) = a_{l+1}\boldsymbol{\omega}_1$$

and hence a_{l+1} is identified. Successively, we can identify the complete alphabet $0, a_2, \ldots, a_{k-1}, 1$ with

$$k = \min\left(l : \ \mathfrak{G} \backslash \{a\boldsymbol{\omega}_1 + a'(1 - \boldsymbol{\omega}_1) : \ a, a' \in \{0, a_2, \ldots, a_l\}\} = \emptyset\right).$$

Finally, identifiability of $\boldsymbol{f}$ follows from $ASB(\boldsymbol{\omega}) > 0$. □

A.1.5 Additional lemmas on the ASB

Lemma A.1.2. *If $\Omega^\delta_{m,M}$ in (2.11) is non-empty for some $m, M \in \mathbb{N}$, then $\delta \leq \frac{\sqrt{M}(1+ma_k)}{\sqrt{2m(m+1)}}$.*

Proof. If $\Omega^\delta_{m,M}$ in (2.11) is non-empty, then there exists an $\omega \in \Omega_{m,M}$ with $\delta \leq ASB(\omega) \leq \sqrt{\sum_{j=1}^M \omega_{1j}^2}$ and $\delta \leq WSB(\omega) \leq (1 + ma_k)/2\left(\|\omega_{i\cdot}\| - \|\omega_{i-1\cdot}\|\right) \leq (1 + ma_k)/2\sqrt{\|\omega_{i\cdot}\|^2 - \|\omega_{i-1\cdot}\|^2}$ for all $i = 1, \ldots, m$, with $\omega_{mj} = 1 - \omega_{1j} - \ldots - \omega_{m-1\,j}$. In particular, there exists $\omega \in \mathbb{R}_+^{m \times M}$ with

$$\frac{4\delta^2}{(1 + ma_k)^2} \leq \min\Big(\sum_{j=1}^M \omega_{1j}^2, \min_{i=2,\ldots,m-1} \sum_{j=1}^M \left(\omega_{ij}^2 - \omega_{i-1\,j}^2\right), \sum_{j=1}^M \left((1 - \omega_{1j} - ... - \omega_{m-1\,j})^2 - \omega_{m-1\,j}^2\right)\Big).$$

Moreover,

$$\begin{aligned}(1-\omega_{1j}-\ldots-\omega_{m-1j})^2 &= 1+(\omega_{1j}+\ldots+\omega_{m-1j})^2-2\omega_{1j}-\ldots-2\omega_{m-1j}\\ &= 1-\sum_{i=1}^{m-1}\omega_{ij}\underbrace{(2-\sum_{s=1}^{m-1}\omega_{sj})}_{\geq 1\geq\omega_{ij}} \leq 1-\omega_{1j}^2-\ldots-\omega_{m-1j}^2.\end{aligned}$$

And thus,

$$\begin{aligned}\frac{\delta^2 4}{(1+ma_k)^2} &\leq \min\Big(\sum_{j=1}^{M}\omega_{1j}^2, \min_{i=2,\ldots,m-1}\sum_{j=1}^{M}\left(\omega_{ij}^2-\omega_{i-1j}^2\right), \sum_{j=1}^{M}\left(1-\omega_{1j}^2-\ldots-2\omega_{m-1j}^2\right)\Big)\\ &\leq \max_{x\in\mathbb{R}^{m-1}}\min\left(x_1, x_2, \ldots, x_{m-1}, (M-mx_1-\ldots-2x_{m-1})\right) = \frac{2M}{m(m+1)},\end{aligned}$$

where for the second inequality we used $x_1 \coloneqq \sum_{j=1}^{M}\omega_{1j}^2$ and $x_i \coloneqq \sum_{j=1}^{M}\omega_{ij}^2 - \sum_{j=1}^{M}\omega_{i-1j}^2$ for $i = 2,\ldots m$. □

Lemma A.1.3. *$\Omega_{m,m}^{0.2\Delta\mathfrak{A}_{\min}}$ as in (2.11) is non-empty for any $m \in \mathbb{N}$, with $\Delta\mathfrak{A}_{\min}$ as in (2.21).*

Proof. For $1/2 > \delta > 0$ define

$$\omega^\delta \coloneqq I_{m\times m} - \frac{2\delta}{1+ma_k}\begin{pmatrix} m-1 & 0 & \ldots & 0 & 0\\ 0 & m-2 & \ldots & 0 & 0\\ & & \vdots & & \\ 0 & 0 & \ldots & 1 & 0\\ -(m-1) & -(m-2) & \ldots & -1 & 0\end{pmatrix}, \tag{A.33}$$

where $I_{m\times m}$ denotes the $m\times m$ identity matrix. As $\frac{2\delta}{1+ma_k}(m-1) < 1$, it holds for $i = m-1,\ldots,1$ that

$$\left|1-\frac{2\delta}{1+ma_k}(i-1)\right| - \left|1-\frac{2\delta}{1+ma_k}i\right| \geq \frac{2\delta}{1+ma_k}$$

and thus $WSB(\omega^\delta) \geq \delta$. Consequently, if $ASB(\omega^\delta) \geq \delta$ it follows that $\Omega_{m,m}^{\delta}$ is non-empty. We have that

$$\begin{aligned}ASB(\omega^\delta) &\geq ASB(I_{m\times m}) - \frac{2\delta}{1+ma_k}\max_{e\neq 0\in\Delta\mathfrak{A}^m}\sqrt{((m-1)(e_1-e_m))^2+\ldots+(e_{m-1}-e_m)^2}\\ &= \Delta\mathfrak{A}_{\min} - \frac{2\delta}{1+ma_k}\max_{e\neq 0\in\Delta\mathfrak{A}^m}\sqrt{((m-1)(e_1-e_m))^2+\ldots+(e_{m-1}-e_m)^2}\\ &\geq \Delta\mathfrak{A}_{\min} - \frac{2\delta}{1+ma_k}2a_k\sqrt{\sum_{i=1}^{m-1}(m-i)} = \Delta\mathfrak{A}_{\min} - \frac{\delta 4a_k}{1+ma_k}\sqrt{\frac{m(m-1)}{2}},\end{aligned}$$

which implies that if

$$\delta \leq \Delta\mathfrak{A}_{\min} - \frac{\delta\sqrt{8}a_k\sqrt{m(m-1)}}{1+ma_k} \quad\Leftrightarrow\quad \delta \leq \Delta\mathfrak{A}_{\min}\left(1+\frac{\sqrt{8}a_k\sqrt{m(m+1)}}{1+ma_k}\right)^{-1} \tag{A.34}$$

then $\Omega^{\delta}_{m,m}$ is non-empty. As

$$\left(1+\frac{\sqrt{8}a_k\sqrt{m(m+1)}}{1+ma_k}\right)^{-1} \geq \left(1+\sqrt{\frac{8(m+1)}{m}}\right)^{-1} \geq 0.2$$

(A.34) holds for $\delta = 0.2\Delta\mathfrak{A}_{\min}$. □

Lemma A.1.4. *If $M/m \in \mathbb{N}$, then $\Omega^{0.2\Delta\mathfrak{A}_{\min}\sqrt{M/m}}_{m,M}$ in (2.11) is non-empty.*

Proof. By Lemma A.1.3 there exists $\omega' \in \Omega^{0.2\Delta\mathfrak{A}_{\min}}_{m,m}$, i.e., $AS\,B(\omega'), WS\,B(\omega') \geq 0.2\Delta\mathfrak{A}_{\min}$. Define

$$\omega = \underbrace{(\omega', \ldots, \omega')}_{M/m\times} \in \Omega_{m,M}.$$

Then $AS\,B(\omega), WS\,B(\omega) \geq 0.2\Delta\mathfrak{A}_{\min}\sqrt{M/m}$. □

Lemma A.1.5. *If $\Omega^{\delta}_{m,M}$ is non-empty for some $\delta > 0$, then there exists $\omega \in \Omega^{\delta}_{m,M}$ with $AS\,B(\omega) = \delta$.*

Proof. Fix some $\omega \in \Omega^{\delta}_{m,M}$ and for $0 \leq \epsilon \leq 1$ define $\omega^{\epsilon} \in \Omega_{m,M}$ as

$$\omega^{\epsilon}_{ij} = \begin{cases} \omega_{ij} & \text{if } i \notin \{1, m\}, \\ \epsilon\,\omega_{1j} & \text{if } i = 1, \\ \omega_{mj} + (1-\epsilon)\omega_{1j} & \text{if } i = m. \end{cases}$$

Then $WS\,B(\omega^{\epsilon}) \geq WS\,B(\omega) \geq \delta$ for all $0 \leq \epsilon \leq 1$ and $\epsilon \mapsto AS\,B(\omega^{\epsilon})$ is continuous with $AS\,B(\omega^0) = 0$ and $AS\,B(\omega^1) \geq \delta$. Thus, there exists an $\epsilon^{\star} \in (0, 1]$ such that $\omega^{\epsilon^{\star}}$ has the desired properties. □

Lemma A.1.6. *If $\Omega^{\delta}_{m,M}$ in (2.11) is non-empty, then there exists an $\omega \in \Omega_{m,m}$ such that $AS\,B(\omega) = \delta\Delta\mathfrak{A}_{\min}/(9\sqrt{M}a_k)$ and $WS\,B(\omega) \geq \delta\Delta\mathfrak{A}_{\min}/(9\sqrt{M}a_k)$.*

Proof. If $\Omega^{\delta}_{m,M}$ is non-empty, it follows from Lemma A.1.2 that $\delta \leq \frac{\sqrt{M}(1+ma_k)}{\sqrt{2m(m+1)}}$ and, hence, $\delta\Delta\mathfrak{A}_{\min}/(9\sqrt{M}a_k) \leq 0.2\Delta\mathfrak{A}_{\min}$. Thus, by Lemma A.1.3 it follows that $\Omega^{\delta\Delta\mathfrak{A}_{\min}/(9\sqrt{M}a_k)}_{m,m} \supset \Omega^{0.2\Delta\mathfrak{A}_{\min}}_{m,m} \neq \emptyset$. i.e., there exists $\omega \in \Omega_{m,m}$ such that $AS\,B(\omega), WS\,B(\omega) \geq \delta\Delta\mathfrak{A}_{\min}/(9\sqrt{M}a_k)$. Now the assertion follows from Lemma A.1.5. □

A.2 Proofs of Chapter 3

Proof of Theorem 3.2.1. Let $\omega \in \Omega_{\boldsymbol{m}}$ be fixed. Analog to $\mathcal{S}(\mathfrak{A})^{\boldsymbol{m}}_{\lambda}$ in (1.12) define

$$\begin{aligned} \mathcal{S}(\mathcal{N}(\omega))^{\boldsymbol{m}}_{\lambda} := \Big\{ \sum_{j=0}^{K} \theta_j \mathbb{1}_{[\tau_j,\tau_{j+1})} : \theta_j \in \mathcal{N}(\omega), \tau_{i+1} - \tau_i \geq \lambda, \\ \tau_0 = 0, \tau_{K+1} = 1, \omega_1, \ldots, \omega_{\boldsymbol{m}} \in \{\theta_0, \ldots, \theta_K\}, K \in \mathbb{N} \Big\}, \end{aligned} \tag{A.35}$$

for the neighborhood of ω-mixture values

$$\mathcal{N}(\omega) := \left\{ e\tilde{\omega} : \ e \in \mathfrak{A}^{\boldsymbol{m}} \text{ and } \|\tilde{\omega} - \omega\|_\infty \leq 2\sigma \frac{q_n(\alpha) + \sqrt{2\ln(e/\lambda)}}{\sqrt{n\lambda}} \right\}.$$

First, we show the following lemma.[1]

Lemma A.2.1. *Conditioned on* $\{\omega \in C_{1-\alpha}(Y)\}$ *and* $\{T_n(Y, \boldsymbol{g}) \leq q_n(\alpha)\}$

$$\inf_{g \in \mathcal{S}(\mathcal{N}(\omega))^{\boldsymbol{m}}_{\lambda/3}} T_n(Y, g) \leq q_n(\alpha) \quad \textit{surely.} \tag{A.36}$$

Proof of Lemma A.2.1. For ease of notation assume that $n\lambda \in \mathbb{N}$. As in R3 define

$$Q(i, j) := \Big[\max_{i \leq u \leq v \leq j} \underline{b}_{uv}, \min_{i \leq u \leq v \leq j} \overline{b}_{uv} \Big] \cap \mathcal{N}(\omega)$$

and note that any $g = \sum_{j=0}^{K} \theta_j \mathbb{1}_{[\tau_j, \tau_{j+1})}$ such that for every $j = 0, \ldots, K$ there exist an interval $[x_u, x_v]$ with $1 \leq u \leq v \leq n$ and $v - u + 1 \geq n\lambda$ such that

1. $[\tau_j, \tau_{j+1}) \subset [x_u, x_v]$,
2. $Q(u, v) \neq \emptyset$, and
3. $\theta_j \in Q(u, v)$,

fulfills the multiscale constraint $T_n(Y, g) \leq q_n(\alpha)$ and takes only values in $\mathcal{N}(\omega)$, that is $g \in \mathcal{S}(\mathcal{N}(\omega))^{\boldsymbol{m}} := \mathcal{S}(\mathcal{N}(\omega))^{\boldsymbol{m}}_0$. Further, note that conditioned on $\{T_n(Y, \boldsymbol{g}) \leq q_n(\alpha)\}$ it follows that $\boldsymbol{\omega} \in C_{1-\alpha}$ (see (1.13)) and, in particular, $\mathfrak{B}^\star \neq \emptyset$ in (1.22). Thus, $\omega \in B := B(i_1^*, j_1^*) \times \ldots \times B(i_m^*, j_m^*)$ for some $B \in \mathfrak{B}^\star$ with $j_r^* - i_r^* + 1 \geq n\lambda$ for $r = 1, \ldots, \boldsymbol{m}$. By definition of B in (1.18)

$$\mathcal{N}(\omega) \supset \{e\tilde{\omega} : e \in \mathfrak{A}^{\boldsymbol{m}}, \tilde{\omega} \in B\}. \tag{A.37}$$

Consequently, it follows directly from R3 and (A.37) that a function g which fulfills 1. - 3. exists. In the following we explicitly construct a function g which has minimal scale $\lambda/3$ and fulfills 1. - 3. such that $g \in \mathcal{S}(\mathcal{N}(\omega))^{\boldsymbol{m}}_{\lambda/3}$, which yields (A.36).
To this end, define $\underline{t}_1 := 1$, $\bar{t}_1 := \max\{i \geq n\lambda : Q(1, i) \neq \emptyset\}$ and successively for $r \geq 2$

$$\begin{aligned} \underline{t}_r &:= \min\{i > \bar{t}_{r-1} : \ \exists j \geq i - 1 + n\lambda \text{ s.t. } Q(i, j) \neq \emptyset\}, \\ \bar{t}_r &:= \max\{i \geq \underline{t}_r : \ Q(\underline{t}_r, i) \neq \emptyset\}, \end{aligned}$$

with the convention that $\min\{\emptyset\} = \infty$. Let $R := \max\{r : \ \underline{t}_r < \infty\}$ and $\underline{t}_{R+1} := n + 1$. Further, for every $r = 1, \ldots, R$ fix some

$$\theta_r \in Q(\underline{t}_r, \bar{t}_r). \tag{A.38}$$

[1] In the original version of (A.36) in (Behr et al., 2017) $\lambda/3$ was falsely replaced by λ and this mistake propagated to the constants c_1, c_2 and $N^\star$ in (3.13), (3.14), and (3.15), respectively.

Note that by construction $Q(\underline{t}_r, \bar{t}_r) \neq \emptyset$ and $\bar{t}_r - \underline{t}_r + 1 \geq n\lambda$. Further, by R3 it follows that $\underline{t}_r - \bar{t}_{r-1} \leq n\lambda$ for $r = 2, \ldots, R+1$. To see this, assume the opposite, i.e., $\underline{t}_r - \bar{t}_{r-1} > n\lambda$ for some $r = 2, \ldots, R+1$. For $k = \underline{t}_r - 1$ in R3 let $[i, j] \in \mathcal{J}_k^\lambda$ be such that (3.8) is non-empty with $j - i + 1 = n\lambda$. By definition of $\mathcal{J}_k^\lambda$ in (3.7) $\underline{t}_r - 1 \in [i, j]$. Hence, $i = j - n\lambda + 1 \geq \underline{t}_r - n\lambda > \bar{t}_{r-1}$ and, by construction of $\underline{t}_r$ and (A.37), it follows that $\underline{t}_r \leq i \leq \underline{t}_r - 1$, which is a contradiction. Next, define for $r = 1, \ldots, R$

$$\begin{aligned}
\overline{s}_r &:= \max\{\bar{t}_r < i \leq \bar{t}_r + n\lambda : \ Q(i + 1 - n\lambda, i) \neq \emptyset\}, \\
\underline{s}_r &:= \min\{\underline{t}_{r+1} - n\lambda \leq i < \underline{t}_{r+1} : \ Q(i, i - 1 + \lambda n) \neq \emptyset\},
\end{aligned}$$

with the convention that $\max\{\emptyset\} = -\infty$. Note that $\overline{s}_r > -\infty$. To see this, for $k = \bar{t}_r + 1$ in R3 let $[i, j] \in \mathcal{J}_k^\lambda$ be such that (3.8) is non-empty with $j - i + 1 = n\lambda$. Then $\bar{t}_r < j = i - 1 + n\lambda \leq \bar{t}_r + n\lambda$ and $Q(j + 1 - n\lambda, j) \neq \emptyset$. Analog, $\underline{s}_r < \infty$. Further, note that $\overline{s}_r \geq \underline{s}_r$. To see this, one can argue similar as above for $k = \overline{s}_r + 1$ in R3. Further, for every $r = 1, \ldots, R$ fix some

$$\overline{\theta}_r \in Q(\overline{s}_r + 1 - \lambda n, \overline{s}_r), \underline{\theta}_r \in Q(\underline{s}_r, \underline{s}_r - 1 + \lambda n). \tag{A.39}$$

Next, for $r = 1, \ldots, R$ consider the following four different cases.

$$\begin{aligned}
&\text{Case 1:} \quad \bar{t}_r + 1 = \underline{t}_{r+1}. \\
&\text{Case 2:} \quad \bar{t}_r + 1 < \underline{t}_{r+1} \text{ and } \overline{s}_r \geq \underline{t}_{r+1} - 1. \\
&\text{Case 3:} \quad \bar{t}_r + 1 < \underline{t}_{r+1}, \overline{s}_r < \underline{t}_{r+1} - 1 \text{ and } \underline{s}_r \leq \bar{t}_r + 1. \\
&\text{Case 4:} \quad \bar{t}_r + 1 < \underline{t}_{r+1}, \overline{s}_r < \underline{t}_{r+1} - 1 \text{ and } \underline{s}_r > \bar{t}_r + 1.
\end{aligned}$$

Define $T_0 := \{1\}$, for $r = 1, \ldots, R-1$

$$\begin{aligned}
T_r &:= \left(\bar{t}_r + 1\right) \text{ in case 1 }, \\
T_r &:= \left(\max(\bar{t}_r + 1 - n\lambda/3, \overline{s}_r + 1 - n\lambda), \min(\underline{t}_{r+1} + 1 + n\lambda/3, \overline{s}_r + 1)\right) \text{ in case 2 }, \\
T_r &:= \left(\max(\bar{t}_r + 1 - n\lambda/3, \underline{s}_r + 1), \min(\underline{t}_{r+1} + 1 + n\lambda/3, \underline{s}_r + 1 + n\lambda)\right) \text{ in case 3 }, \\
T_r &:= (\max(\bar{t}_r + 1 - n\lambda/3, \overline{s}_r + 1 - n\lambda), \left\lceil (\overline{s}_r + \underline{s}_r)/2 \right\rceil, \\
&\quad \min(\underline{t}_{r+1} + 1 + n\lambda/3, \underline{s}_r + 1 + n\lambda)) \text{ in case 4 },
\end{aligned}$$

and

$$\begin{aligned}
T_R &:= (\,) \text{ in case 1 }, \\
T_R &:= \left(\max(\bar{t}_R + 1 - n\lambda/3, \overline{s}_R + 1 - n\lambda)\right) \text{ in case 2 }, \\
T_R &:= \left(\max(\bar{t}_R + 1 - n\lambda/3, \underline{s}_R + 1)\right) \text{ in case 3 }, \\
T_R &:= (\max(\bar{t}_R + 1 - n\lambda/3, \overline{s}_R + 1 - n\lambda), \left\lceil (\overline{s}_R + \underline{s}_R)/2 \right\rceil) \text{ in case 4 }.
\end{aligned}$$

Further, define $\Theta_0 := (\theta_1)$, for $r = 1, \ldots, R-1$

$$\begin{aligned}
\Theta_r &:= (\theta_{r+1}) \text{ in case 1 ,} \\
\Theta_r &:= \left(\overline{\theta}_r, \theta_{r+1}\right) \text{ in case 2 ,} \\
\Theta_r &:= \left(\underline{\theta}_r, \theta_{r+1}\right) \text{ in case 3 ,} \\
\Theta_r &:= \left(\overline{\theta}_r, \underline{\theta}_r, \theta_{r+1}\right) \text{ in case 4}
\end{aligned}$$

and

$$\begin{aligned}
\Theta_R &:= (\,) \text{ in case 1 ,} \\
\Theta_R &:= \left(\overline{\theta}_R\right) \text{ in case 2 ,} \\
\Theta_R &:= \left(\underline{\theta}_R\right) \text{ in case 3 ,} \\
\Theta_R &:= \left(\overline{\theta}_R, \underline{\theta}_R\right) \text{ in case 4 ,}
\end{aligned}$$

with θ_r as in (A.38), $\underline{\theta}_r$ and $\overline{\theta}_r$ as in (A.39). Concatenating the individual vectors $T_0, \ldots, T_R$ and $\Theta_0, \ldots, \Theta_R$, define

$$\tilde{T} = (t_1, \ldots, t_{\tilde{R}}) := (T_0, \ldots, T_R), \quad \tilde{\Theta} = (\theta_1, \ldots, \theta_{\tilde{R}}) := (\Theta_0, \ldots, \Theta_R).$$

Recall that by R1 $B = B(i_1^*, j_1^*) \times \ldots \times B(i_m^*, j_m^*) \notin \mathfrak{B}_{nc}$ as in (3.6) and thus, $Q(i_r^*, j_r^*) \neq \emptyset$ for $r = 1, \ldots, \boldsymbol{m}$. Define $\bar{l}_r$ and $\underline{l}_r$ via

$$t_{\underline{l}_r} := \max\{t \in \tilde{T} : \; t \leq i_r^*\}, \quad t_{\bar{l}_r} := \min\{t \in \tilde{T} : \; t \geq j_r^*\},$$

for $r = 1, \ldots, \boldsymbol{m}$ and define T by replacing $(t_{\underline{l}_r+1}, \ldots, t_{\bar{l}_r-1})$ in $\tilde{T}$ by $(\max(t_{\underline{l}_r} + n\lambda/3 + 1, i_r^*), \min(j_r^* + 1, t_{\bar{l}_r} - n\lambda/3))$. If $\underline{l}_r + 1 = \bar{l}_r$ just insert the latter vector between $t_{\underline{l}_r}$ and $t_{\bar{l}_r}$ in $\tilde{T}$. Analog define Θ by replacing $(\theta_{\underline{l}_r+2}, \ldots, \theta_{\bar{l}_r-2})$ by ω_r. Then, reusing some notation, for $T := (t_1, \ldots, t_R)$, $\Theta := (\theta_1, \ldots, \theta_R)$, and $t_{R+1} := n + 1$ it follows that

$$g := \sum_{i=1}^{R} \theta_i \mathbb{1}_{[(t_i-1)/n, (t_{i+1}-1)/n)} \in \mathcal{S}(\mathcal{N}(\omega))_{\lambda/3}^{\boldsymbol{m}}$$

and g fulfills 1. - 3. . Thus, (A.36) follows. □

For $\epsilon_n := ma_k 2\sigma\left(q_n(\alpha) + \sqrt{2\ln(e/\lambda)}\right) / \sqrt{n\lambda}$ it follows from the definition of $\mathcal{S}(\mathcal{N}(\omega))_{\lambda/3}^{\boldsymbol{m}}$ that

$$\sup_{g \in \mathcal{S}(\mathcal{N}(\omega))_{\lambda/3}^{\boldsymbol{m}}} \min_{f \in \mathcal{S}(\mathfrak{N})_{\lambda/3}^{\boldsymbol{m}}} \|g - f\omega\|_\infty \leq \epsilon_n. \tag{A.40}$$

Further, let $(y_n)_{n \in \mathbb{N}}$ be a fixed sequence in $\mathbb{R}$, and denote $y^n := (y_1, \ldots, y_n)$. Let $\epsilon > 0$, and

$g, g' \in \mathcal{M}_\lambda$ be such that $\sup_{x\in[0,1)} |g(x) - g'(x)| \le \epsilon$. Then by the reverse triangle inequality

$$\begin{aligned}\left|T_n(y^n, g) - T_n(y^n, g')\right| &\le \max_{\substack{1\le i\le j\le n\\ j-i+1\ge n\lambda}} \left| \frac{\left|\sum_{l=i}^{j} y_l - g(x_l)\right| - \left|\sum_{l=i}^{j} y_l - g'(x_l)\right|}{\sigma\sqrt{j-i+1}} \right| \\ &\le \max_{\substack{1\le i\le j\le n\\ j-i+1\ge n\lambda}} \frac{\left|\sum_{l=i}^{j} g(x_l) - g'(x_l)\right|}{\sigma\sqrt{j-i+1}} \le \frac{\sqrt{n\lambda}}{\sigma}\epsilon.\end{aligned}$$

This implies that conditioned on $\{\omega \in C_{1-\alpha}(Y)\}$ and $\{T_n(Y, \boldsymbol{g}) \le q_n(\alpha)\}$

$$\begin{aligned}\inf_{\omega\in\Omega_{\boldsymbol{m}}} \mathbf{P}\left(\min_{f\in\mathcal{S}(\mathfrak{U})^{\boldsymbol{m}}_{\lambda/3}} T_n(Y, f\omega) \le c_3 q_n(\alpha) + c_4 \right) &= \inf_{\omega\in\Omega_{\boldsymbol{m}}} \mathbf{P}\left(\min_{f\in\mathcal{S}(\mathfrak{U})^{\boldsymbol{m}}_{\lambda/3}} T_n(Y, f\omega) \le q_n(\alpha) + \frac{\sqrt{n\lambda/3}}{\sigma}\epsilon_n \right) \\ &\ge \inf_{\omega\in\Omega_{\boldsymbol{m}}} \mathbf{P}\left(\inf_{g\in\mathcal{S}(\mathcal{N}(\omega))^{\boldsymbol{m}}_{\lambda/3}} T_n(Y, g) \le q_n(\alpha) \right) = 1,\end{aligned}$$

where the inequality results from

$$\begin{aligned}\min_{f\in\mathcal{S}(\mathfrak{U})^{\boldsymbol{m}}_{\lambda/3}} T_n(Y, f\omega) &= \inf_{g\in\mathcal{S}(\mathcal{N}(\omega))^{\boldsymbol{m}}_{\lambda/3}} T_n(Y, g) + \left(\min_{f\in\mathcal{S}(\mathfrak{U})^{\boldsymbol{m}}_{\lambda/3}} T_n(Y, f\omega) - \inf_{g\in\mathcal{S}(\mathcal{N}(\omega))^{\boldsymbol{m}}_{\lambda/3}} T_n(Y, g) \right) \\ &\le \inf_{g\in\mathcal{S}(\mathcal{N}(\omega))^{\boldsymbol{m}}_{\lambda/3}} T_n(Y, g) + \sup_{g\in\mathcal{S}(\mathcal{N}(\omega))^{\boldsymbol{m}}_{\lambda/3}} \min_{f\in\mathcal{S}(\mathfrak{U})^{\boldsymbol{m}}_{\lambda/3}} \left| T_n(Y, f\omega) - T_n(Y, g) \right|.\end{aligned}$$

□

Proof of Theorem 3.4.2. A slight modification of (Sieling, 2013, Corollary 4) gives for all $n \in \mathbb{N}$ and $q > C$, for some universal constant $C < \infty$, that

$$\mathbf{P}(T_n > q) \le \exp(-q^2/8), \tag{A.41}$$

which implies

$$q_n(\alpha) \le \sqrt{-8\ln(\alpha)}. \tag{A.42}$$

Thus, for α_n as in (1.25) it follows that

$$q_n(\alpha_n) \le \frac{\delta}{17\boldsymbol{m}a_k\sigma}\ln(n) \tag{A.43}$$

and hence, it follows from (3.14) that for β_n as in (1.25) and $n > N^\star$

$$q_n(\beta_n) \le \frac{\delta}{9\sigma}\ln(n). \tag{A.44}$$

Let

$$\mathcal{I} := \{[x_i, x_j] : 1 \le i \le j \le n \text{ and } j - i + 1 \ge n\lambda/9\}$$

and $\mathfrak{B} := \{B(I) = B(i, j) \ : \ I = [x_i, x_j] \in \mathcal{I}\}$ as in (1.18) with $q = q_n(\beta_n)$. Define $\|B(I)\| := \overline{b} - \underline{b}$

with $B(I) = [\underline{b}, \overline{b}]$ and $q_n \coloneqq q_n(\beta_n)$. Furthermore, let $\mathfrak{B}_{\text{nc}}$ be as in (3.6). Define

$$\epsilon_n \coloneqq \frac{4/9\ \delta + 4\sigma\sqrt{2\ln(9e/\lambda)}}{\sqrt{\lambda/9}} \frac{\ln(n)}{\sqrt{n}} \tag{A.45}$$

and

$$\begin{aligned} A_n \coloneqq &\left\{ \max_j |\hat{\tau}_j - \tau_j| \leq 2\frac{\ln(n)^2}{n} \right\} \cap \left\{ K(\hat{g}) = K(\boldsymbol{g}) \right\} \\ &\cap \left\{ \max_j \max_i \left| \hat{f}^i|_{[\hat{\tau}_j, \hat{\tau}_{j+1})} - \boldsymbol{f}^i|_{[\tau_j, \tau_{j+1})} \right| = 0 \right\} \cap \left\{ \max_i |\hat{\omega}_i - \boldsymbol{\omega}_i| < 2\epsilon_n \right\}. \end{aligned}$$

First, we show that for all $n > N^\star$

$$\mathbf{P}\left(A_n |\ T_n(Y, \boldsymbol{g}) \leq q_n(\alpha_n)\right) = 1. \tag{A.46}$$

Note that conditioned on $\{T_n(Y, \boldsymbol{g}) \leq q_n(\alpha_n)\}$ it follows from (1.13) that $\boldsymbol{\omega} \in C_{1-\alpha_n}$ and thus, by (1.23) it follows that[2]

$$AS\, B(\hat{\omega}) \geq \delta. \tag{A.47}$$

Further, note that conditioned on $\{T_n(Y, \boldsymbol{g}) \leq q_n(\alpha_n)\}$ it follows from Theorem 3.2.1 that

$$\inf_{f \in \mathcal{S}(\mathfrak{U})^{\boldsymbol{m}}_{\lambda/3}} T_n(Y, f\hat{\omega}) \leq q_n(\beta_n).$$

Fix some $f \in \mathcal{S}(\mathfrak{U})^{\boldsymbol{m}}_{\lambda/3}$ such that

$$T_n(Y, f\hat{\omega}) \leq q_n(\beta_n) \tag{A.48}$$

and consider a c.p. of f. Let I_1 and I_2 be intervals of length $\lambda/3$ left and right of this c.p. (note that f is constant on I_1 and I_2 as it has minimal scale $\lambda/3$). Then it follows from (A.44) that for all $n > N^\star$ (see (3.14) and (3.15))

$$\|B(I_1)\| + \|B(I_2)\| = 4\frac{q_n(\beta_n) + \sqrt{2\ln(9e/\lambda)}}{\sqrt{n\lambda/9}/\sigma} < \delta.$$

By (A.47) $f\hat{\omega}$ has minimal jump size δ, in particular, $\left|f|_{I_1} - f|_{I_2}\right| \geq \delta$. Further, by (A.48) $f\hat{\omega}|_{I_1} \in B(I_1)$ and $f\hat{\omega}|_{I_2} \in B(I_2)$. Thus, it follows that $B(I_1)$ and $B(I_2)$ do not intersect and hence, a function g which fulfills $T_n(Y, g) \leq q_n(\beta_n)$ has at least one jump in a $\lambda/9$ neighborhood of a jump of $f\hat{\omega}$. In particular, $\hat{f}$ has at least one jump in a $\lambda/9$ neighborhood of a jump of $f\hat{\omega}$. Moreover, as $\hat{f}$ (and thus also $\hat{g} = \hat{f}\hat{\omega}$) is chosen to have minimal number of jumps (see (1.27)), it follows that $\hat{f}$ (and $\hat{g}$) has exactly one jump in a $\lambda/9$ neighborhood of a jump of $f\hat{\omega}$ and no jumps outside of a $\lambda/9$ neighborhood of a jump of $f\hat{\omega}$. As f (and $f\hat{\omega}$) has minimal scale $\lambda/3$ it follows that $\hat{g} = \hat{f}\hat{\omega}$ has minimal scale $\lambda/9$.[3]

[2] The specific form of $\hat{\omega}$ in (1.23) is irrelevant for (A.47) to hold. One may as well use (1.24), as long as $\hat{\omega}$ is an element of the parameter space $\Omega^\circ_{\boldsymbol{m}}$, which yields Corollary 3.4.3. This should have been stated more clearly in (Behr et al., 2017, Theorem 2.7. and Corollary 2.8.).

[3] In the original version in (Behr et al., 2017) it was falsely stated that $\hat{f}$ has minimal jump size λ instead $\lambda/9$. This additional $1/9$ factor propagates to the constants c_1, c_2 and $N^\star$ in (3.13), (3.14), and (3.15).

Now let $d_n := \ln^2(n)/n$ and define the partition $\mathcal{I} = \mathcal{I}_1 \cup \mathcal{I}_2 \cup \mathcal{I}_3$ as follows.

$$\begin{aligned}
\mathcal{I}_1 &:= \{I \in \mathcal{I} : \ I \text{ contains more than two c.p.'s of } \boldsymbol{g}\},\\
\mathcal{I}_2 &:= \{I \in \mathcal{I} : \boldsymbol{g}|_I = \boldsymbol{g}_1^I \mathbb{1}_{I_1} + \boldsymbol{g}_2^I \mathbb{1}_{I_2} + \boldsymbol{g}_3^I \mathbb{1}_{I_3}, \text{ with } |I_1| \geq |I_2| \geq |I_3|,\\
&\quad |I_2| \leq d_n, \text{ and } \boldsymbol{g}_1^I, \boldsymbol{g}_2^I, \boldsymbol{g}_3^I \in \operatorname{imag}(\boldsymbol{g}) \text{ pairwise different}\}\\
\mathcal{I}_3 &:= \{I \in \mathcal{I} : \boldsymbol{g}|_I = \boldsymbol{g}_1^I \mathbb{1}_{I_1} + \boldsymbol{g}_2^I \mathbb{1}_{I_2} + \boldsymbol{g}_3^I \mathbb{1}_{I_3}, \text{ with } |I_1| \geq |I_2| \geq |I_3|,\\
&\quad |I_2| > d_n, \text{ and } \boldsymbol{g}_1^I, \boldsymbol{g}_2^I, \boldsymbol{g}_3^I \in \operatorname{imag}(\boldsymbol{g}) \text{ pairwise different}\}.
\end{aligned}$$

$\mathcal{I}_2$ contains all intervals of minimal scale $\lambda/9$ which are dominated by a single constant segment of $\boldsymbol{g}$. $\mathcal{I}_1$ contains all intervals where $\boldsymbol{g}$ has at least two constant segments each of minimal scale λ. $\mathcal{I}_3$ contains intervals, where $\boldsymbol{g}$ has at least two (sufficiently long) constant segments, with one of them having at least length $\lambda/9 - 2d_n$ and the other one having at least length d_n.

Define

$$\begin{aligned}
E_1 &:= \bigcap_{I \in \mathcal{I}_1 \cup \mathcal{I}_3} \{B(I) \in \mathfrak{B}_{\text{nc}}\},\\
E_2 &:= \bigcap_{I \in \mathcal{I}_2} \left\{B(I) \subset [\boldsymbol{g}_1^I - \epsilon_n, \boldsymbol{g}_1^I + \epsilon_n]\right\},\\
E_3 &:= \left\{K(\hat{g}) = K(\boldsymbol{g})\right\} \cap \left\{\max_j |\hat{\tau}_j - \tau_j| \leq 2d_n\right\} \cap \left\{\max_j \left|\hat{g}(\hat{\tau}_j) - \boldsymbol{g}(\tau_j)\right| < 2\epsilon_n\right\}.
\end{aligned}$$

First, we show that

$$E_1 \cap E_2 \subset E_3. \tag{A.49}$$

To this end, consider Figure A.1. If $B(I) \in \mathfrak{B}_{\text{nc}}$, then $\hat{g}$ is not constant on I. Therefore, it follows from E_1 and the fact that $\hat{g}$ has minimal scale $\lambda/9$ that $\hat{g}$ is constant only on intervals $I \in \mathcal{I}_2$. Conversely, if $\hat{g}$ is constant on $I \in \mathcal{I}_2$ then $\hat{g}|_I \in B(I)$ (see orange bars in Figure A.1) as $T_n(Y, \hat{g}) \leq q_n(\beta_n)$. Now, consider a c.p. of $\hat{g}$. Let $I, I' \in \mathcal{I}_2$ be the constant parts of $\hat{g}$ left and right of this c.p. and I_1, I_1' be those sub-intervals which contain the largest constant piece of $\boldsymbol{g}$ (see green lines in Figure A.1), with $\boldsymbol{g}|_{I_1} \equiv \boldsymbol{g}_1^I$ and $\boldsymbol{g}|_{I_1'} \equiv \boldsymbol{g}_1^{I'}$. As $\epsilon_n < \delta/4$ for all $n > N^\star$ (see (3.15)) and $\hat{g}$ has minimal jump size δ, E_2 implies that $[\boldsymbol{g}_1^I - \epsilon_n, \boldsymbol{g}_1^I + \epsilon_n] \cap [\boldsymbol{g}_1^{I'} - \epsilon_n, \boldsymbol{g}_1^{I'} + \epsilon_n] = \emptyset$ and thus, $\left|\boldsymbol{g}_1^I - \boldsymbol{g}_1^{I'}\right| > 0$ (see the vertical distance between the left and the right green line in Figure A.1). Consequently, $\boldsymbol{g}$ has at least one jump in a $2d_n$-neighborhood of a jump of $\hat{g}$. Conversely, as $2d_n < \lambda$ for all $n > N^\star$ (see (3.15)) $\boldsymbol{g}$ has at most one jump in a $2d_n$-neighborhood of a jump of $\hat{g}$. Consequently, (A.49) follows.

For all $n > N^\star$ (see (3.15)) $2\epsilon_n < \delta/(2ma_k)$. Thus, if $\hat{f}$ was separable and thus, $(\hat{\omega}, \hat{f})$ δ-separable as in Definition 2.2.1, Theorem 2.2.3 implies

$$E_3 \subset A_n. \tag{A.50}$$

$\hat{f}$ is not separable, in general. However, by Theorem 3.2.1, it follows that there exists a separable $f \in \mathcal{H}(\beta_n)$ as in (1.29) with minimal scale $\lambda/3 > \lambda/9$. As we have not used the particular

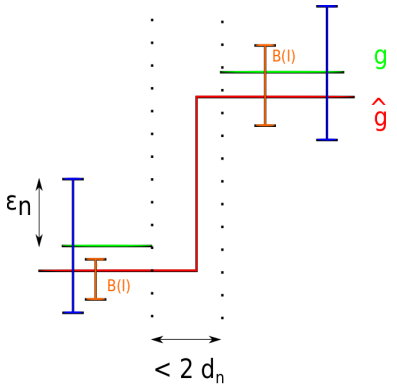

Figure A.1: The key argument underlying $E_1 \cap E_2 \subset E_3$.

choice of $\hat{f}$ in (1.28) it follows that $E_3 \subset \left\{ \max_i |\hat{\omega}_i - \omega_i| < 2\epsilon_n \right\}$. Moreover, it follows from the proof of Theorem 2.2.3 that for the second assertion of the theorem (if the first assertion holds) separability is not needed. Thus (A.50) follows for the SLAM estimates $\hat{\omega}$ and $\hat{f}$.
(A.49) and (A.50) imply that for all $n > N^\star$

$$\mathbf{P}\left(A_n |\, T_n(Y, \boldsymbol{g}) \leq q_n(\alpha_n)\right) \geq \mathbf{P}\left(E_1 \cap E_2 |\, T_n(Y, \boldsymbol{g}) \leq q_n(\alpha_n)\right).$$

First, consider E_1 conditioned on $\{T_n(Y, \boldsymbol{g}) \leq q_n(\alpha_n)\}$. Every interval $I \in \mathcal{I}_1$ includes a sub-interval I', which is the union of two constant pieces of $\boldsymbol{g}$. As $2d_n < \lambda$ for all $n > N^\star$ (see (3.15)), $I' \in \mathcal{I}_3$ and $E_1 \supseteq \bigcap_{I \in \mathcal{I}_3} \{B(I) \in \mathfrak{B}_{\mathrm{nc}}\}$. Moreover, for $I \in \mathcal{I}_3$ with $I = I_1 \cup I_2 \cup I_3$ as in the definition of $\mathcal{I}_3$, conditioned on $\{T_n(Y, \boldsymbol{g}) \leq q_n(\alpha_n)\}$ (recall that $q_n(\alpha_n) < q_n(\beta_n)$) it follows that $\boldsymbol{g}|_{I_1} \in B(I_1)$ and $\boldsymbol{g}|_{I_2} \in B(I_2)$ with $\left|\boldsymbol{g}|_{I_1} - \boldsymbol{g}|_{I_2}\right| \geq \delta$. Thus, if $\delta > \|B(I_1)\| + \|B(I_2)\|$ it follows that $B(I_1) \cap B(I_2) = \emptyset$ and hence, $I \in \mathfrak{B}_{\mathrm{nc}}$. In particular,

$$E_1 \supseteq \bigcap_{I \in \mathcal{I}_3} \{\delta > \|B(I_1)\| + \|B(I_2)\|\}.$$

By the definition of $\mathcal{I}_3$ it follows that $|I_1| \geq \lambda/9 - d_n > d_n$ for all $n > N^\star$ (see(3.15)) and $|I_2| > d_n$. Hence, (1.18) implies

$$\|B(I_1)\| + \|B(I_2)\| \leq 4\left(\frac{q_n + \sqrt{2\ln(e/d_n)}}{\sqrt{nd_n}/\sigma}\right) = \frac{4\sigma\left(q_n + \sqrt{2\ln(e/d_n)}\right)}{\ln(n)}.$$

In summary, we obtain conditioned on $\{T_n(Y, \boldsymbol{g}) \leq q_n(\alpha_n)\}$ for all $n > N^\star$

$$\begin{aligned} E_1 &\supseteq \left\{\delta > \frac{4\sigma\left(q_n + \sqrt{2\ln(e/d_n)}\right)}{\ln(n)}\right\} \\ &= \left\{q_n < \frac{\delta \ln(n)}{4\sigma} - \sqrt{2\ln(e/d_n)}\right\} \supseteq \left\{q_n \leq \frac{\delta}{8\sigma}\ln(n)\right\}, \end{aligned} \tag{A.51}$$

where the second inclusion results from (3.14). In particular, (A.51) and (A.44) yield that $\mathbf{P}(E_1 | T_n(Y, \boldsymbol{g}) \leq q_n(\alpha_n)) = 1$ for all $n > N^\star$.

Second, consider E_2 conditioned on $\{T_n(Y, \boldsymbol{g}) \leq q_n(\alpha_n)\}$. By (A.44), (A.45), and (3.13) it holds for all $I = [x_i, x_j] \in \mathcal{I}$ that

$$\|B(I)\| = 2\sigma \frac{q_n + \sqrt{2\ln(\frac{en}{j-i+1})}}{\sqrt{j-i+1}} \leq 2\sigma \frac{\frac{\delta}{9\sigma}\ln(n) + \sqrt{2\ln(\frac{9e}{\lambda})}}{\sqrt{n\lambda/9}} \leq \epsilon_n/2$$

and as $\bar{\boldsymbol{g}}_I := \sum_{l \in I} \boldsymbol{g}(x_l)/(n\,|I|) \in B(I)$,

$$E_2 \supseteq \bigcap_{I \in \mathcal{I}_2} \{|\bar{\boldsymbol{g}}_I - \boldsymbol{g}_1^I| \leq \epsilon_n - \|B(I)\|\} \supseteq \bigcap_{I \in \mathcal{I}_2} \{|\bar{\boldsymbol{g}}_I - \boldsymbol{g}_1^I| \leq \epsilon_n/2\}.$$

Moreover, for $I \in \mathcal{I}_2$

$$\left|\bar{\boldsymbol{g}}_I - \boldsymbol{g}_1^I\right| = \left|(\boldsymbol{g}_2^I - \boldsymbol{g}_1^I)\frac{|I_2|}{|I|} + (\boldsymbol{g}_3^I - \boldsymbol{g}_1^I)\frac{|I_3|}{|I|}\right| \leq \frac{|I_2| + |I_3|}{|I|} a_k \leq \frac{2d_n}{\lambda/9} a_k. \tag{A.52}$$

Summarizing, conditioned on $\{T_n(Y, \boldsymbol{g}) \leq q_n(\alpha_n)\}$

$$E_2 \supseteq \left\{\frac{2d_n}{\lambda/9} a_k \leq \epsilon_n/2\right\} = \left\{\frac{\sqrt{\lambda n}}{\ln(n)} \geq \frac{36 a_k}{4/3\delta + 12\sigma\sqrt{2\ln(9e/\lambda)}}\right\}. \tag{A.53}$$

(3.15) implies that the right hand side of (A.53) holds for all $n \geq N^\star$ and, in particular, that $\mathbf{P}(E_2 | T_n(Y, \boldsymbol{g}) \leq q_n(\alpha_n)) = 1$ for all $n \geq N^\star$. Together with (A.51), this gives that $\mathbf{P}(E_1 \cap E_2 | T_n(Y, \boldsymbol{g}) \leq q_n(\alpha_n)) = 1$ for all $n > N^\star$. This shows (A.46) and thus,

$$\mathbf{P}(A_n) \geq \mathbf{P}(A_n |\, T_n(Y, \boldsymbol{g}) \leq q_n(\alpha_n))\, \mathbf{P}(T_n(Y, \boldsymbol{g}) \leq q_n(\alpha_n)) = \mathbf{P}(T_n(Y, \boldsymbol{g}) \leq q_n(\alpha_n)) \geq 1 - \alpha_n.$$

Finally, remember that the identifiability condition $AS\,B(\boldsymbol{\omega}) \geq \delta > 0$ implies that $\boldsymbol{g}$ jumps if and only if $\boldsymbol{f}$ jumps. Hence, when $\boldsymbol{f}^i$ and $\hat{f}^i$ take the same function values on constant pieces, results about c.p.'s of $\boldsymbol{g}$ directly translate to results about c.p.'s of $\boldsymbol{f}^1, \ldots, \boldsymbol{f}^m$.

□

Proof of Theorem 3.3.1. It follows from the proof of Theorem 3.4.2 that conditioned on $\{T_n(Y, \boldsymbol{g}) \leq q_n(\alpha_n)\}$ for all $n \geq N^\star$ as in (3.14) and (3.15)

$$\max_{e \in \mathrm{imag}(\boldsymbol{f})} |e\boldsymbol{\omega} - e\hat{\omega}| \leq c_2 \frac{\ln(n)}{\sqrt{n}} \quad \text{and} \quad K(\hat{\omega}^\top \boldsymbol{f}) = K(\hat{g}). \tag{A.54}$$

Let $B(i, j) = [\underline{b}_{ij}, \overline{b}_{ij}]$ be as in (1.18) with $q = q_n(\beta)$ as in (1.19) and

$$\tilde{B}(i, j) := \left[\underline{b}_{ij} - c_2 \frac{\ln(n)}{\sqrt{n}}, \overline{b}_{ij} + c_2 \frac{\ln(n)}{\sqrt{n}}\right].$$

Then, it follows from (A.54) that

$$\begin{aligned}\mathbf{P}\left(\boldsymbol{f} = (\boldsymbol{f}^1, ..., \boldsymbol{f}^{\boldsymbol{m}})^\top \in \tilde{\mathcal{H}}(\beta)\right) &= \mathbf{P}\left(\bigcap_{\substack{1\le i\le j\le n \\ (\boldsymbol{f}\hat{\omega})|_{[i,j]}\equiv(\boldsymbol{f}\hat{\omega})_{ij}}} (\boldsymbol{f}\hat{\omega})_{ij} \in \tilde{B}(i,j) \text{ and } K(\boldsymbol{f}\hat{\omega}) = K(\hat{g})\right) \\ &\ge \mathbf{P}\left(\bigcap_{\substack{1\le i\le j\le n \\ \boldsymbol{g}|_{[ij]}\equiv \boldsymbol{g}_{ij}}} \boldsymbol{g}_{ij} \in B(i,j) \text{ and } T_n(Y,\boldsymbol{g}) \le q_n(\alpha_n)\right) \\ &= \mathbf{P}\left(T_n(Y,\boldsymbol{g}) \le \min(q_n(\beta), q_n(\alpha_n))\right).\end{aligned}$$

Finally, the assertion follows from $\lim_{n\to\infty} \min(q_n(\beta), q_n(\alpha_n)) = q_n(\beta)$ for every fixed $\beta \in (0,1)$. □

A.2.1 Proofs of Section 3.6

For the proof of Theorem 3.6.6 we require the following auxiliary result, which is a direct consequence of Theorem 2.2.5.

Corollary A.2.2. *If $g, \tilde{g} \in \mathcal{M}^{\delta,\lambda}$ and $\mathfrak{m}(g) \neq \mathfrak{m}(\tilde{g})$, then there exists an interval I with $|I| > \lambda/2$ such that g and $\tilde{g}$ are both constant on I and $|g(x) - \tilde{g}(x)| > \delta^{3/2}/(\sqrt{3}a_k)$ for $x \in I$.*

Proof of Theorem 3.6.6. With the notation $\Omega_0^\delta := \mathcal{M}_0^\delta := \emptyset$ (3.20) implies

$$\begin{aligned}\{\hat{m}(q) < \boldsymbol{m}\} \cap \{T_n(Y,\boldsymbol{g}) \le q\} &= \bigcup_{\tilde{m}<\boldsymbol{m}} \bigcup_{\omega\in\Omega_{\tilde{m}}^\delta} \left\{\omega \in C_q^{\tilde{m}}\right\} \cap \{T_n(Y,\boldsymbol{g}) \le q\} \\ &\subset \left\{\inf_{g\in\bigcup_{\tilde{m}<\boldsymbol{m}} \mathcal{M}_{\tilde{m}}^{\delta,\lambda/3}} T_n(Y,g) \le c_3 q + c_4\right\}\end{aligned}$$

and together with (3.23) this gives

$$\{\hat{m}(q) \neq \boldsymbol{m}\} \subset \{T_n(Y,\boldsymbol{g}) > q\} \cup \left\{\inf_{g\in\bigcup_{\tilde{m}<\boldsymbol{m}} \mathcal{M}_{\tilde{m}}^{\delta,\lambda/3}} T_n(Y,g) \le c_3 q + c_4\right\}. \tag{A.55}$$

Consequently,

$$\mathbf{P}(\hat{m}(q) \neq \boldsymbol{m}) \le \alpha_n(q) + \mathbf{P}\left(\inf_{g\in\bigcup_{\tilde{m}<\boldsymbol{m}} \mathcal{M}_{\tilde{m}}^{\delta,\lambda/3}} T_n(Y,g) \le c_3 q + c_4\right). \tag{A.56}$$

Thus, it remains to show that the second probability on the r.h.s. of (A.56) is bounded from above by $\beta_n(q)$. Let $\tilde{I}_1 := [x_1, x_{n\lambda/12})$ and $\tilde{I}_i := [x_{(i-1)n\lambda/12}, x_{in\lambda/12})$ for $i = 2, \dots, \lfloor 12/\lambda \rfloor$ and

$$I := \left\{\tilde{I}_i : \ \boldsymbol{g} \text{ is constant on } \tilde{I}_i \text{ for } i = 1, \dots, \lfloor 12/\lambda \rfloor\right\} := \{I_1, \dots, I_r\}$$

with $r \le 12/\lambda$, and let $\mathfrak{g}_i := \boldsymbol{g}(x)$ for $x \in I_i$. Note that for $\boldsymbol{g}, g \in \mathcal{M}^{\delta,\lambda/3}$, by Corollary A.2.2, there exists an interval $I \subset [0,1)$ with $|I| = \lambda/6$ such that $\boldsymbol{g}$ and g are both constant on I with

$|g(x) - \boldsymbol{g}(x)| \geq \delta^{3/2}/(\sqrt{3}a_k)$ for $x \in I$ and for each such I there exists an $i \in \{1, \ldots, 12/\lambda\}$ such that $\tilde{I}_i \subset I$. Hence, with the events

$$A_i := \left\{ \exists c_i \notin \left[\mathfrak{g}_i \pm \frac{\delta^{3/2}}{\sqrt{3}a_k} \right] \ : \ \left| \sqrt{n\,|I_i|}\, \overline{Y}_{I_i} - \sqrt{n\,|I_i|}\, c_i \right| \leq \sigma\,(q + pen\,(n\,|I_i|)) \right\}$$

it follows from the definition of the multiscale statistic $T_n(Y, g)$ in (1.16) that

$$\mathbf{P}\left(\inf_{g \in \bigcup_{\tilde{m} < \boldsymbol{m}} \mathcal{M}_{\tilde{m}}^{\delta,\lambda}} T_n(Y, g) \leq q \right) \leq \mathbf{P}\left(\bigcup_{i=1}^{r} A_i \right).$$

Let

$$X_i := \frac{1}{\sigma\sqrt{n|I_i|}} \sum_{x_j \in I_i} \epsilon_j \sim \mathcal{N}(0, 1), \tag{A.57}$$

then for

$$d = d(\lambda, \delta, a_k, \sigma) := \frac{\sqrt{\lambda/12n}\delta^{3/2}}{\sqrt{3}a_k\sigma}$$

it holds that

$$\begin{aligned}
\mathbf{P}(A_i) &= \mathbf{P}\left(\exists c_i \notin [\pm d] \ : \ |X_i - c_i| \leq q + \sqrt{2\ln(12e/\lambda)} \right) \\
&\leq \mathbf{P}\left(\exists c_i \notin [\pm d] \ : \ |X_i - c_i| \leq q + \sqrt{2\ln(12e/\lambda)} \bigcap X_i \in [-d, 0] \right) \\
&+ \mathbf{P}\left(\exists c_i \notin [\pm d] \ : \ |X_i - c_i| \leq q + \sqrt{2\ln(12e/\lambda)} \bigcap X_i \in (0, d] \right) + \mathbf{P}\left(|X_i| \geq d \right).
\end{aligned}$$

Moreover,

$$\begin{aligned}
&\mathbf{P}\left(\exists c_i \notin [\pm d] \ : \ |X_i - c_i| \leq q + \sqrt{2\ln(12e/\lambda)} \bigcap X_i \in [-d, 0] \right) \\
&= \mathbf{P}\left(X_i + d \leq q + \sqrt{2\ln(12e/\lambda)} \bigcap X_i \in [-d, 0] \right) \\
&= \mathbf{P}\left(-X_i \geq d - \left(q + \sqrt{2\ln(12e/\lambda)} \right) \bigcap X_i \in [-d, 0] \right) \\
&= \mathbf{P}\left(|X_i| \geq d - \left(q + \sqrt{2\ln(12e/\lambda)} \right) \bigcap X_i \in [-d, 0] \right)
\end{aligned}$$

and analogously

$$\begin{aligned}
&\mathbf{P}\left(\exists c \notin [\pm d] \ : \ |X_i - c| \leq q + \sqrt{2\ln(12e/\lambda)} \bigcap X_i \in (0, d] \right) \\
&= \mathbf{P}\left(|X_i| \geq d - \left(q + \sqrt{2\ln(12e/\lambda)} \right) \bigcap X_i \in (0, d] \right).
\end{aligned}$$

It follows from the above equations and the subgaussian tail estimate, see e.g., (Wainwright, 2017, equation (2.9)), that

$$\begin{aligned}
\mathbf{P}(A_i) &\leq \mathbf{P}\left(|X_i| \geq d - \left(q + \sqrt{2\ln(12e/\lambda)} \right) \bigcap |X_i| \leq d \right) + \mathbf{P}\left(|X_i| \geq d \right) \\
&\leq 2\mathbf{P}\left(|X_i| \geq d - \left(q + \sqrt{2\ln(12e/\lambda)} \right) \right) \leq 4\exp(-\gamma_n(q)n)
\end{aligned}$$

with $\gamma_n(q) := \left(\frac{\sqrt{\lambda/12}\delta^{3/2}}{\sqrt{6}a_k\sigma} - \frac{q + \sqrt{2\ln(12e/\lambda)}}{\sqrt{2n}} \right)_+^2$. As the intervals $I_1, \ldots, I_r$ are disjoint and $r \leq 12/\lambda$,

it follows that

$$\mathbf{P}\left(\inf_{g\in\bigcup_{\tilde{m}<\boldsymbol{m}}\mathcal{M}_{\tilde{m}}^{\delta,\lambda}} T_n(Y,g)\leq q\right)\leq 1-\left(1-4\exp(-\gamma_n(q)n)\right)^{12/\lambda}. \tag{A.58}$$

Replacing q in (A.58) by c_3q+c_4 yields

$$\mathbf{P}\left(\inf_{g\in\bigcup_{\tilde{m}<\boldsymbol{m}}\mathcal{M}_{\tilde{m}}^{\delta,\lambda}} T_n(Y,\tilde{g})\leq q'\right)\leq \beta_n(q)$$

and finishes the proof. □

Proof of Theorem 3.6.7. It follows from Theorem 2.3.10 that $\boldsymbol{m}\leq\sqrt{1/\delta}$ and hence, $c_3/\sqrt{2}\leq\sqrt{8}a_k/\sqrt{3\delta}$. Thus, $\beta_n(q)\searrow 0$ as $n\nearrow\infty$ and $\limsup q_n/\sqrt{n}\leq\sqrt{\lambda}\delta^2/(24\sqrt{2}a_k^2\sigma)$ for $n\to\infty$. Moreover, as the statistic $T_n:=T_n(\epsilon,0)\geq T_n(Y,\boldsymbol{g})$ is known to converge to a certain functional of the Brownian motion $T_n\overset{\mathcal{D}}{\Rightarrow}L(\mathbb{B})<\infty$ a.s. (see (Dümbgen and Spokoiny, 2001)) it follows that $\alpha_n(q)\searrow 0$ for $q\nearrow\infty$. Hence, Theorem 3.6.6 directly yields Theorem 3.6.7. □

Proof of Theorem 3.6.9. It follows from Theorem 2.3.10 that $\boldsymbol{m}\leq\sqrt{1/\delta}$ and hence, for q_n as in Definition 3.6.8

$$q_n=c\sqrt{n}=\frac{\sqrt{\lambda}\delta^2}{24\sqrt{2}a_k^2\sigma}\sqrt{n}\leq\frac{\sqrt{\lambda}\delta^{3/2}}{24\sqrt{2}a_k^2\boldsymbol{m}\sigma}\sqrt{n}.$$

Further, note that for $q=q_n$ the exponential term in the definition of $\beta_n(q)$ in Theorem 3.6.6 gets smaller than 1 for n large enough. Thus, we can apply binomial inequality to obtain that for $q=q_n$ and n large enough

$$\begin{aligned}1-\beta_n(q_n)&\geq 1-\frac{48}{\lambda}\exp\left(-\left(\frac{\sqrt{\lambda}\delta^{3/2}}{\sqrt{72}a_k\sigma}\sqrt{n}-2\boldsymbol{m}a_kq_n-3\boldsymbol{m}a_k\sqrt{\ln(12/\lambda)}\right)^2\right)\\&\geq 1-4\left(\frac{12}{\lambda}\right)^{10\boldsymbol{m}^2a_k^2}\exp\left(-\frac{\lambda\delta^3}{288a_k^2\sigma^2}n\right)\geq 1-4\left(\frac{12}{\lambda}\right)^{10\boldsymbol{m}^2a_k^2}\exp\left(-4c^2n\right)\end{aligned}$$

and with the deviation inequality (Sieling, 2013, Theorem 37) it follows for $\alpha_n(q)$ as in Theorem 3.6.6 that $\alpha_n(q_n)\leq\exp\left(-c^2n/8\right)$. Thus, Theorem 3.6.6 yields

$$\mathbf{P}\left(\hat{m}(q_n)=\boldsymbol{m}\right)\geq 1-\exp\left(-c^2n/8\right)+O\left(\exp\left(-4c^2n\right)\right).$$

□

A.3 Proofs of Chapter 4

Proof of Theorem 4.1.1. The proof of Theorem 4.1.1 is divided into two steps, corresponding to the two different estimation errors of $\hat{\Pi}$ and $\hat{\omega}$, respectively. We start with the first term on the r.h.s. of the assertion which corresponds to the estimation error of $\hat{\omega}$. The idea is to construct a hyperrectangle of maximal size which is a subset of $\mathcal{N}^{\delta,\Lambda}$ and then apply results

of Donoho et al. (1990) (for fixed selection matrix Π). In the following, $\omega^\star$ will denote the center of this hyperrectangle and the matrix E will denote the perturbation (of maximal size) around $\omega^\star$. To this end, let $\omega^\star \in \Omega_{m,M}$ be such that $AS\,B(\omega^\star) = 0.2\Delta\mathfrak{A}_{\min}\sqrt{M/m}$, $WS\,B(\omega^\star) \geq 0.2\Delta\mathfrak{A}_{\min}\sqrt{M/m}$, and $\omega^\star_{mj} \geq 0.4\Delta\mathfrak{A}_{\min}/(1+ma_k)$ for $j = 1,\dots,M$ (existence follows from Lemma A.1.4 and A.1.5). For $\epsilon \in (0,1)^{(m-1)\times M}$ define

$$\omega^\epsilon := \omega^\star + \begin{pmatrix} \epsilon_{11} & \dots & \epsilon_{1M} \\ & \vdots & \\ \epsilon_{(m-1)1} & \dots & \epsilon_{(m-1)M} \\ -\sum_{i=1}^{m-1}\epsilon_{i1} & \dots & -\sum_{i=1}^{m-1}\epsilon_{iM} \end{pmatrix} = \omega^\star + E. \tag{A.59}$$

Let $\overline{\epsilon} := \max_{ij}\left|\epsilon_{ij}\right|$. If

$$\frac{0.4\Delta\mathfrak{A}_{\min}}{1+ma_k} \geq \overline{\epsilon}(m-1), \tag{A.60}$$

then all entries of ω^ϵ are non-negative and $\omega^\epsilon \in \Omega_{m,M}$. For ω^ϵ to be an element of $\Omega^\delta_{m,M}$ we further need that $WS\,B(\omega^\epsilon), AS\,B(\omega^\epsilon) \geq \delta$. To this end, note that

$$\begin{aligned}\left\|\omega^\epsilon_{i\cdot}\right\| - \left\|\omega^\epsilon_{i-1\cdot}\right\| &= \left\|\omega^\star_{i\cdot} + E_{i\cdot}\right\| - \left\|\omega^\star_{i-1\cdot} + E_{i-1\cdot}\right\| \geq \left\|\omega^\star_{i\cdot}\right\| - \left\|\omega^\star_{i-1\cdot}\right\| - \|E_{i\cdot}\| - \|E_{i-1\cdot}\| \\ &\geq \frac{2}{1+ma_k}0.2\Delta\mathfrak{A}_{\min}\sqrt{M/m} - m\sqrt{M}\overline{\epsilon}\end{aligned}$$

and thus

$$WS\,B(\omega^\epsilon) \geq 0.2\Delta\mathfrak{A}_{\min}\sqrt{M/m} - \frac{1+ma_k}{2}m\sqrt{M}\overline{\epsilon}. \tag{A.61}$$

Further, note that for $e \in \Delta\mathfrak{A}^m$ and E as in (A.59)

$$\|eE\|^2 = \sum_{j=1}^{M}\left(\sum_{i=1}^{m-1}(e_i - e_m)\epsilon_{ij}\right)^2 \leq M\left((m-1)2a_k\overline{\epsilon}\right)^2$$

and thus,

$$\begin{aligned}AS\,B(\omega^\epsilon) &= \min_{e\in\Delta\mathfrak{A}^m}\left\|e(\omega^\star + E)\right\| \geq \min_{e\in\Delta\mathfrak{A}}\left\|e\omega^\star\right\| - \|eE\| \\ &= AS\,B(\omega^\star) - \|eE\| \geq 0.2\Delta\mathfrak{A}_{\min}\sqrt{M/m} - 2(m-1)a_k\overline{\epsilon}\sqrt{M}.\end{aligned} \tag{A.62}$$

Summing up, (A.61) and (A.62) yield that $\omega^\epsilon \in \Omega^\delta_{m,M}$ if

$$\delta \leq 0.2\Delta\mathfrak{A}_{\min}\sqrt{M/m} - m^2a_k\sqrt{M}\overline{\epsilon} \tag{A.63}$$

and (A.60) holds. As $\delta \leq \Delta\mathfrak{A}_{\min}\sqrt{M/m}(45\sqrt{2})^{-1}$, (A.63) and (A.60) hold for all $\epsilon \in \mathbb{R}_+^{(m-1)\times M}$ with

$$\overline{\epsilon} \leq \frac{\Delta\mathfrak{A}_{\min}}{6m^{5/2}a_k} =: \epsilon^\star. \tag{A.64}$$

Now let $\Pi^\star$ be the selection matrix such that

$$\Pi^\star A = \begin{pmatrix} e^1 & e^2 & \dots & e^m & e^1 & e^2 & \dots \end{pmatrix}^\top,$$

where $e^r \in \mathbb{R}^m$ is the r-th unit vector in $\mathbb{R}^m$. Then, as $\Lambda \leq n/m$,

$$\Theta := \left\{ \Pi^\star A \omega^\epsilon : \epsilon \in [0, \epsilon^\star]^{m-1 \times M} \right\} \subset \mathcal{N}^{\delta,\Lambda}$$

and for $\Pi^\star A \omega^\epsilon \in \Theta$ one observes in (4.1)

$$Y_1, \dots, Y_{n/m} \overset{i.i.d.}{\sim} N(\omega^\epsilon, \sigma^2 I_{Mm \times Mm}).$$

Define

$$\tilde{\Theta} := \left\{ \omega^\epsilon : \epsilon \in [0, \epsilon^\star]^{m-1 \times M} \right\}.$$

$\tilde{\Theta}$ is almost an hyperractangle. To make it a proper hyperractangle, we have to remove the last column of the matrices in Θ, namely

$$\tilde{\Theta}' := \{ (\omega^\epsilon_{ij})_{\substack{1 \leq i \leq m-1 \\ 1 \leq j \leq M}} : \epsilon \in [0, \epsilon^\star]^{m-1 \times M} \}.$$

Note that

$$\inf_{\hat{\theta}} \sup_{\theta \in \tilde{\Theta}} E_\theta \left(\left\| \hat{\theta} - \theta \right\|_2^2 \right) \geq \inf_{\hat{\theta}} \sup_{\theta \in \tilde{\Theta}'} E_\theta \left(\left\| \hat{\theta} - \theta \right\|_2^2 \right).$$

Then it follows from (Donoho et al., 1990, (2.1), (3.4) and Proposition 3) that

$$\begin{aligned}
\inf_{\hat{\theta}} \sup_{\boldsymbol{\Pi} A \boldsymbol{\omega} \in \mathcal{N}^{\delta,\Lambda}} \mathrm{E}_{\boldsymbol{\Pi} A \boldsymbol{\omega}} \left(\left\| \hat{\theta} - \boldsymbol{\Pi} A \boldsymbol{\omega} \right\|^2 \right) &\geq \inf_{\hat{\theta}} \sup_{\boldsymbol{\Pi} A \boldsymbol{\omega} \in \Theta} \mathrm{E}_{\boldsymbol{\Pi} A \boldsymbol{\omega}} \left(\left\| \hat{\theta} - \boldsymbol{\Pi} A \boldsymbol{\omega} \right\|^2 \right) \\
&= \frac{n}{m} \inf_{\hat{\theta}} \sup_{\boldsymbol{\omega} \in \tilde{\Theta}} \mathrm{E}_{\boldsymbol{\omega}} \left(\left\| \hat{\theta} - \boldsymbol{\omega} \right\|^2 \right) \\
&\geq \frac{n}{m} \inf_{\hat{\theta}} \sup_{\boldsymbol{\omega} \in \tilde{\Theta}'} \mathrm{E}_{\boldsymbol{\omega}} \left(\left\| \hat{\theta} - \boldsymbol{\omega} \right\|^2 \right) \\
&\geq (1.25)^{-1} \frac{n}{m} M(m-1) \frac{(\epsilon^\star)^2 \sigma^2/(n/m)}{(\epsilon^\star)^2 + \sigma^2/(n/m)} \\
&\geq 0.4M \left(\frac{1}{\sigma^2(m-1)} + \frac{2}{n(\epsilon^\star)^2} \right)^{-1}.
\end{aligned}$$

Together with (A.64) this gives

$$\inf_{\hat{\theta}} \sup_{\boldsymbol{\Pi} A \boldsymbol{\omega} \in \mathcal{N}^{\delta}} \mathrm{E}_{\boldsymbol{\Pi} A \boldsymbol{\omega}} \left(\left\| \hat{\theta} - \boldsymbol{\Pi} A \boldsymbol{\omega} \right\|^2 \right) \geq 0.4M \left(\frac{1}{(m-1)\sigma^2} + \frac{72 m^5 a_k^2}{(\Delta \mathfrak{A}_{\min})^2 n} \right)^{-1}.$$

Now we show the second part of the proof which corresponds to the estimation error of $\boldsymbol{\Pi}$. The idea is to fix a suitable mixing matrix $\omega \in \Omega^\delta_{m,M}$ and thus, reduce the estimation problem to a classification problem on the finite set of possible selection matrices Π. This can be considered as a testing problem which allows to apply the Neyman-Pearson lemma. As $\delta \leq$

$\frac{0.2}{9a_k}(\Delta\mathfrak{N}_{\min})^2\sqrt{M}/m$ it follows that $9\delta\sqrt{m}a_k/\Delta\mathfrak{N}_{\min} \leq 0.2\Delta\mathfrak{N}_{\min}\sqrt{M/m}$. Thus, by Lemma A.1.4 it follows that $\Omega_{m,M}^{9\delta\sqrt{m}a_k/\Delta\mathfrak{N}_{\min}}$ is non-empty and hence, by Lemma A.1.6 there exists a quadratic mixing matrix $\omega^\delta \in \Omega_{m,m}$ such that $AS\,B(\omega^\delta) = (9\delta\sqrt{m}a_k/\Delta\mathfrak{N}_{\min})/(9\sqrt{M}a_k/\Delta\mathfrak{N}_{\min}) = \delta/\sqrt{M/m}$ and $WS\,B(\omega^\delta) \geq \delta/\sqrt{M/m}$. Hence,

$$\Theta := \{\Pi A \underbrace{(\omega^\delta, \ldots, \omega^\delta)}_{M/m\times} : \Pi\ \Lambda\text{-separable}\} \subset \mathcal{N}^{\delta,\Lambda}. \tag{A.65}$$

Then for $\Pi A\omega \in \Theta$ one observes in (4.1)

$$Y_1, \ldots, Y_{M/m} \overset{i.i.d.}{\sim} \mathcal{N}(\Pi A\omega^\delta, \sigma^2 I_{nm\times nm}). \tag{A.66}$$

For the finite parameter space $\tilde{\Theta} := \{\Pi A\omega^\delta : \Pi\ \Lambda\text{-separable}\}$ it holds that

$$\min_{\theta\neq\theta'\in\tilde{\Theta}} \left\|\theta-\theta'\right\|^2 = \min_{\theta\neq\theta'\in\tilde{\Theta}} \sum_{j=1}^{n} \left\|\theta_{j\cdot}-\theta'_{j\cdot}\right\|^2 = \min_{\substack{\theta\neq\theta'\in\tilde{\Theta}\\ \exists!\, j^\star:\theta_{j^\star}\neq\theta'_{j^\star}}} \left\|\theta_{j^\star\cdot}-\theta'_{j^\star\cdot}\right\|^2 = AS\,B(\omega^\delta)^2 = \frac{\delta^2 m}{M}.$$

Lemma A.3.1 yields for any estimator $\hat{\theta}$

$$\begin{aligned}\sup_{\Pi A\omega\in\mathcal{N}^{\delta,\Lambda}} \mathrm{E}_{\Pi A\omega}\left(\left\|\hat{\theta}-\Pi A\omega\right\|^2\right) &\geq \sup_{\theta\in\Theta} \mathrm{E}_\theta\left(\left\|\hat{\theta}-\theta\right\|^2\right)\\ &= \sup_{\theta\in\tilde{\Theta}} \frac{M}{m}\,\mathrm{E}_\theta\left(\left\|\hat{\theta}-\theta\right\|^2\right) \geq \delta^2 \sup_{\theta\in\tilde{\Theta}} \mathbf{P}_\theta\left(\hat{\theta}\neq\theta\right).\end{aligned} \tag{A.67}$$

Now let $\theta, \theta' \in \tilde{\Theta}$ be fixed such that $\|\theta-\theta'\|^2 = \frac{\delta^2 m}{M}$. Then the Neyman-Pearson lemma yields for $\bar{Y} := \sum_{i=1}^{M/m} mY_i/M$ with Y_i as in (A.66) and $Z \sim \mathcal{N}(0, m\sigma^2/MI_{nm\times nm})$ that

$$\begin{aligned}\sup_{\theta\in\tilde{\Theta}} \mathbf{P}_\theta\left(\hat{\theta}\neq\theta\right) &\geq \frac{1}{2}\left(\mathbf{P}_\theta\left(\hat{\theta}\neq\theta\right)+\mathbf{P}_{\theta'}\left(\hat{\theta}\neq\theta'\right)\right)\\ &\geq \frac{1}{2}\left(\mathbf{P}_\theta\left(\hat{\theta}\neq\theta\right)+\mathbf{P}_{\theta'}\left(\hat{\theta}=\theta\right)\right)\\ &\geq \frac{1}{2}\inf_{u\in\mathbb{R}}\left(\mathbf{P}_\theta\left(\left\|\bar{Y}-\theta\right\|^2-\left\|\bar{Y}-\theta'\right\|^2>u\right)+\mathbf{P}_{\theta'}\left(\left\|\bar{Y}-\theta\right\|^2-\left\|\bar{Y}-\theta'\right\|^2<u\right)\right)\\ &= \frac{1}{2}\inf_{u\in\mathbb{R}}\left(\mathbf{P}\left(2Z^\top(\theta'-\theta)>u+\left\|\theta-\theta'\right\|^2\right)+\mathbf{P}\left(2Z^\top(\theta'-\theta)<u-\left\|\theta-\theta'\right\|^2\right)\right)\\ &= \mathbf{P}\left(Z^\top(\theta'-\theta)>\frac{\|\theta-\theta'\|^2}{2}\right)\\ &= 1-\Psi\left(\frac{\|\theta-\theta'\|\sqrt{M}}{2\sigma\sqrt{m}}\right) = 1-\Psi\left(\frac{\delta}{2\sigma}\right) \geq \frac{\sigma}{2\delta}e^{-\frac{\delta^2}{8\sigma^2}},\end{aligned}$$

where Ψ denotes the cumulative distribution function of the standard normal and the last inequality follows from Mill's ratio and $1-4\sigma^2/\delta^2 \geq 1/2$ as $\delta \geq \sigma\sqrt{8}$. With (A.67) this gives

$$\sup_{\boldsymbol{\Pi A\omega}\in\mathcal{N}^{\delta,\Lambda}} \mathrm{E}_{\boldsymbol{\Pi A\omega}}\left(\left\|\hat{\theta}-\boldsymbol{\Pi A\omega}\right\|^2\right) \geq \delta\frac{\sigma}{2}e^{-\frac{\delta^2}{8\sigma^2}}$$

This finishes the proof. □

Proof of Theorem 4.1.3. By Theorem 2.2.3 we can write $\hat{\theta} = \hat{\Pi} A \hat{\omega}$ in a unique way. We have that for any $\mathbf{\Pi} A\boldsymbol{\omega} \in \mathcal{N}^{\delta,\Lambda}$

$$\begin{aligned} &\mathrm{E}_{\mathbf{\Pi} A\boldsymbol{\omega}}\left(\left\|\hat{\theta} - \mathbf{\Pi} A\boldsymbol{\omega}\right\|^2\right) \\ &= \mathrm{E}_{\mathbf{\Pi} A\boldsymbol{\omega}}\left(\left\|\hat{\theta} - \mathbf{\Pi} A\boldsymbol{\omega}\right\|^2 \mathbb{1}_{\{\hat{\Pi}=\mathbf{\Pi}\}}\right) + \mathrm{E}_{\mathbf{\Pi} A\boldsymbol{\omega}}\left(\left\|\hat{\theta} - \mathbf{\Pi} A\boldsymbol{\omega}\right\|^2 \mathbb{1}_{\{\hat{\Pi}\neq\mathbf{\Pi}\}}\right). \end{aligned} \tag{A.68}$$

We start with the second term. The idea is to bound it with the classification error, that is $\mathbf{P}_{\mathbf{\Pi} A\boldsymbol{\omega}}\left(\hat{\Pi} \neq \mathbf{\Pi}\right)$, and then apply exact recovery as in Theorem 2.2.3. As the entries of the $n \times M$ matrices $\hat{\theta}$ and $\mathbf{\Pi} A\boldsymbol{\omega}$ are contained in the range of the alphabet $[0, a_k]$, it follows that

$$\mathrm{E}_{\mathbf{\Pi} A\boldsymbol{\omega}}\left(\left\|\hat{\theta} - \mathbf{\Pi} A\boldsymbol{\omega}\right\|^2 \mathbb{1}_{\{\hat{\Pi}\neq\mathbf{\Pi}\}}\right) \leq a_k^2 nM \mathbf{P}_{\mathbf{\Pi} A\boldsymbol{\omega}}\left(\hat{\Pi} \neq \mathbf{\Pi}\right) = a_k^2 nM \sum_{\Pi \neq \mathbf{\Pi}} \mathbf{P}_{\mathbf{\Pi} A\boldsymbol{\omega}}\left(\hat{\Pi} = \Pi\right).$$

For a fixed Λ-separable Π and any $\omega \in \Omega^{\delta}$ it follows from Theorem 2.2.3 that $\|\mathbf{\Pi} A\boldsymbol{\omega} - \Pi A\omega\| \geq \sqrt{\Lambda}\delta/(1 + ma_k) =: c$. Further, as by separability $\operatorname{rank}(\Pi A) = m$ and $\Omega^{\delta} \subset \mathbb{R}^{m\times M}$, there exists a rotation matrix R such that for $\Theta := \{\mathbf{\Pi} A\boldsymbol{\omega} - \Pi A\omega : \ \omega \in \Omega^{\delta}_{m,M}\} \subset \mathbb{R}^{nM}$ and $\tilde{\Theta} := R\Theta$ it holds for all $\theta \in \tilde{\Theta}$ that $\theta_{mM+2} = \ldots = \theta_{nM} = 0$. This gives

$$\begin{aligned} \mathbf{P}_{\mathbf{\Pi} A\boldsymbol{\omega}}\left(\hat{\Pi} = \Pi\right) &\leq \mathbf{P}_{\mathbf{\Pi} A\boldsymbol{\omega}}\left(\|Y - \mathbf{\Pi} A\boldsymbol{\omega}\|^2 > \min_{\omega\in\Omega^{\delta}_{m,M}} \|Y - \Pi A\omega\|^2\right) \\ &= \mathbf{P}_{\mathbf{\Pi} A\boldsymbol{\omega}}\left(\|Z\|^2 > \min_{\theta\in\Theta} \|Z + \theta\|^2\right) \\ &= \mathbf{P}\left(\|Z\|^2 > \min_{\theta\in\tilde{\Theta}} \|Z + \theta\|^2\right) \\ &= \mathbf{P}\left(\max_{\theta\in\tilde{\Theta}} -2Z^{\top}\frac{\theta}{\|\theta\|\,\sigma} - \frac{\|\theta\|}{\sigma} > 0\right) \\ &\leq \mathbf{P}\left(\max_{i=1,\ldots,Mm+1}\left|\frac{Z_i}{\sigma}\right| \max_{\theta\in\tilde{\Theta}} \frac{\sum_{i=1}^{mM+1}|\theta|}{\|\theta\|} > \frac{c}{2\sigma}\right) \\ &\leq (Mm+1)\mathbf{P}\left(\left|\frac{Z_1}{\sigma}\right| \sqrt{mM+1} > \frac{c}{2\sigma}\right) \\ &= (Mm+1)\mathbf{P}\left(|\mathcal{N}(0,1)| > \frac{c}{2\sqrt{mM+1}\sigma}\right) \\ &\leq (Mm+1)\frac{2\sqrt{mM+1}\sigma}{c} e^{-\frac{c^2}{8(mM+1)\sigma^2}}, \end{aligned}$$

where we considered the noise matrix $Z \in \mathbb{R}^{n\times M}$ in (4.1) as a vector $Z \in \mathbb{R}^{nM}$ (with entries $Z_i \overset{i.i.d.}{\sim} \mathcal{N}(0,\sigma^2)$, $i = 1,\ldots,nM$) and for the last inequality we used Mill's ratio. As the number of Λ-separable selection matrices Π is bounded by nmk^m, it follows that

$$\mathbf{P}_{\mathbf{\Pi} A\boldsymbol{\omega}}\left(\hat{\Pi} \neq \mathbf{\Pi}\right) \leq 2\sigma nk^m m(1 + ma_k)\frac{(1+mM)^{3/2}}{\sqrt{\Lambda}\delta} e^{-\frac{\Lambda\delta^2}{8(mM+1)(1+ma_k)^2\sigma^2}}.$$

and

$$\mathrm{E}_{\mathbf{\Pi}A\boldsymbol{\omega}}\left(\left\|\hat{\theta}-\mathbf{\Pi}A\boldsymbol{\omega}\right\|^2 \mathbb{1}_{\{\hat{\Pi}\neq\mathbf{\Pi}\}}\right) \leq 12\sigma n^2 k^m m^{7/2} a_k^3 \frac{M^{5/2}}{\sqrt{\Lambda}\delta} e^{-\frac{\Lambda\delta^2}{8(mM+1)(1+ma_k)^2\sigma^2}}.$$

This gives the second term of the r.h.s. of the assertion.

Now we consider the first summand on the r.h.s. of (A.68). The idea is to bound the minimax risk conditioned on $\hat{\Pi} = \mathbf{\Pi}$ with the minimax risk of the LSE on the linear subvector space $\mathrm{imag}(\mathbf{\Pi}A)$. To this end, let $\mathcal{N}^\delta(\mathbf{\Pi}) \subset \mathcal{N}^{\delta,\Lambda}$ denote the set of all $\Pi A\omega \in \mathcal{N}^{\delta,\Lambda}$ with $\Pi = \mathbf{\Pi}$. Further, let $\hat{\theta}' \in \mathrm{argmin}_{\Pi A\omega\in\mathcal{N}^\delta(\mathbf{\Pi})} \|Y - \Pi A\omega\|^2$ be the least-squares estimator restricted to $\hat{\Pi} = \mathbf{\Pi}$. Then, clearly, $\hat{\theta} = \hat{\theta}'$ on $\{\hat{\Pi} = \mathbf{\Pi}\}$ and thus

$$\mathrm{E}_{\mathbf{\Pi}A\boldsymbol{\omega}}\left(\left\|\hat{\theta}-\mathbf{\Pi}A\boldsymbol{\omega}\right\|^2 \mathbb{1}_{\{\hat{\Pi}=\mathbf{\Pi}\}}\right) = \mathrm{E}_{\mathbf{\Pi}A\boldsymbol{\omega}}\left(\left\|\hat{\theta}'-\mathbf{\Pi}A\boldsymbol{\omega}\right\|^2 \mathbb{1}_{\{\hat{\Pi}=\mathbf{\Pi}\}}\right) \leq \mathrm{E}_{\mathbf{\Pi}A\boldsymbol{\omega}}\left(\left\|\hat{\theta}'-\mathbf{\Pi}A\boldsymbol{\omega}\right\|^2\right).$$

Thus, for all fixed $\mathbf{\Pi}$ as in (4.2)

$$\sup_{\mathbf{\Pi}A\boldsymbol{\omega}\in\mathcal{N}^\delta(\mathbf{\Pi})} \mathrm{E}_{\mathbf{\Pi}A\boldsymbol{\omega}}\left(\left\|\hat{\theta}-\mathbf{\Pi}A\boldsymbol{\omega}\right\|^2 \mathbb{1}_{\{\hat{\Pi}=\mathbf{\Pi}\}}\right) \leq \sup_{\mathbf{\Pi}A\boldsymbol{\omega}\in\mathcal{N}^\delta(\mathbf{\Pi})} \mathrm{E}_{\mathbf{\Pi}A\boldsymbol{\omega}}\left(\left\|\hat{\theta}'-\mathbf{\Pi}A\boldsymbol{\omega}\right\|^2\right).$$

Clearly, $\mathcal{N}^\delta(\mathbf{\Pi}) \subset \mathrm{imag}(\mathbf{\Pi}A)^M$ with $\dim(\mathrm{imag}(\mathbf{\Pi}A)^M) = mM$. Thus, for the LS estimator on $\mathrm{imag}(\mathbf{\Pi}A)^M$, $\hat{\theta}'' \in \mathrm{argmin}_{\tilde{\theta}\in\mathrm{imag}(\mathbf{\Pi}A)^M} \left\|Y-\tilde{\theta}\right\|^2$, it follows from Lemma A.3.2 that

$$\sup_{\mathbf{\Pi}A\boldsymbol{\omega}\in\mathcal{N}^\delta(\mathbf{\Pi})} \mathrm{E}_{\mathbf{\Pi}A\boldsymbol{\omega}}\left(\left\|\hat{\theta}'-\mathbf{\Pi}A\boldsymbol{\omega}\right\|^2\right) \leq 4 \sup_{\theta\in\mathrm{imag}(\mathbf{\Pi}A)^M} \mathrm{E}_\theta\left(\left\|\hat{\theta}''-\theta\right\|^2\right) = 4\sigma^2 mM,$$

which finishes the proof. □

Proof of Theorem 4.2.2. The first assertion follows directly from the first part of Lemma A.3.3 with $\epsilon = \|\Pi A\omega - \Pi' A\omega'\| / (\sqrt{n} m a_k)$. The second assertion follows from the second part of Lemma A.3.3 with $\epsilon \nearrow \|\Pi A\omega - \Pi' A\omega'\|$. □

Proof of Theorem 4.2.3. It follows directly from combining the first part of Theorem 4.2.2 and Corollary 4.1.4 that

$$\inf_{\hat{\Pi},\hat{\omega}} \sup_{\mathbf{\Pi},\boldsymbol{\omega}} \mathrm{E}_{\mathbf{\Pi}A\boldsymbol{\omega}}\left(d\left((\mathbf{\Pi},\boldsymbol{\omega}),(\hat{\Pi},\hat{\omega})\right)^2\right) \gtrsim \sigma^2 M \frac{1}{nma_k^2} + \sigma\sqrt{M}\frac{c_1}{nm^2a_k^2} e^{-\frac{c_1^2}{8}\frac{M}{\sigma^2}}.$$

For $B := \left\{\left\|\mathbf{\Pi}A\boldsymbol{\omega} - \hat{\Pi}A\hat{\omega}\right\| \leq c_1\sqrt{M}/(1+ma_k)\right\}$, Markov's inequality gives

$$\mathbf{P}_{\mathbf{\Pi}A\boldsymbol{\omega}}(B^c) = \mathbf{P}_{\mathbf{\Pi}A\boldsymbol{\omega}}\left(\left\|\mathbf{\Pi}A\boldsymbol{\omega} - \hat{\Pi}A\hat{\omega}\right\| > c_1\sqrt{M}/(1+ma_k)\right) \leq \frac{\mathrm{E}_{\mathbf{\Pi}A\boldsymbol{\omega}}\left(\left\|\mathbf{\Pi}A\boldsymbol{\omega} - \hat{\Pi}A\hat{\omega}\right\|^2\right)}{c_1^2 M/(1+ma_k)^2}.$$

As for any $\mathbf{\Pi}A\boldsymbol{\omega}, \Pi A\omega \in \mathcal{N}^{\delta,\Lambda}$, $d((\mathbf{\Pi},\boldsymbol{\omega}),(\Pi,\omega)) \leq \sqrt{M}(1/m+1) \leq \sqrt{M}3/2$ it follows from

combining the second part of Theorem 4.2.2 and Corollary 4.1.4 that

$$\begin{aligned}
&\inf_{\hat{\Pi},\hat{\omega}} \sup_{\mathbf{\Pi},\boldsymbol{\omega}} \mathrm{E}_{\mathbf{\Pi}A\boldsymbol{\omega}} \left(d\left((\mathbf{\Pi},\boldsymbol{\omega}),(\hat{\Pi},\hat{\omega})\right)^2 \right) \\
&\leq \inf_{\hat{\Pi},\hat{\omega}} \sup_{\mathbf{\Pi},\boldsymbol{\omega}} \mathrm{E}_{\mathbf{\Pi}A\boldsymbol{\omega}} \left(d\left((\mathbf{\Pi},\boldsymbol{\omega}),(\hat{\Pi},\hat{\omega})\right)^2 \mathbb{1}_B \right) + 9/4M\mathbf{P}_{\mathbf{\Pi}A\boldsymbol{\omega}}\left(B^c\right) \\
&\leq \inf_{\hat{\Pi},\hat{\omega}} \sup_{\mathbf{\Pi},\boldsymbol{\omega}} \mathrm{E}_{\mathbf{\Pi}A\boldsymbol{\omega}} \left(\left\| \mathbf{\Pi}A\boldsymbol{\omega} - \hat{\Pi}A\hat{\omega} \right\|^2 \right) + 9/4M \frac{\mathrm{E}_{\mathbf{\Pi}A\boldsymbol{\omega}} \left(\left\| \mathbf{\Pi}A\boldsymbol{\omega} - \hat{\Pi}A\hat{\omega} \right\|^2 \right)}{c_1^2 M/(1+ma_k)^2} \\
&= \inf_{\hat{\Pi},\hat{\omega}} \sup_{\boldsymbol{\omega},\boldsymbol{\omega}} \mathrm{E}_{\mathbf{\Pi}A\boldsymbol{\omega}} \left(\left\| \mathbf{\Pi}A\boldsymbol{\omega} - \hat{\Pi}A\hat{\omega} \right\|^2 \right) \left(1 + \frac{9/4(1+ma_k)^2}{c_1^2} \right) \\
&\lesssim \inf_{\hat{\Pi},\hat{\omega}} \sup_{\boldsymbol{\omega},\boldsymbol{\omega}} \mathrm{E}_{\mathbf{\Pi}A\boldsymbol{\omega}} \left(\left\| \mathbf{\Pi}A\boldsymbol{\omega} - \hat{\Pi}A\hat{\omega} \right\|^2 \right) \left(\frac{ma_k}{c_1} \right)^2 \\
&\lesssim \sigma^2 M \, \frac{m^3 a_k^2}{c_1^2} + \sqrt{M}\sigma \, \frac{m^2 a_k^2}{\sqrt{c_2} c_1^3} \, e^{-\frac{c_2 c_1^2}{16m^3(1+a_k)^2} \frac{M}{\sigma^2}}.
\end{aligned}$$

□

A.3.1 Additional lemmas

Lemma A.3.1. *For a finite parameter space $\Theta \subset \mathbb{R}^n$ and any estimator $\hat{\theta}$*

$$\min_{\theta' \neq \theta''} \left\| \theta' - \theta'' \right\|^2 \leq \frac{\sup_{\theta\in\Theta} \mathrm{E}_\theta \left(\left\| \hat{\theta} - \theta \right\|^2 \right)}{\sup_{\theta\in\Theta} \boldsymbol{P}_\theta \left(\hat{\theta} \neq \theta \right)} \leq \max_{\theta' \neq \theta''} \left\| \theta' - \theta'' \right\|^2.$$

Proof.

$$\sup_{\theta\in\Theta} \mathrm{E}_\theta \left(\left\| \hat{\theta} - \theta \right\|^2 \right) = \sup_{\theta\in\Theta} \sum_{\tilde{\theta}\in\Theta\setminus\theta} \left\| \tilde{\theta} - \theta \right\|^2 \mathbf{P}_\theta \left(\hat{\theta} = \tilde{\theta} \right) = \sup_{\theta\in\Theta} \mathbf{P}_\theta(\hat{\theta} \neq \theta) \sum_{\tilde{\theta}\in\Theta\setminus\theta} \left\| \tilde{\theta} - \theta \right\|^2 \frac{\mathbf{P}_\theta \left(\hat{\theta} = \tilde{\theta} \right)}{\mathbf{P}_\theta(\hat{\theta} \neq \theta)},$$

where, for every $\theta \in \Theta$

$$\min_{\theta' \neq \theta''} \left\| \theta' - \theta'' \right\|^2 \leq \sum_{\tilde{\theta}\in\Theta\setminus\theta} \left\| \tilde{\theta} - \theta \right\|^2 \frac{\mathbf{P}_\theta \left(\hat{\theta} = \tilde{\theta} \right)}{\mathbf{P}_\theta(\hat{\theta} \neq \theta)} \leq \max_{\theta' \neq \theta''} \left\| \theta' - \theta'' \right\|^2.$$

□

Lemma A.3.2. *Let V be a subvector space of $\mathbb{R}^d$, $A \subset V$ an arbitrary subset, and $Y \in \mathbb{R}^d$. Further, let $\hat{\theta}_A(Y) \in \operatorname{argmin}_{\tilde{\theta}\in A} \left\| Y - \tilde{\theta} \right\|$ and $\hat{\theta}_V(Y) \in \operatorname{argmin}_{\tilde{\theta}\in V} \left\| Y - \tilde{\theta} \right\|$. Then*

$$\forall \theta \in A: \quad \left\| \hat{\theta}_A - \theta \right\|^2 \leq 4 \, \left\| \hat{\theta}_V - \theta \right\|^2. \tag{A.69}$$

Proof. Let $\theta \in A$ be fixed. If $\left\| \hat{\theta}_A - \theta \right\|^2 = 0$, (A.69) holds trivially. Further, if $Y \in A$, it holds that $\hat{\theta}_V = \hat{\theta}_A = Y$, and hence, (A.69) follows trivially, too. So assume that $\left\| \hat{\theta}_A - \theta \right\|^2 > 0$ and $Y \notin A$.

Choosing an appropriate coordinate system, we may w.l.o.g. assume that

$$V = \{x \in \mathbb{R}^d : x_1 = \ldots = x_r = 0\},$$

with $\dim(V) = d - r$. Let pr be the orthogonal projection onto V, i.e.,

$$\mathrm{pr} : (x_1, \ldots, x_d)^\top \mapsto (x_{r+1}, \ldots, x_d)^\top.$$

Then,

$$\operatorname*{argmin}_{\tilde{\theta} \in A} \left\|Y - \tilde{\theta}\right\|^2 = \operatorname*{argmin}_{\tilde{\theta} \in A} \sum_{i=1}^{r} Y_i^2 + \left\|\mathrm{pr}(Y) - \mathrm{pr}(\tilde{\theta})\right\|^2 = \operatorname*{argmin}_{\tilde{\theta} \in A} \left\|\mathrm{pr}(Y) - \mathrm{pr}(\tilde{\theta})\right\|^2$$

and analog $\operatorname{argmin}_{\tilde{\theta} \in V} \left\|Y - \tilde{\theta}\right\|^2 = \operatorname{argmin}_{\tilde{\theta} \in V} \left\|\mathrm{pr}(Y) - \mathrm{pr}(\tilde{\theta})\right\|^2$, $\left\|\hat{\theta}_V - \theta\right\|^2 = \left\|\mathrm{pr}(\hat{\theta}_V) - \mathrm{pr}(\theta)\right\|^2$, and $\left\|\hat{\theta}_V - \theta\right\|^2 = \left\|\mathrm{pr}(\hat{\theta}_V) - \mathrm{pr}(\theta)\right\|^2$. Thus, we may w.l.o.g. assume that $V = \mathbb{R}^d$, i.e., $\hat{\theta}_V = Y$. Then

$$\begin{aligned}
\frac{\|Y - \theta\|^2}{\left\|\hat{\theta}_A - \theta\right\|^2} &\geq \left(\min_{x \notin A} \frac{\|x - \theta\|}{\left\|\hat{\theta}_A(x) - \theta\right\|}\right)^2 \geq \left(\min_{x \notin A} \frac{\|x - \theta\|}{\left\|\hat{\theta}_A(x) - x\right\| + \|x - \theta\|}\right)^2 \\
&= \left(1 + \max_{x \notin A} \frac{\left\|x - \hat{\theta}_A(x)\right\|}{\|x - \theta\|}\right)^{-2} \geq \frac{1}{4},
\end{aligned}$$

where the last inequality follows from the definition of $\hat{\theta}_A$.

□

Lemma A.3.3. *Let $\Pi A\omega, \Pi' A\omega' \in \mathcal{N}^\delta$, then for all $\epsilon > 0$*

1. $\|\Pi A\omega - \Pi' A\omega'\| \geq \sqrt{n} m a_k \, \epsilon \quad \Rightarrow \quad d\left((\Pi, \omega), (\Pi', \omega')\right) \geq \epsilon,$
2. *if $\epsilon < \delta/(1 + m a_k)$, then* $\|\Pi A\omega - \Pi' A\omega'\| < \epsilon \quad \Rightarrow \quad d\left((\Pi, \omega), (\Pi', \omega')\right) < \epsilon.$

Proof. From $\|\Pi A\omega - \Pi' A\omega'\| \geq \sqrt{n} m a_k \, \epsilon$ it follows that $\max_{j=1,\ldots,n} \left\|(\Pi A\omega)_{j\cdot} - (\Pi' A\omega')_{j\cdot}\right\| \geq m a_k \, \epsilon$ and $\epsilon \leq \max_{j=1,\ldots,n} \left\|(\Pi A\omega)_{j\cdot} - (\Pi' A\omega')_{j\cdot}\right\| / (m a_k) \leq \sqrt{M}/m$. Hence, by Theorem 2.2.3 $\max_{i=1,\ldots,m} \left\|\omega_{i\cdot} - \omega'_{i\cdot}\right\| \geq \epsilon$ or $\Pi \neq \Pi'$ and thus $d\left((\Pi, \omega), (\Pi', \omega')\right) \geq \epsilon$, which shows the first assertion. If $\epsilon < \delta/(1 + m a_k)$ and $\max_{j=1,\ldots,n} \left\|(\Pi A\omega)_{j\cdot} - (\Pi' A\omega')_{j\cdot}\right\| \leq \|\Pi A\omega - \Pi' A\omega'\| < \epsilon$ it follows from Theorem 2.2.3 that $\max_{i=1,\ldots,m} \left\|\omega_{i\cdot} - \omega'_{i\cdot}\right\| < \epsilon$ and $\Pi = \Pi'$ and thus it follows that $d\left((\Pi, \omega), (\Pi', \omega')\right) < \epsilon$, which shows the second assertion. □

A.4 Proof of Chapter 5

Proof of Theorem 5.1.1. Recall the definition of the ASB in (1.8) and employ the notation

$$\{a - a' : a \neq a' \in \mathfrak{A}^m\} := \{d^1, \ldots, d^D\}.$$

Introducing an auxiliary variable δ (5.6) can be rewritten as

$$\begin{aligned} \max \quad & \delta, \quad \text{s.t.} \\ & \left|\langle \omega, d^i \rangle\right| \geq \delta, \quad i = 1, \ldots, D, \\ & \omega_1 \geq 0 \\ & \omega_i - \omega_{i-1} \geq 0, \quad i = 2, \ldots, m, \\ & \omega_i \geq a_i, \quad i = 1, \ldots, m, \\ & \omega_1 + \ldots + \omega_m = 1 \\ & \omega_i \leq b_i, \quad i = 1, \ldots, m. \end{aligned} \tag{A.70}$$

Define $M := 2(a_k - a_1)$ and note that for all feasible values of (ω, δ) in (A.70) it holds true that $\delta + \left|\langle \omega, d^i \rangle\right| \leq M$ for all $i = 1, \ldots, D$. Thus, introducing further auxiliary binary variables $B_1, \ldots, B_D$ we can rewrite (A.70) as

$$\begin{aligned} \max \quad & \delta, \quad \text{s.t.} \\ & \langle \omega, d^i \rangle + MB_i - \delta \geq 0, \quad i = 1, \ldots, D, \\ & -\langle \omega, d^i \rangle - MB_i - \delta \geq -M, \quad i = 1, \ldots, D, \\ & \omega_1 \geq 0 \\ & \omega_i - \omega_{i-1} \geq 0, \quad i = 2, \ldots, m, \\ & \omega_i \geq a_i, \quad i = 1, \ldots, m, \\ & \omega_1 + \ldots + \omega_m = 1 \\ & \omega_i \leq b_i, \quad i = 1, \ldots, m \\ & B_i \leq 1 \quad i = 1, \ldots, D, \\ & \text{int} \quad B_i \quad i = 1, \ldots, D. \end{aligned} \tag{A.71}$$

In summary, we have rewritten (5.6) as a MILP, with vector of variables $x = (\omega, \delta, B) \in \mathbb{R}^{m+1} \times \{0,1\}^D$, objective function coefficients $c = (0, \ldots, 0, 1, 0, \ldots, 0) \in \mathbb{R}^{m+1} \times \{0,1\}^D$, a matrix of constraint coefficients $A \in \mathbb{R}^{(3(D+m)+2)\times(D+m+1)}$, and a vector of values for the right-hand sides of the constraints $b \in \mathbb{R}^{(3(D+m)+2)}$. □

A.5 Proof of Chapter 8

Proof of Theorem 8.0.1. Note that

$$T_n(Y, \boldsymbol{g}) \leq \max_{\substack{1\leq i\leq j\leq n \\ j-i+1\geq \lambda n}} \frac{\left|\sum_{l=i}^{j} \epsilon_j/\sigma\right|}{\sqrt{j-i+1}} - pen(j-i+1), \tag{A.72}$$

with ϵ_j/σ i.i.d. sub-Gaussian random variables as in (8.1) for $\sigma = 1$, with mean 0 and variance 1. Therefore, the following corollary from Sakhanenko (1985) (see also (Zaitsev, 2002, Theorem 1 and the subsequent remark)) can be applied.

Corollary A.5.1 (Sakhanenko, 1985)**.** *Given i.i.d. sub-Gaussian random variables $\epsilon_1, \ldots, \epsilon_n$ as in (8.1) for $\sigma = 1$, with mean 0 and variance 1, one can construct a sequence of i.i.d. Gaussian random variables $\zeta_1, \ldots, \zeta_n \sim \mathcal{N}(0,1)$ and for all $x > 0$*

$$\boldsymbol{P}(C_1 \Delta(\epsilon, \zeta) > x) \leq (1 + C_2\sqrt{n}) \exp(-x),$$

for some constants $0 < C_1, C_2 < \infty$ and $\Delta(\epsilon, \zeta) := \max_{i\leq n} \left|\sum_{l=1}^{i} (\epsilon_l - \zeta_l)\right|$.

Let $\zeta_1, \ldots, \zeta_n$ be the Gaussian random variables from Corollary A.5.1. Then it follows from (A.72) that

$$\begin{aligned}
\mathbf{P}(T_n(Y, \boldsymbol{g}) > q) \leq \mathbf{P}&\left(\max_{\substack{1\leq i\leq j\leq n \\ j-i+1\geq \lambda n}} \frac{\left|\sum_{l=i}^{j} \zeta_j\right|}{\sqrt{j-i+1}} - pen(j-i+1) > q/2 \right) \\
+\mathbf{P}&\left(\max_{\substack{1\leq i\leq j\leq n \\ j-i+1\geq \lambda n}} \frac{\left|\sum_{l=i}^{j} \epsilon_j/\sigma\right|}{\sqrt{j-i+1}} - pen(j-i+1) - \max_{\substack{1\leq i\leq j\leq n \\ j-i+1\geq \lambda n}} \frac{\left|\sum_{l=i}^{j} \zeta_j\right|}{\sqrt{j-i+1}} - pen(j-i+1) > q/2 \right),
\end{aligned}$$

where (Sieling, 2013, Corollary 4) yields that the first summand on the r.h.s. is bounded by $\exp(-q^2/32)$. Moreover,

$$\begin{aligned}
&\max_{\substack{1\leq i\leq j\leq n \\ j-i+1\geq \lambda n}} \frac{\left|\sum_{l=i}^{j} \epsilon_j/\sigma\right|}{\sqrt{j-i+1}} - pen(j-i+1) - \max_{\substack{1\leq i\leq j\leq n \\ j-i+1\geq \lambda n}} \frac{\left|\sum_{l=i}^{j} \zeta_j\right|}{\sqrt{j-i+1}} - pen(j-i+1) \\
&\leq \max_{\substack{1\leq i\leq j\leq n \\ j-i+1\geq \lambda n}} \frac{\left|\sum_{l=i}^{j} \epsilon_j/\sigma - \zeta_j\right|}{\sqrt{j-i+1}} \leq \frac{2\Delta(\epsilon/\sigma, \zeta)}{\sqrt{n\lambda}}.
\end{aligned}$$

Thus, it follows from Corollary A.5.1 that the second summand is bounded by $(1 + C_2\sqrt{n})$ $\exp(-C_1 q\sqrt{n\lambda}/4)$. □

APPENDIX B

Additional figures from Section 6.2

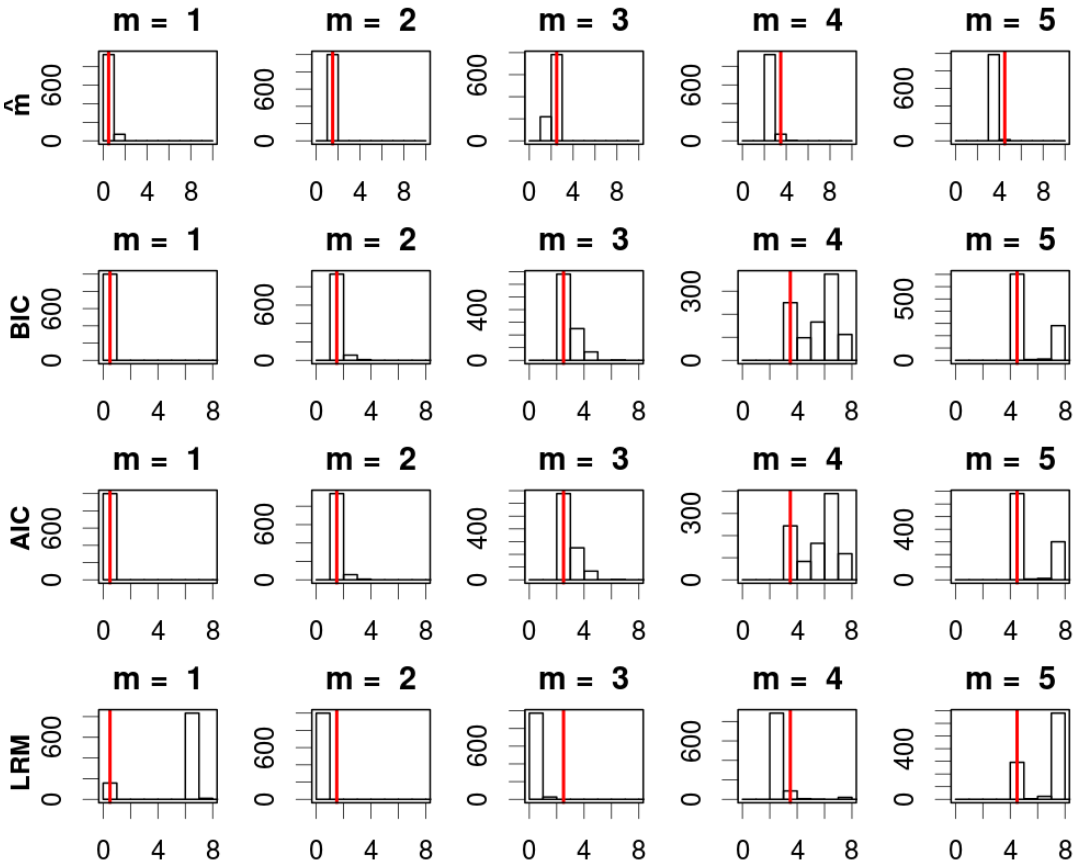

Figure B.1: As in Figure 6.4, but with $\sigma = 0.02$.

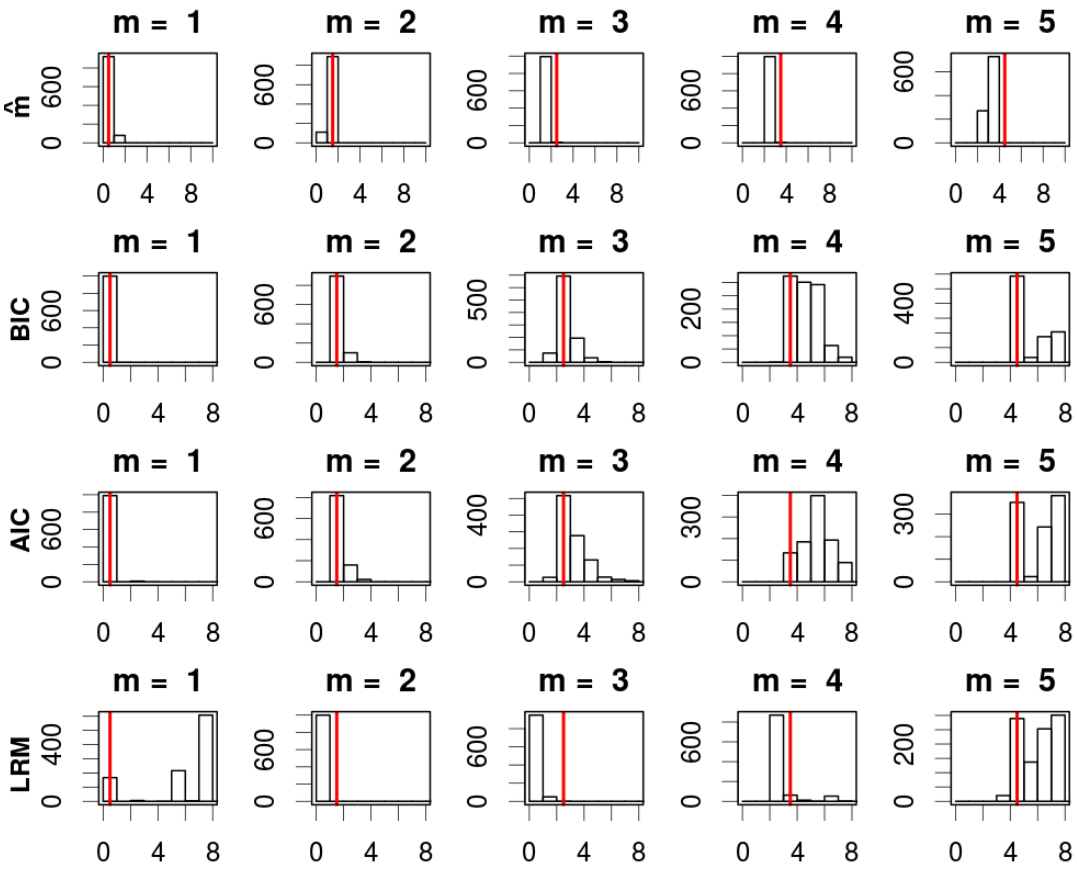

Figure B.2: As in Figure 6.4, but with $\sigma = 0.05$.

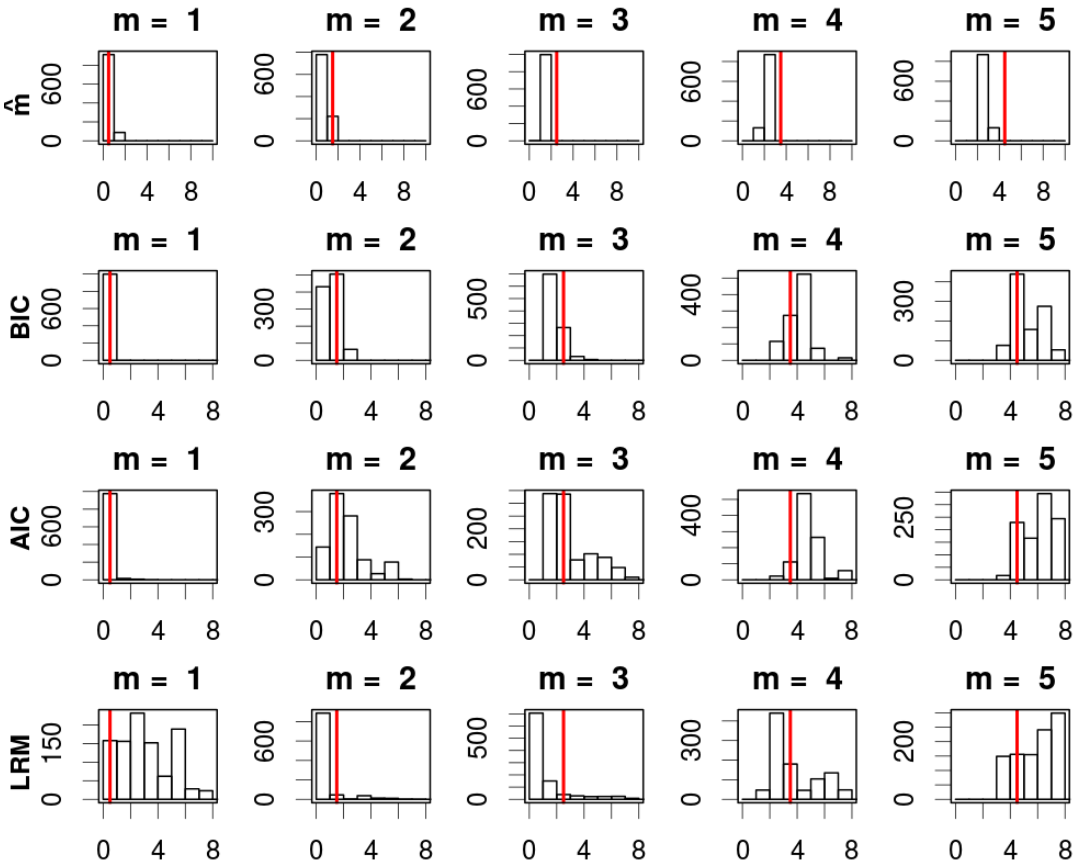

Figure B.3: As in Figure 6.4, but with $\sigma = 0.1$.

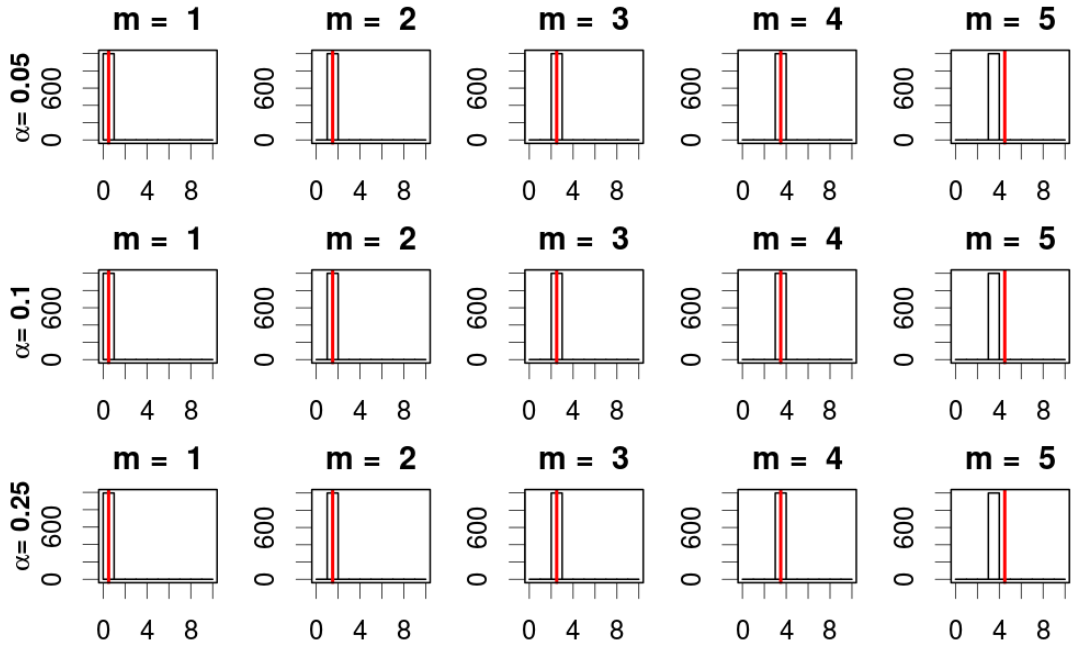

Figure B.4: As in Figure 6.5, but with $\sigma = 0.01$.

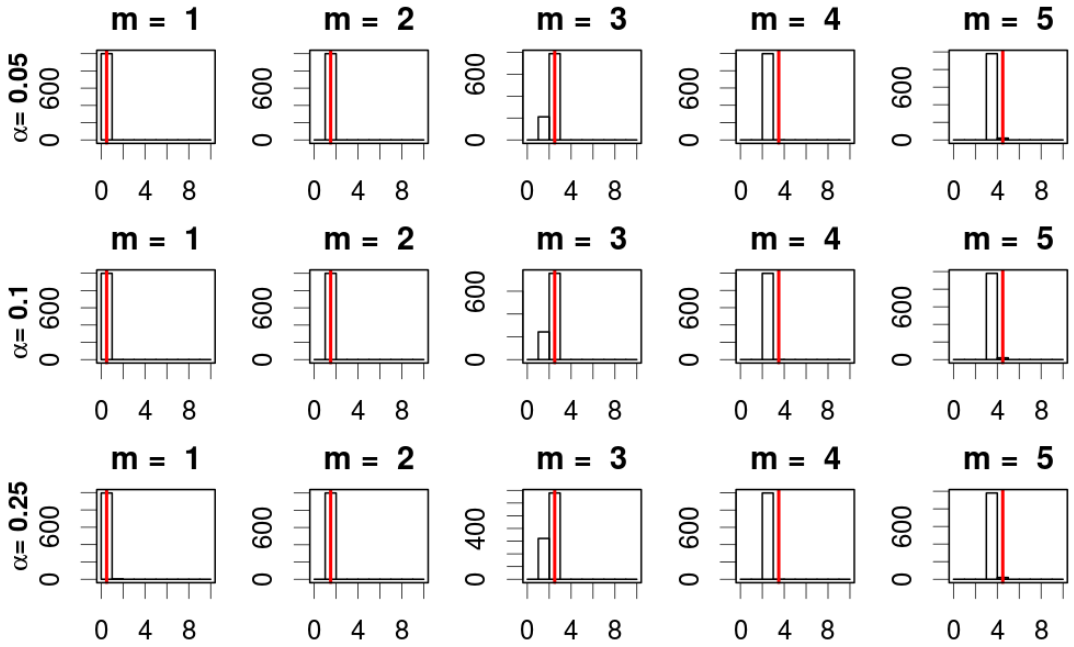

Figure B.5: As in Figure 6.5, but with $\sigma = 0.02$.

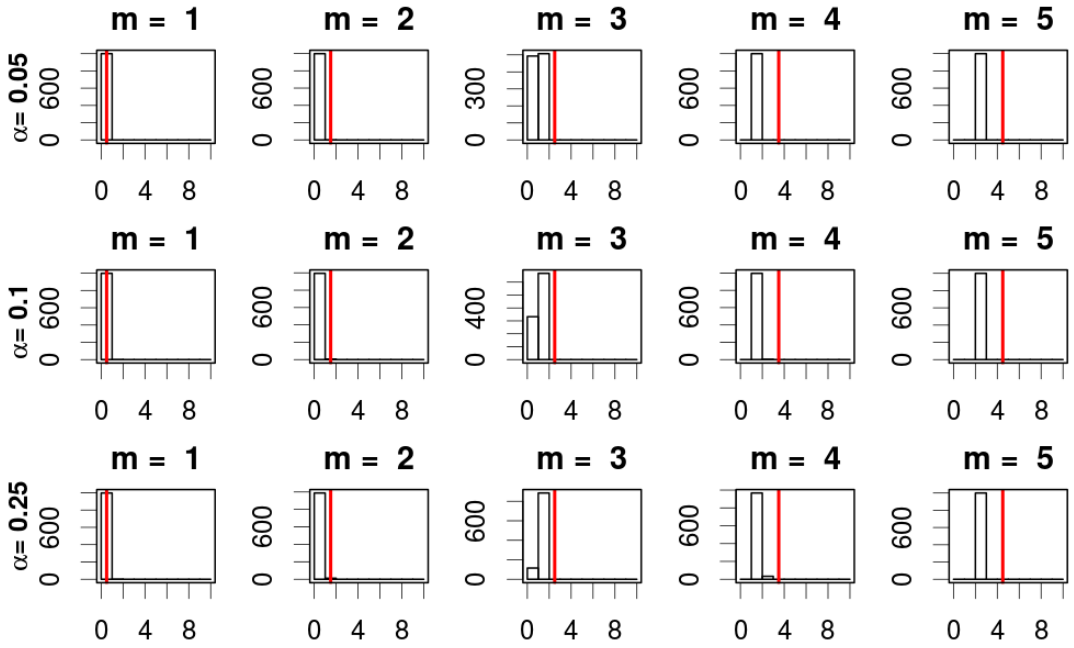

Figure B.6: As in Figure 6.5, but with $\sigma = 0.1$.

Bibliography

Abramowitz, M. and Stegun, I. (1972). *Handbook of Mathematical Functions with Formulas, Graphs, and Mathematical Tables*. Dover Publications, New York.

Abrard, F., Deville, Y., and White, P. (2001). From blind source separation to blind source cancellation in the underdetermined case: A new approach based on time-frequency analysis. In *Proceedings of Third International Conference on Independent Component Analysis and Signal Separation*, pages 734–739. San Diego, CA.

Akaike, H. (1974). A new look at the statistical model identification. *IEEE Transactions on Automatic Control*, 19(6):716–723.

Arora, S., Ge, R., Kannan, R., and Moitra, A. (2012). Computing a nonnegative matrix factorization–provably. In *Proceedings of the Forty-Fourth Annual ACM Symposium on Theory of Computing*, pages 145–162. New York.

Arora, S., Ge, R., Moitra, A., and Sachdeva, S. (2015). Provable ICA with unknown Gaussian noise, and implications for Gaussian mixtures and autoencoders. *Algorithmica*, 72(1):215–236.

Bai, J. and Perron, P. (1998). Estimating and testing linear models with multiple structural changes. *Econometrica*, 66(1):47.

Bandeira, A., Rigollet, P., and Weed, J. (2017). Optimal rates of estimation for multi-reference alignment. *arXiv preprint arXiv:1702.08546*.

Behr, M., Holmes, C., and Munk, A. (2017). Multiscale blind source separation. *arXiv preprint arXiv:1608.07173*. To appear in *The Annals of Statistics*.

Behr, M. and Munk, A. (2017a). Identifiability for blind source separation of multiple finite alphabet linear mixtures. *IEEE Transactions on Information Theory*, 63(9):5506–5517.

Behr, M. and Munk, A. (2017b). Minimax estimation in linear models with unknown finite alphabet design. *arXiv preprint arXiv:1711.04145*.

Belkin, M., Rademacher, L., and Voss, J. (2013). Blind signal separation in the presence of Gaussian noise. *Journal of Machine Learning Research: Proceedings*, 30:270 – 287.

Belouchrani, A., Abed-Meraim, K., Cardoso, J.-F., and Moulines, E. (1997). A blind source separation technique using second-order statistics. *IEEE Transactions on Signal Processing*, 45(2):434–444.

Beroukhim, R., Mermel, C. H., Porter, D., Wei, G., Raychaudhuri, S., Donovan, J., et al. (2010). The landscape of somatic copy-number alteration across human cancers. *Nature*, 463(7283):899–905.

Berthet, Q. and Rigollet, P. (2013). Optimal detection of sparse principal components in high dimension. *The Annals of Statistics*, 41(4):1780–1815.

Bittorf, V., Recht, B., Re, C., and Tropp, J. (2012). Factoring nonnegative matrices with linear programs. In *Advances in Neural Information Processing Systems (NIPS) 25*, pages 1214–1222.

Bofill, P. and Zibulevsky, M. (2001). Underdetermined blind source separation using sparse representations. *Signal Processing*, 81(11):2353–2362.

Boysen, L., Kempe, A., Liebscher, V., Munk, A., and Wittich, O. (2009). Consistencies and rates of convergence of jump-penalized least squares estimators. *The Annals of Statistics*, 37(1):157–183.

Brunet, J.-P., Tamayo, P., Golub, T. R., and Mesirov, J. P. (2004). Metagenes and molecular pattern discovery using matrix factorization. *Proceedings of the National Academy of Sciences*, 101(12):4164–4169.

Burnham, K. P. (2004). Multimodel inference: Understanding AIC and BIC in model selection. *Sociological Methods & Research*, 33(2):261–304.

Carlstein, E., Müller, H.-G., and Siegmund, D. (1994). Change-point problems. *Lecture Notes Monograph Series*, 23. Institute of Mathematical Statistics.

Carter, S. L., Cibulskis, K., Helman, E., McKenna, A., Shen, H., Zack, T., et al. (2012). Absolute quantification of somatic DNA alterations in human cancer. *Nature Biotechnology*, 30(5):413–421.

Chen, H., Xing, H., and Zhang, N. R. (2011). Estimation of parent specific DNA copy number in tumors using high-density genotyping arrays. *PLoS Computational Biology*, 7(1):e1001060.

Cheng, M.-Y. and Hall, P. (1999). Mode testing in difficult cases. *The Annals of Statistics*, 27(4):1294–1315.

Claeskens, G. and Hjort, N. L. (2008). *Model Selection and Model Averaging*. Cambridge Series in Statistical and Probabilistic Mathematics. Cambridge University Press, Cambridge.

Comon, P. (1994). Independent component analysis, a new concept? *Signal Processing*, 36:287–314.

Davies, L., Höhenrieder, C., and Krämer, W. (2012). Recursive computation of piecewise constant volatilities. *Computational Statistics & Data Analysis*, 56(11):3623–3631.

Davies, P. L. and Kovac, A. (2001). Local extremes, runs, strings and multiresolution. *The Annals of Statistics*, 29(1):1–65.

Dette, H., Munk, A., and Wagner, T. (1998). Estimating the variance in nonparametric regression - what is a reasonable choice? *Journal of the Royal Statistical Society: Series B (Statistical Methodology)*, 60(4):751–764.

Diamantaras, K. and Papadimitriou, T. (2011). Blind deconvolution of multi-input single-output systems using the distribution of point distances. *Journal of Signal Processing Systems*, 65(3):525–534.

Diamantaras, K. I. (2006). A clustering approach for the blind separation of multiple finite alphabet sequences from a single linear mixture. *Signal Processing*, 86(4):877–891.

Diamantaras, K. I. (2008). Blind separation of two multi-level sources from a single linear mixture. In *IEEE Workshop on Machine Learning for Signal Processing*, pages 67–72. Cancun.

Diamantaras, K. I. and Chassioti, E. (2000). Blind separation of n binary sources from one observation: A deterministic approach. In *International Workshop on Independent Component Analysis and Blind Signal Separation*, pages 93–98. Helsinki.

Diamantaras, K. I. and Papadimitriou, T. (2009). Blind MISO deconvolution using the distribution of output differences. In *IEEE International Workshop on Machine Learning for Signal Processing*. Grenoble.

Ding, L., Wendl, M. C., McMichael, J. F., and Raphael, B. J. (2014). Expanding the computational toolbox for mining cancer genomes. *Nature Reviews Genetics*, 15(8):556–570.

Donoho, D., Liu, R. C., and MacGibbon, B. (1990). Minimaxristk over hyperrectangles and implications. *The Annals of Statistics*, 18(3):1416–1437.

Donoho, D. and Stodden, V. (2004). When does non-negative matrix factorization give a correct decomposition into parts? In *Advances in Neural Information Processing Systems (NIPS) 16*. MIT Press, Cambridge.

Dörband, W. (1970). Determinantensätze und Simplexeigenschaften (Verallgemeinerung trigonometrischer Lehrsätze auf n-dimensionale Simplexe). *Mathematische Nachrichten*, 44(1-6):295–304.

Du, C., Kao, C.-L. M., and Kou, S. C. (2015). Stepwise signal extraction via marginal likelihood. *Journal of the American Statistical Association*, 111(513):314–330.

Dümbgen, L., Piterbarg, V. I., and Zholud, D. (2006). On the limit distribution of multiscale test statistics for nonparametric curve estimation. *Mathematical Methods of Statistics*, 15(1):20–25.

Dümbgen, L. and Spokoiny, V. (2001). Multiscale testing of qualitative hypotheses. *The Annals of Statistics*, 29(1):124–152.

Dümbgen, L. and Walther, G. (2008). Multiscale inference about a density. *The Annals of Statistics*, 36(4):1758–1785.

Fearnhead, P. (2006). Exact and efficient Bayesian inference for multiple changepoint problems. *Statistics and Computing*, 16(2):203–213.

Flammarion, N., Mao, C., and Rigollet, P. (2016). Optimal rates of statistical seriation. *arXiv preprint arXiv:1607.02435*.

Frick, K., Munk, A., and Sieling, H. (2014). Multiscale change point inference. *Journal of the Royal Statistical Society: Series B (Statistical Methodology)*, 76(3):495–580.

Friedrich, F., Kempe, A., Liebscher, V., and Winkler, G. (2008). Complexity penalized m-estimation: Fast computation. *Journal of Computational and Graphical Statistics*, 17(1):201–224.

Fryzlewicz, P. (2014). Wild binary segmentation for multiple change-point detection. *The Annals of Statistics*, 42(6):2243–2281.

Futschik, A., Hotz, T., Munk, A., and Sieling, H. (2014). Multiscale DNA partitioning: Statistical evidence for segments. *Bioinformatics*, 30(16):2255–2262.

Greaves, M. and Maley, C. C. (2012). Clonal evolution in cancer. *Nature*, 481(7381):306–313.

Gu, F., Zhang, H., Li, N., and Lu, W. (2010). Blind separation of multiple sequences from a single linear mixture using finite alphabet. In *International Conference on Wireless Communications and Signal Processing*. IEEE, Suzhou.

Ha, G., Roth, A., Khattra, J., Ho, J., Yap, D., Prentice, L. M., et al. (2014). TITAN: Inference of copy number architectures in clonal cell populations from tumor whole-genome sequence data. *Genome Research*, 24(11):1881–1893.

Hall, P., Kay, J. W., and Titterinton, D. M. (1990). Asymptotically optimal difference-based estimation of variance in nonparametric regression. *Biometrika*, 77(3):521–528.

Harchaoui, Z. and Lévy-Leduc, C. (2010). Multiple change-point estimation with a total variation penalty. *Journal of the American Statistical Association*, 105(492):1480–1493.

Jeng, X. J., Cai, T. T., and Li, H. (2010). Optimal sparse segment identification with application in copy number variation analysis. *Journal of the American Statistical Association*, 105(491):1156–1166.

Killick, R., Fearnhead, P., and Eckley, I. A. (2012). Optimal detection of changepoints with a linear computational cost. *Journal of the American Statistical Association*, 107(500):1590–1598.

Kim, J. and Park, H. (2008). Sparse nonnegative matrix factorization for clustering. *Georgia Institute of Technology*. Technical Report GT-CSE-08-01.

Kolokoltsov, V. N. (2011). *Markov Processes, Semigroups, and Generators*, volume 38 of *De Gruyter studies in mathematics*. Walter de Gruyter & Co., Berlin.

Lee, D. and Seung, S. (1999). Learning the parts of objects by non-negative matrix factorization. *Nature*, 401:788–791.

Lee, T.-W., Lewicki, M. S., Girolami, M., and Sejnowski, T. J. (1999). Blind source separation of more sources than mixtures using overcomplete representations. *IEEE Signal Processing Letters*, 6(4):87–90.

Li, T. (2005). A general model for clustering binary data. In *Proceedings of the Eleventh ACM SIGKDD International Conference on Knowledge Discovery in Data Mining*, pages 188–197. Chicago.

Li, Y., Amari, S., Cichocki, A., Ho, D., and Shengli Xie (2006). Underdetermined blind source separation based on sparse representation. *IEEE Transactions on Signal Processing*, 54(2):423–437.

Li, Y., Cichocki, A., and Zhang, L. (2003). Blind separation and extraction of binary sources. *IEICE Transactions on Fundamentals of Electronics, Communications and Computer Sciences*, 86(3):580–589.

Liu, B., Morrison, C. D., Johnson, C. S., Trump, D. L., Qin, M., Conroy, J. C., et al. (2013). Computational methods for detecting copy number variations in cancer genome using next generation sequencing: Principles and challenges. *Oncotarget*, 4(11):1868.

Love, D. J., Heath, R. W., Lau, V. K., Gesbert, D., Rao, B. D., and Andrews, M. (2008). An overview of limited feedback in wireless communication systems. *IEEE Journal on Selected Areas in Communications*, 26(8):1341–1365.

Lu, Y. and Zhou, H. H. (2016). Statistical and computational guarantees of Lloyd's algorithm and its variants. *arXiv preprint arXiv:1612.02099*.

Marques, M., Stošić, M., and Costeira, J. (2009). Subspace matching: Unique solution to point matching with geometric constraints. In *IEEE Twelfth International Conference on Computer Vision*, pages 1288–1294. Kyoto.

Matteson, D. S. and James, N. A. (2014). A nonparametric approach for multiple change point analysis of multivariate data. *Journal of the American Statistical Association*, 109(505):334–345.

Müller, H.-G. and Stadtmüller, U. (1987). Estimation of heteroscedasticity in regression analysis. *The Annals of Statistics*, 15(2):610–625.

Neuts, M. F. (1981). *Matrix-Geometric Solutions in Stochastic Models: An Algorithmic Approach*. Johns Hopkins University Press, Baltimore.

Niu, Y. S. and Zhang, H. (2012). The screening and ranking algorithm to detect DNA copy number variations. *The Annals of Applied Statistics*, 6(3):1306.

Olshen, A. B., Venkatraman, E. S., Lucito, R., and Wigler, M. (2004). Circular binary segmentation for the analysis of array-based DNA copy number data. *Biostatistics*, 5(4):557–572.

Pajunen, P. (1997). Blind separation of binary sources with less sensors than sources. In *International Conference on Neural Networks*, pages 1994–1997. Houston.

Pananjady, A., Wainwright, M. J., and Courtade, T. A. (2016). Linear regression with an unknown permutation: Statistical and computational limits. In *54th Annual Allerton Conference on Communication, Control, and Computing*. IEEE, Monticello, IL.

Pananjady, A., Wainwright, M. J., and Courtade, T. A. (2017). Denoising linear models with permuted data. *arXiv preprint arXiv:1704.07461*.

Penny, W., Everson, R., and Roberts, S. (2001). ICA: Model order selection and dynamic source models. In *Independent Component Analysis: Principles and Practice*, pages 299–314. Cambridge University Press.

Proakis, J. G. (2007). *Digital Communications*. McGraw-Hill series in electrical and computer engineering. McGraw-Hill, Boston.

Rosenberg, A. and Hirschberg, J. (2007). V-measure: A conditional entropy-based external cluster evaluation measure. In *Proceedings of Conference on Empirical Methods in Natural Language Processing and Computational Natural Language Learning*, pages 410–420. Prague.

Rostami, M., Babaie-Zadeh, M., Samadi, S., and Jutten, C. (2011). Blind source separation of discrete finite alphabet sources using a single mixture. In *IEEE Statistical Signal Processing Workshop*, pages 709–712. Nice.

Roth, A., Khattra, J., Yap, D., Wan, A., Laks, E., Biele, J., et al. (2014). PyClone: Statistical inference of clonal population structure in cancer. *Nature Methods*, 11(4):396–398.

Sakhanenko, A. (1985). Convergence rate in invariance principle for non-identically distributed variables with exponential moments. In *Limit Theorems for Sums of Random Variables*, Advances in Probablity Theory. Springer.

Sampath, H., Stoica, P., and Paulraj, A. (2001). Generalized linear precoder and decoder design for MIMO channels using the weighted MMSE criterion. *IEEE Transactions on Communications*, 49(12):2198–2206.

Schmidt, M. N., Winther, O., and Hansen, L. K. (2009). Bayesian non-negative matrix factorization. In *International Conference on Independent Component Analysis and Signal Separation*, pages 540–547. Springer, Paraty, Brazil.

Schwarz, G. (1978). Estimating the dimension of a model. *The Annals of Statistics*, 6(2):461–464.

Shah, N. B., Balakrishnan, S., and Wainwright, M. J. (2016). Feeling the bern: Adaptive estimators for bernoulli probabilities of pairwise comparisons. In *IEEE International Symposium on Information Theory*, pages 1153–1157. Barcelona.

Shah, S. P., Roth, A., Goya, R., Oloumi, A., Ha, G., Zhao, Y., et al. (2012). The clonal and mutational evolution spectrum of primary triple-negative breast cancers. *Nature*, 486(7403):395–399.

Siegmund, D. (2013). Change-points: From sequential detection to biology and back. *Sequential Analysis*, 32(1):2–14.

Siegmund, D. and Yakir, B. (2000). Tail probabilities for the null distribution of scanning statistics. *Bernoulli*, 6(2):191.

Sieling, H. (2013). *Statistical Multiscale Segmentation: Inference, Algorithms and Applications*. Ph.D. thesis, University of Goettingen.

Spielman, D. A., Wang, H., and Wright, J. (2012). Exact recovery of sparsely-used dictionaries. In *Conference On Learning Theory (COLT)*. Edinburgh.

Spokoiny, V. (2009). Multiscale local change point detection with applications to value-at-risk. *The Annals of Statistics*, 37(3):1405–1436.

Stein, P. (1966). A note on the volume of a simplex. *The American Mathematical Monthly*, 73(3):299.

Talwar, S., Viberg, M., and Paulraj, A. (1996). Blind separation of synchronous co-channel digital signals using an antenna array. I. Algorithms. *IEEE Transactions on Signal Processing*, 44(5):1184–1197.

Tibshirani, R., Walther, G., and Hastie, T. (2001). Estimating the number of clusters in a data set via the gap statistic. *Journal of the Royal Statistical Society: Series B (Statistical Methodology)*, 63(2):441–423.

Tibshirani, R. and Wang, P. (2008). Spatial smoothing and hot spot detection for CGH data using the fused lasso. *Biostatistics*, 9(1):18–29.

Tong, L., Xu, G., and Kailath, T. (1991). A new approach to blind identification and equalization of multipath channels. In *IEEE Conference Record of the Twenty-Fifth Asilomar Conference on Signals, Systems and Computers*, pages 856–860. Pacific Grove, CA.

Tukey, J. W. (1961). Curves as parameters, and touch estimation. In *Proceedings of the Fourth Berkeley Symposium on Mathematical Statistics and Probability*, volume 1, pages 681–694. University of California Press, Berkely.

Unnikrishnan, J., Haghighatshoar, S., and Vetterli, M. (2015). Unlabeled sensing with random linear measurements. *arXiv preprint arXiv:1512.00115*.

Van den Meersche, K., Soetaert, K., and Van Oevelen, D. (2009). Xsample (): An R function for sampling linear inverse problems. *Journal of Statistical Software*, 30:1–15.

Verdu, S. (1998). *Multiuser Detection*. Cambridge University Press, Cambridge.

Wainwright, M. J. (2017). *High-Dimensional Statistics: A Non-Asymptotic Viewpoint*. University of California, Berkeley. In preparation.

Walther, G. (2010). Optimal and fast detection of spatial clusters with scan statistics. *The Annals of Statistics*, 38(2):1010–1033.

Wang, T., Berthet, Q., and Samworth, R. J. (2016). Statistical and computational trade-offs in estimation of sparse principal components. *The Annals of Statistics*, 44(5):1896–1930.

Yau, C., Papaspiliopoulos, O., Roberts, G. O., and Holmes, C. (2011). Bayesian non-parametric hidden Markov models with applications in genomics. *Journal of the Royal Statistical Society: Series B (Statistical Methodology)*, 73(1):37–57.

Yellin, D. and Porat, B. (1993). Blind identification of FIR systems excited by discrete-alphabet inputs. *IEEE Transactions on Signal Processing*, 41(3):1331–1339.

Yilmaz, O. and Rickard, S. (2004). Blind separation of speech mixtures via time-frequency masking. *IEEE Transactions on Signal Processing*, 52(7):1830–1847.

Zaitsev, A. Y. (2002). Estimates for the strong approximation in multidimensional central limit theorem. In *Proceedings of the ICM*, volume 3, pages 107–116. Beijing.

Zhang, N. R. and Siegmund, D. O. (2007). A modified Bayes information criterion with applications to the analysis of comparative genomic hybridization data. *Biometrics*, 63(1):22–32.

Zhang, N. R. and Siegmund, D. O. (2012). Model selection for high dimensional multi-sequence change-point problems. *Statistica Sinica*, 22(4):1507.

Zhang, Y. and Kassam, S. A. (2001). Blind separation and equalization using fractional sampling of digital communications signals. *Signal Processing*, 81(12):2591–2608.

Zhang, Y., Wainwright, M. J., and Jordan, M. I. (2014). Lower bounds on the performance of polynomial-time algorithms for sparse linear regression. In *Conference On Learning Theory (COLT)*. Barcelona.